BioMed Research International

Aging: Mitigation and Intervention Strategies

Guest Editors: Chi-Feng Hung, Jorge Azofeifa-Navas, Huanran Tan, Chih-Chi Andrew Hu, and Nicole Clarke

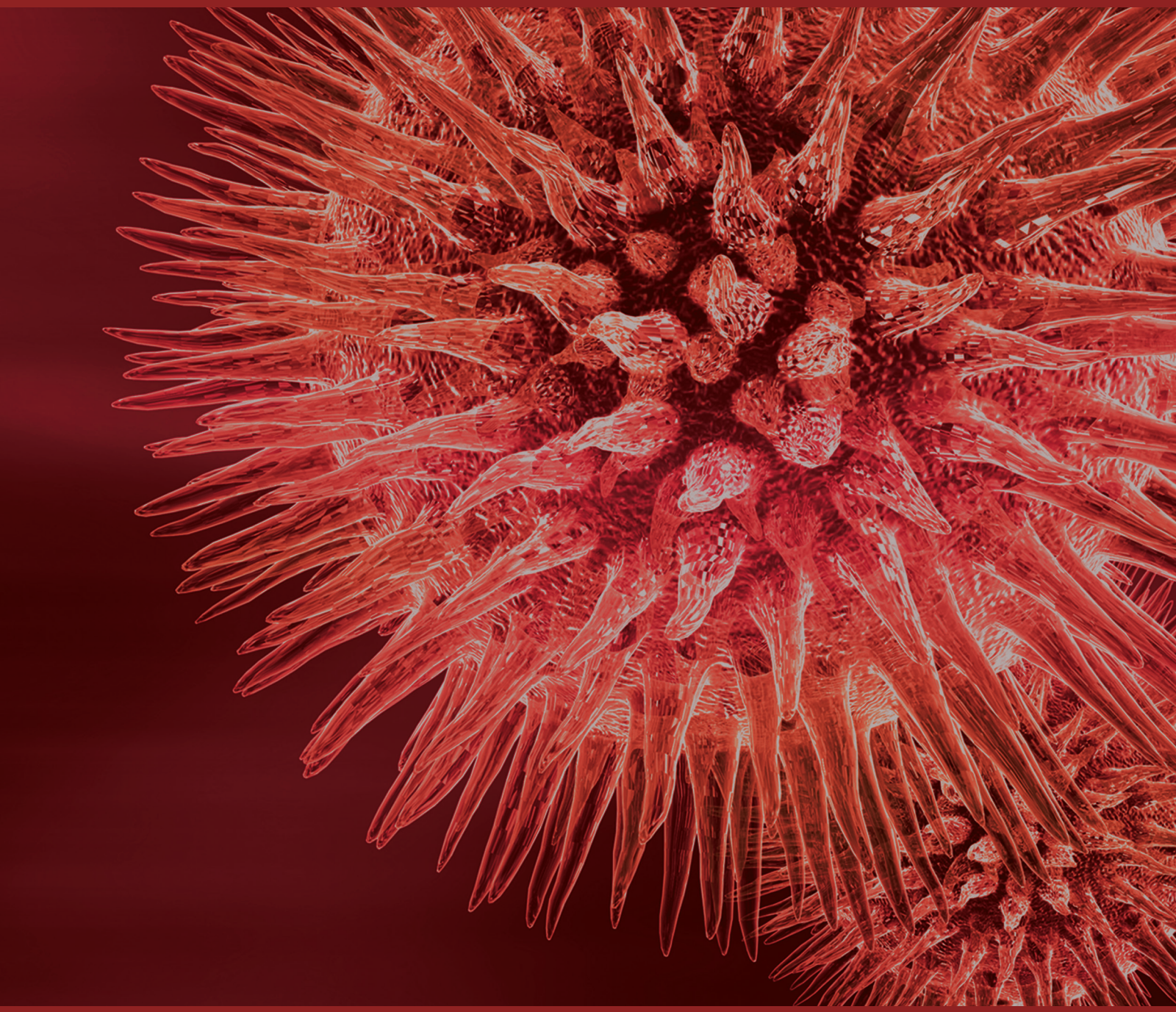

Aging: Mitigation and Intervention Strategies

BioMed Research International

Aging: Mitigation and Intervention Strategies

Guest Editors: Chi-Feng Hung, Jorge Azofeifa-Navas, Huanran Tan, Chih-Chi Andrew Hu, and Nicole Clarke

Contents

Hindawi Publishing Corporation
BioMed Research International
Volume 2015, Article ID 276539, 1 page
http://dx.doi.org/10.1155/2015/276539

Editorial

Aging: Mitigation and Intervention Strategies

Chi-Feng Hung,[1] Jorge Azofeifa-Navas,[2] Huanran Tan,[3] Chih-Chi Andrew Hu,[4] and Nicole Clarke[5]

[1]*School of Medicine, Fu Jen Catholic University, New Taipei City 24205, Taiwan*
[2]*School of Biology, University of Costa Rica, 11501-2060 San José, Costa Rica*
[3]*University Health Science Center, 38 Xueyuan Road, Beijing 100191, China*
[4]*Moffitt Cancer Center, Tampa, FL 33612, USA*
[5]*University of Nottingham, Nottingham NG7 2RD, UK*

Correspondence should be addressed to Chi-Feng Hung; 054317@mail.fju.edu.tw

Received 21 December 2014; Accepted 21 December 2014

Aging is a natural process of life. The causes of aging may come from different sources, both internally and externally. Cellular aging may lead to organ dysfunction during this complicated, irreversible process. Shortening of telomeres during each cell division may lead to cell death; a cell stops dividing while its telomeres shrink to a critical minimum size; and it is one of the causes found in the degeneration of our vision, memory, and immune system. Another contributor to the aging process is oxidative stress. Increased reactive oxygen species (ROS) levels caused by environmental pollution, ionizing radiation, food additives, and so forth may mutate our genes; induce harmful effects on our cells, such as oxidations of lipid, amino acids in proteins, and inactivate specific enzymes; and be a causal factor of cancer development and premature aging. In order to live healthily while we grow old, healthy eating and life style are crucial. Meanwhile, scientists spend a lot of effort trying to investigate ways to support healthy aging and prevent or delay the onset of age-related disease and decline. Many natural ingredients are also found to be beneficial; for example, flavonoids may help fight oxidative stress.

This special issue was to collect information on the mechanism of aging and idea on how to mitigate, delay, or treat age-related decline and diseases. The issue includes studies particularly focusing on the roles of ROS and inflammation and gene in aging and antiaging, as well as investigations of natural products and medications related to antiaging, anticancer, and prevention of cardiovascular diseases, thus promoting a healthy aging from different aspects.

Chi-Feng Hung
Jorge Azofeifa-Navas
Huanran Tan
Chih-Chi Andrew Hu
Nicole Clarke

Hindawi Publishing Corporation
BioMed Research International
Volume 2015, Article ID 235709, 6 pages
http://dx.doi.org/10.1155/2015/235709

Review Article

A Low-Dose Combination of Fluvastatin and Valsartan: A New "Drug" and a New Approach for Decreasing the Arterial Age

Miodrag Janić, Mojca Lunder, and Mišo Šabovič

Department of Vascular Diseases, University of Ljubljana Medical Centre, Zaloška Cesta 7, 1000 Ljubljana, Slovenia

Correspondence should be addressed to Mišo Šabovič; miso.sabovic@kclj.si

Received 11 July 2014; Accepted 27 October 2014

Academic Editor: Nicole Clarke

We have developed a new "drug" and approach that appear to be effective in reducing arterial age. This "drug" represents a low, subtherapeutic dose of statin and sartan and particularly their low-dose combination. The improvement of arterial wall characteristics, also reflecting in a decrease of arterial age, was achieved after a short period of treatment (one month) with the above-mentioned drugs. In addition, we have also implemented a new, innovative therapeutic approach, consisting of intermittent (cyclic) treatment—alternating short "treatment" periods and much longer "rest" periods (when the beneficial effects are still present but gradually decline). This new "drug" and approach both merit further investigation in order to confirm their antiaging efficacy.

1. Introduction

Arterial aging is a process that occurs as part of whole body aging. The role, contribution, and importance of arterial aging to whole body aging have not yet been clarified. Nevertheless, it seems logical that arterial aging should have an important, if not pivotal, role in the aging of the whole body. Therefore, arterial aging could be a valuable target for antiaging interventions. Furthermore, arterial aging also substantially contributes to cardiovascular disorders and represents an important risk factor. It is also of note that a person's age is reflected in their arterial aging.

Although significant advances have been achieved in the prevention and treatment of cardiovascular diseases, they still remain the most important factor of morbidity and mortality in the developed world [1]. Consequently, new strategies for their more effective prevention are desirable [2], as are strategies to allow successful aging. Thus, at least in theory, slowing or even reversing arterial aging could result in both antiaging and cardiovascular preventive effects and benefits. We have previously described and introduced a new, innovative preventive approach, which we have now explored even further. In contrast to other implemented approaches, our concept targets the arterial wall directly rather than the risk factors for aging and atherosclerosis. Notably, the treatment of arterial aging has not been described as an antiaging approach.

We therefore propose a new "drug(s)": low, subtherapeutic doses of statins and sartans and particularly their combination. In addition, we propose a new innovative approach. The approach consists of "intermittent" treatment, that is, one-month therapy followed by a 6–12 month free-of-treatment "rest" period (when the beneficial effects are still present but gradually decline). This period is then followed by a new treatment cycle [3]. The efficacy of the described approach has been studied on apparently healthy male individuals [4–6], as well as patients with diabetes mellitus type 1 [7] and type 2 and patients surviving myocardial infarction. Herein, we describe and present our approach in detail, combining data from the spectrum of our different studies.

2. Arterial Age

Age is an important risk factor for cardiovascular events and cardiovascular risk calculators are based on age, such as the most widely used Framingham Risk Score and SCORE [8]. With regard to age, some studies suggest that arterial (vascular) age should be considered in risk prediction models instead of chronological age, especially for young or middle-age people with low cardiovascular risk [9–11]. Thus, arterial

(vascular) age can be defined as an individual's age after considering their functional and structural arterial wall properties and represents the age at which an individual's arterial wall parameter level would be in the healthy population mean [11]. Importantly, it should be considered that chronological and arterial (vascular) age are not always strictly parallel. Moreover, it is much more common that both "types" of aging continue at a different pace. From a clinical point of view, arterial age seems to be more important as a risk and prognostic factor for cardiovascular events, since it more reliably reflects the real age of an individual than his or her chronological age.

For an individual, the concept of arterial age is more understandable than cardiovascular disease risk [10–12]. Several methods exist for calculating arterial age, some of which are based on coronary calcium score determination [13], such as the MESA (Multi-Ethnic Study in Atherosclerosis) arterial age calculator [14]. In another study, arterial age calculation was based on nomograms of carotid intima-media thickness (cIMT) [9]. Arterial age calculation can be based directly on the structural and functional arterial wall parameters, such as in pulse wave velocity (PWV) and cIMT [11]. The importance of arterial aging has been confirmed by calculations of vascular aging from SCORE and Framingham scores that have recently been extended for arterial age determination and calculations [10, 15].

We believe that arterial age is a very important factor in the aging process, since arteries are the body's main system that interconnects all body organs. Consequently, arterial age could be a surrogate for biological age. If we can achieve arterial age decrease, we can logically expect an improvement of the function of other body systems, resulting in a decrease in the whole body's age. Thus, arterial age could be an ideal target for any antiaging intervention. Decreasing arterial age could result in double benefits: a decrease in arterial age and whole body age and a decrease in cardiovascular risk. Research targets should therefore be focused on arterial age in order to try to obtain efficacious treatment for arterial health prevention in the near future. Taken all together, the rationale is to reduce arterial age. Both age and cardiovascular risk decrease would be possible by targeting the arterial age. In this regard, a new "drug" and approach, which would effectively target arterial age, seem to be a straightforward solution in antiaging medicine.

3. Innovative "Drug"

We propose a new "drug," which, at least in theory, could be beneficial in reducing injury of the arterial wall induced by aging. It consists of two widely used drug groups with known beneficial effects on the arterial wall: statins and sartans or their combination. These beneficial effects are so-called "pleiotropic effects" and are beyond their primary mode of action, namely, plasma cholesterol reduction and blood pressure lowering. Beneficial pleiotropic effects are manifested through various mechanisms, the most important being those that are similar in both drug groups: oxidative stress reduction, inflammation lowering, and other potential mechanisms, exerted directly on the arterial wall [16–18]. Due to the described mechanisms, these two drug groups represent a fairly logical choice for arterial antiaging, as the aging process is the consequence of their perpetual activation. Their efficacy on arterial function improvement has also been explored, and they have been proved to be efficient to a certain extent in therapeutic doses. At therapeutic doses, their effect could be purely the result of their primary mode of action [19–22]. It is very important to consider that the pleiotropic effects of the drugs described appear even when they are administered at low doses, that is, doses that do not exert their primary effect on cholesterol or blood pressure [23, 24]. This phenomenon is of paramount importance for our approach. In addition, in subtherapeutic doses, these drugs have almost no side effects and are particularly safe [25, 26].

As mentioned above, pleiotropic effects are not strictly dose-dependent as they do not always appear in parallel with therapeutic effects. For example, if a higher dose of a certain statin reduces cholesterol to a higher degree, this does not mean that its pleiotropic effects are also greater at a higher dose. Thus differences appear in the pleiotropic effects of low and high doses, particularly in the pleiotropic effects on the arterial wall. For example, rosuvastatin was shown to possess more beneficial pleiotropic effects at low doses than at high doses. In low doses, rosuvastatin significantly increased capillary density and accelerated blood flow in a mouse model of surgically induced limb ischemia. This was accompanied by an increase in circulating endothelial progenitor cells, dependent on endothelial NO-synthase activation. These effects were not observed with rosuvastatin at high doses [27].

Based on the aforementioned assumptions, we proposed a new approach to improving arterial wall characteristics, choosing statin, sartan, or their combination at low doses. Low doses were selected in order to achieve maximal pleiotropic beneficial effects on the arterial wall and to avoid any potential side effects. We chose low-dose fluvastatin, valsartan, or their low-dose combination for our clinical studies. We found that already after a short period (14 days to 1 month) of treatment with a low-dose combination of fluvastatin and valsartan or separate drugs, the functional and structural arterial wall characteristics improved; that is, PWV and beta-stiffness were reduced and flow-mediated dilation (FMD) improved (Figure 1). These results confirm the strong efficacy of such a low-dose drug combination. At the low doses used, the drugs do not exhibit their primary mode of action [3]. These facts were confirmed in our previous studies, along with the fact that combination treatment was superior to separate drugs [4–6]. This effect could be additive or even synergistic [28–31]. Notably, since this kind of low-dose combination has not been investigated previously, it represents an innovative "drug."

4. Innovative Approach

We introduced intermittent or cyclic treatment, where a cycle means a short period of treatment and a long period without treatment. We believe that intermittent treatment is more effective, since it does not allow rebound mechanisms

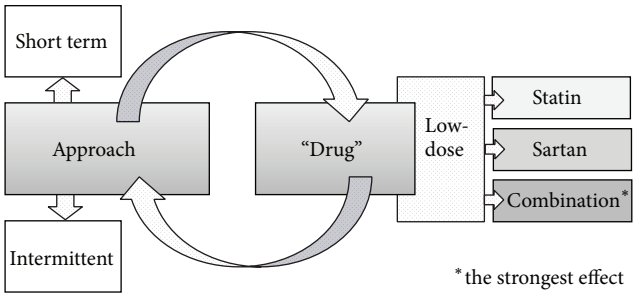

Figure 1: Schematic presentation of the "drug" and approach. The approach is formed of a short-term treatment period, followed by much longer period without treatment, that is, intermittent approach. The "drug" consists of two widely used drug groups with known beneficial effects on the arterial wall: low-dose statins and sartans or their low-dose combination.

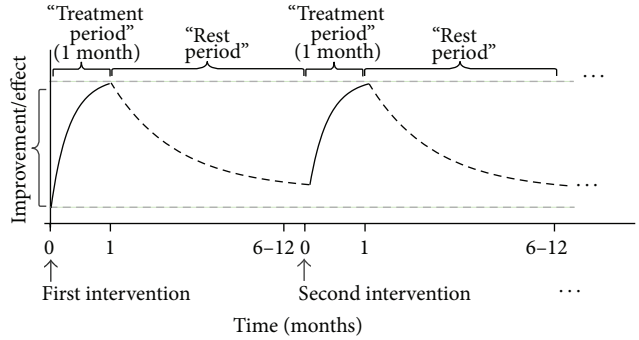

Figure 2: A scheme representing the intermittent approach. The approach consists of a short (one-month) treatment period followed by a relatively much longer rest period (from a few to 12 months). During the rest period, the beneficial effects are still present but gradually decline.

to develop that could be particularly important for the inhibition of the pleiotropic effects. It is worthy of mention that in animal studies we observed that, after reaching a peak, the effects decline with the continuation of the same treatment; this is probably due to the reasons described above [32]. Additionally, better compliance and almost no side effects are achieved by short-term treatment.

We have tested this intermittent cycling approach in several studies. The approach consists of a short (one-month) treatment period followed by a relatively much longer rest period (from a few to 12 months). During the rest period, the beneficial effects are still present but gradually decline (Figure 2). We observed that the so-called "rest" period should be shorter in participants with already injured arterial wall (patients with diabetes mellitus, after myocardial infarction) and longer in healthy persons [7]. This observation is quite logical and supports our idea.

5. Improvement of Arterial Wall Characteristics

The drug combination and therapeutic approach described above specifically target the arterial wall. The latter has two types of characteristics: functional, represented by endothelial function, and structural, represented by the arterial stiffness. However, arterial stiffness is more complex, as it is influenced by functional and structural changes.

The functional characteristics of the arterial stiffness are regulated by the vascular smooth muscle cells (VSMC), which are in turn regulated by vasoactive hormones, the most important one being nitric oxide (NO), released by the endothelium. These characteristics might therefore be improved through improvement of the endothelium. For this kind of improvement, the effects can vary from immediate to long-term, but on the other hand, for structural characteristics improvement, a longer time is needed to allow for remodeling. The structural characteristics are defined by the ratio between collagen and elastin in the arterial media, as well as the amount of viable VSMC that produce these compounds. The higher the amount of elastin, the more elastic the artery, while, on the other hand, the artery becomes stiffer with age, when collagen predominates and becomes cross-linked. This particular characteristic is also influenced by the functional characteristics of the arterial wall. For arterial stiffness improvement/decrease, two possible approaches could be used: (i) decrease in functional and (ii) decrease in structural effects on arterial stiffness. Our approach interferes with and influences both.

A one-month treatment with a low-dose combination of fluvastatin and valsartan improves the functional arterial wall characteristics. Through these and additional mechanisms, it also subsequently influences the structural arterial wall characteristics, leading to overall beneficial effects on the arterial function. The improvement in functional characteristics is evident in an increase in FMD, while the structural characteristics' improvement is evidenced by a decrease in both PWV and β-stiffness [4–6]. In addition to these observations, we have shown that these effects can at least in part be explained by a reduction in inflammation and oxidative stress [33].

6. Decrease of Arterial Age

We have proposed the following concept—if arterial stiffness increases with age, a decrease in arterial stiffness will result in decreasing arterial age. The decrease of arterial age was achieved by our approach in all studied groups of apparently healthy participants. After one month of treatment, low-dose fluvastatin or low-dose valsartan separately decreased arterial age by approximately 7 years, whereas a low-dose combination decreased arterial age by approximately 10 years. These calculations are based on nomograms for PWV and β-stiffness [34, 35].

7. Proof of the Concept

Aging influences the arterial wall through two basic interconnected mechanisms: structural and dynamic. Structural aging is the consequence of a higher collagen to elastin fibers ratio, leading to stiffer arteries. Dynamic aging is

the consequence of reduced nitric oxide (NO) bioavailability, leading to endothelial dysfunction and a higher tone of smooth muscle cells in the arterial media. All these derangements have a similar pathophysiological background, namely, increased oxidative stress and inflammation in the arterial wall [36]. Additional, not yet fully discovered mechanisms probably also play a role. Nevertheless, all of the described derangements could be influenced, amongst other, also by the new "drug" and approach [33, 36].

In our studies, we have thoroughly tested the described new, innovative "drug" and approach. In apparently healthy middle-aged men, we tested the effect of one-month therapy with low-dose fluvastatin, valsartan, or their low-dose combination. We have consistently obtained improvement of arterial wall characteristics in every participant. These results were all statistically significant to a very high degree. In participants treated only with low-dose fluvastatin, PWV decreased by 6% and β-stiffness decreased by 11%, while FMD improved by 92%, all compared to the baseline values [4]. Low-dose valsartan showed slightly better results, with PWV decreasing by 8% and β-stiffness by 12% and FMD improving by 150% [5]. As expected, the low-dose combination of fluvastatin and valsartan proved to be the most potent. In the latter group of participants, PWV decreased by 11% and β-stiffness by 12% and FMD improved by 170% [6]. These results were further supported by an accompanying significant decrease in inflammatory markers, namely, high sensitivity C-reactive protein (hsCRP), vascular cell adhesion molecule-1 (VCAM-1), and interleukin 6 (IL-6) in the low-dose combination group. Additionally, oxidative stress parameters also significantly changed only in the low-dose combination group, with total antioxidant status (TAS) and glutathione peroxidase (GPx) increasing and selenium levels decreasing [33]. These molecular results partially elucidate the mechanism behind the approach. Furthermore, the effectiveness of a 30-day treatment with a low-dose combination of fluvastatin and valsartan was also proved in patients with diabetes mellitus type 1; PWV decreased by 7.5% and β-stiffness decreased by 10% while FMD improved by 73% [7]. Importantly, we have observed no side effects in any of our study participants. This was somehow expected, as low, subtherapeutic doses of statins and sartans were used, thus not producing any blood pressure or lipids reduction.

When the arterial wall parameters were monitored after discontinuation of the one-month treatment, the protective pleiotropic effects were still present over a certain period of time but gradually declined. The decline was the fastest in the low-dose fluvastatin group, followed by the low-dose valsartan group [4, 5]. In the low-dose combination group, the residual effect five months after treatment discontinuation was somehow surprisingly still at almost 80% and was halved only after 10 months (therefore not yet reaching the basal level) [6], thus allowing for a probable one-year cycle period. Our preliminary observations show that after these effects reached the basal level, repeating a one-month treatment with the same drug/combination as the previous time gave the same results as the first treatment. When these results are taken together, a constant cyclical achievement of the basal level results or basal level arterial age could be achieved with the described intermittent approach over several years or even longer. Evidently, the arterial aging process can be slowed down. Furthermore, on the one hand, such treatment leads to obtaining or regaining some "arterial" years that would be otherwise lost and would lead to a more rapid decline in arterial function, preclinical atherosclerotic changes, and later on to atherosclerotic manifestation. On the other hand, such treatment leads to the slowing of whole body aging.

This concept was proven even further in animal studies with isolated rat heart and aorta, where we obtained the highest increase in endothelium-dependent thoracic aorta relaxation and coronary flow after six weeks of treatment with low-dose statin, sartan, or their low-dose combination. As in human studies, the low-dose combination was the most effective. It should be emphasized that, after eight weeks of treatment, the described protective effects declined, thus proving the assumption on the activation of counter compensatory mechanisms [32]. Therefore, an optimal length of therapy should be used in order to obtain the maximal possible effect on the one hand and avoid triggering the compensatory mechanisms that diminish protective effects on the other. The results in animal studies were further backed by gene expression experiments, where the expression of endothelin receptor type A (EDNRA) gene was reduced, while the expression of endothelial nitric oxide synthase 3 (NOS3) gene increased [37].

8. Future Perspectives

We have shown that our new "drug" and approach are effective in a varied range of participants, from apparently healthy to unhealthy ones. We believe that ideal candidates for treatment would be middle-aged males and females, still healthy or with existing cardiovascular disease, diabetes mellitus, or overt atherosclerotic disease, and also the elderly. We believe that the new "drug" and approach could be somehow effective in these people as well, despite their different characteristics and the drugs they already use.

All in all, our previous studies have confirmed the effectiveness of our new innovative "drug" and approach to improving arterial wall properties and consequently decreasing arterial age. We propose that repetition of treatment cycles (alternating treatment and rest periods) through the years could preserve arterial age at approximately the same level for a longer period of time. Obviously, several additional studies are necessary to confirm the effectiveness of our preventive approach. Further animal and human studies exploring the exact mechanisms underlying the observed beneficial effect are also required. Larger and long-lasting studies are needed in order to test whether this approach influences whole body aging and reduces cardiovascular events in the long term.

Conflict of Interests

The authors declare that there is no conflict of interests regarding the publication of this paper.

References

[1] J. G. Robinson and S. S. Gidding, "Curing atherosclerosis should be the next major cardiovascular prevention goal," *Journal of the American College of Cardiology*, vol. 63, no. 25PA, pp. 2779–2785, 2014.

[2] S. C. Smith Jr., D. Chen, A. Collins et al., "Moving from political declaration to action on reducing the global burden of cardiovascular diseases: a statement from the global cardiovascular disease taskforce," *Circulation*, vol. 128, no. 23, pp. 2546–2548, 2013.

[3] M. Janić, M. Lunder, and M. Šabovič, "A new anti-ageing strategy focused on prevention of arterial ageing in the middle-aged population," *Medical Hypotheses*, vol. 80, no. 6, pp. 837–840, 2013.

[4] M. Lunder, M. Janić, S. Habjan, and M. Šabovič, "Subtherapeutic, low-dose fluvastatin improves functional and morphological arterial wall properties in apparently healthy, middle-aged males—a pilot study," *Atherosclerosis*, vol. 215, no. 2, pp. 446–451, 2011.

[5] M. Lunder, M. Janić, and M. Šabovič, "Reduction of age-associated arterial wall changes by low-dose valsartan," *European Journal of Preventive Cardiology*, vol. 19, no. 6, pp. 1243–1249, 2012.

[6] M. Lunder, M. Janić, B. Jug, and M. Šabovič, "The effects of low-dose fluvastatin and valsartan combination on arterial function: a randomized clinical trial," *European Journal of Internal Medicine*, vol. 23, no. 3, pp. 261–266, 2012.

[7] V. Savic, B. Erzen, M. Janic et al., "Improvement of arterial wall characteristics by the low-dose fluvastatin and valsartan combination in type 1 diabetes mellitus patients," *Diabetes and Vascular Disease Research*, vol. 10, no. 5, pp. 420–425, 2013.

[8] R. A. Payne, "Cardiovascular risk," *British Journal of Clinical Pharmacology*, vol. 74, no. 3, pp. 396–410, 2012.

[9] J. H. Stein, M. C. Fraizer, S. E. Aeschlimann, J. Nelson-Worel, P. E. McBride, and P. S. Douglas, "Vascular age: integrating carotid intima-media thickness measurements with global coronary risk assessment," *Clinical Cardiology*, vol. 27, no. 7, pp. 388–392, 2004.

[10] J. I. Cuende, N. Cuende, and J. Calaveras-Lagartos, "How to calculate vascular age with the SCORE project scales: a new method of cardiovascular risk evaluation," *European Heart Journal*, vol. 31, no. 19, pp. 2351–2358, 2010.

[11] D. B. Santana, Y. A. Zócalo, I. F. Ventura et al., "Health informatics design for assisted diagnosis of subclinical atherosclerosis, structural, and functional arterial age calculus and patient-specific cardiovascular risk evaluation," *IEEE Transactions on Information Technology in Biomedicine*, vol. 16, no. 5, pp. 943–951, 2012.

[12] E. K. Kerut, "Coronary risk assessment and arterial age calculation using coronary artery calcium scoring and the framingham risk score," *Echocardiography*, vol. 28, no. 6, pp. 686–693, 2011.

[13] K. Ebeling and P. Nischan, "Nonexperimental evaluation of the effectiveness of a screening program for lung cancer," *International Journal of Technology Assessment in Health Care*, vol. 8, no. 2, pp. 245–254, 1992.

[14] J. A. Munir, H. Wu, K. Bauer et al., "Impact of coronary calcium on arterial age and coronary heart disease risk estimation using the MESA arterial age calculator," *Atherosclerosis*, vol. 211, no. 2, pp. 467–470, 2010.

[15] R. B. D'Agostino Sr., R. S. Vasan, M. J. Pencina et al., "General cardiovascular risk profile for use in primary care: the Framingham heart study," *Circulation*, vol. 117, no. 6, pp. 743–753, 2008.

[16] P. Jankowski, M. E. Safar, and A. Benetos, "Pleiotropic effects of drugs inhibiting the renin-angiotensin-aldosterone system," *Current Pharmaceutical Design*, vol. 15, no. 5, pp. 571–584, 2009.

[17] C. G. Mihos, M. J. Salas, and O. Santana, "The pleiotropic effects of the hydroxy-methyl-glutaryl-CoA reductase inhibitors in cardiovascular disease: a comprehensive review," *Cardiology in Review*, vol. 18, no. 6, pp. 298–304, 2010.

[18] M. Wang, R. E. Monticone, and E. G. Lakatta, "Arterial aging: a journey into subclinical arterial disease," *Current Opinion in Nephrology and Hypertension*, vol. 19, no. 2, pp. 201–207, 2010.

[19] D. Z. I. Cherney, J. W. Scholey, S. Jiang et al., "The effect of direct renin inhibition alone and in combination with ACE inhibition on endothelial function, arterial stiffness, and renal function in type 1 diabetes," *Diabetes Care*, vol. 35, no. 11, pp. 2324–2330, 2012.

[20] A. M. El-Barbary, M. S. Hussein, E. M. Rageh, H. E. Hamouda, A. A. Wagih, and R. G. Ismail, "Effect of atorvastatin on inflammation and modification of vascular risk factors in rheumatoid arthritis," *Journal of Rheumatology*, vol. 38, no. 2, pp. 229–235, 2011.

[21] R. G. Fassett, I. K. Robertson, M. J. Ball, D. P. Geraghty, J. E. Sharman, and J. S. Coombes, "Effects of atorvastatin on arterial stiffness in chronic kidney disease: a randomised controlled trial," *Journal of Atherosclerosis and Thrombosis*, vol. 17, no. 3, pp. 235–241, 2010.

[22] K. Hayashi, K. Miyagawa, K. Sato, R. Ueda, and Y. Dohi, "Temocapril, an angiotensin converting enzyme inhibitor, ameliorates age-related increase in carotid arterial stiffness in normotensive subjects," *Cardiology*, vol. 106, no. 3, pp. 190–194, 2006.

[23] M. Hongo, S. Kumazaki, A. Izawa et al., "Low-dose rosuvastatin improves arterial stiffness in high-risk Japanese patients with dyslipdemia in a primary prevention group: a comparison with fluvastatin," *Circulation Journal*, vol. 75, no. 11, pp. 2660–2667, 2011.

[24] A. Ichihara, M. Hayashi, Y. Kaneshiro et al., "Low doses of losartan and trandolapril improve arterial stiffness in hemodialysis patients," *American Journal of Kidney Diseases*, vol. 45, no. 5, pp. 866–874, 2005.

[25] R. C. Pasternak, S. C. Smith Jr., C. N. Bairey-Merz, S. M. Grundy, J. I. Cleeman, and C. Lenfant, "ACC/AHA/NHLBI clinical advisory on the use and safety of statins," *Journal of the American College of Cardiology*, vol. 40, no. 3, pp. 567–572, 2002.

[26] M. Burnier, "Angiotensin II type 1 receptor blockers," *Circulation*, vol. 103, no. 6, pp. 904–912, 2001.

[27] J. Zhou, M. Cheng, Y. H. Liao et al., "Rosuvastatin enhances angiogenesis via eNOS-dependent mobilization of endothelial progenitor cells," *PLoS ONE*, vol. 8, no. 5, Article ID e63126, 2013.

[28] S. H. Han, E. W. Kang, S.-J. Yoon et al., "Combined vascular effects of HMG-CoA reductase inhibitor and angiotensin receptor blocker in non-diabetic patients undergoing peritoneal dialysis," *Nephrology Dialysis Transplantation*, vol. 26, no. 11, pp. 3722–3728, 2011.

[29] M. Horiuchi, T.-X. Cui, Z. Li, J.-M. Li, H. Nakagami, and M. Iwai, "Fluvastatin enhances the inhibitory effects of a selective angiotensin II type 1 receptor blocker, valsartan, on vascular neointimal formation," *Circulation*, vol. 107, no. 1, pp. 106–112, 2003.

[30] O. Hussein, J. Shneider, M. Rosenblat, and M. Aviram, "Valsartan therapy has additive anti-oxidative effect to that of fluvastatin therapy against low-density lipoprotein oxidation: studies in hypercholesterolemic and hypertensive patients," *Journal of Cardiovascular Pharmacology*, vol. 40, no. 1, pp. 28–34, 2002.

[31] L. Liu, S.-P. Zhao, H.-N. Zhou, Q.-Z. Li, and J.-X. Li, "Effect of fluvastatin and valsartan, alone and in combination, on postprandial vascular inflammation and fibrinolytic activity in patients with essential hypertension," *Journal of Cardiovascular Pharmacology*, vol. 50, no. 1, pp. 50–55, 2007.

[32] M. Lunder, L. Žiberna, M. Janić et al., "Low-dose atorvastatin, losartan, and particularly their combination, provide cardiovascular protection in isolated rat heart and aorta," *Heart and Vessels*, vol. 28, no. 2, pp. 246–254, 2013.

[33] M. Janić, M. Lunder, M. Prezelj, and M. Šabovič, "A combination of low-dose fluvastatin and valsartan decreases inflammation and oxidative stress in apparently healthy middle-aged males," *Journal of Cardiopulmonary Rehabilitation and Prevention*, vol. 34, no. 3, pp. 208–212, 2014.

[34] S. Carerj, C. Nipote, C. Zimbalatti et al., "388 normal vascular aging evaluated by a new tool: e-tracking," *European Heart Journal—Cardiovascular Imaging*, vol. 7, supplement 1, p. S49, 2006.

[35] M.-J. Jurašić, S. Josef-Golubić, R. Šarac, A. Lovrencic-Huzjan, and V. Demarin, "Beta stiffness—setting age standards," *Acta Clinica Croatica*, vol. 48, no. 3, pp. 253–258, 2009.

[36] M. Janić, M. Lunder, and M. Šabovič, "Arterial stiffness and cardiovascular therapy," *BioMed Research International*, vol. 2014, Article ID 621437, 11 pages, 2014.

[37] M. Lunder, G. Drevenšek, D. Černe, J. Marc, M. Janić, and M. Šabovič, "Treatment with low-dose atorvastatin, losartan, and their combination increases expression of vasoactive-related genes in rat aortas," *Journal of Cardiovascular Pharmacology and Therapeutics*, vol. 18, no. 2, pp. 177–183, 2013.

Hindawi Publishing Corporation
BioMed Research International
Volume 2015, Article ID 906039, 6 pages
http://dx.doi.org/10.1155/2015/906039

Research Article

The Differential Effects of a Selective Kappa-Opioid Receptor Agonist, U50488, in Guinea Pig Heart Tissues

Chi-Feng Hung,[1,2] Hsin-Ju Li,[3] Hsun-Hao Chang,[4] Gon-Ann Lee,[3] and Ming Jai Su[5]

[1]*School of Medicine, Fu Jen Catholic University, No. 510 Zhongzheng Road, Xinzhuang District, New Taipei City 24205, Taiwan*
[2]*Big Data Research Centre, Fu Jen Catholic University, New Taipei City, Taiwan*
[3]*Department of Chemistry, Fu Jen Catholic University, New Taipei City, Taiwan*
[4]*Department of Cardiology, Tainan Municipal Hospital, No. 670 Chongde Road, East District, Tainan 70173, Taiwan*
[5]*Department of Pharmacology, College of Medicine, National Taiwan University, No. 1 Jen-Ai Road, Section 1, Zhongzheng District, Taipei 10051, Taiwan*

Correspondence should be addressed to Chi-Feng Hung; 054317@mail.fju.edu.tw

Received 11 July 2014; Revised 2 November 2014; Accepted 4 November 2014

Academic Editor: Adair Santos

The differential effects of a selective kappa- (κ-) opioid receptor agonist, U50488, were elucidated by monitoring the contraction of isolated guinea pig atrial and ventricular muscles. In electrically driven left atria, U50488 in nanomolar concentration range decreased the contractile force. Norbinaltorphimine (norBNI), a selective κ-receptor antagonist, and pertussis toxin (PTX) abolished the negative inotropic effect of U50488. In contrast, the inhibitory effect was not affected by the pretreatment of atropine or propranolol. Even though U50488 exerted a negative inotropic effect in the left atrium, it did not affect the contractile force of the right atrium and ventricles paced at 2 Hz. Similarly, the beating rate of the spontaneously beating right atrium was also unaffected by U50488. These results indicate that the activation of κ-opioid receptors can only produce negative inotropic effect in left atria via activation of PTX-sensitive G protein in guinea pigs. The absence of negative inotropic effects in right atria and ventricles suggests that there may be a greater distribution of functional κ-opioid receptors in guinea pig left atria than in right atria and ventricles, and the distribution of the receptors may be species-specific.

1. Introduction

Many studies have indicated that κ-opioid receptors exist in the heart by receptor binding assay [1–3] and physiological studies [4, 5]. Stimulation of κ-opioid receptors in the heart may evoke negative inotropic [6, 7] and chronotropic effects [8]. Prior investigators also suggested that activation of cardiac κ-opioid receptors could mediate cardioprotective and antiarrhythmic effect during myocardial ischemia and reperfusion [9–12]; modulation of cardiac function by opioid peptide receptor agonists or antagonists, and future drug development to improve myocardial salvage would be possible [2, 3].

While U50488, a selective κ-opioid receptor agonist, decreases the electrically induced $[Ca^{2+}]_i$ transient in rat cardiac myocytes at a higher concentration (μmol/L) by activating the phosphoinositol pathway [13, 14], it inhibits the augmentation of the electrically induced $[Ca^{2+}]_i$ transient by β-adrenoceptor stimulation in the heart at a lower concentration (nmol/L) [13]. Electrophysiological studies showed that U50488 could inhibit the P-type calcium channel in brain Purkinje cells through activation of κ-opioid receptors [15, 16]; it could also inhibit the L-type calcium, sodium, and potassium channels in ventricular myocytes directly at a higher concentration [17, 18].

Several studies have reported that 5-hydroxytryptamine (5-HT), calcitonin gene-related peptide (CGRP), angiotensin II, somatostatin, adenosine, and diadenosine tetraphosphate changed the contractile force more in atrial than in ventricular tissues [19–23]. However, opioid receptors exist in both atria and ventricles; it is still unknown whether there is any response difference in the κ-opioid receptors between these

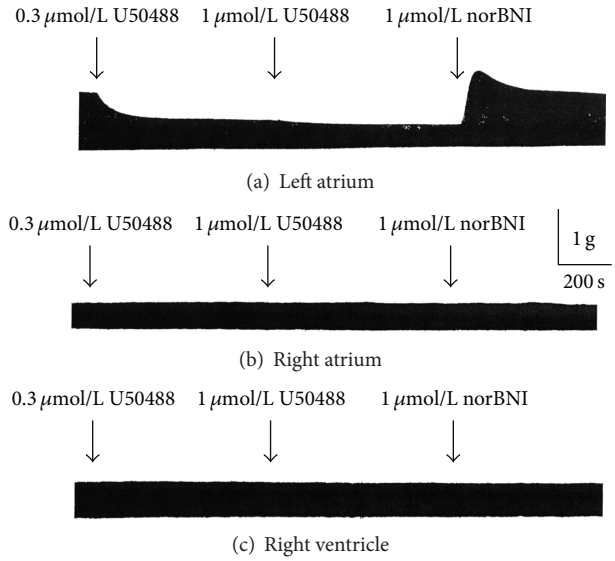

Figure 1: Effect of U50488 on the contractile force in guinea pig atria and ventricle. Sinoatrial node of right atrium was removed. Atria and ventricle were paced at 2 Hz. After equilibrium for 30 min, U50488 and norBNI were added sequentially. (a) Left atrium. (b) Right atrium. (c) Right ventricle.

tissues. This study was planned to examine the effects of a selective κ-receptor agonist, U50488, on atrial and ventricular muscles isolated from guinea pigs.

2. Materials and Methods

2.1. Chemicals. NorBNI (norbinaltorphimine), U50488 (trans-3,4-dichloro-N-methyl-N-[2-(1-pyrrolidinyl)cyclohexyl]-benzeneacetamide), U69593 ((+)-(5α,7α,8β)-N-methyl-N-[7-(1-pyrrolidinyl)-1-oxaspiro[4.5]dec-8-yl]-benzeneacetamide), and PTX (pertussis toxin) were purchased from Research Biochemicals International (RBI) Chem. Co. (USA). Propranolol, atropine, and carbachol were purchased from Sigma Chem. Co. (USA).

2.2. Isolated Cardiac Preparations and Mechanical Response. Preparations of isolated left and right atria (or ventricles) from male guinea pigs (Hartley strain, 0.2–0.5 kg) were used. The preparations were bathed in Tyrode solution, and the Tyrode solution (composition in mM: NaCl 137.0, KCl 5.4, $MgCl_2$ 1.1, $NaHCO_3$ 11.9, NaH_2PO_4 0.33, dextrose 11.0, and $CaCl_2$ 1.8) was aerated with 5% CO_2 and 95% O_2 at 37 ± 0.5°C. Contractions of spontaneously beating right atrial preparations, as well as the electrically driven left atrial, right atrial, and right ventricular strips, were measured by connecting one end of the preparation to a force displacement transducer (type BG 25, Gould Inc., Cleveland, Ohio, USA) by a fine silk thread and were recorded on a Gould RS 3400 recorder. To obtain the maximum developed tension, an optimal preload (1.0 g) was used. Left atria, right atria, and right ventricular strips were stimulated at a frequency of 2 Hz by rectangular pulse of 2 ms duration at supramaximal intensity via an isolated Grass S88 stimulator (Grass Instruments Co., Quincy, MA, USA).

2.3. Assessment of the Effects of PTX. To assess a possible role of pertussis toxin-sensitive G protein in the actions of U50488, guinea pigs were pretreated with PTX 150 μg/kg (i.p.) for 24 h before sacrifice. The influence of PTX on cardiac tissues was verified by the contractile responses of left atrial strips to carbachol. Carbachol (0.1 μmol/L) decreased the basal contractile force from 0.8 ± 0.1 g to 0.5 ± 0.1 g (decrease about 44% in control group, $n = 5$), whereas a less decrease was found, from 0.8 ± 0.1 g to 0.6 ± 0.1 g (decrease about 24%, $n = 5$), in PTX-treated group.

2.4. Statistics. Data are expressed as mean ± SE. Statistics comparison was made by Student's paired or unpaired t-test with the level of significance taken as $P < 0.05$.

3. Results

3.1. The Differential Effects of κ Receptor Agonists on Cardiac Contractility. Figure 1 shows the original tracings of continuous tension recordings of three different guinea pig atrial and ventricular preparations in cumulative response to 300 nmol/L and 1 μmol/L U50488. In the left atrium, U50488 exerted a significant and immediate negative inotropic effect (Figure 1(a)). This inhibitory effect reached a steady state in 10 min and could be eliminated by norBNI (1 μmol/L), a selective κ-opioid receptor antagonist. In contrast, the inhibitory effect was not found in the preparations of right atrium, right ventricle (Figures 1(b) and 1(c)), and left ventricle (not shown). Average data of the influence of U50488 on the contractile force of left atrial preparations are shown in Figure 2. U50488 started to reduce the contractile force significantly at 30 nmol/L. At 100 nmol/L, 300 nmol/L, and 1 μmol/L, it reduced the force to 77.3 ± 5.0%, 60.6 ± 7.7%, and 49.8 ± 6.9% ($n = 5$) of the control, respectively. Similarly,

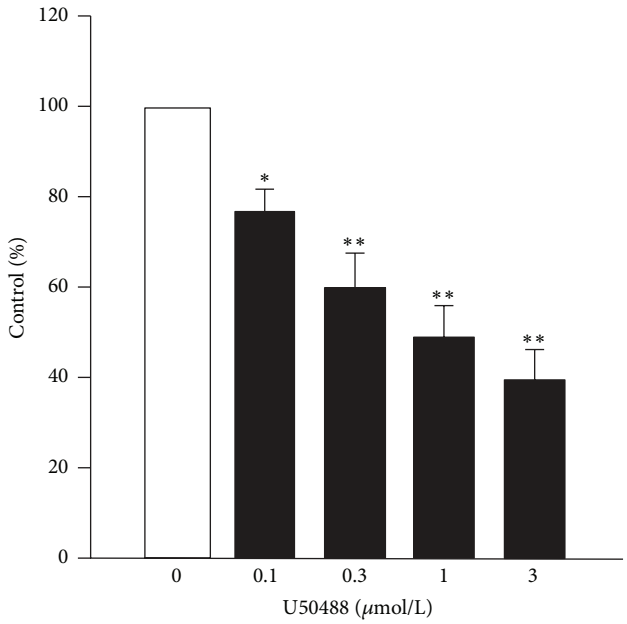

Figure 2: The concentration-dependent effects of U50488 on contractile force of left atrium illustrated as percentage of control. Vertical lines are SE. $*$ and $**$ indicate $P < 0.05$ and $P < 0.01$ as compared with control ($n = 5$).

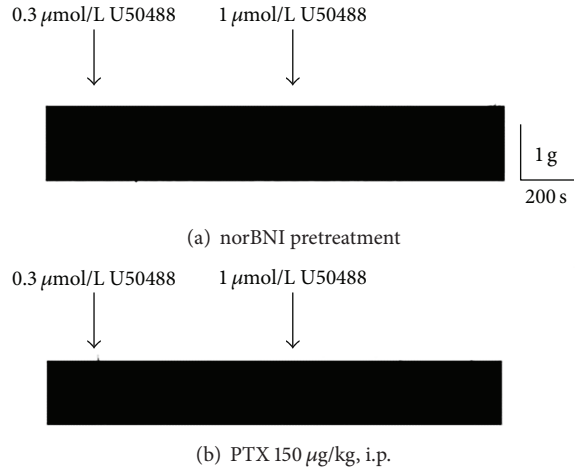

Figure 3: Representative tracings show the effect of norBNI and PTX on the effect of U50488 in left atria. (a) A norBNI (1 μmol/L) pretreated atrium. (b) An atrium from PTX-pretreated guinea pig (150 μg/kg for 24 h).

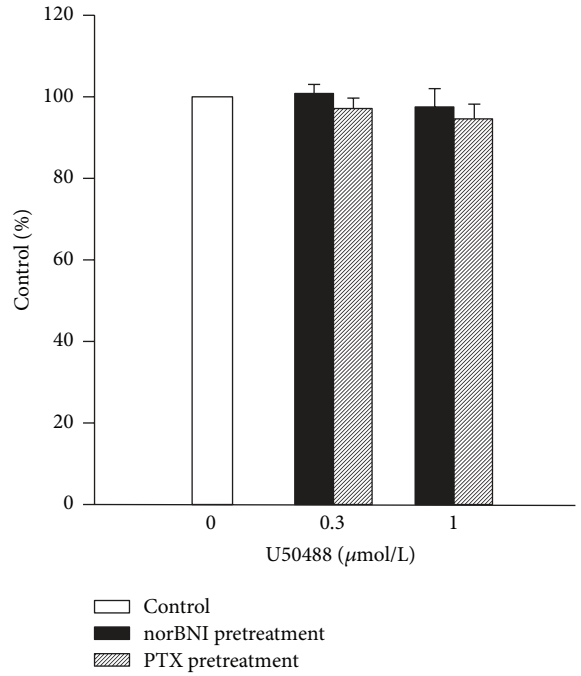

Figure 4: Effect of U50488 on left atria pretreated with norBNI ($n = 4$) and PTX ($n = 5$).

we found that U69593, another selective κ-receptor agonist, also has the same negative inotropic effect on left atria but not the preparations of right atria and ventricles (figure not shown) in our other experiments. The inhibitory effect could also be abolished by norBNI (1 μmol/L). At 300 nmol/L and 1 μmol/L, it reduced the force to 54.4 ± 5.3% and 45.9 ± 6.4% ($n = 4$) of the control, respectively. As higher concentrations of U50488 and U69593 may elicit effects not mediated via opioid receptor [24], they were not investigated with the κ-opioid receptor antagonist.

3.2. Effects of norBNI and PTX on the Negative Inotropic Action of U50488. To further evaluate whether the inhibitory effects of U50488 on left atria were due to κ-opioid receptors and the coupling of inhibitory G protein, $G_{i/o}$, the muscle strips were pretreated with a selective κ_2-receptor antagonist, norBNI (1 μmol/L), for 10 min. We found that norBNI at 1 μM alone did not affect the contractile force of the left atrial preparations, but it prevented the inhibitory effects of U50488 (Figure 3(a)). In left atria isolated from guinea pigs pretreated with PTX (150 μg/kg, i.p.), which catalyzes the adenine nucleotide ribosylation of $G_{i/o}$ protein α-subunits, U50488 also failed to exert any inhibitory response (Figure 3(b)). The average data of U50488 after norBNI or PTX pretreatment are shown in Figure 4.

3.3. Effects of Propranolol and Atropine on the Negative Inotropic Action of U50488. It had been reported that propranolol could modify the inhibitory effect of U50488 in isolated right atria of rat [4, 7], and the κ-receptor agonist could inhibit norepinephrine release from cardiac sympathetic nerve [25]. Therefore, we evaluated whether the inhibitory effects of U50488 in isolated left atria of guinea pig could be affected by propranolol (3 μmol/L). A representative example of the effect of propranolol pretreatment on the U50488-induced negative inotropic action is shown in Figure 5(a), and the average result is shown in Figure 5(b). The average amplitudes of the contractile force of the left atrial preparations were decreased to 62.7 ± 4.3%, 54.2 ± 5.1%, and 46.0 ± 5.7% ($n = 6$) of the control by 0.3, 1, and 3 μmol/L of U50488, respectively. Decreases in contractile force induced by 0.3

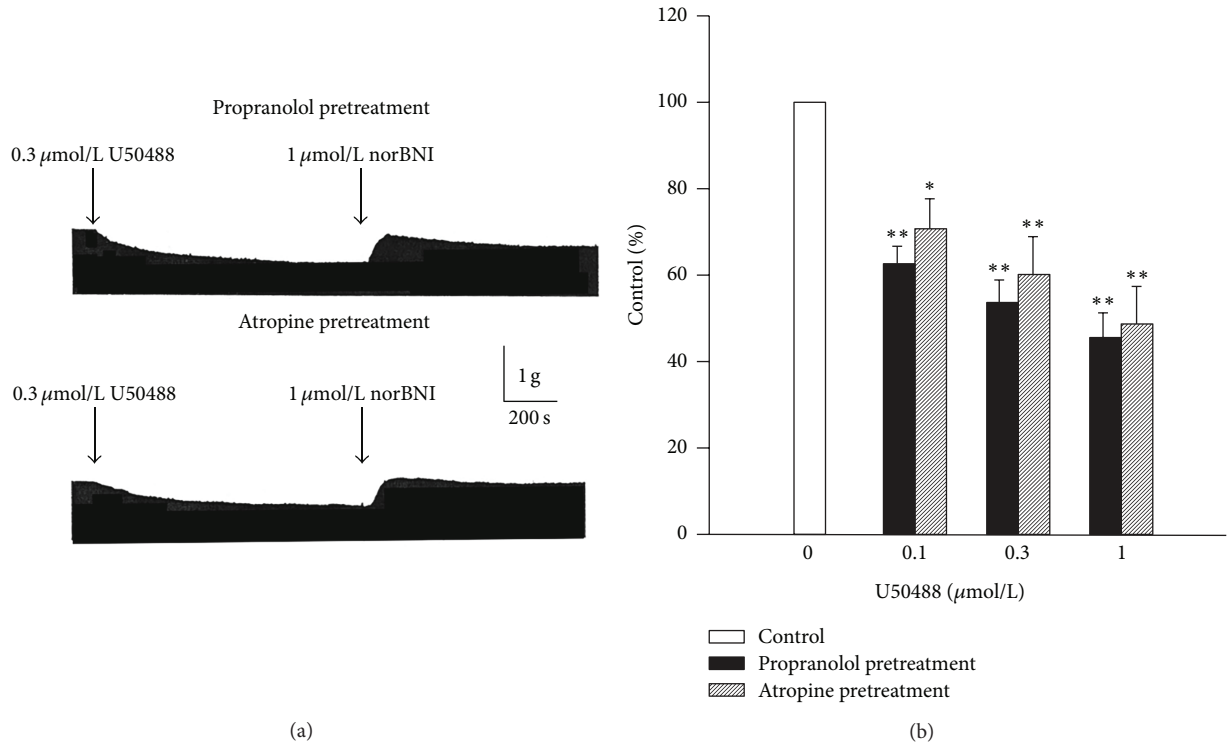

Figure 5: Negative inotropic effect of U50488 in left atria pretreated with propranolol (3 μmol/L, $n = 6$) or atropine (1 μmol/L, $n = 5$). (a) Representative traces show the effect of U50488 on the contractile force in left atria pretreated with propranolol or atropine for 20 min. (b) Concentration-dependent effects of U50488 on contractile of left atria in the presence of propranolol or atropine. Values are expressed as percentage of control. Vertical lines are SE. $*$ and $**$ indicate $P < 0.05$ and $P < 0.01$ as compared with control.

and 1 μmol/L of U50488 were also completely eliminated by norBNI. In comparison with the decrease in contractile force induced by U50488 alone, propranolol did not affect the negative inotropic effect of U50488 on left atrial preparations. Considering the release of acetylcholine being another possibility which may contribute to the negative inotropic effect of U50488, we examined the negative inotropic effect of U50488 on left atria pretreated with atropine (1 μmol/L). Our data showed that the negative inotropic effect of U50488 was unaffected by atropine. The average amplitudes in contractile force were decreased to 70.6 ± 7.0%, 60.4 ± 8.6%, and 49.0 ± 8.6% ($n = 5$) of the control by 0.3, 1, and 3 μmol/L of U50488, respectively (Figures 5(a) and 5(b)).

3.4. Effect of U50488 on the Spontaneous Beating Rate of Guinea Pig Right Atria. U50488 could evoke negative chronotropic effect on isolated right atria of rat [6, 7]. However, we did not find any change in the spontaneous beating rate in guinea pig right atria in our study (Figure 6).

4. Discussion

In this study, we compared the inotropic effects of U50488 and U69593, two selective κ-opioid receptor agonists, in guinea pig left atria to their effects in right atria and ventricles. We observed that both U50488 and U69593 dose-dependently decreased the contractile force of guinea pig atrial muscles, and this effect was exerted only in left atria. The absence of negative inotropic effect in right atria and ventricles suggests that κ-opioid receptors in these two regions may be less or absent in guinea pigs. However, missing signaling pathway for coupling of κ-opioid receptor activation to negative inotropism in these two cardiac tissues may also be another possibility. These speculations remain for further identification, and radioligand binding studies using appropriate radioligands may be necessary.

Corresponding to previous observations which showed the coupling of the κ-opioid receptor to activation of the $G_{i/o}$ protein [16], our results showed that the negative inotropic effect of U50488 on left atrial tissues could be abolished by norBNI and PTX, which suggests that the action is mediated through κ-opioid receptors by activation of PTX-sensitive G protein. At a higher concentration (3 μmol/L), U50488 was found to decrease the contractile force of right ventricular preparations that could not be eliminated by norBNI in this study. The negative inotropic effect at the higher concentration of U50488 may be due to its directly inhibitory effect instead of the activation of κ-opioid receptors. These observations agree with the study that showed a direct inhibition of calcium current in guinea pig ventricular myocytes by U50488 at similar concentration range [24]. The 15.0 ± 4.0% ($n = 6$) inhibition of the contractile force of right ventricular strips by 3 μM U50488 in our study is comparable to the 18% inhibition of calcium current in guinea pig ventricular cell by Utz et al. [24].

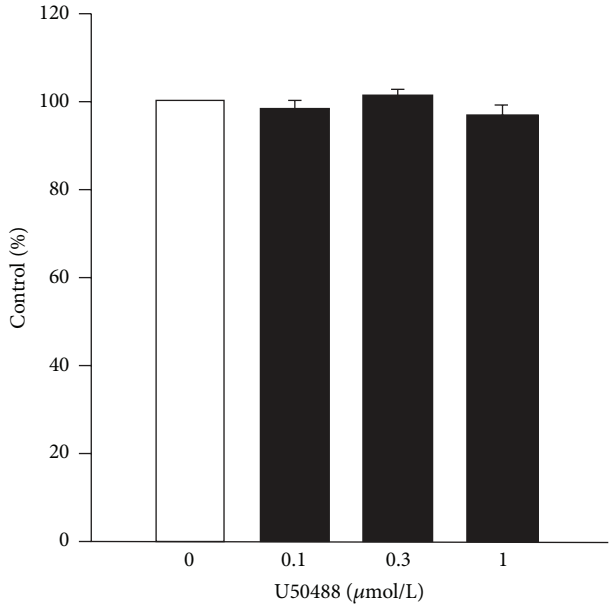

Figure 6: Effect of U50488 on spontaneously beating rate of right atria in guinea pig. Values are presented as percentages of control ($n = 6$).

Previously, U50488 had been shown to exert negative inotropic effects in both atrial and ventricular preparations by the activation of κ receptors in rats [7]. The different results in this study may be due to the difference in experimental conditions or animal model. In addition, Niroomand et al. [26] have shown that functional κ-opioid receptors may not present in canine cardiac sarcolemma because the κ-receptor agonist, U50488, did not inhibit adenylate cyclase activities. These observations strongly suggest that the distribution of κ-opioid receptors in cardiac myocardium may be species-specific. Therefore, functional study of the κ-opioid receptor on human cardiac preparation is necessary.

In general, agents and interventions that increase K^+ conductance (G_k) shorten action potential duration (APD) and tend to have negative inotropic effects, whereas agents that decrease K^+ current lengthen APD and may have positive inotropic effects [27]. Therefore, the shortening of the action potential duration is a possible mechanism responsible for the negative inotropic effect of U50488. In our unpublished data, we found that U50488 could shorten the duration of action potential and decrease the contractile force in guinea pig left atrial preparations. This effect could also be eliminated by the selective κ-opioid receptor antagonist, norBNI (1 μmol/L). Because the delayed rectifier and inward rectifier potassium channels play a key role during repolarization of action potential in guinea pig [28–30], the shortening of action potential may be related to these channels being affected by U50488. However, further voltage clamp studies will be needed to characterize the effect of U50488 on the delayed rectifier or inward rectifier potassium current.

To our knowledge this report demonstrates for the first time that the opioid receptor agonist elicits a negative inotropic response in left atria without having a corresponding effect in right atria and ventricles. Whether the different effects of U50488 exist in human tissues remains to be studied. Several studies have shown that postischemic contractile dysfunction or "stunning of myocardium" occurred especially during ischemia-reperfusion [31–33]. During a period of stunning, left ventricular ejection fraction may be significantly impaired. Myocardial stunning may delay recovery from cardiogenic shock or left ventricular failure. Therefore, it is important to avoid stunning of ventricular tissue during ischemia-reperfusion. While there is an increase in κ-opioid peptide release in myocardial ischemia-reperfusion [34], the absence of significant negative inotropic properties of κ-opioid receptor agonist in the right ventricle may be beneficial to cardiac performance during ischemia-reperfusion. In addition, decrease in contractile force in the left atrium may slightly alleviate the loading of the left ventricle and be beneficial to the failing left ventricular myocardium.

Conflict of Interests

The authors declare that there is no conflict of interests regarding the publication of this paper.

Acknowledgments

This work was supported by a research grant from the National Science Council and Fu Jen Catholic University of Taiwan.

References

[1] P. Sobanski, M. Krajnik, M. Shaqura, E. Bloch-Boguslawska, M. Schäfer, and S. A. Mousa, "The presence of mu-, delta-, and kappa-opioid receptors in human heart tissue," *Heart and Vessels*, vol. 29, no. 6, pp. 855–863, 2014.

[2] K. Tanaka, J. R. Kersten, and M. L. Riess, "Opioid-induced cardioprotection," *Current Pharmaceutical Design*, vol. 20, no. 36, pp. 5696–5705, 2014.

[3] M. M. Theisen, S. Schlottmann, C. August et al., "Detection and distribution of opioid peptide receptors in porcine myocardial tissue," *Pharmacological Research*, vol. 84, pp. 45–49, 2014.

[4] T. V. Lasukova, L. N. Maslov, S. W. Nizkodubova, A. S. Gorbunov, and S. Y. Zibulnikov, "Role of intracellular calcium and cyclic nucleotides in realization of cardioprotective effects of δ_1- and κ_1-Opioid receptor agonists," *Bulletin of Experimental Biology and Medicine*, vol. 148, no. 6, pp. 877–880, 2009.

[5] L.-W. Fu and J. C. Longhurst, "Functional role of peripheral opioid receptors in the regulation of cardiac spinal afferent nerve activity during myocardial ischemia," *American Journal of Physiology: Heart and Circulatory Physiology*, vol. 305, no. 1, pp. H76–H85, 2013.

[6] C.-F. Hung, W.-L. Chang, H.-C. Liang, and M.-J. Su, "Identification of opioid receptors in the sympathetic and parasympathetic nerves of guinea-pig atria," *Fundamental & Clinical Pharmacology*, vol. 14, no. 4, pp. 387–394, 2000.

[7] C. Bolte, G. Newman, and J. E. J. Schultz, "Kappa and delta opioid receptor signaling is augmented in the failing heart," *Journal of Molecular and Cellular Cardiology*, vol. 47, no. 4, pp. 493–503, 2009.

[8] T. V. Lasukova, L. N. Maslov, A. A. Platonov, N. V. Guzarova, and I. B. Lishmanov, "Role of kappa1 opioid receptors and cAMP in regulation of cardiac tolerance to ischemia and reperfusion," *Izvestiia Akademii Nauk*, no. 5, pp. 580–588, 2008.

[9] Q.-Y. Zhang, W. Wang, Q.-X. Shi et al., "Antiarrhythmic effect mediated by κ-opioid receptor is associated with Cx43 stabilization," *Critical Care Medicine*, vol. 38, no. 12, pp. 2365–2376, 2010.

[10] L. O. Karlsson, N. Bergh, L. Li et al., "Dose-dependent cardioprotection of enkephalin analogue Eribis peptide 94 and cardiac expression of opioid receptors in a porcine model of ischaemia and reperfusion," *European Journal of Pharmacology*, vol. 674, no. 2-3, pp. 378–383, 2012.

[11] A. Y. Lishmanov, L. N. Maslov, T. V. Lasukova, D. Crawford, and T. M. Wong, "Activation of k_1-opioid receptor as a method for prevention of ischemic and reperfusion arrhythmias: role of protein kinase C and K_{ATP} channels," *Bulletin of Experimental Biology and Medicine*, vol. 143, no. 2, pp. 187–190, 2007.

[12] L. Cheng, S. Ma, L.-X. Wei et al., "Cardioprotective and antiarrhythmic effect of U50,488H in ischemia/reperfusion rat heart," *Heart and Vessels*, vol. 22, no. 5, pp. 335–344, 2007.

[13] J.-Z. Sheng and T.-M. Wong, "Chronic U50,488H abolishes inositol 1,4,5-trisphosphate and intracellular Ca^{2+} elevations evoked by κ-opioid receptor in rat myocytes," *European Journal of Pharmacology*, vol. 307, no. 3, pp. 323–329, 1996.

[14] C.-M. Cao, Q. Xia, Y.-Y. Chen, X. Zhang, and Y.-L. Shen, "Opioid receptor-mediated effects of interleukin-2 on the $[Ca^{2+}]_i$ transient and contraction in isolated ventricular myocytes of the rat," *Pflugers Archiv European Journal of Physiology*, vol. 443, no. 4, pp. 635–642, 2002.

[15] T. Kanemasa, K. Asakura, and M. Ninomiya, "κ-Opioid agonist U50488 inhibits P-type Ca^{2+} channels by two mechanisms," *Brain Research*, vol. 702, no. 1-2, pp. 207–212, 1995.

[16] B. Hassan and V. Ruiz-Velasco, "The κ-opioid receptor agonist U-50488 blocks Ca2+ channels in a voltage- and G protein-independent manner in sensory neurons," *Regional Anesthesia & Pain Medicine*, vol. 38, no. 1, pp. 21–27, 2013.

[17] D. Chao and Y. Xia, "Ionic storm in hypoxic/ischemic stress: can opioid receptors subside it?" *Progress in Neurobiology*, vol. 90, no. 4, pp. 439–470, 2010.

[18] M. Chen, J.-J. Zhou, K. W.-L. Kam et al., "Roles of K_{ATP} channels in delayed cardioprotection and intracellular Ca^{2+} in the rat heart as revealed by kappa-opioid receptor stimulation with U50488H," *British Journal of Pharmacology*, vol. 140, no. 4, pp. 750–758, 2003.

[19] W. A. Macdonald, O. B. Nielsen, and T. Clausen, "Effects of calcitonin gene-related peptide on rat soleus muscle excitability: mechanisms and physiological significance," *American Journal of Physiology: Regulatory Integrative and Comparative Physiology*, vol. 295, no. 4, pp. R1214–R1223, 2008.

[20] K. B. Olsen, T. H. Braunstein, C. M. Sørensen, L. N. Axelsen, N. H. Holstein-Rathlou, and M. S. Nielsen, "Angiotensin II does not acutely regulate conduction velocity in rat atrial tissue," *Scandinavian Journal of Clinical and Laboratory Investigation*, vol. 71, no. 6, pp. 492–499, 2011.

[21] A. Pousti, T. Deemyad, G. Malihi, and K. Brumand, "A preliminary study on the interaction of fluvoxamine and adenosine receptor on isolated guinea-pig atria," *International Journal of Neuroscience*, vol. 116, no. 12, pp. 1491–1499, 2006.

[22] F. Speroni, A. Rebolledo, S. Salemme, M. C. Añón, F. Tanzi, and V. Milesi, "Genistein inhibits contractile force, intracellular Ca^{2+} increase and Ca^{2+} oscillations induced by serotonin in rat aortic smooth muscle," *Journal of Physiology and Biochemistry*, vol. 63, no. 2, pp. 143–152, 2007.

[23] A. Kovács, L. G. Hársing Jr., and G. Szénási, "Vasoconstrictor 5-HT receptors in the smooth muscle of the rat middle cerebral artery," *European Journal of Pharmacology*, vol. 689, no. 1–3, pp. 160–164, 2012.

[24] J. Utz, R. Eckert, and W. Trautwein, "Inhibition of L-type calcium currents in guinea pig ventricular myocytes by the κ-opioid agonist U50488h does not involve binding to opiate receptors," *Journal of Pharmacology and Experimental Therapeutics*, vol. 274, no. 2, pp. 627–633, 1995.

[25] T. R. L. Romero, L. S. Guzzo, and I. D. G. Duarte, "Mu, Delta, and Kappa opioid receptor agonists induce peripheral antinociception by activation of endogenous noradrenergic system," *Journal of Neuroscience Research*, vol. 90, no. 8, pp. 1654–1661, 2012.

[26] F. Niroomand, R. A. Mura, L. Piacentini, and W. Kübler, "Opioid receptor agonists activate pertussis toxin-sensitive G proteins and inhibit adenylyl cyclase in canine cardiac sarcolemma," *Naunyn-Schmiedeberg's Archives of Pharmacology*, vol. 354, no. 5, pp. 643–649, 1996.

[27] J. E. de Menezes-Filho, A. N. Santana Gondim, J. Santos Cruz et al., "Geraniol blocks calcium and potassium channels in the mammalian myocardium: useful effects to treat arrhythmias," *Basic & Clinical Pharmacology & Toxicology*, 2014.

[28] M. Zhao, J. Zhao, G. He, X. Sun, X. Huang, and L. Hao, "Effects of astragaloside IV on action potentials and ionic currents in guinea-pig ventricular myocytes," *Biological and Pharmaceutical Bulletin*, vol. 36, no. 4, pp. 515–521, 2013.

[29] K. Ishihara, N. Sarai, K. Asakura, A. Noma, and S. Matsuoka, "Role of Mg_{2+} block of the inward rectifier K^+ current in cardiac repolarization reserve: a quantitative simulation," *Journal of Molecular and Cellular Cardiology*, vol. 47, no. 1, pp. 76–84, 2009.

[30] M. Yamada, K. Ohta, A. Niwa, N. Tsujino, T. Nakada, and M. Hirose, "Contribution of L-type Ca^{2+} channels to early afterdepolarizations induced by IKr and IKs channel suppression in guinea pig ventricular myocytes," *Journal of Membrane Biology*, vol. 222, no. 3, pp. 151–166, 2008.

[31] Y.-H. Choi, D. B. Cowan, T. C. W. Wahlers, R. Hetzer, P. J. del Nido, and C. Stamm, "Calcium sensitisation impairs diastolic relaxation in post-ischaemic myocardium: implications for the use of Ca^{2+} sensitising inotropes after cardiac surgery," *European Journal of Cardio-Thoracic Surgery*, vol. 37, no. 2, pp. 376–383, 2010.

[32] W. R. Ford, A. S. Clanachan, C. Robin Hiley, and B. I. Jugdutt, "Angiotensin II reduces infarct size and has no effect on post-ischaemic contractile dysfunction in isolated rat hearts," *British Journal of Pharmacology*, vol. 134, no. 1, pp. 38–45, 2001.

[33] T. Bragadeesh, A. R. Jayaweera, M. Pascotto et al., "Post-ischaemic myocardial dysfunction (stunning) results from myofibrillar oedema," *Heart*, vol. 94, no. 2, pp. 166–171, 2008.

[34] Y. Wu, J. Wan, W.-Z. Zhen et al., "The effect of butorphanol post-conditioning on myocardial ischaemia reperfusion injury in rats," *Interactive Cardiovascular and Thoracic Surgery*, vol. 18, no. 3, pp. 308–312, 2014.

Hindawi Publishing Corporation
BioMed Research International
Volume 2015, Article ID 564738, 8 pages
http://dx.doi.org/10.1155/2015/564738

Clinical Study

Effect of Supplemental Lutein and Zeaxanthin on Serum, Macular Pigmentation, and Visual Performance in Patients with Early Age-Related Macular Degeneration

Yang-Mu Huang,[1] Hong-Liang Dou,[2] Fei-Fei Huang,[1] Xian-Rong Xu,[1] Zhi-Yong Zou,[1] and Xiao-Ming Lin[1]

[1] *Peking University Health Science Center, 38 Xueyuan Road, Beijing 100191, China*
[2] *Peking University Eye Center, Peking University Third Hospital, 49 Huayuan North Road, Beijing 100191, China*

Correspondence should be addressed to Hong-Liang Dou; douhongliang3736@sina.cn and Xiao-Ming Lin; linbjmu@bjmu.edu.cn

Received 9 July 2014; Revised 21 September 2014; Accepted 21 September 2014

Academic Editor: Huanran Tan

Purpose. To compare the 2-year effect of multiple doses of lutein/zeaxanthin on serum, macular pigmentation, and visual performance on patients with early age-related macular degeneration (AMD). *Methods*. In this randomized, double-blinded, and placebo-controlled trial, 112 early AMD patients randomly received either 10 mg lutein, 20 mg lutein, a combination of lutein (10 mg) and zeaxanthin (10 mg), or placebo daily for 2 years. Serum concentration of lutein/zeaxanthin, macular pigment optical density (MPOD), visual functions including best-spectacle corrected visual acuity (BCVA), contrast sensitivity (CS), flash recovery time (FRT), and vision-related quality of life (VFQ25) was quantified. *Results*. Serum lutein concentration and MPOD significantly increased in all the active treatment groups. Supplementation with 20 mg lutein was the most effective in increasing MPOD and CS at 3 cycles/degree for the first 48 weeks. However, they both significantly increased to the same peak value following supplementation with either 10 mg or 20 mg lutein during the intervention. No statistical changes of BCVA or FRT were observed during the trial. *Conclusions*. Long-term lutein supplementation could increase serum lutein concentration, MPOD, and visual sensitivities of early AMD patients. 10 mg lutein daily might be an advisable long-term dosage for early AMD treatment.

1. Introduction

Age-related macular degeneration (AMD) is the leading cause of irreversible vision loss among people aged over 50, especially in developed countries [1]. With the average population age increasing, the number of AMD patients is estimated to triple to 60–75 million worldwide in the next 30–40 years [2]. Since late AMD not only jeopardizes a patient's visual function and quality of life, but also brings a tremendous socioeconomic burden, most treatment strategies are focused on addressing late AMD [3, 4]. However, the treatment of AMD at an earlier stage might slow the progression before irreversible visual impairment occurs, which would be more effective in enhancing or maintaining visual performances [1, 5]. Unfortunately, no clinically proven therapies for early AMD exist at present, and few studies focus on early AMD [6, 7].

Substantial evidence suggested that lutein and its isomer zeaxanthin, also known as macular pigment (MP), might prevent the progression of AMD resulting from photooxidative damage [2, 8]. A meta-analysis showed that the dietary intake of lutein and zeaxanthin could lead to a 4% reduction in the risk of developing early AMD, as opposed to a 26% reduction for late AMD, indicating that lutein/zeaxanthin might be more effective in reducing the risk of progression from early AMD to late AMD [9].

Some intervention studies have shown putative functional benefits of lutein/zeaxanthin supplementation by increasing MPOD and visual functions; however, the evidence is limited and inconclusive [10–14]. Given the common recommendation to use long-term supplementation of lutein/zeaxanthin to treat AMD patients and the controversy around which dosage (20–40 mg/d versus 6–12 mg/d)

is more effective [10, 15], it is surprising that only a few studies have specifically compared the long-term effects of different lutein/zeaxanthin dosages on early AMD without any interference from other nutrients. Moreover, although the amounts of zeaxanthin and lutein in the central 3 mm of macula are approximately the same, few researchers have studied the effect of using a supplementation where lutein and zeaxanthin are combined in equal doses [10, 11, 16]. Besides, few studies have observed the effects of lutein/zeaxanthin supplementation from multidimensions, including serum and macular concentrations, visual functions, and subjective evaluations.

Therefore, we conducted this 2-year randomized, placebo-controlled, double-blinded dose-ranging trial to determine the effects of lutein/zeaxanthin on serum concentration, MPOD, and visual performances in early AMD patients and to use the results to discuss the daily lutein/zeaxanthin dosage currently used for long-term treatment.

2. Methods

2.1. Subjects. Subjects with AMD aged over 50 years were recruited in Beijing, China. Inclusion criteria included a clinical diagnosis of early AMD (defined as the presence of soft drusen, presence of retinal pigmentary abnormalities with no signs of late AMD, or both) according to the Age-Related Eye Disease Study System [17], clear ocular media, and agreement to adhere to the study regimen. Those who had other ocular disorders or unstable systemic or chronic illness or consumed dietary supplements containing antioxidants or carotenoids within the previous 6 months were excluded. This study was performed in accordance with the principles of the Declaration of Helsinki and was approved by the Medical Ethics Committee of Peking University. Written consent was obtained from all subjects.

2.2. Study Design. All subjects were screened for eligibility based on the protocol criteria. Diagnosis of early AMD was confirmed by 2 ophthalmologists using funduscope and fundus photographs. After enrollment, subject information on characteristics and demographics was collected using questionnaires and examinations. Serum total cholesterol (TC), triglyceride (TG), high density lipoprotein-cholesterol (HDL-C), low density lipoprotein-cholesterol (LDL-C), and glucose were measured within 2 days of collection by Beijing Laweekse Health Laboratory using an autoanalyzer.

In this 2-year randomized, double-blinded, placebo-controlled trial, all subjects were randomly assigned to take either 10 mg lutein, 20 mg lutein, lutein (10 mg) + zeaxanthin (10 mg), or a placebo daily. All the supplements were packaged identically with the same labels. Serum lutein/zeaxanthin concentrations, MPOD, and visual performance indices including best-spectacle corrected visual acuity (BCVA), contrast sensitivity (CS), and flash recovery time (FRT) were quantified at baseline, 24 weeks, 48 weeks, and 2 years. All clinical examinations were performed by the qualified ophthalmic technicians in Peking University Eye Center, Peking University Third Hospital. Vision-related quality of life (VFQ-25) was measured at baseline, 48 weeks, and 2 years. Diet stability was assessed using a validated 120-item food frequency questionnaire conducted at baseline, 48 weeks, and 2 years. All subjects, examiners, and study staff were masked to treatment assignment.

Subjects were required to maintain their normal dietary and living habits and were asked to visit our office monthly to collect capsules of the following month and to return the remaining capsules from the month together with the daily checklist. They were encouraged to report any adverse effects immediately and were asked specifically about adverse events such as carotenoderma during visits.

2.3. Serum Lutein/Zeaxanthin. Serum concentrations of lutein and zeaxanthin were extracted and analyzed using a modified high-performance liquid chromatograph (HPLC) method, which is discussed in detail elsewhere [18]. The analysis was performed on a Hewlett-Packard/Agilent Technology Model 1100 HPLC System with a C30 column (5 μm, 4.6 × 250 mm, Develosil, Japan) under the temperature of 25°C, detected at 450 nm. All procedures including the blood sample collections were performed under dim light.

2.4. MPOD. MPOD was determined using a confocal scanning laser ophthalmoscope (Heidelberg Retina Angiograph II, Heidelberg Engineering Inc., Heidelberg, Germany) and has been detailed elsewhere [19]. Argon laser light (488 nm) was used to excite autofluorescence (AF) after using infrared light, and a series of AF images were obtained for the excitation wavelengths quickly before recovery. All images were centered on the fovea and aligned to one average image according to their anatomic details. MPOD was quantified from this average image by comparing foveal and parafoveal AF. This measurement technique has been used in multiple clinical studies, and its accuracy and reliability were reported with a coefficient of variation of less than 5% [19–21].

2.5. Visual Performance. After diopter correction, BCVA was measured according to the Early Treatment Diabetic Retinopathy Study (ETDRS) protocol, and the results were converted to the logarithm of the minimum angle of resolution (logMAR) [22]. CS was measured with CSV-1000 test system (Vector-Vision, Dayton, OH) at 4 spatial frequencies (3, 6, 12, and 18 cycles/degree) with a grade scale from 1 (high contrast) to 8 (low contrast). The contrast level of the last correct response was defined as the CS of each frequency and is reported as log CS.

FRT was recorded using a macular adaptometer (MDD-2; Avenue Optical Flash LLC, Lighthouse Point, FL), which included a xenon arc, and flash filtered for infrared, ultraviolet, visible short wavelengths and was delivered through an aperture in a hand-held tube. Technicians pressed a push button to activate the flash and the timer and pressed it again to stop the timer when the first stimuli of vision recovery were reported by the subject. The time was recorded as FRT [23].

VFQ-25 was our primary patient-reported outcome to evaluate qualitative changes in visual function and health-related quality of life. Scores were calculated with a 0 to 100 scale where higher scores indicate better functioning

[24]. The Chinese version of VFQ-25 used in this study has proven reliability and validity as a measure of vision-related functioning outcomes [25].

2.6. Sample Size and Statistical Analyses. Sample size estimations indicated that 26 patients per group were needed to be able to distinguish a 30% difference for MPOD change in treatment groups (5% significance level, power 80%), and a total of 112 patients were enrolled assuming a dropout rate of 10%. As for randomization, the sequence was computer generated in a 1 : 1 : 1 : 1 ratio within permuted blocks of size 8.

Baseline comparisons among groups were assessed using ANOVA or the chi-square analysis. Skewed data was logarithmically transformed for analysis. Differences between baseline and follow-up measurements within a group were assessed using paired t-tests, while between-group differences at each time point were tested using analysis of covariance. Changes between groups over time were assessed using repeated-measures ANOVA including a time × treatment interaction. The linear correlation between 2 variables was assessed using the Pearson test. Statistical analyses were conducted using SPSS 11.0 for Windows software (SPSS, Inc., Chicago, Illinois, USA). A 2-tailed P value of less than 0.05 was considered significant.

3. Results

3.1. Baseline Findings. Of the 334 screened participants, 112 subjects met all the criteria and were subsequently enrolled and randomized. Four subjects (3.6%) were excluded from the analysis due to their failure to attend scheduled examinations. Subject characteristics were well balanced across groups at baseline (Table 1). Of all subjects, 7 subjects (6.5%) were smokers and 7 (6.5%) were former smokers, with no differences among groups. Dietary intakes of lutein, zeaxanthin, beta-carotene, and other antioxidants were not significantly different among the groups or during the intervention (for all, $P > 0.05$). No adverse events related to the study were observed or reported. During the intervention, approximately 97% (105/108) of the subjects took at least 93% (missing 2 days) of their supplements every month.

3.2. Serum Lutein/Zeaxanthin Concentration and MPOD. Serum and macular concentrations of lutein/zeaxanthin in all the active treatment groups progressively increased (all $P < 0.05$), and the increases were all negatively correlated with their baseline values (all $P < 0.001$), whereas no such increases were seen in the placebo arm. Those who received 20 mg lutein showed a greater increase (6.75-fold) in serum lutein, compared to those who received 10 mg (4.30-fold) or lutein + zeaxanthin (5.57-fold) (Figure 1(a)). Serum zeaxanthin concentration significantly increased only in lutein + zeaxanthin group (3.87-fold, $P < 0.001$). The time × treatment interaction was significant for both serum lutein and zeaxanthin concentrations (both $P < 0.001$).

Likewise, the effect of 20 mg lutein on increasing MPOD was more effective at the first 24 weeks (increased by 25.4%, $P < 0.01$) and at 48 weeks (increased by 34.6%, $P < 0.01$). However, by year 2, the 10 mg lutein group reached the same MPOD level (0.442 D.U.) as the 20 mg lutein group (0.441 D.U.) (Figure 1(b)). Repeated-measures analyses showed a significant time × treatment interaction of MPOD ($P = 0.046$). MPOD significantly increased during the supplementation ($P < 0.001$), whereas no statistical treatment effect was shown ($P = 0.072$).

3.3. Visual Performance. Changes of CS among groups are shown in Table 2. By year 2, increments of CS at 3 and 6 cycles/degree from baseline were observed in all the active treatment groups, whereas a significant increase of CS at 18 cycles/degree was only seen in the lutein + zeaxanthin group. During the first 48 weeks, the increases of CS at 3 and 6 cycles/degree were higher and more significant ($P < 0.01$) after receiving 20 mg lutein. However, at 2 years, CS at 3 cycles/degree in the 10 mg lutein group significantly increased (+16.1%, $P < 0.05$) to a similar peak value to the 20 mg lutein group. Table 3 showed that the effect of lutein/zeaxanthin supplementation on BCVA was not significant; however, significant differences of FRT compared to the placebo group were seen after receiving 10 mg lutein and 20 mg lutein at 2 years ($P < 0.05$). Repeated-measures analyses of the above variables did not reveal any differential treatment effects, except a significant time effect observed for CS at 3 cycles/degree ($P < 0.05$).

The VFQ25 scores did not show any significant change over the first 48 weeks; however, they slightly increased at 2 years, especially in the lutein + zeaxanthin group (increased by 7.9%, $P < 0.01$). Using a repeated-measures analysis of variance, the score increased significantly during the supplementation ($P < 0.001$), whereas no significant treatment effect was observed. The changes in VFQ25 scores from baseline to 2 years were correlated negatively with baseline scores in all active treatment groups (correlation coefficients from $r = -0.40$ to $r = -0.60$, all $P < 0.05$). Correlation analysis showed that baseline VFQ25 score was positively correlated with baseline BCVA ($r = 0.24$, $P < 0.05$) and CS at 4 spatial frequencies (correlation coefficients from $r = 0.21$ to $r = 0.30$, $P < 0.05$ for all).

4. Discussion

This trial demonstrated that 2 years of lutein/zeaxanthin supplementation increased serum lutein/zeaxanthin concentrations, MPOD, and visual performances in patients with early AMD, without leading to any detectable adverse effect. More interestingly, we found that though body lutein/zeaxanthin concentrations and visual performances increased the most after receiving 20 mg lutein within the first 48 weeks, the increases of MPOD and visual functions (BCVA and CS) were similar between the 10 mg lutein and the 20 mg lutein groups at 2 years. Additionally, our results indicate that a combined equal dose of lutein and zeaxanthin might be more effective in improving CS at 18 cycles/degree and patient-reported visual performance (VFQ25 scores).

Consistent with previous studies, lutein/zeaxanthin supplementation increased their serum concentrations dose-dependently [26]. Higher lutein or zeaxanthin dosage led

Table 1: Baseline characteristics of subjects with early age-related macular degeneration[a,b].

	Placebo (n = 28)	10 mg lutein (n = 26)	20 mg lutein (n = 27)	10 mg lutein + 10 mg zeaxanthin (n = 27)
Age (y)	69.0 ± 7.5	69.7 ± 8.3	69.3 ± 6.9	68.5 ± 6.9
Sex, male [n (%)]	11 (39.3)	9 (34.6)	14 (51.9)	12 (44.4)
Education (y)	12.2 ± 2.8	10.8 ± 2.7	12.2 ± 2.9	10.5 ± 4.1
BMI (kg/m^2)	24.8 ± 3.0	24.1 ± 3.4	25.1 ± 3.3	24.6 ± 3.6
Serum lipids (mmol/L)				
Total cholesterol	5.022 ± 1.756	4.984 ± 1.068	5.091 ± 0.883	5.247 ± 0.952
Triglyceride	1.571 ± 1.575	1.538 ± 0.684	1.491 ± 0.821	1.777 ± 0.791
HDL cholesterol	1.388 ± 0.438	1.386 ± 0.319	1.408 ± 0.258	1.481 ± 0.291
LDL cholesterol	3.091 ± 0.606	3.190 ± 0.746	3.203 ± 0.605	3.338 ± 0.605
Early cataracts [n (%)][c]	6 (21.4)	6 (23.0)	5 (18.5)	8 (29.6)
MPOD (D.U.)	0.315 ± 0.144	0.307 ± 0.142	0.315 ± 0.122	0.320 ± 0.118
Serum concentration (μmol/L)				
Lutein	0.337 ± 0.397	0.319 ± 0.250	0.308 ± 0.231	0.251 ± 0.260
Zeaxanthin	0.066 ± 0.075	0.048 ± 0.050	0.050 ± 0.042	0.046 ± 0.055

[a]D.U.: density unit; MPOD: macular pigment optical density. There were no significant differences among groups in any of the baseline study characteristics noted.
[b]For continuous variables, all values are mean ± SDs. For categorical variables, all values are n values, percentages of the total in parentheses. Comparisons among groups were derived from analysis of variance for continuous variables or the chi-square test for categorical variables.
[c]Cataracts diagnosed and graded according to the Lens Opacities Classification System III.

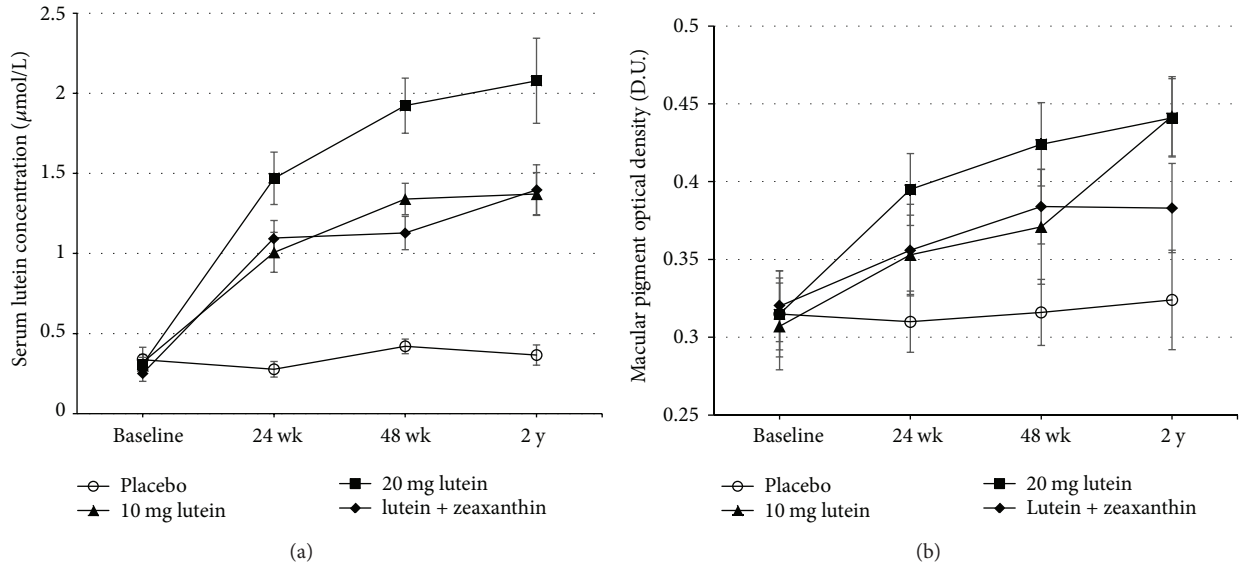

Figure 1: Changes in serum lutein concentration (a) and macular pigment optical density (b) at baseline, 24 weeks, 48 weeks, and 2 years in patients with early age-related macular degeneration, treated with 10 mg/d lutein, 20 mg/d lutein, lutein (10 mg/d) + zeaxanthin (10 mg/d), or placebo. Values are expressed as group mean ± SEMs. Significant increase was observed in all non-placebo groups compared to that of baseline or placebo group (all $P < 0.05$, paired t-test). Significant time and treatment effects were observed in serum lutein concentration, $P < 0.001$ (repeated-measures ANOVA), whereas only significant time effect was seen in MPOD, $P < 0.001$ (repeated-measures ANOVA).

to higher serum concentration, which is consistent with the straightforward kinetics of their transport in human blood [18]. However, although MPOD in the 20 mg lutein group was higher than that in other groups at 48 weeks, MPOD in the 10 mg lutein group steadily increased to a similar level to the 20 mg lutein group at 2 years. This indicated that the incorporation of lutein/zeaxanthin into the retinal tissue is not driven simply by diffusion [26] but is influenced by unique transport proteins in serum and binding proteins in human retina [27, 28]. The saturability of macular xanthophylls-binding protein may be responsible for the same MPOD level in the 10 mg and 20 mg lutein groups at 2 years [29]. This macular saturation of xanthophyll was also seen in the macula of rhesus monkeys [30]. Weigert's study also indirectly supports

Table 2: Changes of contrast sensitivity among different groups during the intervention[a].

	Placebo ($n = 28$)	10 mg lutein ($n = 26$)	20 mg lutein ($n = 27$)	10 mg lutein + 10 mg zeaxanthin ($n = 27$)
Contrast sensitivity, log				
3 cycles/degree				
Baseline	1.22 ± 0.37	1.26 ± 0.36	1.24 ± 0.39	1.25 ± 0.32
24 weeks	1.22 ± 0.34	1.32 ± 0.39	1.34 ± 0.29	1.34 ± 0.34
48 weeks	1.13 ± 0.36	1.45 ± 0.37†	1.47 ± 0.39**†	1.40 ± 0.31*
2 years	1.25 ± 0.32	1.47 ± 0.34*	1.32 ± 0.25†	1.39 ± 0.39*
6 cycles/degree				
Baseline	1.40 ± 0.39	1.41 ± 0.34	1.40 ± 0.39	1.45 ± 0.38
24 weeks	1.34 ± 0.34	1.47 ± 0.35	1.52 ± 0.37	1.51 ± 0.383
48 weeks	1.30 ± 0.31	1.57 ± 0.37	1.62 ± 0.36***	1.52 ± 0.38
2 years	1.25 ± 0.30	1.50 ± 0.33	1.54 ± 0.36†	1.50 ± 0.36
12 cycles/degree				
Baseline	0.97 ± 0.37	1.02 ± 0.33	1.00 ± 0.34	1.06 ± 0.36
24 weeks	1.02 ± 0.36	1.06 ± 0.42	1.06 ± 0.38	1.09 ± 0.35
48 weeks	0.91 ± 0.32	1.07 ± 0.35	1.12 ± 0.38	1.16 ± 0.40
2 years	0.87 ± 0.33	1.10 ± 0.35	1.05 ± 0.36	1.09 ± 0.35
18 cycles/degree				
Baseline	0.50 ± 0.35	0.57 ± 0.39	0.49 ± 0.35	0.53 ± 0.37
24 weeks	0.52 ± 0.36	0.60 ± 0.42	0.57 ± 0.38	0.63 ± 0.35
48 weeks	0.39 ± 0.28	0.62 ± 0.34	0.63 ± 0.38	0.68 ± 0.42
2 years	0.40 ± 0.34	0.59 ± 0.45	0.65 ± 0.39	0.74 ± 0.33*†

All values are mean ± SDs. Mean values were significantly different from baseline within the same group: $^{*}P < 0.05$, $^{**}P < 0.01$, and $^{***}P < 0.001$. Mean values were significantly different from those of the placebo control group: $^{\dagger}P < 0.05$.
[a]Repeated-measures analyses of the above variables did not reveal any differential treatment effects, and the only significant time effect was observed at 3 cycles/degree ($P < 0.05$).

Table 3: Changes of visual performance among different groups during the intervention[a].

	Placebo ($n = 28$)	10 mg lutein ($n = 26$)	20 mg lutein ($n = 27$)	10 mg lutein + 10 mg zeaxanthin ($n = 27$)
Best-corrected visual acuity, log MAR				
Baseline	0.34 ± 0.19	0.31 ± 0.21	0.31 ± 0.21	0.32 ± 0.25
24 weeks	0.33 ± 0.25	0.32 ± 0.21	0.27 ± 0.17	0.28 ± 0.30
48 weeks	0.34 ± 0.22	0.28 ± 0.22	0.26 ± 0.20	0.27 ± 0.35
2 years	0.30 ± 0.25	0.26 ± 0.15	0.28 ± 0.16	0.27 ± 0.24
Photorecovery time, sec				
Baseline	18.57 ± 16.78	16.68 ± 14.22	15.86 ± 11.17	17.38 ± 12.00
24 weeks	19.02 ± 10.59	18.90 ± 17.71	14.13 ± 8.11	16.41 ± 14.69
48 weeks	19.70 ± 12.16	15.50 ± 11.27	14.61 ± 13.43	17.80 ± 16.48
2 years	24.41 ± 14.40	15.00 ± 8.40†	15.36 ± 12.75†	15.67 ± 11.04
VFQ25 score				
Baseline	76.04 ± 18.09	75.46 ± 14.60	75.58 ± 15.35	74.26 ± 14.46
48 weeks	74.97 ± 17.10	75.02 ± 13.01	72.56 ± 14.46	76.32 ± 11.20
2 years	77.31 ± 17.05	79.61 ± 13.52	76.65 ± 16.32	80.13 ± 11.73**

log MAR: logarithm of minimum angle of resolution; VFQ25: Visual Function Questionnaire 25.
All values are mean ± SDs.
Mean values were significantly different from baseline within the same group: $^{**}P < 0.01$.
Mean values were significantly different from those of the placebo control group: $^{\dagger}P < 0.05$.
[a]Repeated-measures analyses of the above variables did not reveal any differential treatment or time effects.

our notion, showing that MPOD higher than 0.5 D.U. was unlikely to increase during lutein supplementation [31]. Our study indicated that though higher lutein supplementation could rapidly increase its serum and macular concentration, a lower lutein dosage (10 mg/d) could reach and maintain an efficient MP level in the long term [11, 32].

In this study, a tendency of increase in BCVA and FRT was observed in all the active treatment groups ($P > 0.01$) [14, 33]. The latest Age-Related Eye Disease Study 2 (AREDS2) also showed nonsignificant increase of BCVA after 5 years of intervention using AREDS formulation (antioxidant vitamins C and E, beta carotene, and zinc) adding lutein (10 mg) + zeaxanthin (2 mg) and suggested that the inadequate dose and/or duration of treatment might be attributable to the lack of efficacy [34]. The insensitivity of BCVA and FRT tests might also be one explanation for the nonsignificant change. Significant morphologic changes usually do not adversely impact visual functions at an early stage, therefore leaving little room for measurable improvement [1, 5].

However, CS is a more sensitive visual indicator compared to BCVA and FRT, which could provide additional information at the very beginning of visual dysfunction. Significant increases of CS were indeed detected at different spatial frequencies at 48 weeks and 2 years in all the active treatment groups, which is in line with other studies [13, 35]. This might be due to the preferential absorption of MP on blue light (short-wave light that produces a veiling luminance), which would attenuate the adverse impact of chromatic aberration and improve visual function [36, 37]. We found that the increase patterns of CS at 3 cycles/degree after receiving 10 mg lutein and 20 mg lutein were in accordance with those of MPOD. However, unlike the significant increase of MPOD from baseline to 24 weeks, no statistical changes of CS were observed before 48 weeks. Our results indicated that MPOD might be the foundation for the improvements in visual functions; CS could only improve after MPOD had reached and maintained a relatively high level. This hypothesis is also supported by the positive correlation between changes in MPOD and improvements in visual functions as mentioned in other studies [38, 39].

We noticed that the change of MPOD and visual functions from baseline was smaller in this study compared to similar studies [13, 14]. One possible reason is that the baselines in our study were higher since the morphologic and functional macular impairments in early AMD did not seriously affect visual functions, and this may have left limited space for improvement. This in turn supports the notion that early intervention might be more effective and essential in enhancing or maintaining visual function. Though AREDS2 concluded that addition of lutein + zeaxanthin supplementation could not further reduce risk of progression to advanced AMD, we believe their results may not illustrate the actual effect of xanthophyll on AMD, since the supplemental lutein/zeaxanthin they used was combined with other antioxidants [34].

It should be noted that no significant improvement of VFQ25 score was observed until the second year, and the only significant change was seen in the lutein + zeaxanthin group. Similarly, in Richer's study, the VFQ25 score increased by only 2% after 12 months of lutein and/or zeaxanthin supplementation [10]. This is possibly because improved visual functions are the foundation for better vision-related quality of life and thus VFQ25 score could only increase after visual functions reached a certain level. Our notion was also supported by the positive correlation between VFQ25 scores and visual functions (BCVA and CS) detected in our study. Likewise, Revicki's study showed that mean VFQ25 scores correlated significantly with BCVA in eyes of AMD patients ($P < 0.0001$) [24].

There are some noteworthy limitations in this study. First, the high selective criteria for subjects may affect generalization. Second, since the progression of AMD from early stage to late stage is much longer than our intervention period, our study could not use late AMD as the ultimate outcome and, therefore, is not powered adequately to find a reduction in late AMD incidence. Larger-scale and longer-term studies should be undertaken to focus on the effects of lutein and/or zeaxanthin on early AMD, and more sensitive measurements should be used.

In conclusion, our study has shown that lutein/zeaxanthin supplementation could increase their serum concentrations, MPOD, and reverse visual impairment in subjects with early AMD. Most interestingly, our findings suggest that supplementation with either 10 mg or 20 mg lutein could be equally effective after 2 years. Thus, it might be advisable for early AMD patients to take a lower dosage (10 mg/d) for long-term treatment.

Conflict of Interests

None of the authors declared any conflict of interests regarding the publication of this paper.

Authors' Contribution

Each author (1) contributed to the conception and design, acquisition of data, analysis, and interpretation of data and (2) revised the paper critically for important intellectual content and final approval of the version to be published.

Acknowledgment

The authors gratefully acknowledge the financial support from the National Natural Science Foundation of China (Grant no. 81273063).

References

[1] L. S. Lim, P. Mitchell, J. M. Seddon, F. G. Holz, and T. Y. Wong, "Age-related macular degeneration," *The Lancet*, vol. 379, no. 9827, pp. 1728–1738, 2012.

[2] A. Chopdar, U. Chakravarthy, and D. Verma, "Age related macular degeneration," *British Medical Journal*, vol. 326, no. 7387, pp. 485–488, 2003.

[3] V. E. S. Jeganathan and N. Verma, "Safety and efficacy of intravitreal anti-VEGF injections for age-related macular degeneration," *Current Opinion in Ophthalmology*, vol. 20, no. 3, pp. 223–225, 2009.

[4] R. L. Avery, "New treatments for age-related macular degeneration," *The Lancet*, vol. 370, no. 9597, pp. 1479–1480, 2007.

[5] J. H. Woo, S. Sanjay, and K. G. Au Eong, "Benefits of early awareness in age-related macular degeneration," *Eye*, vol. 23, no. 12, pp. 2271–2272, 2009.

[6] I. J. Murray, M. Makridaki, R. L. P. van der Veen, D. Carden, N. R. A. Parry, and T. T. J. M. Berendschot, "Lutein supplementation over a one-year period in early AMD might have a mild beneficial effect on visual acuity: the CLEAR study," *Investigative Ophthalmology & Visual Science*, vol. 54, no. 3, pp. 1781–1788, 2013.

[7] L. Ma, H.-L. Dou, Y.-M. Huang et al., "Improvement of retinal function in early age-related macular degeneration after Lutein and zeaxanthin supplementation: a randomized, double-masked, placebo-controlled trial," *American Journal of Ophthalmology*, vol. 154, no. 4, pp. 625–634, 2012.

[8] N. I. Krinsky, J. T. Landrum, and R. A. Bone, "Biologic mechanisms of the protective role of lutein and zeaxanthin in the eye," *Annual Review of Nutrition*, vol. 23, pp. 171–201, 2003.

[9] L. Ma, H.-L. Dou, Y.-Q. Wu et al., "Lutein and zeaxanthin intake and the risk of age-related macular degeneration: a systematic review and meta-analysis," *British Journal of Nutrition*, vol. 107, no. 3, pp. 350–359, 2012.

[10] S. P. Richer, W. Stiles, K. Graham-Hoffman et al., "Randomized, double-blind, placebo-controlled study of zeaxanthin and visual function in patients with atrophic age-related macular degeneration: the Zeaxanthin and Visual Function Study (ZVF) FDA IND #78, 973," *Optometry*, vol. 82, no. 11, pp. 667–680, 2011.

[11] M. Trieschmann, S. Beatty, J. M. Nolan et al., "Changes in macular pigment optical density and serum concentrations of its constituent carotenoids following supplemental lutein and zeaxanthin: the LUNA study," *Experimental Eye Research*, vol. 84, no. 4, pp. 718–728, 2007.

[12] J. M. Rosenthal, J. Kim, F. de Monastario et al., "Dose-ranging study of lutein supplementation in persons aged 60 years or older," *Investigative Ophthalmology and Visual Science*, vol. 47, no. 12, pp. 5227–5233, 2006.

[13] S. Richer, W. Stiles, L. Statkute et al., "Double-masked, placebo-controlled, randomized trial of lutein and antioxidant supplementation in the intervention of atrophic age-related macular degeneration: the Veterans LAST study (Lutein Antioxidant Supplementation Trial)," *Optometry*, vol. 75, no. 4, pp. 216–230, 2004.

[14] F. E. Cangemi, "TOZAL study: an open case control study of an oral antioxidant and omega-3 supplement for dry AMD," *BMC Ophthalmology*, vol. 7, article 3, 2007.

[15] S. Carpentier, M. Knaus, and M. Suh, "Associations between lutein, zeaxanthin, and age-related macular degeneration: an overview," *Critical Reviews in Food Science and Nutrition*, vol. 49, no. 4, pp. 313–326, 2009.

[16] E. Y. Chew, T. Clemons, J. P. Sangiovanni et al., "The age-related eye disease study 2 (AREDS2): study design and baseline characteristics (AREDS2 report number 1)," *Ophthalmology*, vol. 119, no. 11, pp. 2282–2289, 2012.

[17] M. D. Davis, R. E. Gangnon, L.-Y. Lee et al., "The age-related eye disease study severity scale for age-related macular degeneration: AREDS report no. 17," *Archives of Ophthalmology*, vol. 123, no. 11, pp. 1484–1498, 2005.

[18] Y.-M. Huang, S.-F. Yan, L. Ma et al., "Serum and macular responses to multiple xanthophyll supplements in patients with early age-related macular degeneration," *Nutrition*, vol. 29, no. 2, pp. 387–392, 2013.

[19] L. Ma, S.-F. Yan, Y.-M. Huang et al., "Effect of lutein and zeaxanthin on macular pigment and visual function in patients with early age-related macular degeneration," *Ophthalmology*, vol. 119, no. 11, pp. 2290–2297, 2012.

[20] N. Lois, A. S. Hatfyard, A. C. Bird, and F. W. Fitzke, "Quantitative evaluation of fundus autofluorescence imaged "in vivo" in eyes with retinal disease," *British Journal of Ophthalmology*, vol. 84, no. 7, pp. 741–745, 2000.

[21] M. Trieschmann, B. Heimes, H. W. Hense, and D. Pauleikhoff, "Macular pigment optical density measurement in autofluorescence imaging: comparison of one- and two-wavelength methods," *Graefe's Archive for Clinical and Experimental Ophthalmology*, vol. 244, no. 12, pp. 1565–1574, 2006.

[22] H.-K. Kuo, M.-T. Kuo, I.-S. Tiong, P.-C. Wu, Y.-J. Chen, and C.-H. Chen, "Visual acuity as measured with Landolt C chart and Early Treatment of Diabetic Retinopathy Study (ETDRS) chart," *Graefe's Archive for Clinical and Experimental Ophthalmology*, vol. 249, no. 4, pp. 601–605, 2011.

[23] D. A. Newsome and M. Negreiro, "Reproducible measurement of macular light flash recovery time using a novel device can indicate the presence and worsening of macular diseases," *Current Eye Research*, vol. 34, no. 2, pp. 162–170, 2009.

[24] D. A. Revicki, A. M. Rentz, N. Harnam, V. S. Thomas, and P. Lanzetta, "Reliability and validity of the National Eye Institute Visual Function Questionnaire-25 in patients with age-related macular degeneration," *Investigative Ophthalmology & Visual Science*, vol. 51, no. 2, pp. 712–717, 2010.

[25] C. W. S. Chan, D. Wong, C. L. K. Lam, S. McGhee, and W. W. Lai, "Development of a Chinese version of the National Eye Institute Visual Function Questionnaire (CHI-VFQ-25) as a tool to study patients with eye diseases in Hong Kong," *British Journal of Ophthalmology*, vol. 93, no. 11, pp. 1431–1436, 2009.

[26] R. A. Bone and J. T. Landrum, "Dose-dependent response of serum lutein and macular pigment optical density to supplementation with lutein esters," *Archives of Biochemistry and Biophysics*, vol. 504, no. 1, pp. 50–55, 2010.

[27] P. Bhosale, B. Li, M. Sharifzadeh et al., "Purification and partial characterization of a lutein-binding protein from human retina," *Biochemistry*, vol. 48, no. 22, pp. 4798–4807, 2009.

[28] J. E. Romanchik, D. W. Morel, and E. H. Harrison, "Distributions of carotenoids and α-tocopherol among lipoproteins do not change when human plasma is incubated in vitro," *Journal of Nutrition*, vol. 125, no. 10, pp. 2610–2617, 1995.

[29] B. Li, P. Vachali, and P. S. Bernstein, "Human ocular carotenoid-binding proteins," *Photochemical & Photobiological Sciences*, vol. 9, no. 11, pp. 1418–1425, 2010.

[30] M. Neuringer, M. M. Sandstrom, E. J. Johnson, and D. M. Snodderly, "Nutritional manipulation of primate retinas, I: Effects of lutein or zeaxanthin supplements on serum and macular pigment in xanthophyll-free Rheus monkeys," *Investigative Ophthalmology & Visual Science*, vol. 45, no. 9, pp. 3234–3243, 2004.

[31] G. Weigert, S. Kaya, B. Pemp et al., "Effects of lutein supplementation on macular pigment optical density and visual acuity in patients with age-related macular degeneration," *Investigative Ophthalmology and Visual Science*, vol. 52, no. 11, pp. 8174–8178, 2011.

[32] R. A. Bone, J. T. Landrum, L. H. Guerra, and C. A. Ruiz, "Lutein and zeaxanthin dietary supplements raise macular pigment density and serum concentrations of these carotenoids in humans," *Journal of Nutrition*, vol. 133, no. 4, pp. 992–998, 2003.

[33] H. E. Bartlett and F. Eperjesi, "A randomised controlled trial investigating the effect of lutein and antioxidant dietary supplementation on visual function in healthy eyes," *Clinical Nutrition*, vol. 27, no. 2, pp. 218–227, 2008.

[34] T. A. E. D. Group, "Lutein + zeaxanthin and omega-3 fatty acids for age-related macular degeneration: the Age-Related Eye Disease Study 2 (AREDS2) randomized clinical trial," *he Journal of the American Medical Association*, vol. 309, no. 19, pp. 2005–2015, 2013.

[35] Y. Sasamoto, F. Gomi, M. Sawa, M. Tsujikawa, and K. Nishida, "Effect of 1-year lutein supplementation on macular pigment optical density and visual function," *Graefe's Archive for Clinical and Experimental Ophthalmology*, vol. 249, no. 12, pp. 1847–1854, 2011.

[36] J. M. Stringham and B. R. Hammond Jr., "Dietary lutein and zeaxanthin: possible effects on visual function," *Nutrition Reviews*, vol. 63, no. 2, pp. 59–64, 2005.

[37] B. R. Wooten and B. R. Hammond, "Macular pigment: influences on visual acuity and visibility," *Progress in Retinal and Eye Research*, vol. 21, no. 2, pp. 225–240, 2002.

[38] J. M. Nolan, J. Loughman, M. C. Akkali et al., "The impact of macular pigment augmentation on visual performance in normal subjects: COMPASS," *Vision Research*, vol. 51, no. 5, pp. 459–469, 2011.

[39] J. Loughman, M. C. Akkali, S. Beatty et al., "The relationship between macular pigment and visual performance," *Vision Research*, vol. 50, no. 13, pp. 1249–1256, 2010.

Hindawi Publishing Corporation
BioMed Research International
Volume 2015, Article ID 425380, 8 pages
http://dx.doi.org/10.1155/2015/425380

Research Article

Curcumin Mitigates Accelerated Aging after Irradiation in *Drosophila* by Reducing Oxidative Stress

Ki Moon Seong,[1] Mira Yu,[2] Kyu-Sun Lee,[3] Sunhoo Park,[1] Young Woo Jin,[1] and Kyung-Jin Min[2]

[1] *National Radiation Emergency Medical Center, Korea Institute of Radiological & Medical Sciences, Seoul 139-706, Republic of Korea*
[2] *Department of Biological Sciences, Inha University, 100 Inha Street, Incheon 402-751, Republic of Korea*
[3] *Bionanotechnology Research Center, Korean Research Institute of Bioscience and Biotechnology, Daejeon 305-806, Republic of Korea*

Correspondence should be addressed to Kyung-Jin Min; minkj@inha.ac.kr

Received 24 June 2014; Revised 15 September 2014; Accepted 17 September 2014

Academic Editor: Huanran Tan

Curcumin, belonging to a class of natural phenol compounds, has been extensively studied due to its antioxidative, anticancer, anti-inflammatory, and antineurodegenerative effects. Recently, it has been shown to exert dual activities after irradiation, radioprotection, and radiosensitization. Here, we investigated the protective effect of curcumin against radiation damage using *D. melanogaster*. Pretreatment with curcumin (100 μM) recovered the shortened lifespan caused by irradiation and increased eclosion rate. Flies subjected to high-dose irradiation showed a mutant phenotype of outstretched wings, whereas curcumin pretreatment reduced incidence of the mutant phenotype. Protein carbonylation and formation of γH2Ax foci both increased following high-dose irradiation most likely due to generation of reactive oxygen species. Curcumin pretreatment reduced the amount of protein carbonylation as well as formation of γH2Ax foci. Therefore, we suggest that curcumin acts as an oxidative stress reducer as well as an effective protective agent against radiation damage.

1. Introduction

Out of several hundred aging theories, the most popular aging theory is oxidative stress theory of aging. It claims that aging is caused by oxidative damage to macromolecules. Oxidative stress is the result of an imbalance between generation of reactive oxygen species by essential life systems and detoxification of reactive radicals by defense mechanisms within organisms [1]. Disruption of the normal redox state of cells induces cytotoxic effects through production of reactive intermediates, which inflict damage to all cellular components, including proteins, lipids, and DNA [2]. Reactive oxygen species such as superoxide ($O_2^{\bullet -}$), hydroxyl ($OH^{\bullet}$), peroxyl ($RO_2^{\bullet}$), and hydroperoxyl ($HO_2^{\bullet}$) are generated by natural respiration in animals and environmental stresses such as radiation, chemicals, and heat [3, 4].

Although the biological effects of low-dose radiation less than 100 mSv have not been fully established, exposure to high-dose radiation caused by unexpected accidents related to artificial sources has many deleterious consequences in humans, including organ malfunction, malignant cancer development, genetic mutagenesis, and developmental abnormalities [5–7]. Moreover, ionizing radiation has long been used as a standard medical treatment to kill cancer cells and shrink tumors [8]. Cancer radiotherapy destroys chromosomes by making it impossible for them to proliferate. Normal cells are also damaged by this therapy, which is the main drawback of this medical procedure. Several antioxidative natural extracts have been combined together in order to reduce radiation injury and protect normal cells [9]. For example, melatonin has been shown to imbue significant radiation protection against chromosomal aberrations and micronuclei formation when administered to mice prior to radiation exposure [10]. Further, several flavonoid compounds such as quercetin, myricetin, and orientin have been reported as potent antioxidants with radioprotective ability [11]. Resveratrol, a polyphenolic plant product, was

also shown to attenuate radiation damage in *C. elegans* by scavenging ROS [12].

Curcumin derived from turmeric is a representative plant phenolic compound possessing therapeutic properties [13, 14]. It is known to eliminate oxygen free radicals, inhibit lipid peroxidation, and protect cellular macromolecules such as DNA from oxidative stress [15, 16]. Curcumin has been shown to reduce chromosomal aberrations in models of human breast cancer, probably due to its antioxidative activity [17]. Fruit flies fed a curcumin diet have shown an extended lifespan, improved health, and modulated expression of aging-associated genes [18, 19].

Due to its antioxidative activity, curcumin has been proposed as a radiation protector. Pretreatment with curcumin has been shown to protect lymphocytes against γ-radiation-induced cellular damage [15]. Curcumin also was found to protect against cutaneous radiation-induced damage in mice [20]. However, several previous studies showed that curcumin has no protective effect against the clastogenicity of γ-radiation [21–23]. Therefore, it remains unclear whether or not curcumin indeed acts as a radiation protector. Moreover, most studies on the radioprotective effects of curcumin have been performed at the cellular level [24–26]. Studies using model animals would more strongly support the conclusion that curcumin protects against radiation damage. Therefore, we evaluated the protective effect of curcumin against ionizing radiation using *D. melanogaster* and found that curcumin may be effective as a radiation protector.

2. Materials and Methods

2.1. Fly Husbandry. We performed all experiments using wild-type Canton-S flies. Larvae of the Canton-S strain were grown on standard cornmeal-sugar-yeast (CSY) medium (5.2 g of cornmeal, 11 g of sucrose, 11 g of yeast [MP Biomedicals, Solon, OH], 1.1 mL of 20% tegosept, and 0.79 g of agar per 100 mL of water) supplemented with several grains of live yeast. The rearing room was maintained at 25°C with 45% humidity on a 12 h : 12 h light-dark cycle.

2.2. Curcumin Pretreatment. Stock solution of curcumin (5 mM) was prepared dissolving curcumin (218580100, Acros Organics) in 99% ethanol and was supplemented to sucrose-yeast (SY) food at a concentration of 100 μM. Same amount of ethanol was supplemented to food without curcumin. Collected eggs were reared in the SY food containing curcumin before irradiation at the 3rd instar larvae stage.

2.3. γ-Irradiation Exposure. Eggs were collected from young female flies over 12–14 h and reared on SY medium. 3rd instar larvae were irradiated in a γ-irradiation machine (^{137}Cs, IBL 437N; CIS Bio International, Gifsur-Yvette, France) at a dose rate of 0.8 Gy/min. Following irradiation, nonirradiated and irradiated flies were maintained contemporaneously in the same incubator at 25°C.

2.4. Pupation and Eclosion Rates. Irradiated larvae were checked daily to determine pupation and eclosion rates. Pupation rate was calculated based on the total number of pupae divided by the number of larvae, whereas eclosion frequency was calculated based on the total number of eclosed flies divided by the number of larvae.

2.5. Lifespan. When irradiated larvae were eclosed, adult flies were collected over 48 h and randomly assigned to 500 mL demography cages to achieve a final density of 100 females and 100 males per cage. SY diets were prepared with 10 g of sucrose, 10 g of yeast, 1.1 mL of 20% tegosept (w/v in ethanol), and 0.79 g of agar per 100 mL of water. The vials containing SY diets were changed every 2 days, and all mortalities were recorded. Three replicates were established for each dose level.

2.6. Detection of Protein Oxidation (Protein Carbonylation). Protein carbonylation was measured using an OxyBlot protein oxidation detection kit according to the manufacturer's instructions (Millipore). Briefly, radiation-exposed larvae under each condition were homogenized in lysis buffer (50 mM Tris-HCL pH 7.4, 150 mM NaCl with protease inhibitor cocktail). For the positive control, protein sample was prepared from larvae fed 20 mM paraquat for 16 h. Protein samples were then treated with 2,4-dinitrophenylhydrazine (DNPH). Reaction of DNPH with carbonylated proteins allows the formation of 2-4-dinitrophenylhydrazone (DNP), which can be detected with anti-DNP antibody. Samples were subjected to 10% SDS-PAGE and transferred onto a PVDF membrane (Roche). DNP groups were then immunodetected with rabbit anti-DNP antibody, followed by secondary anti-HRP antibody and ECL revelation. To normalize protein loading, the transferred SDS-PAGE gel was stained with Coomassie blue.

2.7. γH2Ax Foci Staining. To detect double-strand breaks, irradiated larvae were dissected in cold PBS and fixed for 20 min at room temperature in PBS containing 4% paraformaldehyde. After washing and blocking with PBS containing 0.1% Triton and 2% BSA, wing imaginal discs were incubated with antiphosphorylated H2Ax (γH2Ax, Upstate Biotechnology). For visualization, samples were mounted in VECTASHIELD Mounting Media (Vector Lab), and fluorescence images were acquired using a FluoView confocal microscope (Olympus).

2.8. Statistical Analyses. All demographic data were presented as the mean ± SEM and analyzed with a one-way analysis of variance (ANOVA) on ranked data using standard survival models in the JMP statistical package and Prism software (GraphPad, La Jolla, CA). Asterisk indicates significant difference from the control ($^{**}P < 0.001$ and $^{*}P < 0.05$). The tests used and sample sizes for each experiment are indicated.

3. Results

3.1. Effect of Curcumin Pretreatment on Drosophila Lifespan after Radiation Exposure. Previous studies have reported

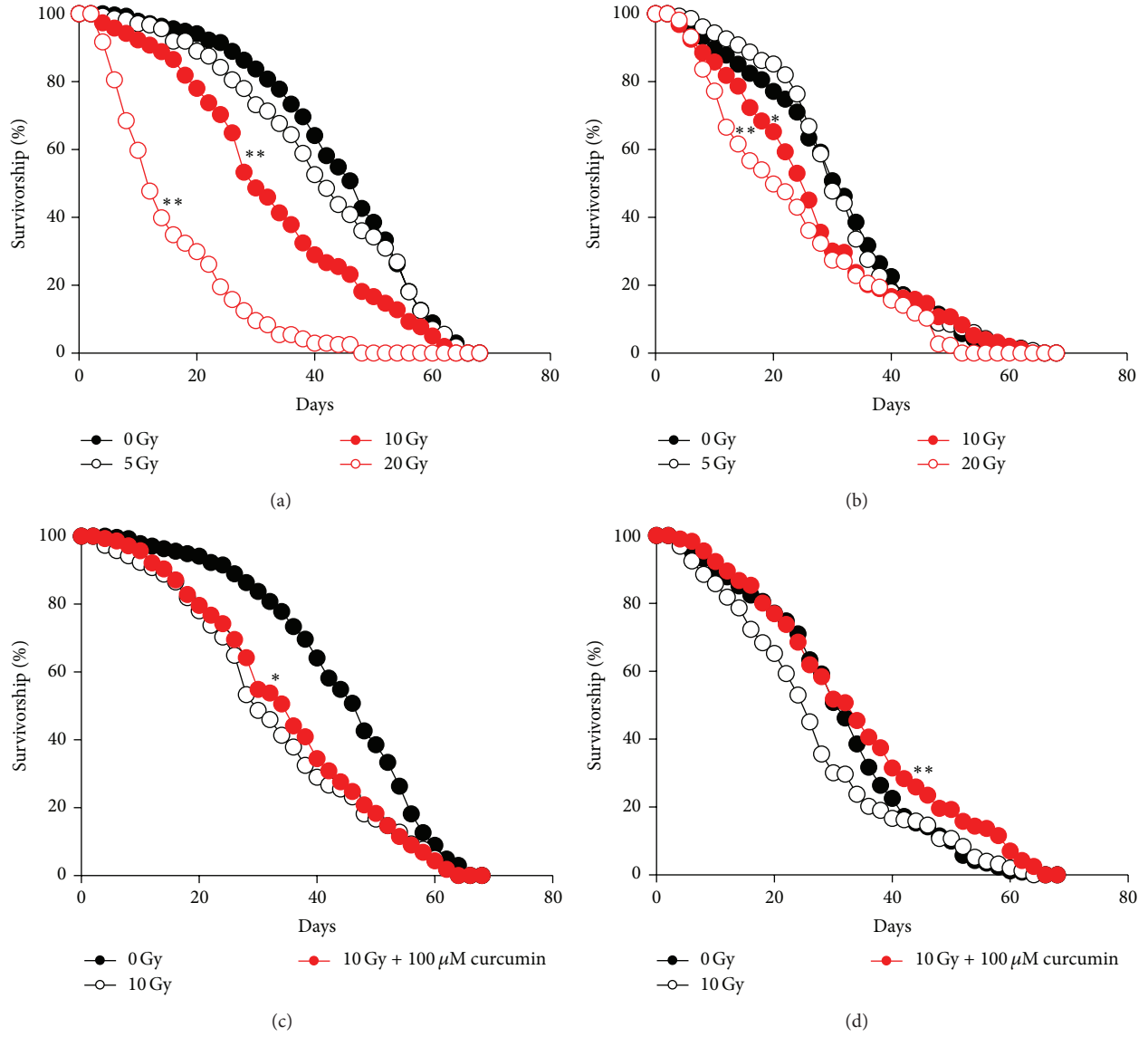

Figure 1: Curcumin pretreatment recovers shortened fly lifespan by ionizing radiation. Several doses of ionizing radiation were administered at the 3rd larval stage, and the lifespans of adult males (a) and females (b) were measured. Larvae were fed 100 μM curcumin from egg hatching before 10 Gy of irradiation at the 3rd larval stage, and the lifespans of adult males (c) and females (d) were measured ($^{*}P < 0.05$, $^{**}P < 0.01$).

that ionizing radiation reduces the lifespan of *Drosophila* to various degrees depending on the irradiation dosage and strain genetic background [27, 28]. Here, we first subjected larvae of fruit flies to irradiation at several doses and then recorded lifespans of adults in order to determine the optimal dose to analyze the effects of curcumin (Figures 1(a) and 1(b)). The effect of curcumin pretreatment was evaluated in flies irradiated at 10 Gy, which showed a mean lifespan of approximately 30 days in both males and females (Table 1). We reared Canton-S flies after egg hatching with fly medium containing 100 μM curcumin, and ionizing radiation was administered at the 3rd instar larva stage. 100 μM curcumin was chosen as the most effective dose based on preliminary experiment. Flies pretreated with curcumin showed significant extension of their mean lifespan—5.5% for males ($P < 0.01$) and 26.5% for females ($P < 0.01$) (Table 1, Figures 1(c), 1(d)). These data indicate that curcumin pretreatment extended the lifespan of irradiated flies by mitigating the harmful effects of ionizing radiation.

3.2. Effect of Curcumin Pretreatment on Drosophila Development after Radiation Exposure. All insects, including *Drosophila*, undergo marked morphological changes during their development to adult stage known as metamorphosis, which is an excellent parameter to detect physiological effects following environmental fluctuation. Here, we measured pupation and eclosion rates of flies pretreated with curcumin after irradiation. The pupation rate of curcumin-pretreated flies was not significantly different after irradiation ($P > 0.07$) (Figure 2(a)). However, the eclosion rate of flies was

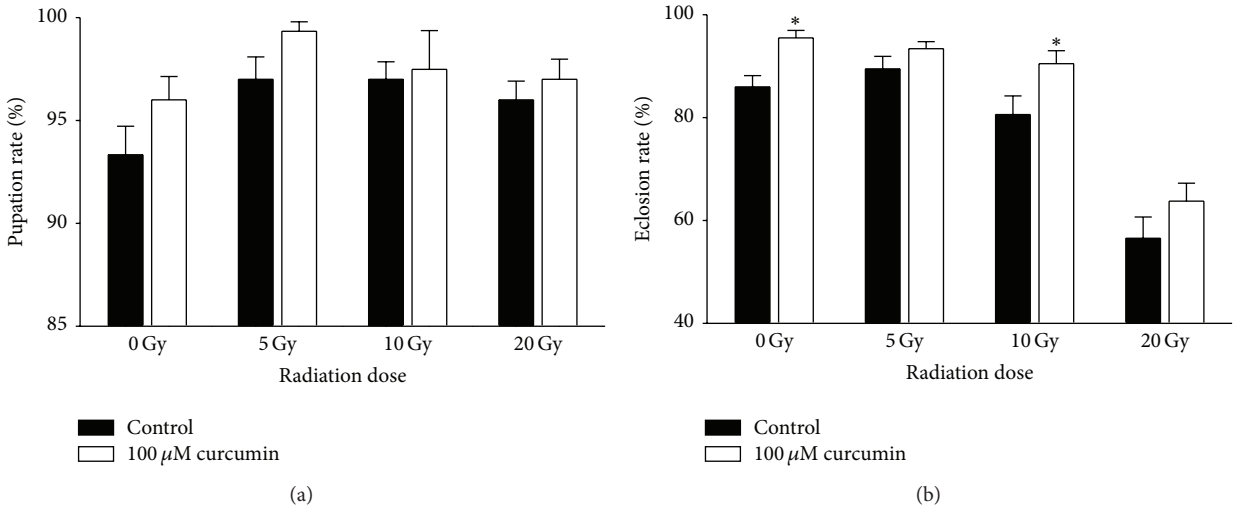

Figure 2: Curcumin pretreatment increases the eclosion rate of fruit flies. Pupation rate (a) and eclosion rate (b) of irradiated flies were recorded as described in the materials and methods section. Pretreatment with curcumin improved the eclosion rate in some treatments ($^{*}P < 0.05$).

Table 1: Mean longevity recovery by pretreatment of curcumin.

Treatment	Flies numbers	Mean longevity	SD	P value
Male				
Control	270	44.6889	0.82040	—
IR[a]	259	33.2819	0.96298	<0.0001*
IR + curcumin[b]	279	35.1183	0.89536	<0.0001**
Female				
Control	262	31.1908	0.84744	—
IR[a]	253	27.0119	0.93228	0.0151*
IR + curcumin[b]	286	34.1748	0.95931	<0.0001**

[a]Radiation at 10 Gy was irradiated at 3rd instar larval stage.
[b]Flies were cultivated in the medium containing 100 μM of curcumin until irradiation.
*Compared with control, **compared with IR group.

reduced as the radiation dose increased. The eclosion rate of control flies was 83%, whereas that of flies irradiated at 20 Gy was reduced to 58%. Curcumin pretreatment distinctly augmented the eclosion rate in irradiated flies with statistical significance ($P < 0.05$) (Figure 2(b)). Curcumin pretreatment without irradiation also increased the eclosion rate ($P < 0.05$).

3.3. Effect of Curcumin Pretreatment on Drosophila Phenotype after Radiation Exposure. High-dose irradiation has been shown to induce chromosomal mutations and malformation of external organs [29–31]. Here, we analyzed the specific phonotype caused by irradiation to determine whether or not curcumin reduces the mutagenic effects of ionizing radiation. Irradiation with 20 Gy at the 3rd instar larval stage resulted in outstretched wings on bodies of adult flies (Figure 3(a)), and the frequency of the mutant phenotype increased as the radiation dose increased (Figure 3(b)). Specifically, no mutant phenotype was observed at 0 Gy of irradiation, whereas about 60% of flies showed the mutant phenotype at 20 Gy of irradiation. Although curcumin pretreatment did not significantly reduce the frequency of mutation, lower frequency of the mutant phenotype was a tendency in all curcumin-pretreated groups (Figure 3(b)).

3.4. Effect of Curcumin Pretreatment on ROS Generation after Radiation Exposure. The phenotypic data acquired in this study indicate that curcumin reduced the various stresses caused by ionizing radiation. Since it is well known that radiation induces oxidative stress and curcumin is an excellent antioxidant, we examined whether or not curcumin detoxifies radiation-induced oxidative damage. Protein carbonylation is known to be a key biomarker of oxidative stress generated by carbonyl (CO) groups (aldehydes and ketones), which are produced on protein side chains, especially in proline, arginine, lysine, and threonine, following their oxidation [32]. Here, we extracted protein lysates from flies and performed protein carbonylation assay as described in Section 2. Protein carbonylation increased upon irradiation, whereas curcumin pretreatment obviously reversed this in irradiated flies. Paraquat, known to be a chemical inducing cellular protein carbonylation, was used as a positive control (Figure 4).

3.5. Effect of Curcumin Pretreatment on DNA Damage after Radiation Exposure. Reduced oxidative stress by curcumin could diminish the damage inflicted by ionizing radiation. DNA double-strand breaks caused by radiation-induced ROS impair normal cellular survival. In mammal, phosphorylated H2Ax (γH2Ax) foci, an indicator of DNA double-strand breaks, are found in the nucleosomes near radiolytic damaged region [33]. Since antibody to mammalian γH2Ax can recognize *Drosophila* γH2Av based on sequence homology [34], we monitored the radiation-mediated DNA damage

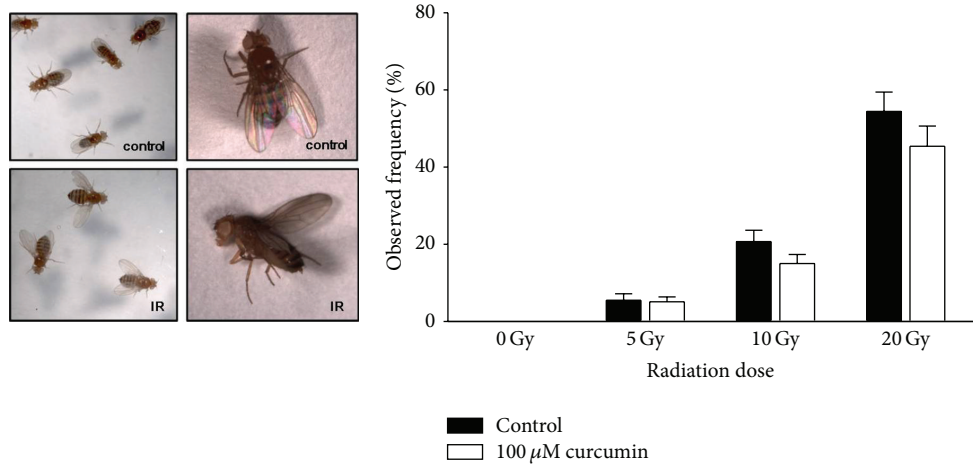

(a) (b)

FIGURE 3: Irradiation increases incidence of flies with outstretched wings. Some irradiated flies emerged with outstretched wings (a). The incidence of flies with outstretched wings increased as the radiation dose increased. Curcumin pretreatment tended to reduce incidence, but the difference was not significant in all treatments.

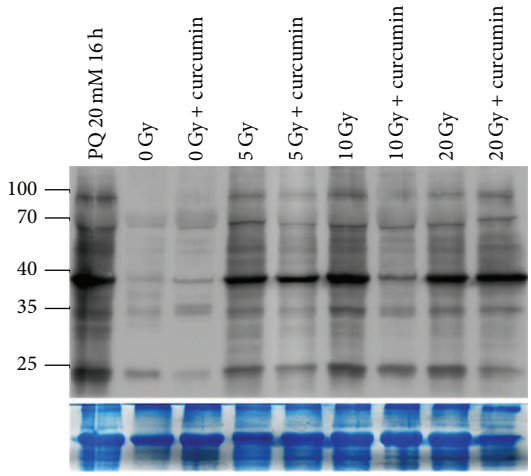

FIGURE 4: Curcumin pretreatment reduces radiation-induced protein carbonylation. Both paraquat (positive control) and irradiation increased protein carbonylation, whereas curcumin pretreatment decreased protein carbonylation. A gel image stained with Coomassie blue was used as an internal control of protein loading amount in SDS-PAGE.

with γH2Ax foci in larval wing disc. Here, ionizing radiation induced DNA breaks in a dose-dependent manner, whereas curcumin pretreatment significantly reduced formation of γH2Ax foci in the larval wing disc of *Drosophila* (Figure 5). These data indicate that curcumin reduced radiation induced the genome instability in *Drosophila* by increasing resistance to oxidative stress.

4. Discussion

In this paper, we presented data showing that curcumin reversed the shortened lifespan of irradiated flies as well as increased the eclosion rate. Curcumin also attenuated oxidative stress and DNA alterations caused by ionizing radiation. Interestingly, irradiation caused a larger reduction in lifespan in males than in females, whereas curcumin pretreatment was more effective in females than in males (Figure 1). This sexually dimorphic difference may be due to differential hormonal regulation of male and female fecundity [35–37]. It may also be due to gender differences in susceptibility to oxidative stress between males and females. Some parameters of free radical processes are different between male and female *Drosophila*. For example, a previous study showed differences in oxygen consumption of extracted mitochondria and mitochondrial DNA copy number between male and female *Drosophila* [37].

To our knowledge, this is the first report showing that high-dose irradiation of larvae results in an abnormal outstretched wing phenotype (Figure 3). Generally, *Drosophila* adults are quite resistant to irradiation. Even 500 Gy of radiation has been shown to have little effect on adult survival following irradiation at the adult stage (unpublished data), which may be due to the cuticular exoskeleton of flies. Unlike adults, *Drosophila* larvae are susceptible to irradiation due to their soft cuticular structure. As mentioned above, in this study, lifespans were greatly reduced and incidence of the outstretched wing phenotype increased as the radiation dose increased. Actually, half of the flies emerged with the outstretched wing phenotype when 20 Gy of radiation was administered to 3rd instar larvae. It remains unknown which signaling pathway is involved in the formation of the outstretched wing phenotype, but we suspect the JAK/STAT signaling pathway since it participates in the formation of the imaginal wing disc [38, 39]. Further investigation is necessary to determine the molecular mechanisms of outstretched wing formation after irradiation.

Eclosion rates of nonirradiated or irradiated flies were improved by curcumin pretreatment (Figure 2). As an explanation, curcumin has the potential to remove ROS generated

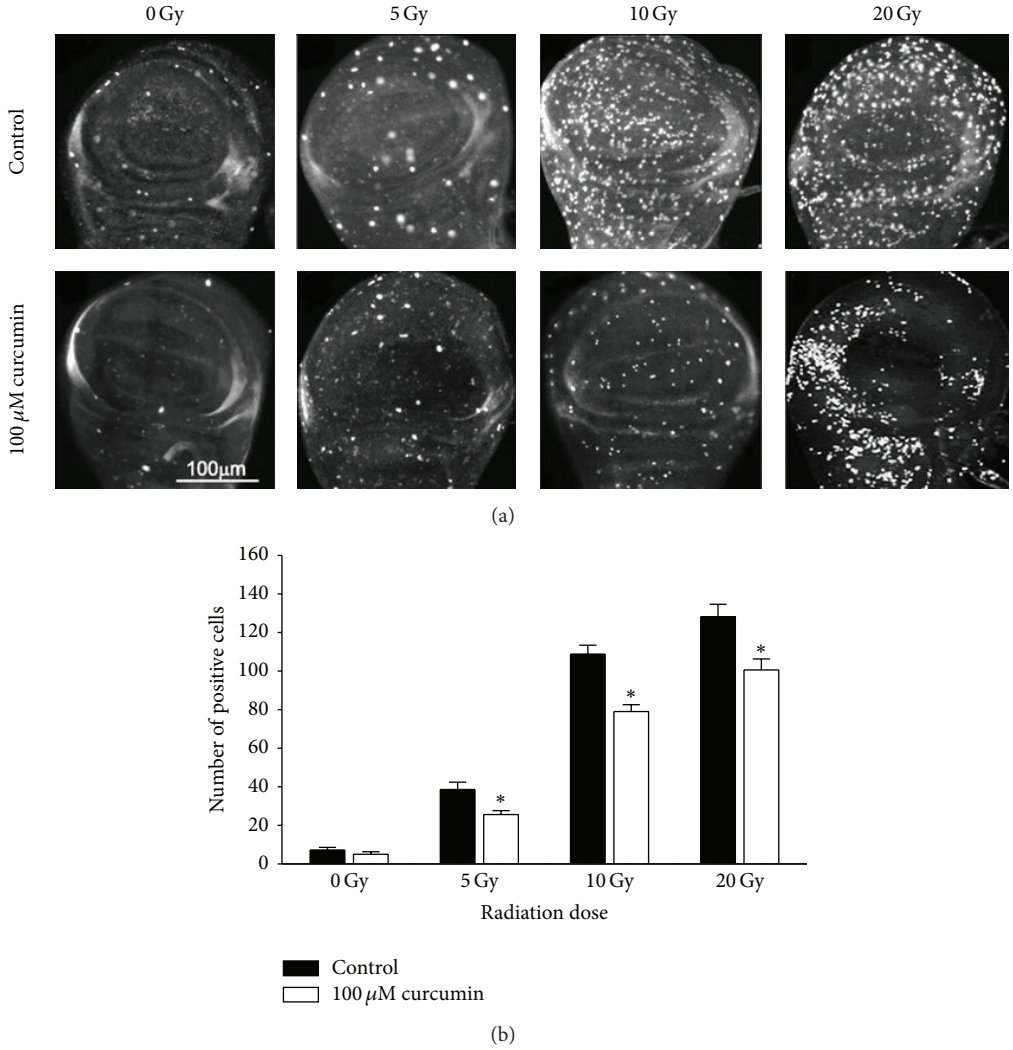

Figure 5: Curcumin reduces formation of radiation-induced γH2Ax foci. Phosphorylated H2Ax was used as a marker of DNA double-strand breaks. Foci on wing discs were detected by immunostaining with specific antibodies for γH2Ax (a). The incidence was measured by counting spots (b) and analyzed statistically ($^{*}P < 0.05$).

during development and/or radiation exposure. A previous report of delayed aging upon curcumin treatment supports our observations since aging is tightly coupled with ROS generation [18]. Both 20 mM paraquat and irradiation increased protein carbonylation, which itself was reduced by curcumin treatment (Figure 4). Similarly, pretreatment with curcumin to irradiated lymphocytes reduced lipid peroxidation and increased antioxidative properties, thereby preventing injury to lymphocytes [15]. Overall, curcumin provided *Drosophila* with augmented resistance to overcome radiation-induced oxidative stresses.

Collectively, these effects of curcumin may be due to its scavenging activity and distinct structural characteristics. First, curcumin has a hydrophobic structure that allows it to easily pass through the plasma membrane into the cytoplasm, where it can scavenge ROS more easily than hydrophobic molecules [40]. Second, curcumin has electron-donating groups such as phenolic hydroxyl groups and a β-diketone structure responsible for removing free radicals from cells [15]. Increased resistance to oxidative stress by curcumin could be attributed to its transcriptional regulation; namely, curcumin can activate transcriptional factors and increase the expression of genes involved in oxidative defense [41, 42].

However, some scientists have remarked that curcumin could be a "double-edged sword," similar to other herbal antioxidants in tumorigenesis [43, 44]. The carcinogenic or prooxidant effects of curcumin have been shown to be mediated by mechanisms such as iron depletion, inhibition of cytochrome p450, and interference with the p53 tumor suppressor pathway [40, 45, 46]. Moreover, other lines of evidence raise concerns about the safety of curcumin for cancer treatment. Specifically, curcumin shows diverse clinical effects depending on its concentration [47]. To develop curcumin into a preventive or therapeutic drug, the optimal dose that elicits only desirable effects should be determined.

The development of radioprotectors is an area of great significance due to its wide applications in planned radiotherapy as well as unexpected radiation exposure. Although

some conflicting behaviors of curcumin on radioprotective function were reported, there are number of studies showing that curcumin offers protection to normal cells from radiation [15, 20, 48]. Our present data using *Drosophila* prove that curcumin improved radioresistance by relieving oxidative stress, thereby consolidating the radioprotective effects of curcumin.

5. Conclusions

In this paper, we have presented data showing that that curcumin relieves the oxidative stress and DNA damage caused by high-dose radiation in *Drosophila*. Curcumin pretreatment extends lifespan and decreases the frequency of mutagenic phenotype caused by ionizing radiation. Given antiaging benefits of curcumin from antioxidative properties, it will be of interest to determine whether curcumin can be used as a radioprotective agent in mammalian models.

Conflict of Interests

The authors declare that there is no conflict of interests regarding the publication of this paper.

Authors' Contribution

Ki Moon Seong and Mira Yu contributed equally.

Acknowledgments

This work was supported by the research funds of the Ministry of Science, ICT and Future Planning (MISP) (no. 50586-2014) and the Basic Science Research Program through the National Research Foundation of Korea (NRF), funded by the Ministry of Education, Science, and Technology (no. 2012R1A1A2041099).

References

[1] T. Finkel and N. J. Holbrook, "Oxidants, oxidative stress and the biology of ageing," *Nature*, vol. 408, no. 6809, pp. 239–247, 2000.

[2] K. S. Fritz and D. R. Petersen, "Exploring the biology of lipid peroxidation-derived protein carbonylation," *Chemical Research in Toxicology*, vol. 24, no. 9, pp. 1411–1419, 2011.

[3] P. J. Hansen, "Effects of heat stress on mammalian reproduction," *Philosophical Transactions of the Royal Society B: Biological Sciences*, vol. 364, no. 1534, pp. 3341–3350, 2009.

[4] F. Caputo, R. Vegliante, and L. Ghibelli, "Redox modulation of the DNA damage response," *Biochemical Pharmacology*, vol. 84, no. 10, pp. 1292–1306, 2012.

[5] K. M. Seong, C. S. Kim, B.-S. Lee et al., "Low-dose radiation induces drosophila innate immunity through toll pathway activation," *Journal of Radiation Research*, vol. 53, no. 2, pp. 242–249, 2012.

[6] S. A. Lorimore, P. J. Coates, and E. G. Wright, "Radiation-induced genomic instability and bystander effects: inter-related nontargeted effects of exposure to ionizing radiation," *Oncogene*, vol. 22, no. 45, pp. 7058–7069, 2003.

[7] K. B. Moysich, R. J. Menezes, and A. M. Michalek, "Chernobyl-related ionising radiation exposure and cancer risk: an epidemiological review," *The Lancet Oncology*, vol. 3, no. 5, pp. 269–279, 2002.

[8] N. J. Curtin, "DNA repair dysregulation from cancer driver to therapeutic target," *Nature Reviews Cancer*, vol. 12, no. 12, pp. 801–817, 2012.

[9] F. E. Koehn and G. T. Carter, "The evolving role of natural products in drug discovery," *Nature Reviews Drug Discovery*, vol. 4, no. 3, pp. 206–220, 2005.

[10] F. M. Badr, O. H. M. El Habit, and M. M. Harraz, "Radioprotective effect of melatonin assessed by measuring chromosomal damage in mitotic and meiotic cells," *Mutation Research—Genetic Toxicology and Environmental Mutagenesis*, vol. 444, no. 2, pp. 367–372, 1999.

[11] V. Benkovic, A. Horvat Knezevic, D. Dikic et al., "Radioprotective effects of propolis and quercetin in γ-irradiated mice evaluated by the alkaline comet assay," *Phytomedicine*, vol. 15, no. 10, pp. 851–858, 2008.

[12] K. Ye, C.-B. Ji, X.-W. Lu et al., "Resveratrol attenuates radiation damage in Caenorhabditis elegansby preventing oxidative stress," *Journal of Radiation Research*, vol. 51, no. 4, pp. 473–479, 2010.

[13] L. Pari, D. Tewas, and J. Eckel, "Role of curcumin in health and disease," *Archives of Physiology and Biochemistry*, vol. 114, no. 2, pp. 127–149, 2008.

[14] B. B. Aggarwal and B. Sung, "Pharmacological basis for the role of curcumin in chronic diseases: an age-old spice with modern targets," *Trends in Pharmacological Sciences*, vol. 30, no. 2, pp. 85–94, 2009.

[15] M. Srinivasan, N. R. Prasad, and V. P. Menon, "Protective effect of curcumin on γ-radiation induced DNA damage and lipid peroxidation in cultured human lymphocytes," *Mutation Research: Genetic Toxicology and Environmental Mutagenesis*, vol. 611, no. 1-2, pp. 96–103, 2006.

[16] Q.-Y. Wei, W.-F. Chen, B. Zhou, L. Yang, and Z.-L. Liu, "Inhibition of lipid peroxidation and protein oxidation in rat liver mitochondria by curcumin and its analogues," *Biochimica et Biophysica Acta—General Subjects*, vol. 1760, no. 1, pp. 70–77, 2006.

[17] S. Somasundaram, N. A. Edmund, D. T. Moore, G. W. Small, Y. Y. Shi, and R. Z. Orlowski, "Dietary curcumin inhibits chemotherapy-induced apoptosis in models of human breast cancer," *Cancer Research*, vol. 62, no. 13, pp. 3868–3875, 2002.

[18] K. S. Lee, B. S. Lee, S. Semnani et al., "Curcumin extends life span, improves health span, and modulates the expression of age-associated aging genes in drosophila melanogaster," *Rejuvenation Research*, vol. 13, no. 5, pp. 561–570, 2010.

[19] L.-R. Shen, F. Xiao, P. Yuan et al., "Curcumin-supplemented diets increase superoxide dismutase activity and mean lifespan in Drosophila," *Age*, vol. 35, no. 4, pp. 1133–1142, 2013.

[20] P. Okunieff, J. Xu, D. Hu et al., "Curcumin protects against radiation-induced acute and chronic cutaneous toxicity in mice and decreases mRNA expression of inflammatory and fibrogenic cytokines," *International Journal of Radiation Oncology Biology Physics*, vol. 65, no. 3, pp. 890–898, 2006.

[21] N. Aravindan, J. Veeraraghavan, R. Madhusoodhanan, T. S. Herman, and M. Natarajan, "Curcumin regulates low-linear energy transfer γ-radiation-induced NFκB-dependent telomerase activity in human neuroblastoma cells," *International Journal of Radiation Oncology Biology Physics*, vol. 79, no. 4, pp. 1206–1215, 2011.

[22] J. Veeraraghavan, M. Natarajan, P. Lagisetty, V. Awasthi, T. S. Herman, and N. Aravindan, "Impact of curcumin, raspberry extract, and neem leaf extract on rel protein-regulated cell death/radiosensitization in pancreatic cancer cells," *Pancreas*, vol. 40, no. 7, pp. 1107–1119, 2011.

[23] P. Javvadi, A. T. Segan, S. W. Tuttle, and C. Koumenis, "The chemopreventive agent curcumin is a potent radiosensitizer of human cervical tumor cells via increased reactive oxygen species production and overactivation of the mitogen-activated protein kinase pathway," *Molecular Pharmacology*, vol. 73, no. 5, pp. 1491–1501, 2008.

[24] R. Parshad, K. K. Sanford, F. M. Price et al., "Protective action of plant polyphenols on radiation-induced chromatid breaks in cultured human cells," *Anticancer Research A*, vol. 18, no. 5, pp. 3263–3266, 1998.

[25] S. M. Khopde, K. I. Priyadarsini, S. N. Guha, J. G. Satav, P. Venkatesan, and M. N. Aswathanarana Rao, "Inhibition of radiation-induced lipid peroxidation by tetrahydrocurcumin: possible mechanisms by pulse radiolysis," *Bioscience, Biotechnology and Biochemistry*, vol. 64, no. 3, pp. 503–509, 2000.

[26] S. Kapoor and K. I. Priyadarsini, "Protection of radiation-induced protein damage by curcumin," *Biophysical Chemistry*, vol. 92, no. 1-2, pp. 119–126, 2001.

[27] K. M. Seong, C. S. Kim, S.-W. Seo et al., "Genome-wide analysis of low-dose irradiated male *Drosophila melanogaster* with extended longevity," *Biogerontology*, vol. 12, no. 2, pp. 93–107, 2011.

[28] A. A. Moskalev, A. S. Iatskiv, and V. G. Zaĭnullin, "Effect of low-dose irradiation on the lifespan in various strains of Drosophila melanogaster," *Genetika.*, vol. 42, no. 6, pp. 773–782, 2006.

[29] D. R. Boreham, J. A. Dolling, C. Somers, J. Quinn, and R. E. Mitchel, "The adaptive response and protection against heritable mutations and fetal malformation," *Dose-Response*, vol. 4, no. 4, pp. 317–326, 2006.

[30] S. J. Garte and F. J. Burns, "Oncogenes and radiation carcinogenesis," *Environmental Health Perspectives*, vol. 93, pp. 45–49, 1991.

[31] O. Vos, "Effects and consequences of prenatal irradiation," *Bollettino della Società Italiana di Biologia Sperimentale*, vol. 65, no. 6, pp. 481–500, 1989.

[32] I. Dalle-Donne, R. Rossi, D. Giustarini, A. Milzani, and R. Colombo, "Protein carbonyl groups as biomarkers of oxidative stress," *Clinica Chimica Acta*, vol. 329, no. 1-2, pp. 23–38, 2003.

[33] H. V. Goutham, K. D. Mumbrekar, B. M. Vadhiraja et al., "DNA double-strand break analysis by γ-H2AX foci: a useful method for determining the overreactors to radiation-induced acute reactions among head-and-neck cancer patients," *International Journal of Radiation Oncology Biology Physics*, vol. 84, no. 5, pp. e607–e612, 2012.

[34] J. P. Madigan, H. L. Chotkowski, and R. L. Glaser, "DNA double-strand break-induced phosphorylation of *Drosophila* histone variant H2Av helps prevent radiation-induced apoptosis," *Nucleic Acids Research*, vol. 30, no. 17, pp. 3698–3705, 2002.

[35] T. O. Hansen, P. Sarup, V. Loeschcke, and S. I. S. Rattan, "Age-related and sex-specific differences in proteasome activity in individual Drosophila flies from wild type, longevity-selected and stress resistant strains," *Biogerontology*, vol. 13, no. 4, pp. 429–438, 2012.

[36] K. G. Iliadi, N. N. Iliadi, and G. L. Boulianne, "Regulation of drosophila life-span: effect of genetic background, sex, mating and social status," *Experimental Gerontology*, vol. 44, no. 8, pp. 546–553, 2009.

[37] J. W. O. Ballard, R. G. Melvin, J. T. Miller, and S. D. Katewa, "Sex differences in survival and mitochondrial bioenergetics during aging in Drosophila," *Aging Cell*, vol. 6, no. 5, pp. 699–708, 2007.

[38] B. A. Callus and B. Mathey-Prevot, "SOCS36E, a novel Drosophila SOCS protein, suppresses JAK/STAT and EGF-R signalling in the imaginal wing disc," *Oncogene*, vol. 21, no. 31, pp. 4812–4821, 2002.

[39] L. Sefton, J. R. Timmer, Y. Zhang, F. Béranger, and T. W. Cline, "An extracellular activator of the Drosophila JAK/STAT pathway is a sex- determination signal element," *Nature*, vol. 405, no. 6789, pp. 970–971, 2000.

[40] S. Oetari, M. Sudibyo, J. N. M. Commandeur, R. Samhoedi, and N. P. E. Vermeulen, "Effects of curcumin on cytochrome P450 and glutathione S-transferase activities in rat liver," *Biochemical Pharmacology*, vol. 51, no. 1, pp. 39–45, 1996.

[41] T.-S. Huang, S.-C. Lee, and J.-K. Lin, "Suppression of c-Jun/AP-1 activation by an inhibitor of tumor promotion in mouse fibroblast cells," *Proceedings of the National Academy of Sciences of the United States of America*, vol. 88, no. 12, pp. 5292–5296, 1991.

[42] L. Korutla and R. Kumar, "Inhibitory effect of curcumin on epidermal growth factor receptor kinase activity in A431 cells," *Biochimica et Biophysica Acta*, vol. 1224, no. 3, pp. 597–600, 1994.

[43] S. A. Marathe, I. Dasgupta, D. P. Gnanadhas, and D. Chakravortty, "Multifaceted roles of curcumin: two sides of a coin!," *Expert Opinion on Biological Therapy*, vol. 11, no. 11, pp. 1485–1499, 2011.

[44] W. Kim, K. M. Seong, and B. Youn, "Phenylpropanoids in radioregulation: double edged sword," *Experimental and Molecular Medicine*, vol. 43, no. 6, pp. 323–333, 2011.

[45] P. Tsvetkov, G. Asher, V. Reiss, Y. Shaul, L. Sachs, and J. Lotem, "Inhibition of NAD(P)H:quinone oxidoreductase 1 activity and induction of p53 degradation by the natural phenolic compound curcumin," *Proceedings of the National Academy of Sciences of the United States of America*, vol. 102, no. 15, pp. 5535–5540, 2005.

[46] Y. Jiao, J. Wilkinson IV, X. Di et al., "Curcumin, a cancer chemopreventive and chemotherapeutic agent, is a biologically active iron chelator," *Blood*, vol. 113, no. 2, pp. 462–469, 2009.

[47] E. Burgos-Morón, J. M. Calderón-Montaño, J. Salvador, A. Robles, and M. López-Lázaro, "The dark side of curcumin," *International Journal of Cancer*, vol. 126, no. 7, pp. 1771–1775, 2010.

[48] G. C. Jagetia, "Radioprotection and radiosensitization by curcumin," *Advances in Experimental Medicine and Biology*, vol. 595, pp. 301–320, 2007.

Hindawi Publishing Corporation
BioMed Research International
Volume 2015, Article ID 620643, 7 pages
http://dx.doi.org/10.1155/2015/620643

Clinical Study

Temozolomide and Radiotherapy versus Radiotherapy Alone in High Grade Gliomas: A Very Long Term Comparative Study and Literature Review

Salvatore Parisi,[1,2] Pietro Corsa,[1] Arcangela Raguso,[1] Antonio Perrone,[1] Sabrina Cossa,[1] Tindara Munafò,[1] Gerardo Sanpaolo,[1] Elisa Donno,[1] Maria Antonietta Clemente,[1] Michele Piombino,[3] Federico Parisi,[4] and Guido Valle[5]

[1] *Unit of Radiation Therapy of IRCCS "Casa Sollievo della Sofferenza", 71013 San Giovanni Rotondo, Italy*
[2] *Radiotherapy Unit, Scientific Institute "Casa Sollievo della Sofferenza", Viale Cappuccini, 71013 San Giovanni Rotondo, Italy*
[3] *Unit of Radiation Therapy of Policlinico, 70124 Bari, Italy*
[4] *University of Chieti, 66100 Chieti, Italy*
[5] *Unit of Nuclear Medicine of IRCCS "Casa Sollievo della Sofferenza", San Giovanni Rotondo, Italy*

Correspondence should be addressed to Salvatore Parisi; s.parisi@operapadrepio.it

Received 7 July 2014; Revised 4 November 2014; Accepted 5 November 2014

Academic Editor: Chi-Feng Hung

Temozolomide (TMZ) is the first line drug in the care of high grade gliomas. The combined treatment of TMZ plus radiotherapy is more effective in the care of brain gliomas then radiotherapy alone. Aim of this report is a survival comparison, on a long time (>10 years) span, of glioma patients treated with radiotherapy alone and with radiotherapy + TMZ. *Materials and Methods*. In this report we retrospectively reviewed the outcome of 128 consecutive pts with diagnosis of high grade gliomas referred to our institutions from April 1994 to November 2001. The first 64 pts were treated with RT alone and the other 64 with a combination of RT and adjuvant or concomitant TMZ. *Results*. Grade 3 (G3) haematological toxicity was recorded in 6 (9%) of 64 pts treated with RT and TMZ. No G4 haematological toxicity was observed. Age, histology, and administration of TMZ were statistically significant prognostic factors associated with 2 years overall survival (OS). PFS was for GBM 9 months, for AA 11. *Conclusions*. The combination of RT and TMZ improves long term survival in glioma patients. Our results confirm the superiority of the combination on a long time basis.

1. Introduction

Despite advances in the last years in the treatment of neoplastic diseases, the prognosis of patients (pts) with high grade gliomas is still dismal.

The survival of glioma patients treated with surgical resection alone is approximately 6 months [1]. The combination of surgery and postoperative radiation therapy (RT) increases the survival up to 9-10 months in pts with glioblastoma multiforme (GBM) and 36 months in anaplastic astrocytoma (AA) [2].

In order to get further improvements in the last decades many studies have tested multimodality treatment schedules incorporating chemotherapy (CT) with nitrosourea based regimens, with questionable survival advantages [1–6].

A meta-analysis published in 2002 [7] including many different chemotherapeutic regimes has pointed out that the association of chemotherapy is, in general, more effective than RT alone in prolonging survival and in delaying recurrences in glioma patients. Particularly this meta-analysis showed a mild but significant benefit with the addition of CT, with a 15% relative reduction in the risk of death and an increase in 2-year survival from 9% to 13% in individuals with GBM and from 31% to 37% in pts with AA. These evidences encouraged research with new chemotherapeutic agents.

Temozolomide (TMZ) (Temodal, Temodar; Schering-Plough, Kenilworth, NJ) is one of second-generation imidazotetrazinone prodrugs that spontaneously converts into the active metabolite without the need for enzymatic demethylation in the liver [8]. Nowadays TMZ is the first choice drug in

Table 1: Group A and group B: patients' characteristics.

	Group A	Group B
Patients' number	31	33
Age		
Range	41–78 years	26–74 years
Median	62 years	57 years
Sex		
Male	17 pts	18 pts
Female	14 pts	15 pts
Karnofsky Index		
Range	60–90	60–90
Medium	70	70
Surgery		
Stereotactic biopsy	3 pts	9 pts
Subtotal resection	18 pts	12 pts
Total resection	10 pts	12 pts
Histology		
Anaplastic astrocytoma	11 pts	10 pts
Glioblastoma multiforme	20 pts	23 pts
RT total dose		
Median	64 Gy	63 Gy
Range	45 Gy–66 Gy	45 Gy–64 Gy
<50 Gy	2 pts	1 pts
≥50 Gy <60 Gy	5 pts	2 pts
≥60 Gy	24 pts	30 pts

Table 2: Groups A + B and group C: patients' characteristics.

	Groups A + B	Group C
Patients' number	64	64
Age		
Range	26–78 years	29–74 years
Median	59 years	60 years
Sex		
Male	35 pts	39 pts
Female	29 pts	25 pts
Karnofsky Index		
Range	60–90	60–90
Medium	70	70
Surgery		
Stereotactic biopsy	12 pts	11 pts
Subtotal resection	30 pts	35 pts
Total resection	22 pts	18 pts
Histology		
Anaplastic astrocytoma	21 pts	14 pts
Glioblastoma multiforme	43 pts	50 pts
RT total dose		
Median	61 Gy	59 Gy
Range	45 Gy–66 Gy	35 Gy–66 Gy
<50 Gy	3 pts	3 pts
≥50 Gy <60 Gy	7 pts	6 pts
≥60 Gy	54 pts	55 pts

the chemotherapy of gliomas and is largely used after surgery and together or after RT.

Accordingly, 64 consecutive pts, with diagnosis of high grade glioma, with irradiation and adjuvant TMZ (group A, $n = 31$ pts) or adjuvant/concomitant (group B, $n = 33$ pts) [9] were treated at the Departments of Radiotherapy of Bari University and "Casa Sollievo della Sofferenza" Hospital in San Giovanni Rotondo. The survival data of these subjects (groups A + B) were compared with a group of 64 other patients with similar clinical characteristics treated in the same institutions only with radiotherapy from April 1994 to December 1996 (group C).

This study is aimed at comparing the outcome of the 31 pts treated with RT and adjuvant TMZ (group A) from January 1997 to June 1999 versus the 33 pts treated with RT and concomitant TMZ (group B) from July 1999 to November 2001 and at comparing, on a long term basis, the subjects that received both RT and TMZ with the historical group (group C) that was treated with radiotherapy alone. The survival data have been evaluated also according to the histology of the neoplasm: glioblastoma multiforme (GBM, in 43 patients of groups A + B and in 50 pts of group C) and anaplastic astrocytoma (AA, in 21 pts of groups A + B and in 14 pts of group C).

2. Patients and Methods

2.1. Inclusion Criteria. Our retrospective analysis included pts aged >18 years with pathologically proven diagnosis of AA or GBM. All histologic specimens were classified according to World Health Organisation (WHO) criteria, after surgery or stereotactic biopsy. Other inclusion criteria were a Karnofsky Index (KI) of 60–100, normal haematological, renal, and hepatic functions, absence of previous (with the exception of nonmelanoma skin cancer and carcinoma in situ of the cervix) or concurrent neoplasm, and absence of any other remarkable disease.

2.2. Patients' Characteristics. The study refers to 64 consecutive pts referred to our Departments of Radiotherapy that started brain neoplasm treatment from January 1997 to November 2001.

Out of 64 pts, 29 were females and 35 males, with age ranging from 26 to 78 years, with a median of 59 years. In 12 pts, with inoperable diseases, only a stereotactic biopsy was performed and in 52 pts a surgical resection was performed (30 subtotal and 22 total) (Tables 1 and 2).

The histology of the neoplasm was glioblastoma multiforme (GBM, in 43 patients of groups A + B) and anaplastic astrocytoma (AA, in 21 pts of groups A + B). The control group histology (group C) included 50 pts with GBM and 14 pts with AA.

2.3. Treatment. The 64 pts of groups A + B were treated with RT and oral TMZ. Median total dose of RT delivered was 63.5 Gy (range 45 Gy–66 Gy), with conventional fractionation, according to ICRU recommendations (Table 1). Ten pts

were treated with a total dose less than 60 Gy because of their low (60 to 75) KI or disease progression during the treatment.

Irradiation volume was determined on preoperative computed tomography (CT) and magnetic resonance (MR) of the brain and planning target volume (PTV) included the neoplasm, the surrounding oedema, and a margin of 2 cm in all directions [10]. All pts were immobilised with a customised thermoplastic mask. Three-dimensional treatment planning was obtained on the basis of CT performed with pt immobilised in therapy position.

The first 31 pts from January 1997 to June 1999 (group A) were treated with RT and adjuvant TMZ (200 mg/m^2/d × 5 days, every 28 days for 6 cycles) and the other 33 from July 1999 to November 2001 (group B) with RT and concomitant TMZ (75 mg/m^2/d × 7 d/wk for 6 weeks) followed by adjuvant TMZ (200 mg/m^2/d × 5 days, every 28 days for 5-6 cycles).

During the concomitant and adjuvant radiochemotherapeutic regimens, prophylactic antiemetic therapy (Ondansetron 8 mg/die or Granisetron 2 mg/die) was routinely prescribed. Anticonvulsant and corticosteroids were used only as required.

The results obtained in the 31 pts of group A have been compared with those of the 33 of group B. Finally we have compared the results obtained in these 64 pts (group A + group B) with those of a historical group of 64 consecutive pts (group C), with similar clinical characteristics, treated with RT alone at the same institutions from April 1994 to December 1996 (Table 2).

2.4. Statistical Analysis. Survival was calculated actuarially using the Kaplan Meier method, and significance was assessed using the log-rank test. Multivariate analysis by the Cox Regression Model was performed for identifying the independent prognostic variables governing the clinical end points.

The length of survival was considered from the end of radiation treatment until the last follow-up or the death.

3. Results

3.1. Survival. At the time of this analysis, May 2014, 3 pts (9.6%) in group A with AA and 5 pts (15.1%) in group B with AA are still alive, and 56 pts are dead (28 pts in group A and 28 pts in group B). The median follow-up in group A pts has been 18 months (range 6–89) and in group B 16 months (range 3–70).

On the basis of Kaplan Meiers estimates, the 1- and 2-year overall survival rates (OS) were, respectively, 74% and 29% in group A pts and 73% and 30% in group B ($P = 0.8$ not statistically significant) (Figure 1).

On the contrary, a statistically significant better 2-year OS was observed in pts with age ≤55 years ($P = 0.04$) and/or with diagnosis of AA ($P < 0.0001$) and/or with total dose delivered ≥60 Gy ($P = 0.001$) (Table 4).

The multivariate analysis, using stratified Cox regression, disclosed a significant better 2-year OS associated with age ≤55 years ($P = 0.04$), diagnosis of AA ($P = 0.0003$), and type of surgery ($P = 0.05$). Timing of TMZ administration (group A versus group B) was not statistically significant (Table 5).

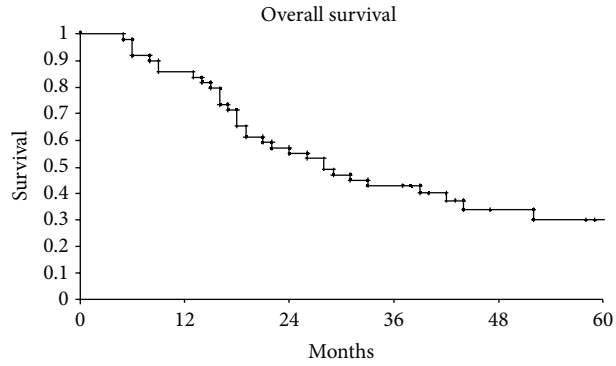

Figure 1: Overall survival of our series.

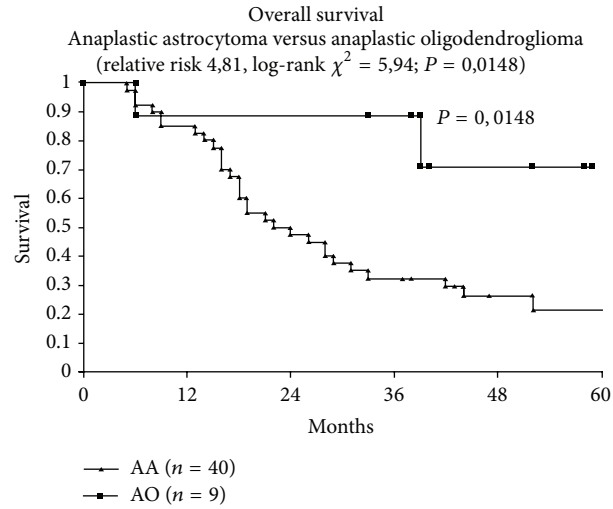

Figure 2: Overall survival anaplastic astrocytoma versus anaplastic oligodendroglioma.

Comparing the results of the 64 pts of groups A + B versus the 64 pts of group C, the median follow-up in groups A + B pts has been 17.5 months (range 3–89) and in group C pts 14 months (range 4–62). On the basis of Kaplan Meier estimates, the median OS was 15 months: 14 months in subjects not treated with TMZ (group C) and 17.5 months in the patients (groups A + B) that received TMZ ($P = 0.0001$) (Figure 2). Age, AA histology, and administration of TMZ were statistically significant prognostic factors for 2-year OS in the univariate analysis using Kaplan Meier method and compared with log-rank test: age ≤ 55 years $P = 0.007$; AA histology $P < 0.0001$; administration of TMZ $P = 0.0001$ (Table 6).

PFS was for GBM 9 months and for AA 11.

The salvage therapies employed in local recurrence are fotemustine, antiangiogenic drugs, and temozolomide.

3.2. Toxicity. We analysed complications of the 64 pts treated with RT and TMZ according to the WHO-RTOG scale. Grade 3 (G3) haematological toxicity was scored in 6 pts

Table 3: G3 haematological toxicity in group A and group B patients.

	Group A	Group B
Patients' number	31	33
Haematological toxicity	6.4%	12.1%
Thrombocytopenia	0%	3%
Neutropenia	3.2%	6%
Thrombocytopenia-neutropenia	3.2%	3%

Table 4: Univariate analysis group A and group B patients.

Prognostic factors	Pts' number	2-year OS	P
Age			
≤55 years	26	38.4%	0.04
>55 years	38	23.7%	
Sex			
Male	35	28.6%	n.s.
Female	29	31%	
Histology			
Anaplastic astrocytoma	21	52.4%	<0.0001
Glioblastoma Multiforme	43	16.3%	
Surgery			
Stereotactic biopsy	12	25%	
Subtotal resection	30	23.3%	n.s.
Total resection	22	36.6%	
Timing TMZ			
Adjuvant	31	29%	n.s.
Concomitant/adjuvant	33	30%	
RT total dose			
≥60 Gy	54	33.3%	0.001
<60 Gy	10	10%	

(9% of pts): 2 belonging to group A and 4 to group B ($P = 0.6$ not statistically significant) (Table 3).

In group A pts, during adjuvant chemotherapy, only one patient developed G3 neutropenia-thrombocytopenia and a further subject showed G3 neutropenia alone. No pts of group A experienced thrombocytopenia alone. In the subjects treated with concomitant TMZ and RT (group B) we observed G3 neutropenia in 2 cases, G3 thrombocytopenia in 1, and neutropenia and thrombocytopenia in a further r patient (Table 3).

No G4 haematological toxicity was observed.

The other acute side effects (G1-G2 nausea, vomiting, and fatigue), reported in 10 pts, of groups A + B were mild or easily controlled with medications.

4. Discussion

Malignant gliomas are among the most uncontrollable, devastating, and fatal cancers. The benefit of RT alone, in inoperable pts, or in combination with surgery, has been demonstrated in phase III trials at the end of seventies [11–14]. In order to improve the outcome, various combinations of surgery, RT, and chemotherapy have been tried in several studies, unfortunately with inconclusive results [1–6]. A meta-analysis [7] has pointed out significant improvement in survival adding nitrosourea based regimens.

TMZ is nowadays the first line chemotherapeutic drug in GBM therapy. Our study confirms its usefulness and the lack of heavy side effects.

Experimental studies demonstrated in vitro synergistic effect, in inhibiting glioblastoma cell lines growth, by using

Table 5: Multivariate analysis group A and group B patients.

Prognostic factors	P
Age	
≤55 years–>55 years	0.04
Sex	
Male—female	n.s.
Histology	
AA—GBM	0.0003
Surgery	
Stereotactic Biopsy—subtotal resection—total resection	0.05
Timing TMZ	
Adjuvant—concomitant/adjuvant	n.s.
RT total dose	
<60 Gy–≥60 Gy	0.0001

Table 6: Univariate analysis groups A + B and group C patients.

Prognostic factors	Pts' number	2-year OS	P
Age			
≤55 years	47	29%	0.007
>55 years	81	15%	
Sex			
Male	74	17.5%	n.s.
Female	54	22%	
Histology			
Anaplastic astrocytoma	36	40%	<0.0001
Glioblastoma multiforme	92	11.8%	
Surgery			
Stereotactic biopsy	23	25%	
Subtotal resection	65	14%	n.s.
Total resection	40	26%	
Treatment schedule			
RT + TMZ	64	29.6%	0.0001
RT alone	64	9.3%	
RT total dose			
≥60 Gy	109	22%	0.003
<60 Gy	19	10.5%	

TMZ and fractionated RT [15]. On the basis of these suggestions, phase I and II clinical trials investigated the efficacy of this association, with promising results [16–24].

According to these encouraging experiences in 1997 we started to treat pts affected by high grade gliomas with a combination of TMZ and RT. The results of our study confirm the literature data regarding tolerability and usefulness of this schedule.

The main toxicity in our experience has been haematological, with G3 neutropenia, thrombocytopenia, or both observed in 9% of cases and above all in concomitant/adjuvant TMZ administration, without statistical significance. Similar incidence of haematological toxicity has been reported in Stupp phase II trial [22] and in other preliminary experiences [16, 25]. In our series we observed neither G4 haematological side effects nor infections of *Pneumocystis carinii* [17, 22]. Moreover nonhaematological toxicities were mild and easily controlled by medical therapies.

The median survival obtained in our pts is similar to that reported in other publications [26–30]. Two-year OS in groups A + B pts was 29.6% but 9.3% in group C ($P = 0.0001$), suggesting a significant improvement of prognosis by combined treatment. Similar results, using RT and TMZ, have been shown in other phase II trials with 2-year survival ranging from 29% to 38% [26–30]. Moreover in the multicentric randomized EORTC-NCIC 26981 trial 2-year survival was 26% in the 287 pts of RT + TMZ arm versus 8% in the 286 pts of RT alone arm ($P < 0.0001$) [24, 31].

In our pts no statistically significant difference in OS between adjuvant and concomitant/adjuvant TMZ administration was observed. Anyway preclinical studies and larger clinical trials have suggested additive or perhaps synergistic activity combining TMZ and RT [22].

In agreement with literature [22, 32, 33], our data confirm that age and histology represent important prognostic factors in this disease. In fact both univariate and multivariate analyses showed that pts with age ≤55 years and diagnosis of anaplastic astrocytoma have a significantly better survival.

Improvement of prognosis, obtained using RT and TMZ in malignant gliomas in several phase II series and above all in the phase III EORTC-NCIC 26981 trial on GBM, suggests that actually this treatment can be used routinely in clinical practice [24].

Despite these interesting results the prognosis of malignant gliomas remains poor. Concerning this, great advances could come from research into genetic features of brain tumours, with the aim of characterising molecular profiles of neoplasm [34]. These developments will identify novel drug targets and therapeutic strategies, in order to individuate subgroups of pts receiving tailored treatments, on the basis of the genetic findings of their cancers [34]. According to these remarks, some recent reports show the preliminary results of combining TMZ with other drugs active against biological targets, particularly antiangiogenic drugs like thalidomide [35] and rofecoxib [36] and other proposed "old" drugs like metformin and arsenic trioxide [37].

In order to increase the efficacy of TMZ, Brock et al. [35] have employed in 67 pts with glioblastoma an association of TMZ, thalidomide, and RT. They observed an acceptable tolerance and a favourable survival outcome when compared with a historical group of pts treated with RT alone or RT and nitrosourea adjuvant chemotherapy.

Similar findings were reported by Baumann et al. [36] in a recent publication, whereas in a preliminary study TMZ was tested in pts with GBM in combination with the COX-2 inhibitor rofecoxib, another antiangiogenic agent, in order to evaluate the safety and activity of this association [38].

Moreover several phase I and II trials are exploring possible therapeutic approaches with schedules containing TMZ and new drugs [23, 39, 40].

Some authors believe that the additions of TMZ do not change the pattern of progression of GBM after radiotherapy (GUNJUR A. J. M. I. and RADIATION ONCOLOGY 2012).

On the contrary, the majority, considering that patients aged 75 or older represent half of all patients with GBM, retain that older cohort (>65 years) should not be excluded from treatments as was shown in NOA-8 phase III study; data from randomized and nonrandomized studies show encouraging results.

Finally, elderly patients will soon represent the vast majority of patients with GBM and they deserve to be treated at the best way possible; future studies should include the older patients with stratification of comorbidities and PS.

For what concerns anaplastic astrocytomas, the treatment of anaplastic glioma varies depending on histopathology of the tumor, molecular markers, and individual patient characteristics. As opposed to the standard treatment of glioblastoma, based on Stupp trial, there is no accepted standard treatment for AG. AA is most often treated with radiotherapy, with or without concomitant TMZ and with or without adjuvant temozolomide. Temozolomide has largely replaced PCV (procarbazine, CCNU, and vincristine) as the chemotherapeutic agent for AO and AOA, largely due to greater tolerability and less potential for toxicity. However, whether temozolomide has similar efficacy to PCV has not been fully evaluated. Patients, who have progressed after RT alone, may be treated with TMZ or PCV. A valid option, at the recurrence, is stereotactic radiosurgery and we employ this modality in many patients.

In conclusion there is, today, an improvement in surgical techniques, such as fluorescence guided resection and neuroendoscopic approaches; new discoveries will be made in basic and translation research, with block of cancer proliferation (e.g., TMZ, BEVACIZUMAB, IHDAC, anti-P53 inhibitors, inhibition of cancer stem cells, more advanced and precise radiation techniques, inhibitors of EGFR, TKI, NF-KB, inhibitors of mTOR, Pi 3k/AKT, and proteasome) and new delivery of drugs in nanoparticles and liposomes and the introduction in clinical practice of antipsychotic drugs (like haloperidol of II and III generation). All that will, probably, improve survival and quality of life in such a devastating disease.

5. Conclusions

Continuous daily TMZ and concomitant RT followed by adjuvant TMZ are safe and can prolong survival in pts with

high grade gliomas. Our report confirms the beneficial role of the association RT + TMZ on long (>10 y) follow-up. It must be stressed that this association resulted in life-saving on a 13-year time span in 3 out the 21 patients (14.1%) with anaplastic astrocytoma.

There is today a large interest in new treatments in gliomas like improvement in surgical techniques such as fluorescence guided resection and neuroendoscopic approaches. New discoveries are made in basic and translation research, and old and new drugs have been proposed as promising agents in brain tumors care [41–50]. More advanced and precise radiation techniques, inhibitors of EGFR, TKI, NF-KB, inhibitors of mTOR, Pi 3k/AKT, proteasome, and new delivery of drugs in nanoparticles, liposomes, and the introduction in clinical practice of antipsychotic drugs (like haloperidol of II and III generation) could be beneficial. All these improvements and developments will, probably, improve survival and quality of life in such a devastating disease.

Conflict of Interests

The authors declare that there is no conflict of interests regarding the publication of this paper.

References

[1] L. M. DeAngelis, P. C. Burger, S. B. Green, and J. G. Cairncross, "Malignant glioma: who benefits from adjuvant chemotherapy?" *Annals of Neurology*, vol. 44, no. 4, pp. 691–695, 1998.

[2] E. Galanis and J. Buckner, "Chemotherapy for high-grade gliomas," *British Journal of Cancer*, vol. 82, no. 8, pp. 1371–1380, 2000.

[3] J. Del Rowe, C. Scott, M. Werner-Wasik et al., "Single-arm, open-label phase II study of intravenously administered tirapazamine and radiation therapy for glioblastoma multiforme," *Journal of Clinical Oncology*, vol. 18, no. 6, pp. 1254–1259, 2000.

[4] H. A. Fine, K. B. G. Dear, J. S. Loeffler, P. M. Black, and G. P. Canellos, "Meta-analysis of radiation therapy with and without adjuvant chemotherapy for malignant gliomas in adults," *Cancer*, vol. 71, no. 8, pp. 2585–2597, 1993.

[5] B. J. Fisher, C. Scott, D. R. Macdonald, C. Coughlin, and W. J. Curran, "Phase I study of topotecan plus cranial radiation for glioblastoma multiforme: results of Radiation Therapy Oncology Group trial 9507," *Journal of Clinical Oncology*, vol. 19, no. 4, pp. 1111–1117, 2001.

[6] D. Thomas, M. Brada, S. Stenning et al., "Randomized trial of procarbazine, lomustine, and vincristine in the adjuvant treatment of high-grade astrocytoma: a Medical Research Council Trial," *Journal of Clinical Oncology*, vol. 19, no. 2, pp. 509–518, 2001.

[7] Glioma Meta-Analysis Trialist (GMT) Group, "Chemotherapy in adult high-grade glioma: a systematic review and meta-analysis of individual patient data from 12 randomised trials," *The Lancet*, vol. 359, no. 9311, pp. 1011–1018, 2002.

[8] R. Stupp, M. Gander, S. Leyvraz, and E. Newlands, "Current and future developments in the use of temozolomide for the treatment of brain tumours," *The Lancet Oncology*, vol. 2, no. 9, pp. 552–560, 2001.

[9] P. Corsa, S. Parisi, M. Piombino et al., "A preliminary retrospective study with temozolomide and radiotherapy versus radiotherapy alone for the treatment of high-grade gliomas," *International Journal of Radiation Oncology, Biology, Physics*, vol. 57, supplement 2, p. S378, 2003.

[10] E. P. M. Jansen, L. G. H. Dewit, M. Van Herk, and H. Bartelink, "Target volumes in radiotherapy for high-grade malignant glioma of the brain," *Radiotherapy and Oncology*, vol. 56, no. 2, pp. 151–156, 2000.

[11] A. P. Andersen, "Postoperative irradiation of glioblastomas. Results in a randomized series," *Acta Radiologica: Oncology*, vol. 17, pp. 474–484, 1978.

[12] K. Kristiansen, S. Hagen, T. Kollevold et al., "Combined modality therapy of operated astrocytomas grade III and IV. Confirmation of the value of postoperative irradiation and lack of potentiation of bleomycin on survival time: a prospective multicenter trial of the Scandinavian Glioblastoma Study Group," *Cancer*, vol. 47, no. 4, pp. 649–652, 1981.

[13] W. R. Shapiro and D. F. Young, "Treatment of malignant glioma. A controlled study of chemotherapy and irradiation," *Archives of Neurology*, vol. 33, no. 7, pp. 494–500, 1976.

[14] M. D. Walker, E. Alexander Jr., W. E. Hunt et al., "Evaluation of BCNU and/or radiotherapy in the treatment of anaplastic gliomas. A cooperative clinical trial," *Journal of Neurosurgery*, vol. 49, no. 3, pp. 333–343, 1978.

[15] J. Van Rijn, J. J. Heimans, J. Van Den Berg, P. Van Der Valk, and B. J. Slotman, "Survival of human glioma cells treated with various combination of temozolomide and X-rays," *International Journal of Radiation Oncology Biology Physics*, vol. 47, no. 3, pp. 779–784, 2000.

[16] M. Brada, K. Hoang-Xuan, R. Rampling et al., "Multicenter phase II trial of temozolomide in patients with glioblastoma multiforme at first relapse," *Annals of Oncology*, vol. 12, no. 2, pp. 259–266, 2001.

[17] S. M. Chang, K. R. Lamborn, M. Malec et al., "Phase II study of temozolomide and thalidomide with radiation therapy for newly diagnosed glioblastoma multiforme," *International Journal of Radiation Oncology, Biology, Physics*, vol. 60, no. 2, pp. 353–357, 2004.

[18] O. L. Chinot, S. Honore, H. Dufour et al., "Safety and efficacy of temozolomide in patients with recurrent anaplastic oligodendrogliomas after standard radiotherapy and chemotherapy," *Journal of Clinical Oncology*, vol. 19, no. 9, pp. 2449–2455, 2001.

[19] H. S. Friedman, R. E. McLendon, T. Kerby et al., "DNA mismatch repair and O6-alkylguanine-DNA alkyltransferase analysis and response to temodal in newly diagnosed malignant glioma," *Journal of Clinical Oncology*, vol. 16, no. 12, pp. 3851–3857, 1998.

[20] M. Gilbert, J. Olson, and W. Yung, "Preradiation treatment of newly diagnosed anaplastic astrocytomas and glioblastoma multiforme using temozolomide," *Neuro-Oncology*, vol. 2, abstract 77, p. 264, 2000.

[21] E. S. Newlands, M. F. G. Stevens, S. R. Wedge, R. T. Wheelhouse, and C. Brock, "Temozolomide: a review of its discovery, chemical properties, pre-clinical development and clinical trials," *Cancer Treatment Reviews*, vol. 23, no. 1, pp. 35–61, 1997.

[22] R. Stupp, P.-Y. Dietrich, S. O. Kraljevic et al., "Promising survival for patients with newly diagnosed glioblastoma multiforme treated with concomitant radiation plus temozolomide followed by adjuvant temozolomide," *Journal of Clinical Oncology*, vol. 20, no. 5, pp. 1375–1382, 2002.

[23] B. Yamini, X. Yu, G. Y. Gillespie, D. W. Kufe, and R. R. Weichselbaum, "Transcriptional targeting of adenovirally delivered tumor necrosis factor α by temozolomide in experimental glioblastoma," *Cancer Research*, vol. 64, no. 18, pp. 6381–6384, 2004.

[24] R. Stupp, W. P. Mason, M. J. van den Bent et al., "Radiotherapy plus concomitant and adjuvant temozolomide for glioblastoma," *The New England Journal of Medicine*, vol. 352, no. 10, pp. 987–996, 2005.

[25] W. K. A. Yung, R. E. Albright, J. Olson et al., "A phase II study of temozolemide vs. procarbazine in patients with glioblastoma multiforme at first relapse," *British Journal of Cancer*, vol. 83, no. 5, pp. 588–593, 2000.

[26] H. Athanassiou, M. Synodinou, E. Maragoudakis et al., "Randomized phase II study of temozolomide and radiotherapy compared with radiotherapy alone in newly diagnosed glioblastoma multiforme," *Journal of Clinical Oncology*, vol. 23, no. 10, pp. 2372–2377, 2005.

[27] S. Chibbaro, L. Benvenuti, A. Caprio et al., "Temozolomide as first-line agent in treating high-grade gliomas: phase II study," *Journal of Neuro-Oncology*, vol. 67, no. 1-2, pp. 77–81, 2004.

[28] L. Cionini, A. Tagliagambe, L. Fatigante et al., "A phase 2 study with concurrent and sequential temozolomide combined with radiation therapy in high grade gliomas," *International Journal of Radiation Oncology ∗ Biology ∗ Physics*, vol. 51, supplement 3, p. S206, 2001.

[29] S. E. Combs, S. Gutwein, D. Schulz-Ertner et al., "Phase I/II-study of temozolomide combined with radiation as postoperative treatment in primary glioblastoma multiforme," *International Journal of Radiation Oncology, Biology, Physics*, vol. 60, supplement 1, pp. S258–S259, 2004.

[30] G. Lanzetta, C. Campanella, A. Rozzi et al., "Temozolomide in radio-chemotherapy combined treatment for newly-diagnosed glioblastoma multiforme: phase II clinical trial," *Anticancer Research*, vol. 23, no. 6, pp. 5159–5164, 2003.

[31] R. O. Mirimanoff, W. Mason, R. Kortmann et al., "Radiotherapy (RT) and concomitant and adjuvant Temozolomide (TMZ) versus Radiotherapy alone for newly diagnosed glioblastoma (GBM): overall results and Recursive Partitioning Analysis (RPA) of a phase III randomized trial of the EORTC Brain Tumor and Radiotherapy Groups and NCIC Clinical Trial Group," *International Journal of Radiation Oncology, Biology, Physics*, vol. 60, supplement 1, p. S162, 2004.

[32] W. J. Curran Jr., C. B. Scott, J. Horton et al., "Recursive partitioning analysis of prognostic factors in three radiation therapy oncology group malignant glioma trials," *Journal of the National Cancer Institute*, vol. 85, no. 9, pp. 704–710, 1993.

[33] C. B. Scott, C. Scarantino, R. Urtasun et al., "Validation and predictive power of Radiation Therapy Oncology Group (RTOG) recursive partitioning analysis classes for malignant glioma patients: a report using RTOG 90-06," *International Journal of Radiation Oncology Biology Physics*, vol. 40, no. 1, pp. 51–55, 1998.

[34] D. R. Macdonald, "New frontiers in the treatment of malignant glioma," *Seminars in Oncology*, vol. 30, no. 6, pp. 72–76, 2003.

[35] C. S. Brock, E. S. Newlands, S. R. Wedge et al., "Phase I trial of temozolomide using an extended continuous oral schedule," *Cancer Research*, vol. 58, no. 19, pp. 4363–4367, 1998.

[36] F. Baumann, M. Bjeljac, S. S. Kollias et al., "Combined thalidomide and temozolomide treatment in patients with glioblastoma multiforme," *Journal of Neuro-Oncology*, vol. 67, no. 1-2, pp. 191–200, 2004.

[37] M. Carmignani, M. Aldea, O. Soritau et al., "Glioblastoma stem cells: a new target for metformin and arsenic trioxide," *Journal of Biological Regulators and Homeostatic Agents*, vol. 2, pp. 1–15, 2014.

[38] J. Tuettenberg, R. Grobholz, T. Korn, F. Wenz, R. Erber, and P. Vajkoczy, "Continuous low-dose chemotherapy plus inhibition of cyclooxygenase-2 as an antiangiogenic therapy of glioblastoma multiforme," *Journal of Cancer Research and Clinical Oncology*, vol. 131, no. 1, pp. 31–40, 2005.

[39] M. Bartolomei, C. Mazzetta, D. Handkiewicz-Junak et al., "Combined treatment of glioblastoma patients with locoregional pre-targeted ^{90}Y-biotin radioimmunotherapy and temozolomide," *Quarterly Journal of Nuclear Medicine and Molecular Imaging*, vol. 48, no. 3, pp. 220–228, 2004.

[40] R. Ravizza, E. Cereda, E. Monti, and M. B. Gariboldi, "The piperidine nitroxide Tempol potentiates the cytotoxic effects of temozolomide in human glioblastoma cells," *International Journal of Oncology*, vol. 25, no. 6, pp. 1817–1822, 2004.

[41] P. Corsa, S. Parisi, A. Raguso et al., "Temozolomide and radiotherapy as first-line treatment of high-grade gliomas," *Tumori*, vol. 92, no. 4, pp. 299–305, 2006.

[42] C. A. Barker, A. J. Bishop, M. Chang, K. Beal, and T. A. Chan, "Valproic acid use during radiation therapy for glioblastoma associated with improved survival," *International Journal of Radiation Oncology Biology Physics*, vol. 86, no. 3, pp. 504–509, 2013.

[43] G. D. Guthrie and S. Eljamel, "Impact of particular antiepileptic drugs on the survival of patients with glioblastoma multiforme," *Journal of Neurosurgery*, vol. 118, no. 4, pp. 859–865, 2013.

[44] P. Evers, P. P. Lee, J. DeMarco et al., "Irradiation of the potential cancer stem cell niches in the adult brain improves progression-free survival of patients with malignant glioma," *BMC Cancer*, vol. 10, article 384, 2010.

[45] H. C. Tsai, K. C. Wei, C. N. Tsai et al., "Effect of valproic acid on the outcome of glioblastoma multiforme," *British Journal of Neurosurgery*, vol. 26, no. 3, pp. 347–354, 2012.

[46] S. Scoccianti, S. M. Magrini, U. Ricardi et al., "Patterns of care and survival in a retrospective analysis of 1059 patients with glioblastoma multiforme treated between 2002 and 2007: a multicenter study by the central nervous system study group of Airo (Italian association of radiation oncology)," *Neurosurgery*, vol. 67, no. 2, pp. 446–458, 2010.

[47] T. Iuchi, K. Hatano, T. Kodama et al., "Phase 2 trial of hypofractionated high-dose intensity modulated radiation therapy with concurrent and adjuvant temozolomide for newly diagnosed glioblastoma," *International Journal of Radiation Oncology Biology Physics*, vol. 88, no. 4, pp. 793–800, 2014.

[48] S. Scoccianti, S. M. Magrini, U. Ricardi et al., "Radiotherapy and temozolomide in anaplastic astrocytoma: a retrospective multicenter study by the Central Nervous System Study Group of AIRO (Italian Association of Radiation Oncology)," *Neuro-Oncology*, vol. 14, no. 6, pp. 798–807, 2012.

[49] T. S. Armstrong, J. S. Wefel, M. Wang et al., "Net clinical benefit analysis of radiation therapy oncology group 0525: a phase III trial comparing conventional adjuvant temozolomide with dose-intensive temozolomide in patients with newly diagnosed glioblastoma," *Journal of Clinical Oncology*, vol. 31, no. 32, pp. 4076–4084, 2013.

[50] A. Gunjur, M. Bressel, and G. Ryan, "The addition of temozolomide does not change the pattern of progression of glioblastoma multiforme post-radiotherapy," *Journal of Medical Imaging and Radiation Oncology*, vol. 56, no. 5, pp. 567–573, 2012.

Hindawi Publishing Corporation
BioMed Research International
Volume 2014, Article ID 297293, 10 pages
http://dx.doi.org/10.1155/2014/297293

Review Article

Natural Compounds and Aging: Between Autophagy and Inflammasome

Shih-Yi Chuang,[1,2] Chih-Hung Lin,[3,4] and Jia-You Fang[1,2,5]

[1] *Pharmaceutics Laboratory, Graduate Institute of Natural Products, Chang Gung University, 259 Wen-Hwa 1st Road, Kweishan, Taoyuan 333, Taiwan*
[2] *Research Center for Industry of Human Ecology, Chang Gung University of Science and Technology, Kweishan, Taoyuan 333, Taiwan*
[3] *Center for General Education, Chang Gung University of Science and Technology, Kweishan, Taoyuan 333, Taiwan*
[4] *Chronic Diseases and Health Promotion Research Center, Chang Gung University of Science and Technology, Kweishan, Taoyuan 333, Taiwan*
[5] *Chinese Herbal Medicine Research Team, Healthy Aging Research Center, Chang Gung University, Kweishan, Taoyuan 333, Taiwan*

Correspondence should be addressed to Jia-You Fang; fajy@mail.cgu.edu.tw

Received 7 July 2014; Accepted 21 August 2014; Published 14 September 2014

Academic Editor: Chi-Feng Hung

Aging, a natural physiological process, is characterized by a progressive loss of physiological integrity. Loss of cellular homeostasis in the aging process results from different sources, including changes in genes, cell imbalance, and dysregulation of the host-defense systems. Innate immunity dysfunctions during aging are connected with several human pathologies, including metabolic disorders and cardiovascular diseases. Recent studies have clearly indicated that the decline in autophagic capacity that accompanies aging results in the accumulation of dysfunctional mitochondria, reactive oxygen species (ROS) production, and further process dysfunction of the NACHT, LRR, and PYD domains-containing protein 3 (NLRP3) inflammasome activation in the macrophages, which produce the proinflammatory cytokines. These factors impair cellular housekeeping and expose cells to higher risk in many age-related diseases, such as atherosclerosis and type 2 diabetes. In this review, we investigated the relationship between dysregulation of the inflammasome activation and perturbed autophagy with aging as well as the possible molecular mechanisms. We also summarized the natural compounds from food intake, which have potential to reduce the inflammasome activation and enhance autophagy and can further improve the age-related diseases discussed in this paper.

1. Introduction

Aging is a natural physiological process that affects a person with a progressive loss of physiological integrity over the passage of time. According to the World Health Organization (WHO), the proportion of the world's population over the age of 60 will rise to 22% by 2050 [1]. However, although everyone grows older as time passes, the degree of change of physiological function in different individuals may differ. Aging factors may have a variety of different sources, including changes in genes, cell imbalance, and organ senescence. Table 1 summarizes the cellular and molecular mechanisms related to the change process of aging. Several of the pathologies associated with aging, such as atherosclerosis and inflammation, involve uncontrolled cellular overgrowth or hyperactivity [2]. The immune system declines in reliability and efficiency with age, resulting in higher risk in the elderly for compromised pathology as a consequence of chronic inflammation such as atherosclerosis, Alzheimer's disease, and an increased susceptibility to infectious disease. Given the complexity of the issue, we attempted to elucidate and categorize the cellular and molecular mechanisms between the inflammasome activation and autophagy that occur with aging. In addition, several studies have indicated that food intake can reduce inflammation activation or increase autophagy to achieve health and longevity. We also discussed the usefulness of natural foods for promoting anti-inflammasome activity.

Table 1: The impact of aging on lifespans.

The molecular hallmarks of age	Age-related changes	Reference
Genomic instability		
Nuclear DNA	Chromosomal aneuploidies and copy number variations	[71–73]
Mitochondrial DNA	Replication errors cause polyclonal expansion of mtDNA mutations	[74]
Telomere exhaustion	Shortened telomeres exhibit decreased lifespans	[75, 76]
Epigenetic alterations		
Histone modifications	Deficiency in SIRT6 exhibits accelerated aging	[77]
DNA methylation	Polycomb target genes become hypermethylated with age	[78]
Chromatin remodeling	HP1α effects longevity in flies	[79]
Transcriptional alterations	Micro-RNA mir-71 is required for the lifespan extension	[80]
Loss of proteostasis		
Chaperone-mediated protein folding and stability	HSPs decline on longevity Accumulation and aggregation of abnormal proteins occur in aged organism	[81, 82]
Delay or dysfunction of autophagy	mTOR signaling in the regulation of mammalian lifespan	[83]
The ubiquitin-proteasome system	Enhancement of proteasome activity extends replicative lifespan in yeast	[84]
Deregulated nutrient sensing		
The insulin- and IGF-1-signaling pathway	Levels decline and dysfunction of GH/IGF-1 signaling pathway	[39, 85]
mTOR and AMPK	Inhibition of mTOR/DR pathway extends lifespan	[86, 87]
Mitochondrial dysfunction		
ROS	Amphibious effects of ROS on aging	[88–91]
Mitochondrial Integrity and Biogenesis	Reduced efficiency of telomerase activation with aging	[92]
Cellular senescence		
The INK4a/ARF Locus	Ink4a/ARF expression increases aging	[93, 94]
Stem cell attrition	Hematopoiesis declines with age resulting in a diminished production of adaptive immune cells Reduced in cell-cycle activity of hematopoietic stem cells (HSCs) on aged mice	[7, 95]
Inflammation	Activation of the NLRP3 inflammasome leading to increased production of IL-1β, TNF, and interferons	[36, 96]

SIRT6: sirtuin-6; HP1α: heterochromatin protein 1α; HSPs: heat shock proteins; mTOR: mammalian target of rapamycin; IGF-1: insulin/insulin growth factor 1; DR: dietary restriction; ROS: reactive oxygen species; AMPK: AMP-activated protein kinase; HSCs: hematopoietic stem cells; NLRP3: nucleotide-binding domain, leucine rich family (NLR), pyrin containing 3; IL-1β: interleukin-1β; TNF: tumor necrosis factor.

2. The Innate Immune System and Aging

The immune system, which protects an organism from disease, comprises two branches: innate and acquired immunity, including phagocyte lineages, such as macrophages, monocytes, dendritic cells (DCs), neutrophils and natural killer (NK) cells in an innate part, and B and T lymphocytes in an acquired part. Table 2 summarizes the process of aging-related changes in the immune system.

Innate immunity is the first line of host defense against microbe infection through diverse germline-encoded pattern-recognition receptors (PRRs) in phagocytes, such as Toll-like receptors (TLRs) and nucleotide-binding oligomerization domain- (NOD-) like receptors (NLRs), which recognize pathogen-associated molecular patterns (PAMPs) from pathogens or danger-associated molecular patterns (DAMPs) from damaged tissue in the body [3, 4].

Macrophages, one of the phagocytic cell lineages presented in most tissues, contribute to the innate immunity and are responsible for numerous inflammatory, immunological, and metabolic processes [5]. Macrophages play an important role in the recognition of danger signaling and the initiation of inflammatory responses, including clearance of pathogens via direct phagocytosis of invading pathogens or indirect release of cytokines and chemokines, which can activate and recruit other inflammatory cells to damaged sites. They also activate acquired immunity through the procession of antigens and presentation of peptides to T lymphocytes [5]. Aging-related changes to the macrophages contribute to the aging process via a functional shift toward a proinflammatory phenotype, which constitutively produces more interleukin- (IL-) 6, IL-1beta (IL-1β), and tumor necrosis factor (TNF) and reduced phagocytic function [6, 7]. Elevated plasma concentrations of IL-6, IL-1β, and TNF have been described in

Table 2: Alterations in the immune system associated with aging.

Immune system	Age-related changes	References
Innate immunity		
Monocytes or macrophages	Reduced levels of MHC class II complexes, reduced phagocytic capacity, and enhanced oxidative stress	[97, 98]
Neutrophils	Reduction in phagocytosis ability, impaired free radical production, and decreased rescue from apoptosis	[99]
Dendritic cells	Reduced antigen presentation and impaired phagocytic capability to clean apoptotic cells	[100]
Natural killer cells	Increased number of NK cells, reduced cytotoxicity, and impaired proliferation ability in response to IL-2 stimulation	[98]
Acquired immunity		
T cells	Reductions in T-cell thymopoiesis, accumulated highly differentiated memory T cells, loss of CD28 antigen and CD69 antigen for T cell activation and signal transduction, and reduced CD8+ cell proliferation in response to antigen stimulation	[101, 102]
B cells	Reductions in B-cell lymphopoiesis, increased memory B cells and fewer naive B cells, impaired antibody response to vaccination, and increased production of low-affinity antibodies due to decreased isotype switching	[98]

MHC II: major histocompatibility complex class II.

elderly populations and are postulated as predictive markers of functional disability, frailty, and mortality. The macrophage populations of the elderly appear to have reduced levels of major histocompatibility complex (MHC) class II, which contribute to poor $CD4^+$ T lymphocyte responses [8]. Furthermore, it has been found that the phagocytic function of macrophages in aging individuals declines. Aging also results in reduced secretion levels of chemokines, such as macrophage inflammatory protein- (MIP-) 1alpha (MIP-1α), MIP-1β, MIP-2, and eotaxin [9]. A significant decrease in macrophage precursors and macrophages in the bone marrow of elderly individuals has been described previously [10]. These results suggest that an age-related decline in macrophage function may reduce both innate and adaptive immunities.

Neutrophils are short-lived immune cells that play an important role in the antimicrobial host defense that protects the individual from both bacterial and fungal infections [11]. Phagocytosis, chemotaxis, and ROS production of neutrophils could be changed with aging [12]. Studies measuring phagocytosis of bacteria by the neutrophils have found a significant reduction in phagocytic ability in the elderly population [13, 14]. Larbi et al. [15] demonstrated that the age-related decline in neutrophil functions can be partially explained by the reduced Fc-gamma receptor expression. It has been shown that Fc-gamma receptor-mediated free radical generation and phagocytosis are altered with aging, which is clearly the result of changes in p42/p44 mitogen-activated protein kinase (MAPK) signaling pathways.

DCs play a critical role in linking the innate and the adaptive immune system. DCs are the most potent antigen-presenting cells that can prime naive $CD4^+$ T cells via antigen presentation. After Toll-like receptors (TLRs) stimulation such as TLR7 and TLR9, for example, the plasmacytoid dendritic cells (pDCs) produce type I interferon to defend against viral infections and activate NK cells to amplify the host response and help to clear the virus [16–18]. Myeloid dendritic cells (mDCs) are professional antigen-presenting cells to T lymphocytes. They express TLRs and C-type lectin receptors (CLRs) for the detection of viruses. They also produce cytokines, such as IL-12, to induce cytotoxic T-cell responses, which clear virus-infected cells [19]. Epidermal Langerhans cells (LCs), originally described as epidermal DCs, maintain immune homeostasis in the skin by activating skin-resident regulatory T cells. These contain langerin, large granules capable of phagocytosis [20]. LCs are impaired in their phagocytic ability to induce ovalbumin- (OVA-) specific $CD4^+$ and $CD8^+$ T-cell proliferation in aged mice [20]. Besides presenting the antigens, they also provide the costimulatory signals for optimal activation of NK cells and produce the cytokine IL-17, which is known to recruit neutrophils [21].

3. Inflammasome and Aging

In mammals, the inflammasome is a group of cytosolic receptors that recognize not only intracellular PAMPs, but also host-derived signal DAMPs. They control the production of proinflammatory cytokines, such as proinflammatory cytokines IL-1β and IL-18. The inflammasome is a multiprotein complex that contains at least two distinct classes of the NLR family or the pyrin domain (PYD) and HIN domain-containing (PYHIN) family. The inflammasome mediates the activation of caspase-1, leading to pro-IL-1β and pro-IL-18 processing [22]. In addition to the production of IL-1β and IL-18, the inflammasome/caspase-1 complexes may target different effector molecules to regulate diverse physiological functions, such as pyroptosis and tissue repair [23]. During inflammasome activation, NLRP3 can oligomerize through the central nucleotide-binding domain and then recruit an adaptor protein apoptosis-associated

speck-like protein containing CARD (ASC) with PYD and an amino-terminal caspase-recruitment-and-activation domain (CARD domain). NLRP3 would interact with the PYD domain of ASC through its own PYD domains, whereas the CARD domain of ASC recruits procaspase-1. Assembly of the inflammasome initiates self-cleavage of caspase-1 and the formation of the active heterotetrameric caspase-1. Active caspase-1 further proteolytically processes pro-IL-1β and pro-IL-18 to their mature forms [24]. At least six inflammasome complexes of the NLR family, including NACHT, LRR and PYD domains-containing protein (NLRP)1, NLRP3, CARD domain containing (NLRC)4, NLRP6, NLRP12, and PYHIN family, absent in melanoma 2 (AIM2), have been characterized [4].

Among the numerous inflammasome complexes, the NLRP3 inflammasome has been extensively studied and shown to be activated by a large variety of activators that do not share any structural similarities [3]. The NLRP3 inflammasome is proposed to be activated through a secondary mediator, including potassium efflux, reactive oxygen species (ROS), or lysosomal proteases [4]. The NLRP3 inflammasome requires two signals for its activation in macrophages. Stimulation with lipopolysaccharides (LPS) leads to TLR4 signaling-pathway activation in a nuclear factor kappa-light-chain-enhancer of activated B cells- (NF-κB-) dependent manner. This results in the synthesis of precursor forms of proinflammatory cytokines, including pro-IL-1β and NLRP3 proteins [25]. Further stimulation of cells with ATP activates the P_2X7 receptor, causing K^+ efflux through membrane pores, which results in the NLRP3 inflammasome assembly. Another proposed mechanism suggests the activation of NLRP3 by cathepsin B released from ruptured lysosomes following the phagocytosis of monosodium urate and alum. It is demonstrated by using cathepsin B inhibitors and lysosome inhibitors *in vitro* [26, 27]. ROS was proposed to be an upstream activator of the NLRP3 inflammasome, originating from the mitochondria (mROS). In contrast, mROS generation from a series of electron transport through the mitochondrial oxidative phosphorylation complex was essential for inflammasome activation. A finding by Zhou et al. [28] reveals that mitochondrial dysfunction activates mROS production. Treatment with NLRP3 activators results in the recruitment of NLRP3 to the mitochondria-associated ER membrane (MAM) where NLRP3 recruited ASC for inflammasome activation. Nakahira et al. [29] also demonstrated that LPS together with ATP causes loss of mitochondrial membrane potential and mROS generation due to the release of mitochondrial DNA (mtDNA). Furthermore, cytosolic mtDNA levels correlate with NLRP3-dependent IL-1β production. Interestingly, the findings by Zhou et al. [28] correlated with those by Nakahira et al. [29], which also suggested a role for autophagy in attenuating IL-1β production where caspase-1 activation is limited and where the NLRP3 relocates to MAMs through the clearance of damaged mROS production. Other critical effectors of NLRP3 activation have been reported in recent years. Thioredoxin-(TRX-) interacting protein (TXNIP) upon oxidative stress has been shown to dissociate from TRX and bind to NLRP3 to promote the NLRP3 activation and to be linked to the regulation of lipid and glucose metabolism [28]. MicroRNA-223 and ubiquitination of the NLRP3 are reported as negative regulators of the NLRP3 [30–32]. The NLRP3 inflammasome has been demonstrated to play a critical role in microbial pathogen infection [3, 33]. Nevertheless, dysregulation of the NLRP3 inflammasome activation has been associated with a variety of human diseases, including autoinflammatory diseases, Crohn's disease, type 2 diabetes, atherosclerosis, and cancers [22, 34].

A prominent age-dependent alteration is a slowly progressing proinflammatory phenotype, contributing to a long-term stimulation of the immune system. This can result in a low-grade proinflammatory status referred to as inflammaging, which accompanies the aging process in mammals [35, 36]. Several studies focused on the pattern of transcriptional factors on aging tissues found that overactivation of the I kappa B kinase- (IKK-) NF-κB pathway is one of the signatures of aging, revealing the inflammatory pathways in aging [37, 38]. More evidence shows that systemic inflammation links to inflammaging, including the accumulation of proinflammatory cytokines in metabolic organs, the overexpression of the NF-κB transcription factor in damaged tissue, or a defective autophagy-signaling pathway in phagocytes [36]. Dysregulation of the inflammatory cytokines response, such as IL-1β, TNF, and interferon, elicits pathological changes of type 2 diabetes and atherosclerosis, correlated with aging in the human population [22, 34, 39, 40].

4. Autophagy and Aging

Autophagy is considered an evolutionarily conserved cellular catabolic process, which facilitates the recycling of damaged proteins and organelles [41]. Three distinct types of autophagy coexist in most cells, including macroautophagy (usually referred to as autophagy), microautophagy, and chaperon-mediated autophagy (CMA). The three types of autophagy are well established and carry cytosolic proteins into the lysosomes for degradation. During autophagy, dysfunctional protein or organelles are sequestered into a double-membrane vesicle known as the autophagosome. The origin of the autophagosome, called the phagophore or isolation membrane, may be derived from the plasma membrane, Golgi, mitochondria, and endoplasmic reticulum (ER). Classical autophagy initiation is induced by nutrient deprivation followed by the inhibition of the mammalian target of rapamycin (mTOR), which recruits the UNC-51-like kinase (ULK) complex from the cytosol to the isolation membrane. This leads to the nucleation of the isolation membrane through the assembly of ATG14, Beclin 1, vacuolar protein sorting (VPS)15, class III phosphatidylinositol-3-OH kinase (PI(3)K), and VPS34 complexes. Additional proteins, such as Ambra 1, double FYVE-containing protein (DFCP)1, ATG9, and WD-repeat domain phosphoinositide-interacting (WIPI) protein, also regulate the nucleation step of autophagosome formation [41]. The next step is the elongation of the isolation membrane, which requires two ubiquitin-like protein conjugation systems. The first is the conjugation of ATG12-ATG5, which is covalently linked by

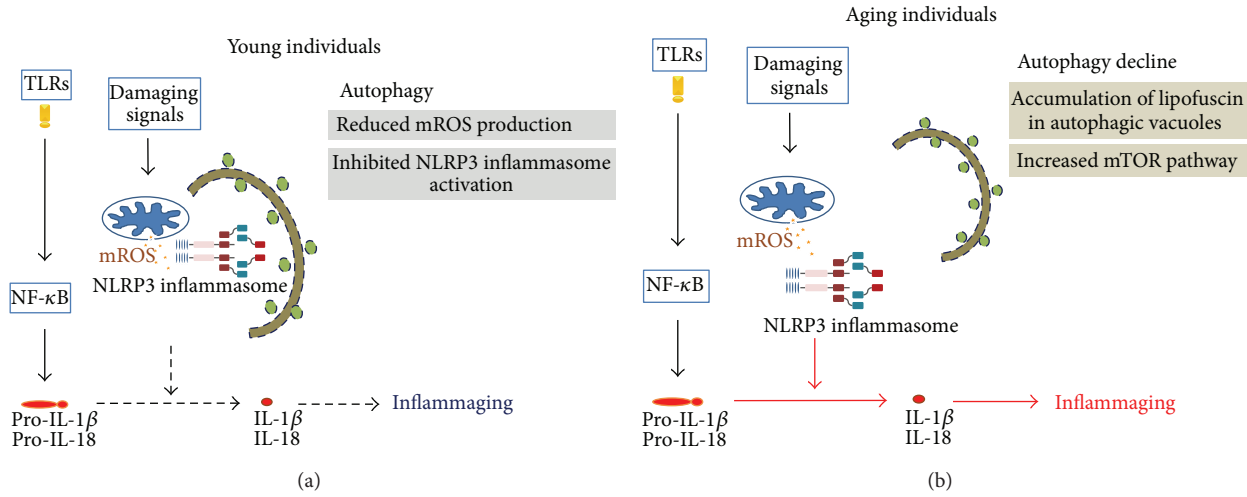

Figure 1: The schematic diagrams represent an overview of the signaling pathways between autophagy and inflammaging. In young individuals (left), autophagy may contribute to maintain the innate physiological lifespan through distinct mechanisms in clearing intracellular mitochondrial ROS (mROS) and NLRP3 inflammasome resulting in decreased inflammaging (black dashed lines), whereas dysfunction of autophagy homeostasis during aging results in increased inflammaging (red lines). However, autophagy protects against the NLRP3 inflammasome-dependent aging process. Aging is only one of the consequences that regulate the depicted signal transduction pathways.

ATG7 (E1-like) and ATG10 (E2-like) enzymes, and serves as a dimer complex that associates with ATG16L1. This multiple protein complex is crucial in autophagosome formation. The second is the conjugation of phosphatidylethanolamine- (PE-) microtubule-associated protein 1 light chain 3 (LC3), which is covalently linked by ATG7 (E1-like) and ATG3 (E2-like) enzymes. The ATG5-ATG12–ATG16 complex serves as the E3-like enzyme to generate PE-LC3 (LC3-II), which is incorporated into both the inner and outer membranes of the autophagosome. Autophagy is originally considered to be a nonselective bulk degradation process. Several lines of evidence suggest that selective autophagy occurs through the recognition of autophagy substrates, such as degradation of intracellular bacteria and viruses (xenophagy), regulation of the turnover of mitochondria (mitophagy), the clearance of polyubiquitinated protein aggregates (aggrephagy), and regulation of lipid metabolism (lipophagy). Increasing evidence has revealed that autophagy plays an important role in regulating immune responses and inflammation [41]. The engagement of TLR4 by LPS recruits the Toll-receptor-associated activator of interferon (TRIF) and the myeloid differentiation factor 88 (MyD88) adaptor. This leads to enhanced TRAF6 E3 ligase activity, which results in the K63-linked ubiquitination of Beclin 1 and the oligomerization of Beclin 1. This promotes the activation of PI(3)K and helps the formation of autophagosomes [42, 43]. Another study [44] reported that heat shock protein 90 (HSP90) plays an important role in mediating TLR4-induced autophagy. HSP90 mediates TLR4-induced autophagy through interaction with Beclin 1 and protects Beclin 1 from proteasome-mediated degradation. In addition, HSP90 and the kinase-specific cochaperone Cdc37 interact with ULK1 and promote its stability and activation. This in turn plays an important role in autophagy-mediated mitochondrial clearance [45]. Both TLRs and NLRs can induce autophagy through the activation of Beclin 1. NLRP4, on the other hand, displays an ability to inhibit autophagy [46]. Several studies have reported that autophagy and/or autophagy-related proteins play an important role in regulating mitochondria integrity, ROS generation, and the subsequent NLRP3 activation. Macrophages treated with 3-methyladenine (3MA), a chemical inhibitor of autophagy, or macrophages with the deletion of several autophagic components, including ATG16L1, ATG7, Beclin 1, and LC3, impair mitochondrial homeostasis and further induce more caspase-1 activation and IL-1β secretion in response to solely LPS or LPS+NLRP3 agonists [29, 47]. These data strongly suggest that autophagy negatively regulates the NLRP3 inflammasome activity. Autophagy is also a critical regulator of the organelles' homeostasis, particularly for aggregated protein and mitochondria in cells [41]. Damaged mitochondria that have lost their membrane potential and are more likely to release toxic apoptotic mediators and ROS serve as signaling to recruit selective autophagy (mitophagy) [29]. The aging process causes the deficient maintenance of proteostasis (see Table 1), resulting in the accumulation of damaged cellular components in old cells; for example, lipofuscin would destroy lysosome function, thus failing to clear the dysfunctional mitochondria [48]. In particular, dysfunction of mitochondrial homeostasis can increase mROS production and stimulate the NLRP3 inflammasome activation. Thus, autophagy declines with aging, enhancing the inflammaging process (Figure 1). Several regulatory mechanisms indicate that the age-related deficiency of autophagy can enhance the appearance of the inflammation phenotype in cells. It is well known that several redox-sensitive protein kinases, phosphatases, and proinflammatory cytokines can stimulate IKK-NF-κB signaling and ROS production, and the increased levels of ROS can feedback-activate NF-κB signaling. All of

Table 3: Classification of compounds from food sources associated with anti-NLRP3 inflammasome.

Category	Compounds	Molecular mechanism		Resources	References
Stilbenoids	Resveratrol	Inhibited NLRP3 activation Induced autophagy	Impaired caspase-1 and IL-1β expression Reduced the acetylation of cytoplasmic proteins	*Veratrum album*	[57, 58]
Flavonoids					
Flavonols	Quercetin	Suppressed renal NLRP3 activation	Impaired caspase-1 and IL-1β expression	Quercetum	[64, 65]
Flavones	Luteoloside	Inhibited NLRP3 activation	Reduced ROS accumulation Impaired NLRP3, caspase-1, and IL-1β expression	Honeysuckle	[61]
Flavan-3-ols	Catechins	Inhibited NLRP3 activation Enhanced autophagy	Impaired caspase-1 and IL-1β expression Enhanced Beclin 1 expression	Green tea	[37, 38]
	EGCG	Inhibited NLRP3 activation Enhanced autophagy	Reduced ROS accumulation, NF-κB activation, and NLRP3 expression Impaired caspase-1 and IL-1β expression	Green tea	[103–105]
Other phenolic compounds	Creosol	Impaired NLRP3 activation	Reduced iNOS expression and NO levels Decreased ROS production Impaired IL-1β expression	Bamboo vinegar (BV)	[59]
	Propolis extracts	Inhibited NLRP3 activation	Reduced the IL-1β secretion	Brazilian propolis	[60]

iNOS: inducible nitric oxide synthase; ROS: reactive oxygen species; IL: interleukin; MAPK: mitogen-activated protein kinase; EGCG: epigallocatechin-3-gallate; NF-κB: nuclear factor kappa-light-chain-enhancer of activated B cells.

them can produce prime activation of the inflammasome. Moreover, declines in autophagy can result in the loss of control activity of the NF-κB complex, which is degraded via selective autophagy [49, 50]. The loss of clearance function of autophagy with aging generates a comfortable situation for stimulating NF-κB signaling directly or indirectly, resulting in inflammasome-dependence in an age-related proinflammatory phenotype manner.

5. The Impact of Natural Compounds on Inflammaging

Aging in humans is associated with a high incidence of some chronic diseases and inflammaging-associated diseases, such as type 2 diabetes, atherosclerosis, and Alzheimer's disease. There is a need to develop a preventive strategy for prolonging the period of healthy life and preventing the pathogenesis of these inflammaging-associated diseases. Interestingly, inflammaging-associated diseases are highly related to NLRP3 activation or a decline in autophagy, which increases metabolic and oxidative stress and elevates a low-grade inflammation, which increases the levels of damage.

Food intake including vegetables, fruits, tea, and wine can reduce the development of age-related diseases [51, 52]. Emerging studies suggest that some phytochemical compounds have potential as inflammation inhibitors to impair NLRP3 activation or enhance autophagy. Four main categories of phytochemical compounds may improve inflammaging-related diseases through impaired NLRP3 activation or enhanced autophagy (Table 3).

Resveratrol is a stilbenoid compound that exists in many plant-derived foods such as grapes and red wine [53]. Several discoveries provide evidence demonstrating that a significant amount of resveratrol in the diet has beneficial effects on various chronic diseases and aging. It has been found that resveratrol can protect against type 2 diabetes, heart disease, and Alzheimer's disease [54–56]. In humans, there is still no solid evidence that resveratrol intake can extend lifespan. However, it has been found that resveratrol can protect against NLRP3 inflammasome activation and enhance autophagy [57, 58], which may be able to suppress oxidative stress and inflammation and point to a promising antiaging process.

Other phenolic compounds are described as being linked to anti-inflammatory activity. These compounds include creosol in bamboo vinegar [59] and propolis extracts in Brazilian propolis [60]. They are demonstrated potentially to inhibit NLRP3 activation through the reduction of MAPK and NF-κB activation, decrease ROS production, and impair IL-1β expression. All of them are suggested to improve the aging process [52].

Luteoloside and quercetin, naturally occurring flavonoids in food, exhibit health-beneficial properties and an antiaging effect for humans [52]. Luteoloside, isolated from the medicinal plant *Gentiana macrophylla*, has been demonstrated to show an anticancer effect against hepatocellular carcinoma

(HCC) cells through its effect of inhibiting the NLRP3 inflammasome through inhibiting proliferation, invasion, and metastasis of HCC cells in a mouse lung metastasis model [61]. Quercetin isolated from herbal foods has been reported previously to exhibit potential for anti-inflammation and antihyperlipidemia [62, 63]. Recent studies [64, 65] have demonstrated that quercetin could impair NLRP3 inflammasome activation to improve renal inflammation.

Catechins and epigallocatechin-3-gallate (EGCG) are abundant in teas derived from the tea plant *Camellia sinensis*. These products show the effect of ameliorating a variety of human diseases such as cancers, atherosclerotic lesions, and Alzheimer's disease [66–70]. Recent studies [37, 38] have shown that they also attenuate the *Helicobacter pylori*-triggered caspase-1 signaling pathway, oxidative stress, and apoptosis in the gastric mucosa of the *Helicobacter pylori*-infected mouse model.

6. Conclusion

A healthy lifestyle to avoid premature aging is achievable through maintaining a happy, relaxed mood, engaging in regular sports and exercise, not smoking or drinking, and following a nutrient-rich, low-calorie diet. Studies have shown that people who do not have a healthy lifestyle and do not adhere to a nutritious diet are at high risk of age-related diseases such as type 2 diabetes, cancer, and cardiovascular disease. In this review, we summarize the relationship between inflammaging and autophagy. There are indications that autophagic capacity is dysfunctional in age-related diseases. Autophagy declines with aging, triggering NLRP3 activation, and enhancing the inflammaging process. Decreased NLRP3 activation and increased autophagy can extend the lifespan. In this respect, the effective function of autophagic uptake in the clearance of dysfunctional mitochondria reduced oxidative stress and impaired NLRP3 activation is critical to maintaining cell homeostasis. Growing evidence shows that some foods containing natural compounds, such as resveratrol, catechins, EGCG, propolis extracts, creosol, and luteoloside, are categorized as antiaging molecules [52]. There is suggestion that dietary intake of these compounds may promote health and extend the lifespan via multiple mechanisms, including the reduction of oxidative stress, induction of autophagy, and suppression of NLRP3 activation. This can lead to a healthier and longer lifespan.

Conflict of Interests

The authors declare that there is no conflict of interests regarding the publication of this paper.

Authors' Contribution

Shih-Yi Chuang and Chih-Hung Lin are contributed equally to this paper.

Acknowledgments

The authors are grateful to the financial support by Chang Gung University and Chang Gung Memorial Hospital (Grant nos. EMRPD1D901 and CMRPD1B0332).

References

[1] A. Larbi, P. Rymkiewicz, A. Vasudev et al., "The immune system in the elderly: a fair fight against diseases?" *Aging Health*, vol. 9, no. 1, pp. 35–47, 2013.

[2] M. V. Blagosklonny, "Aging: ROS or TOR," *Cell Cycle*, vol. 7, no. 21, pp. 3344–3354, 2008.

[3] B. K. Davis, H. Wen, and J. P.-Y. Ting, "The Inflammasome NLRs in immunity, inflammation, and associated diseases," *Annual Review of Immunology*, vol. 29, pp. 707–735, 2011.

[4] V. A. K. Rathinam, S. K. Vanaja, and K. A. Fitzgerald, "Regulation of inflammasome signaling," *Nature Immunology*, vol. 13, no. 4, pp. 333–342, 2012.

[5] A. Chow, B. D. Brown, and M. Merad, "Studying the mononuclear phagocyte system in the molecular age," *Nature Reviews Immunology*, vol. 11, no. 11, pp. 788–798, 2011.

[6] H. M. Sadeghi, J. F. Schnelle, J. K. Thomas, P. Nishanian, and J. L. Fahey, "Phenotypic and functional characteristics of circulating monocytes of elderly persons," *Experimental Gerontology*, vol. 34, no. 8, pp. 959–970, 1999.

[7] A. C. Shaw, S. Joshi, H. Greenwood, A. Panda, and J. M. Lord, "Aging of the innate immune system," *Current Opinion in Immunology*, vol. 22, no. 4, pp. 507–513, 2010.

[8] C. Q. Wang, K. B. Udupa, H. Xiao, and D. A. Lipschitz, "Effect of age on marrow macrophage number and function," *Aging*, vol. 7, no. 5, pp. 379–384, 1995.

[9] M. E. Swift, A. L. Burns, K. L. Gray, and L. A. DiPietro, "Age-related alterations in the inflammatory response to dermal injury," *Journal of Investigative Dermatology*, vol. 117, no. 5, pp. 1027–1035, 2001.

[10] T. Ogawa, M. Kitagawa, and K. Hirokawa, "Age-related changes of human bone marrow: a histometric estimation of proliferative cells, apoptotic cells, T cells, B cells and macrophages," *Mechanisms of Ageing and Development*, vol. 117, no. 1–3, pp. 57–68, 2000.

[11] A. Mócsai, "Diverse novel functions of neutrophils in immunity, infammation, and beyond," *Journal of Experimental Medicine*, vol. 210, no. 7, pp. 1283–1299, 2013.

[12] A. C. Shaw, D. R. Goldstein, and R. R. Montgomery, "Age-dependent dysregulation of innate immunity," *Nature Reviews Immunology*, vol. 13, no. 12, pp. 875–887, 2013.

[13] R. Khanfer, D. Carroll, J. M. Lord, and A. C. Phillips, "Reduced neutrophil superoxide production among healthy older adults in response to acute psychological stress," *International Journal of Psychophysiology*, vol. 86, no. 3, pp. 238–244, 2012.

[14] C. Wenisch, S. Patruta, F. Daxböck, R. Krause, and W. Hörl, "Effect of age on human neutrophil function," *Journal of Leukocyte Biology*, vol. 67, no. 1, pp. 40–45, 2000.

[15] A. Larbi, N. Douziech, C. Fortin, A. Linteau, G. Dupuis, and T. Fulop Jr., "The role of the MAPK pathway alterations in GM-CSF modulated human neutrophil apoptosis with aging," *Immunity and Ageing*, vol. 2, article 6, 2005.

[16] A. Agrawal and S. Gupta, "Impact of aging on dendritic cell functions in humans," *Ageing Research Reviews*, vol. 10, no. 3, pp. 336–345, 2011.

[17] C. Romagnani, M. Della Chiesa, S. Kohler et al., "Activation of human NK cells by plasmacytoid dendritic cells and its modulation by CD4+ T helper cells and CD4+ CD25hi T regulatory cells," *European Journal of Immunology*, vol. 35, no. 8, pp. 2452–2458, 2005.

[18] R. Lande and M. Gilliet, "Plasmacytoid dendritic cells: key players in the initiation and regulation of immune responses," *Annals of the New York Academy of Sciences*, vol. 1183, pp. 89–103, 2010.

[19] T. Kawai and S. Akira, "Signaling to NF-κB by Toll-like receptors," *Trends in Molecular Medicine*, vol. 13, no. 11, pp. 460–469, 2007.

[20] J. Seneschal, R. A. Clark, A. Gehad, C. M. Baecher-Allan, and T. S. Kupper, "Human epidermal Langerhans cells maintain immune homeostasis in skin by activating skin resident regulatory T cells," *Immunity*, vol. 36, no. 5, pp. 873–884, 2012.

[21] H. W. Stout-Delgado, W. Du, A. C. Shirali, C. J. Booth, and D. R. Goldstein, "Aging promotes neutrophil-induced mortality by augmenting IL-17 production during viral infection," *Cell Host and Microbe*, vol. 6, no. 5, pp. 446–456, 2009.

[22] L. Zitvogel, O. Kepp, L. Galluzzi, and G. Kroemer, "Inflammasomes in carcinogenesis and anticancer immune responses," *Nature Immunology*, vol. 13, no. 4, pp. 343–351, 2012.

[23] E. A. Miao, J. V. Rajan, and A. Aderem, "Caspase-1-induced pyroptotic cell death," *Immunological Reviews*, vol. 243, no. 1, pp. 206–214, 2011.

[24] E. Latz, T. S. Xiao, and A. Stutz, "Activation and regulation of the inflammasomes," *Nature Reviews Immunology*, vol. 13, no. 6, pp. 397–411, 2013.

[25] G. Guarda, M. Zenger, A. S. Yazdi et al., "Differential expression of NLRP3 among hematopoietic cells," *Journal of Immunology*, vol. 186, no. 4, pp. 2529–2534, 2011.

[26] F. Martinon, V. Pétrilli, A. Mayor, A. Tardivel, and J. Tschopp, "Gout-associated uric acid crystals activate the NALP3 inflammasome," *Nature*, vol. 440, no. 7081, pp. 237–241, 2006.

[27] V. Hornung, F. Bauernfeind, A. Halle et al., "Silica crystals and aluminum salts activate the NALP3 inflammasome through phagosomal destabilization," *Nature Immunology*, vol. 9, no. 8, pp. 847–856, 2008.

[28] R. Zhou, A. Tardivel, B. Thorens, I. Choi, and J. Tschopp, "Thioredoxin-interacting protein links oxidative stress to inflammasome activation," *Nature Immunology*, vol. 11, no. 2, pp. 136–140, 2010.

[29] K. Nakahira, J. A. Haspel, V. A. K. Rathinam et al., "Autophagy proteins regulate innate immune responses by inhibiting the release of mitochondrial DNA mediated by the NALP3 inflammasome," *Nature Immunology*, vol. 12, no. 3, pp. 222–230, 2011.

[30] F. Bauernfeind, A. Rieger, F. A. Schildberg, P. A. Knolle, J. L. Schmid-Burgk, and V. Hornung, "NLRP3 inflammasome activity is negatively controlled by miR-223," *Journal of Immunology*, vol. 189, no. 8, pp. 4175–4181, 2012.

[31] M. Haneklaus, M. Gerlic, M. Kurowska-Stolarska et al., "Cutting edge: miR-223 and EBV miR-BART15 regulate the NLRP3 inflammasome and IL-1β production," *The Journal of Immunology*, vol. 189, no. 8, pp. 3795–3799, 2012.

[32] C. Juliana, T. Fernandes-Alnemri, S. Kang, A. Farias, F. Qin, and E. S. Alnemri, "Non-transcriptional priming and deubiquitination regulate NLRP3 inflammasome activation," *Journal of Biological Chemistry*, vol. 287, no. 43, pp. 36617–36622, 2012.

[33] L. Franchi, R. Muñoz-Planillo, and G. Núñez, "Sensing and reacting to microbes through the inflammasomes," *Nature Immunology*, vol. 13, no. 4, pp. 325–332, 2012.

[34] C.-S. Yang, D.-M. Shin, and E.-K. Jo, "The role of NLR-related protein 3 inflammasome in host defense and inflammatory diseases," *International Neurourology Journal*, vol. 16, no. 1, pp. 2–12, 2012.

[35] C. Franceschi, M. Bonafè, S. Valensin et al., "Inflamm-aging: an evolutionary perspective on immunosenescence," *Annals of the New York Academy of Sciences*, vol. 908, pp. 244–254, 2000.

[36] A. Salminen, K. Kaarniranta, and A. Kauppinen, "Inflammaging: disturbed interplay between autophagy and inflammasomes," *Aging*, vol. 4, no. 3, pp. 166–175, 2012.

[37] J.-C. Yang, H.-C. Yang, C.-T. Shun, T.-H. Wang, C.-T. Chien, and J. Y. Kao, "Catechins and sialic acid attenuate helicobacter pylori -triggered epithelial caspase-1 activity and eradicate helicobacter pylori infection," *Evidence-Based Complementary and Alternative Medicine*, vol. 2013, Article ID 248585, 13 pages, 2013.

[38] J. C. Yang, C. T. Shun, C. T. Chien, and T. H. Wang, "Effective prevention and treatment of Helicobacter pylori infection using a combination of catechins and sialic acid in AGS cells and BALB/c mice," *Journal of Nutrition*, vol. 138, no. 11, pp. 2084–2090, 2008.

[39] N. Barzilai, D. M. Huffman, R. H. Muzumdar, and A. Bartke, "The critical role of metabolic pathways in aging," *Diabetes*, vol. 61, no. 6, pp. 1315–1322, 2012.

[40] I. Tabas, "Macrophage death and defective inflammation resolution in atherosclerosis," *Nature Reviews Immunology*, vol. 10, no. 1, pp. 36–46, 2010.

[41] B. Levine, N. Mizushima, and H. W. Virgin, "Autophagy in immunity and inflammation," *Nature*, vol. 469, no. 7330, pp. 323–335, 2011.

[42] Y. Xu, C. Jagannath, X. D. Liu, A. Sharafkhaneh, K. E. Kolodziejska, and N. T. Eissa, "Toll-like receptor 4 is a sensor for autophagy associated with innate immunity," *Immunity*, vol. 27, no. 1, pp. 135–144, 2007.

[43] C.-S. Shi and J. H. Kehrl, "Traf6 and A20 differentially regulate TLR4-induced autophagy by affecting the ubiquitination of Beclin 1," *Autophagy*, vol. 6, no. 7, pp. 986–987, 2010.

[44] C. Xu, J. Liu, L.-C. Hsu, Y. Luo, R. Xiang, and T.-H. Chuang, "Functional interaction of heat shock protein 90 and Beclin 1 modulates Toll-like receptor-mediated autophagy," *The FASEB Journal*, vol. 25, no. 8, pp. 2700–2710, 2011.

[45] J. H. Joo, F. C. Dorsey, A. Joshi et al., "Hsp90-Cdc37 chaperone complex regulates Ulk1- and Atg13-mediated mitophagy," *Molecular Cell*, vol. 43, no. 4, pp. 572–585, 2011.

[46] N. Jounai, K. Kobiyama, M. Shiina, K. Ogata, K. J. Ishii, and F. Takeshita, "NLRP4 negatively regulates autophagic processes through an association with Beclin1," *The Journal of Immunology*, vol. 186, no. 3, pp. 1646–1655, 2011.

[47] T. Saitoh, N. Fujita, M. H. Jang et al., "Loss of the autophagy protein Atg16L1 enhances endotoxin-induced IL-1β production," *Nature*, vol. 456, no. 7219, pp. 264–268, 2008.

[48] A. Terman, T. Kurz, M. Navratil, E. A. Arriaga, and U. T. Brunk, "Mitochondrial Turnover and aging of long-lived postmitotic cells: The mitochondrial-lysosomal axis theory of aging," *Antioxidants and Redox Signaling*, vol. 12, no. 4, pp. 503–535, 2010.

[49] C. P. Chang, Y. C. Su, C. W. Hu, and H. Y. Lei, "TLR2-dependent selective autophagy regulates NF-κB lysosomal degradation in hepatoma-derived M2 macrophage differentiation," *Cell Death and Differentiation*, vol. 20, no. 3, pp. 515–523, 2013.

[50] S. Paul, A. K. Kashyap, W. Jia, Y.-W. He, and B. C. Schaefer, "Selective autophagy of the adaptor protein Bcl10 modulates T cell receptor activation of NF-kappaB," *Immunity*, vol. 36, no. 6, pp. 947–958, 2012.

[51] A. V. Everitt, S. N. Hilmer, J. C. Brand-Miller et al., "Dietary approaches that delay age-related diseases," *Clinical Interventions in Aging*, vol. 1, no. 1, pp. 11–31, 2006.

[52] H. Si and D. Liu, "Dietary antiaging phytochemicals and mechanisms associated with prolonged survival," *The Journal of Nutritional Biochemistry*, vol. 25, no. 6, pp. 581–591, 2014.

[53] X. Gu, L. Creasy, A. Kester, and M. Zeece, "Capillary electrophoretic determination of resveratrol in wines," *Journal of Agricultural and Food Chemistry*, vol. 47, no. 8, pp. 3223–3227, 1999.

[54] E. N. Frankel, A. L. Waterhouse, and J. E. Kinsella, "Inhibition of human LDL oxidation by resveratrol," *The Lancet*, vol. 341, no. 8852, pp. 1103–1104, 1993.

[55] J. M. Smoliga, J. A. Baur, and H. A. Hausenblas, "Resveratrol and health—a comprehensive review of human clinical trials," *Molecular Nutrition and Food Research*, vol. 55, no. 8, pp. 1129–1141, 2011.

[56] J. A. Baur and D. A. Sinclair, "Therapeutic potential of resveratrol: the in vivo evidence," *Nature Reviews Drug Discovery*, vol. 5, no. 6, pp. 493–506, 2006.

[57] S. J. Yang and Y. Lim, "Resveratrol ameliorates hepatic metaflammation and inhibits NLRP3 inflammasome activation," *Metabolism-Clinical and Experimenta*, vol. 63, no. 5, pp. 693–701, 2014.

[58] F. Pietrocola, G. Mariño, D. Lissa et al., "Pro-autophagic polyphenols reduce the acetylation of cytoplasmic proteins," *Cell Cycle*, vol. 11, no. 20, pp. 3851–3860, 2012.

[59] C. L. Ho, C. Y. Lin, S. M. Ka et al., "amboo vinegar decreases inflammatory mediator expression and NLRP3 inflammasome activation by inhibiting reactive oxygen species generation and protein kinase C-alpha/delta activation," *PLoS ONE*, vol. 8, no. 10, Article ID e75738, 2013.

[60] J. I. Hori, D. S. Zamboni, D. B. Carrão, G. H. Goldman, and A. A. Berretta, "The inhibition of inflammasome by Brazilian propolis (EPP-AF)," *Evidence-Based Complementary and Alternative Medicine*, vol. 2013, Article ID 418508, 11 pages, 2013.

[61] S. H. Fan, Y. Y. Wang, J. Lu et al., "Luteoloside suppresses proliferation and metastasis of hepatocellular carcinoma cells by inhibition of NLRP3 inflammasome," *PLoS ONE*, vol. 9, no. 2, Article ID e89961, 2014.

[62] S. Egert, A. Bosy-Westphal, J. Seiberl et al., "Quercetin reduces systolic blood pressure and plasma oxidised low-density lipoprotein concentrations in overweight subjects with a high-cardiovascular disease risk phenotype: a double-blinded, placebo-controlled cross-over study," *The British Journal of Nutrition*, vol. 102, no. 7, pp. 1065–1074, 2009.

[63] J. X. Zhu, Y. Wang, L. D. Kong, C. Yang, and X. Zhang, "Effects of Biota orientalis extract and its flavonoid constituents, quercetin and rutin on serum uric acid levels in oxonate-induced mice and xanthine dehydrogenase and xanthine oxidase activities in mouse liver," *Journal of Ethnopharmacology*, vol. 93, no. 1, pp. 133–140, 2004.

[64] C. Wang, Y. Pan, Q.-Y. Zhang, F.-M. Wang, and L.-D. Kong, "Quercetin and allopurinol ameliorate kidney injury in STZ-treated rats with regulation of renal NLRP3 inflammasome activation and lipid accumulation," *PLoS ONE*, vol. 7, no. 6, Article ID e38285, 2012.

[65] Q.-H. Hu, X. Zhang, Y. Pan, Y.-C. Li, and L.-D. Kong, "Allopurinol, quercetin and rutin ameliorate renal NLRP3 inflammasome activation and lipid accumulation in fructose-fed rats," *Biochemical Pharmacology*, vol. 84, no. 1, pp. 113–125, 2012.

[66] I. C. W. Arts, D. R. Jacobs Jr., L. J. Harnack, M. Gross, and A. R. Folsom, "Dietary catechins in relation to coronary heart disease death among postmenopausal women," *Epidemiology*, vol. 12, no. 6, pp. 668–675, 2001.

[67] P. V. A. Babu and D. Liu, "Green tea catechins and cardiovascular health: an update," *Current Medicinal Chemistry*, vol. 15, no. 18, pp. 1840–1850, 2008.

[68] J. V. Higdon and B. Frei, "Tea catechins and polyphenols: health effects, metabolism, and antioxidant functions," *Critical Reviews in Food Science and Nutrition*, vol. 43, no. 1, pp. 89–143, 2003.

[69] S. Shankar, S. Ganapathy, S. R. Hingorani, and R. K. Srivastava, "EGCG inhibits growth, invasion, angiogenesis and metastasis of pancreatic cancer," *Frontiers in Bioscience*, vol. 13, no. 2, pp. 440–452, 2008.

[70] A. M. Haque, M. Hashimoto, M. Katakura, Y. Tanabe, Y. Hara, and O. Shido, "Long-term administration of green tea catechins improves spatial cognition learning ability in rats," *Journal of Nutrition*, vol. 136, no. 4, pp. 1043–1047, 2006.

[71] C. López-Otín, M. A. Blasco, L. Partridge, M. Serrano, and G. Kroemer, "The hallmarks of aging," *Cell*, vol. 153, no. 6, pp. 1194–1217, 2013.

[72] L. A. Forsberg, C. Rasi, H. R. Razzaghian et al., "Age-related somatic structural changes in the nuclear genome of human blood cells," *The American Journal of Human Genetics*, vol. 90, no. 2, pp. 217–228, 2012.

[73] F. Faggioli, T. Wang, J. Vijg, and C. Montagna, "Chromosome-specific accumulation of aneuploidy in the aging mouse brain," *Human Molecular Genetics*, vol. 21, no. 24, pp. 5246–5253, 2012.

[74] B. A. I. Payne, I. J. Wilson, C. A. Hateley et al., "Mitochondrial aging is accelerated by anti-retroviral therapy through the clonal expansion of mtDNA mutations," *Nature Genetics*, vol. 43, no. 8, pp. 806–810, 2011.

[75] M. Jaskelioff, F. L. Muller, J. H. Paik et al., "Telomerase reactivation reverses tissue degeneration in aged telomerase-deficient mice," *Nature*, vol. 469, no. 7328, pp. 102–107, 2011.

[76] J. J. Boonekamp, M. J. P. Simons, L. Hemerik, and S. Verhulst, "Telomere length behaves as biomarker of somatic redundancy rather than biological age," *Aging Cell*, vol. 12, no. 2, pp. 330–332, 2013.

[77] R. Mostoslavsky, K. F. Chua, D. B. Lombard et al., "Genomic instability and aging-like phenotype in the absence of mammalian SIRT6," *Cell*, vol. 124, no. 2, pp. 315–329, 2006.

[78] S. Maegawa, G. Hinkal, H. S. Kim et al., "Widespread and tissue specific age-related DNA methylation changes in mice," *Genome Research*, vol. 20, no. 3, pp. 332–340, 2010.

[79] K. Larson, S.-J. Yan, A. Tsurumi et al., "Heterochromatin formation promotes longevity and represses ribosomal RNA synthesis," *PLoS Genetics*, vol. 8, no. 1, Article ID e1002473, 2012.

[80] K. Boulias and H. R. Horvitz, "The C. elegans MicroRNA mir-71 acts in neurons to promote germline-mediated longevity through regulation of DAF-16/FOXO," *Cell Metabolism*, vol. 15, no. 4, pp. 439–450, 2012.

[81] G. A. Walker and G. J. Lithgow, "Lifespan extension in *C. elegans* by a molecular chaperone dependent upon insulin-like signals," *Aging Cell*, vol. 2, no. 2, pp. 131–139, 2003.

[82] H. Koga, S. Kaushik, and A. M. Cuervo, "Protein homeostasis and aging: the importance of exquisite quality control," *Ageing Research Reviews*, vol. 10, no. 2, pp. 205–215, 2011.

[83] D. E. Harrison, R. Strong, Z. D. Sharp et al., "Rapamycin fed late in life extends lifespan in genetically heterogeneous mice," *Nature*, vol. 460, no. 7253, pp. 392–395, 2009.

[84] U. Kruegel, B. Robison, T. Dange et al., "Elevated proteasome capacity extends replicative lifespan in saccharomyces cerevisiae," *PLoS Genetics*, vol. 7, no. 9, Article ID e1002253, 2011.

[85] B. Schumacher, I. van der Pluijm, M. J. Moorhouse et al., "Delayed and accelerated aging share common longevity assurance mechanisms," *PLoS Genetics*, vol. 4, no. 8, Article ID e1000161, 2008.

[86] S. C. Johnson, P. S. Rabinovitch, and M. Kaeberlein, "MTOR is a key modulator of ageing and age-related disease," *Nature*, vol. 493, no. 7432, pp. 338–345, 2013.

[87] W. Mair, I. Morantte, A. P. C. Rodrigues et al., "Lifespan extension induced by AMPK and calcineurin is mediated by CRTC-1 and CREB," *Nature*, vol. 470, no. 7334, pp. 404–408, 2011.

[88] D. Harman, "The free radical theory of aging: effect of age on serum copper levels," *Journal of Gerontology*, vol. 20, pp. 151–153, 1965.

[89] S. Hekimi, J. Lapointe, and Y. Wen, "Taking a "good" look at free radicals in the aging process," *Trends in Cell Biology*, vol. 21, no. 10, pp. 569–576, 2011.

[90] H. van Remmen, Y. Ikeno, M. Hamilton et al., "Life-long reduction in MnSOD activity results in increased DNA damage and higher incidence of cancer but does not accelerate aging," *Physiological Genomics*, vol. 16, no. 1, pp. 29–37, 2003.

[91] M. Ristow and S. Schmeisser, "Extending life span by increasing oxidative stress," *Free Radical Biology and Medicine*, vol. 51, no. 2, pp. 327–336, 2011.

[92] E. Sahin and R. A. DePinho, "Axis of ageing: telomeres, p53 and mitochondria," *Nature Reviews—Molecular Cell Biology*, vol. 13, no. 6, pp. 397–404, 2012.

[93] J. Krishnamurthy, C. Torrice, M. R. Ramsey et al., "Ink4a/Arf expression is a biomarker of aging," *Journal of Clinical Investigation*, vol. 114, no. 9, pp. 1299–1307, 2004.

[94] S. Ressler, J. Bartkova, H. Niederegger et al., "p16INK4A is a robust in vivo biomarker of cellular aging in human skin," *Aging Cell*, vol. 5, no. 5, pp. 379–389, 2006.

[95] D. J. Rossi, D. Bryder, J. Seita, A. Nussenzweig, J. Hoeijmakers, and I. L. Weissman, "Deficiencies in DNA damage repair limit the function of haematopoietic stem cells with age," *Nature*, vol. 447, no. 7145, pp. 725–729, 2007.

[96] D. R. Green, L. Galluzzi, and G. Kroemer, "Mitochondria and the autophagy-inflammation-cell death axis in organismal aging," *Science*, vol. 333, no. 6046, pp. 1109–1112, 2011.

[97] J. Plowden, M. Renshaw-Hoelscher, C. Engleman, J. Katz, and S. Sambhara, "Innate immunity in aging: impact on macrophage function," *Aging Cell*, vol. 3, no. 4, pp. 161–167, 2004.

[98] D. Weiskopf, B. Weinberger, and B. Grubeck-Loebenstein, "The aging of the immune system," *Transplant International*, vol. 22, no. 11, pp. 1041–1050, 2009.

[99] T. Fulop, A. le Page, C. Fortin et al., "Cellular signaling in the aging immune system," *Current Opinion in Immunology*, vol. 29, pp. 105–111, 2014.

[100] A. Agrawal, S. Agrawal, and S. Gupta, "Dendritic cells in human aging," *Experimental Gerontology*, vol. 42, no. 5, pp. 421–426, 2007.

[101] J. A. Serra, B. Fernandez-Gutierrez, C. Hernandez-Garcia et al., "Early T cell activation in elderly humans," *Age and Ageing*, vol. 25, no. 6, pp. 470–478, 1996.

[102] D. Baylis, D. B. Bartlett, H. P. Patel, and H. C. Roberts, "Understanding how we age: insights into inflammaging," *Longevity and Healthspan*, vol. 2, no. 1, article 8, 2013.

[103] L. Z. Ellis, W. Liu, Y. Luo et al., "Green tea polyphenol epigallocatechin-3-gallate suppresses melanoma growth by inhibiting inflammasome and IL-1β secretion," *Biochemical and Biophysical Research Communications*, vol. 414, no. 3, pp. 551–556, 2011.

[104] P.-Y. Tsai, S.-M. Ka, J.-M. Chang et al., "Epigallocatechin-3-gallate prevents lupus nephritis development in mice via enhancing the Nrf2 antioxidant pathway and inhibiting NLRP3 inflammasome activation," *Free Radical Biology and Medicine*, vol. 51, no. 3, pp. 744–754, 2011.

[105] W. Li, S. Zhu, J. Li et al., "EGCG stimulates autophagy and reduces cytoplasmic HMGB1 levels in endotoxin-stimulated macrophages," *Biochemical Pharmacology*, vol. 81, no. 9, pp. 1152–1163, 2011.

Hindawi Publishing Corporation
BioMed Research International
Volume 2014, Article ID 151479, 10 pages
http://dx.doi.org/10.1155/2014/151479

Research Article

GHK and DNA: Resetting the Human Genome to Health

Loren Pickart, Jessica Michelle Vasquez-Soltero, and Anna Margolina

Skin Biology, Research & Development Department, 4122 Factoria Boulevard SE, Suite No. 200, Bellevue, WA 98006, USA

Correspondence should be addressed to Loren Pickart; lorenpickart@skinbiology.com

Received 8 July 2014; Accepted 27 August 2014; Published 11 September 2014

Academic Editor: Chi-Feng Hung

During human aging there is an increase in the activity of inflammatory, cancer promoting, and tissue destructive genes plus a decrease in the activity of regenerative and reparative genes. The human blood tripeptide GHK possesses many positive effects but declines with age. It improves wound healing and tissue regeneration (skin, hair follicles, stomach and intestinal linings, and boney tissue), increases collagen and glycosaminoglycans, stimulates synthesis of decorin, increases angiogenesis, and nerve outgrowth, possesses antioxidant and anti-inflammatory effects, and increases cellular stemness and the secretion of trophic factors by mesenchymal stem cells. Recently, GHK has been found to reset genes of diseased cells from patients with cancer or COPD to a more healthy state. Cancer cells reset their programmed cell death system while COPD patients' cells shut down tissue destructive genes and stimulate repair and remodeling activities. In this paper, we discuss GHK's effect on genes that suppress fibrinogen synthesis, the insulin/insulin-like system, and cancer growth plus activation of genes that increase the ubiquitin-proteasome system, DNA repair, antioxidant systems, and healing by the TGF beta superfamily. A variety of methods and dosages to effectively use GHK to reset genes to a healthier state are also discussed.

1. Introduction

According to the Administration on Aging (http://www.aoa.gov/), there were 39 million people aged 65 and older in 2009 which constituted 12% of the American population. By 2030 it is expected that 19% of the population will be over 65. With life expectancy continuing to increase, we may expect that this trend is here to stay. Unfortunately, with advanced age comes not only wisdom but also many age-related pathological conditions that account for the high rates of hospitalization, increased cost of health care and decreased quality of life. Today, more than ever, there is an urgent need to find safe, easy-to-administer, cost-effective methods, which could not only delay the onset of the age related diseases, but also restore health.

It now becomes increasingly clear that the primary cause of human aging and its attendant diseases is changes in the activity of the human genome. During aging there is an increase in the activity of inflammatory, cancer promoting, and tissue destructive genes plus a decrease in the activity of regenerative and reparative genes [1].

The most exciting discovery of the past decades is that these changes in gene activity can be reversed, often by quite simple and natural molecules [2]. Recent discoveries on the actions of the human tripeptide GHK (glycyl-L-histidyl-L-lysine) to reset gene expression of human cells to a more healthy state may open a door to the therapeutic resetting of genes in the elderly. This can be useful as a preventative measure and a complimentary treatment for conditions typically associated with aging such as cancer, Alzheimer's, chronic obstructive lung disease (COPD), nephropathy, and retinopathy.

GHK was discovered during studies comparing the effect of human plasma from young persons (age 20–25) to plasma from older persons (age 50–70) on the functioning of incubated slices of human hepatic tissue. The younger plasma more effectively induced a profile associated with youth by suppressing fibrinogen synthesis. The active factor was found to be GHK. Since then numerous studies over the course of four decades demonstrated that this simple molecule improves wound healing and tissue regeneration (skin, hair follicles, bones, stomach, intestinal linings, and liver), increases collagen and glycosaminoglycans, stimulates synthesis of decorin, increases angiogenesis, and nerve outgrowth; possesses antioxidant and anti-inflammatory effects,

and increases cellular stemness and the secretion of trophic factors by mesenchymal stem cells [3–6].

GHK's actions on gene expression were determined by the Broad Institute and, using their data, we determined that GHK increased or decreased gene expression (UP or DOWN more than 50%) in 32.1% of the human genes [7]. In a recent gene study, the Broad Institute's Connectivity Map was used to find potential therapeutic agents for aggressive, metastatic colon cancer [8]. The gene analysis computer program selected GHK from 1,309 bioactive molecules as the best choice to reset the diseased gene patterns to a healthier pattern. When three lines of human cancer cells (SH-SY5Y neuroblastoma cells, U937 histolytic cells, breast cancer cells) were incubated in culture with 1 to 10 nanomolar GHK, the programmed cell death system (apoptosis) was reactivated and cell growth inhibited [9]. When cells derived from the damaged areas of the lungs of COPD patients were incubated with 10 nanomolar GHK, the tripeptide recapitulated TGF beta induced genes expression patterns which led to the organization of the actin cytoskeleton and elevated the expression of integrin. This restored proper collagen contraction and remodeling by lung fibroblasts [10]. These results, combined with GHK's broad spectrum of positive actions on many systems that maintain human health, suggest that therapies using GHK might provide health benefits to the elderly.

In this paper, we discuss the following actions of GHK on genes important in healthy aging.

(1) The Suppression of Fibrinogen Synthesis. Fibrinogen is an excellent predictor of mortality especially in patients with cardiovascular complications [11, 12]. GHK was isolated as a plasma factor that suppressed fibrinogen synthesis in liver tissue and in mice.

(2) Activation of the Ubiquitin/Proteasome System (UPS). The UPS removes damaged proteins. Higher activities of the UPS appear to retard aging effects [13, 14].

(3) Activation of DNA Repair Genes. DNA damage is promptly repaired in young and healthy cells, however, as we age, DNA damage starts accumulating. Resetting activity of DNA repair genes can diminish deleterious effects of aging.

(4) Antioxidant Genes. Free radicals and toxic end products of lipid peroxidation are linked to atherosclerosis, cancer, cataracts, diabetes, nephropathy, Alzheimer's disease and other severe pathological conditions of aging.

(5) Suppression of Insulin and Insulin-Like Genes. The insulin family has been proposed as a negative controller of longevity; higher levels of insulin and insulin-like proteins reduce the lifespan [15].

(6) Tissue Repair by TGF Superfamily. General tissue repair by the TGF superfamily as exemplified by COPD (chronic obstructive pulmonary disease).

(7) Cancer Controlling Genes. Caspase, growth regulatory, and DNA repair genes are important in cancer suppression.

Table 1: GHK and fibrinogen.

Gene title	Percent change in gene expression
Fibrinogen alpha chain, FGA	121
Fibrinogen beta chain, FGB	−475

In addition to discussing GHK actions in this paper, we suggest administrative methods and dosages that should be effective in humans.

2. Methods and Results

2.1. Gene Expression Analysis. The connectivity map was used to acquire our gene expression data (retrieved March 5, 2013) [16]. Within the Connectivity Map repository there are three GHK gene signatures. Each signature was produced using the GeneChip HT Human Genome U133A Array. GHK was tested on 2 of the 5 cell lines used by the Connectivity Map. Two of the profiles were created using the PC3 cell line while the third used the MCF7 cell line. Our studies utilized all three gene expression profiles.

This genomic data was then analyzed using GenePattern [17]. The CEL files were processed with MAS5 and background correction. Files were then uploaded to the ComparativeMarkerSelectionViewer module in order to view fold changes for each probe set.

Since many probe sets map to the same gene we converted the fold changes in m-RNA production produced by GenePattern to percentages and then averaged all probe sets representing the same gene. It was determined that the 22,277 probe sets in the Broad data represent 13,424 genes. This ratio (1.66) was used to calculate the overall number of genes that are affected by GHK at various cutoff points (rather than probe sets). The number of genes stimulated or suppressed by GHK with a change greater than or equal to 50% is 31.2%.

2.2. Fibrinogen Suppression. Fibrinogen consists of three polypeptide chains; alpha, beta, and gamma. GHK strongly suppresses the gene for the beta chain of fibrinogen. A lack of adequate FGB will effectively stop fibrinogen syntheses since equal amounts of all three polypeptide chains are needed to produce fibrinogen. See Table 1.

GHK also suppresses the production of the inflammatory cytokine interleukin-6 (IL-6) which is a main positive regulator of fibrinogen synthesis, through its interaction with fibrinogen genes [18]. In cell culture systems, GHK suppresses IL-6 secretion in skin fibroblasts and IL-6 gene expression in SZ95 sebocytes [19, 20].

In summary, the effects of GHK on the FGB gene plus its effects on IL-6 production imply a suppression of overall fibrinogen production.

2.3. Ubiquitin/Proteasome System. GHK stimulated gene expression in 41 UPS genes while suppressing only 1 UPS gene. See Table 2.

Table 2: Ubiquitin/proteasome system and GHK.

Up	Gene title	Percent change in gene expression
1	Ubiquitin specific peptidase 29, USP29	1056
2	Ubiquitin protein ligase E3 component n-recognin 2, UBR2	455
3	Gamma-aminobutyric acid (GABA) B receptor, 1 /// ubiquitin D, GABBR1 /// UBD	310
4	Ubiquitin specific peptidase 34, USP34	195
5	Parkinson protein 2, E3 ubiquitin protein ligase (parkin), PARK2	169
6	Ubiquitin-conjugating enzyme E2I (UBC9 homolog, yeast), UBE2I	150
7	Ubiquitin protein ligase E3 component n-recognin 4, UBR4	146
8	Ubiquitin protein ligase E3B, UBE3B	116
9	Ubiquitin specific peptidase 2, USP2	104
10	Ubiquitin-like modifier activating enzyme 6, UBA6	104
11	Ubiquitination factor E4B (UFD2 homolog, yeast), UBE4B	97
12	Ubiquitin-conjugating enzyme E2M (UBC12 homolog, yeast), UBE2M	92
13	Ubiquitin-like modifier activating enzyme 7, UBA7	88
14	HECT, C2 and WW domain containing E3 ubiquitin protein ligase 1, HECW1	81
15	Proteasome (prosome, macropain) 26S subunit, ATPase, 3, PSMC3	81
16	Ubiquitin-conjugating enzyme E2D 1 (UBC4/5 homolog, yeast), UBE2D1	79
17	Proteasome (prosome, macropain) subunit, beta type, 2, PSMB2	79
18	Ubiquitin protein ligase E3 component n-recognin 5, UBR5	77
19	Ubiquitin specific peptidase 21, USP21	76
20	OTU domain, ubiquitin aldehyde binding 2, OTUB2	76
21	Proteasome (prosome, macropain) inhibitor subunit 1 (PI31), PSMF1	75
22	Ubiquitin-conjugating enzyme E2H (UBC8 homolog, yeast), UBE2H	73
23	Ubiquitin-conjugating enzyme E2N (UBC13 homolog, yeast), UBE2N	72
24	Ubiquitin carboxyl-terminal hydrolase L5, UCHL5	71
25	Proteasome (prosome, macropain) 26S subunit, non-ATPase, 13, PSMD13	70
26	Ubiquitin associated protein 1, UBAP1	70
27	Ubiquitin-conjugating enzyme E2B (RAD6 homolog), UBE2B	69
28	TMEM189-UBE2V1 readthrough /// ubiquitin-conjugating enzyme E2 variant 1, TMEM189-UBE2V1 /// UBE2V1	67
29	Proteasome (prosome, macropain) 26S subunit, non-ATPase, 1, PSMD1	64
30	Proteasome (prosome, macropain) 26S subunit, non-ATPase, 3, PSMD3	64
31	Ariadne homolog, ubiquitin-conjugating enzyme E2 binding protein, 1 (drosophila), ARIH1	61
32	BRCA1 associated protein-1 (ubiquitin carboxy-terminal hydrolase), BAP1	60
33	Ubiquitin interaction motif containing 1, UIMC1	60
34	Ubiquitin associated protein 2-like, UBAP2L	57
35	Ubiquitin protein ligase E3 component n-recognin 7 (putative), UBR7	56
36	Ubiquitin-conjugating enzyme E2G 1 (UBC7 homolog, yeast), UBE2G1	54
37	Itchy E3 ubiquitin protein ligase homolog (mouse), ITCH	54
38	Ubiquitin-conjugating enzyme E2D 4 (putative), UBE2D4	51
39	Proteasome (prosome, macropain) 26S subunit, non-ATPase, 10, PSMD10	50
40	WW domain containing E3 ubiquitin protein ligase 1, WWP1	50
41	Ubiquitin-like 3, UBL3	50
Down	Gene title	Percent change in gene expression
1	Ubiquitin associated and SH3 domain containing A, UBASH3A	−89

Table 3: GHK and DNA repair.

Percent change in gene expression	Genes up	Genes down
50%–100%	41	4
100%–150%	2	1
150%–200%	1	0
200%–250%	2	0
250%–300%	1	0

Table 4: The most affected DNA repair genes.

Up	Gene title	Percent change in gene expression
1	Poly (ADP-ribose) polymerase family, member 3, PARP3	253
2	Polymerase (DNA directed), mu, POLM	225
3	MRE11 meiotic recombination 11 homolog A MRE11A	212
4	RAD50 homolog (S. cerevisiae), RAD50	175
5	Eyes absent homolog 3 (Drosophila), EYA3	128
6	Retinoic acid receptor, alpha, RARA	123
Down	Gene title	Percent change in gene expression
1	Cholinergic receptor, nicotinic, alpha 4, CHRNA4	−105

2.4. DNA Repair Genes. GHK was primarily stimulatory for DNA repair genes (47 UP, 5 DOWN). See Tables 3 and 4.

2.5. Antioxidant Genes. Among the 13,424 available genes in the Broad Institute data, we were able to identify 14 antioxidant genes in which GHK stimulates as well as two prooxidant genes that GHK suppresses. GHK increases the expression of the oxidative/inflammatory gene NF-κB2 103% but also increases the expression of two inhibitors of NF-κB, TLE1 by 762% and IL18BP by 295%, thus possibly inhibiting the activity of the NF-κB protein. See Table 5.

2.6. Insulin and Insulin-Like System. GHK stimulates 3 genes in this system and suppresses 6 genes. See Table 6.

3. Discussion

Even though numerous and diverse beneficial effects of GHK have been known for decades, it was not clear how one simple molecule could accomplish so much. The use of gene expression data greatly extends our understanding of GHK's effects and its potential treatments of some of the diseases and biochemical changes associated with aging. As a potential therapeutic agent GHK has a clear advantage over many other active chemicals that may also show promising results in gene profiling experiments, its gene modulating effects correspond to findings from *in vivo* experiments. When GHK is administered internally to an animal, it induces actions throughout the body.

The treatment of rats, mice, and pigs with GHK was shown to effectively activate systemic healing throughout the animal. For example, if GHK is injected into the thigh muscles of rats, it induces accelerated healing in implanted Hunt-Schilling wound chambers. If the GHK is injected into the thigh muscles of mice, it accelerates the healing of an experimental full thickness surgical defect wound model on its back. If injected into thigh muscles of pigs, it induces accelerates healing of full thickness surgical defect wounds on its back [37]. If GHK is injected intraperitoneally into rats, it heals tubular bone fractures [38]. Wound healing requires activation of gene expression for numerous pathways and wound healing data confirms that GHK is able to activate gene expression in animals [39–45].

There is still not enough information to translate gene profiling data into biological effects. However, based on the documented activity of GHK *in vivo*, we can predict the following beneficial actions from our gene profiling data.

3.1. Fibrinogen. Fibrinogen, the protein which is used to make blood clots, is also a strong predictor of mortality in cardiovascular patients. After vascular incidents, such as myocardial infarction, fibrinogen concentrations increase sharply. The free, unclotted fibrinogen protein increases the "stickiness" of red blood cells which stack together forming rouleaux. This increases the time of the "solid" blood state which decreases blood flow through the microcirculation where blood flows like a thixotropic fluid, switching between a solid phase and a liquid phase, somewhat like toothpaste. As a solid, it stops oxygen and nutrient flow to the tissues. This, in itself, can cause tissue damage.

The gene data on GHK's suppression of FGB (the fibrinogen beta chain) combined with its actions on lowering IL-6 secretion on fibroblasts and sebocytes appears to be sufficient to explain its lowering effect on fibrinogen.

3.2. Ubiquitin Proteasome System. The ubiquitin proteasome system (UPS) functions in the removal of damaged or misfolded proteins. Aging is a natural process that is characterized by a progressive accumulation of unfolded, misfolded, or aggregated proteins. In particular, the proteasome is responsible for the removal of normal as well as damaged or misfolded proteins. Recent work has demonstrated that proteasome activation by either genetic means or use of compounds retards aging [13, 14].

In our screening of UPS genes with a percent change of at least ±50%, GHK increased gene expression in 41 UPS genes while suppressing 1 UPS gene. Thus, it should have a positive effect on this system [13, 14, 46].

3.3. DNA Repair. It is estimated that normal metabolic activities and environmental factors such as UV light and radiation can cause DNA damage, resulting in somewhere between 1000 and as many as 1 million individual molecular lesions per cell per day. Lack of sufficient DNA repair is

Table 5: GHK effects on antioxidant genes.

Up	Genes	Percent change in gene expression	Comments
1	TLE1	762	Inhibits the oxidative/inflammatory gene NF-κB [21].
2	SPRR2C	721	This proline-rich, antioxidant protein protects outer skin cells from oxidative damage from ROS. When the ROS level is low, the protein remains in the outer cell membrane but when the ROS level is high, the protein clusters around the cell's DNA to protect it [22, 23].
3	ITGB4	609	Upregulation of ITGB4 promotes wound repair ability and antioxidative ability [24].
4	APOM	403	Binds oxidized phospholipids and increases the antioxidant effect of HDL [25].
5	PON3	319	Absence of PON3 (paraoxonase 3) in mice resulted in increased rates of early fetal and neonatal death. Knockdown of PON3 in human cells reduced cell proliferation and total antioxidant capacity [26].
6	IL18BP	295	The protein encoded by this gene is an inhibitor of the proinflammatory cytokine IL18. IL18BP abolished IL18 induction of interferon-gamma (IFNgamma), IL8, and activation of NF-κB *in vitro*. Blocks neutrophil oxidase activity [27].
7	HEPH	217	Inhibits the conversion of Fe(2+) to Fe(3+). HEPH increases iron efflux, lowers cellular iron levels, suppresses reactive oxygen species production, and restores mitochondrial transmembrane potential [28].
8	FABP1	186	Reduces intracellular ROS level. Plays a significant role in reduction of oxidative stress [29, 30].
9	PON1	149	PON1 (paraoxonase 1) is a potent antioxidant and a major anti-atherosclerotic component of high-density lipoprotein [31].
10	MT3	142	Metallothioneins (MTs) display *in vitro* oxyradical scavenging capacity, suggesting that they may specifically neutralize hydroxyl radicals. Metallothioneins and metallothionein-like proteins isolated from mouse brain act as neuroprotective agents by scavenging superoxide radicals [32, 33].
11	PTGS2	120	Produces cyclooxygenase-II (COX-II) which has antioxidant activities [34].
12	NF-κB2	103	NF-κB, an oxidative/inflammatory protein, is involved in cellular responses to stimuli such as stress, cytokines, free radicals, ultraviolet irradiation, oxidized LDL, and bacterial or viral antigens [21].
13	NFE2L2	56	Nuclear respiratory factor 2 helps activate antioxidant responsive element regulated genes which contribute to the regulation of the cellular antioxidant defense systems [35].
14	PTGS1	50	Produces cyclooxygenase-I (COX-I) which has antioxidant activity [34].
Down	Genes	Percent change in gene expression	Comments
1	IL17A	−1018	This strongly suppressed cytokine can stimulate the expression of IL6 and cyclooxygenase-2 (PTGS2/COX-2), as well as enhancing the production of nitric oxide (NO). High levels of this cytokine are associated with several chronic inflammatory diseases including rheumatoid arthritis, psoriasis, and multiple sclerosis (NCBI GENE entry).
2	TNF	−115	GHK suppresses this prooxidant TNF gene which inhibits the antioxidant IL18 [36].

considered a cause of cell senescence, programmed cell death, and unregulated cell division, which can lead to the formation of a tumor that is cancerous [47–50].

GHK was stimulatory for DNA repair genes (47 stimulated, 5 suppressed) suggesting an increased DNA repair activity.

3.4. Antioxidant Defense. Free radicals and toxic end products of lipid peroxidation are linked to atherosclerosis, cancer, cataracts, diabetes, nephropathy, Alzheimer's disease, and other severe pathological conditions of aging. Reactive oxygen species (ROS) and reactive carbonyl species (RCS) are produced in cells in small quantities under physiological

Table 6: GHK and insulin/insulin-like genes.

Up	Gene title	Percent change in gene expression
1	Insulin-like 6, INSL6	188
2	Insulin-like growth factor 2 mRNA binding protein 3, IGF2BP3	136
3	Insulin-like growth factor binding protein 3, IGFBP3	82
Down	Gene title	Percent change in gene expression
1	Insulin-like growth factor 1 (somatomedin C), IGF1	−522
2	Insulin receptor-related receptor, INSRR	−437
3	Insulin, INS	−289
4	Insulin-like 3 (Leydig cell), INSL3	−188
5	Insulin-like growth factor binding protein 7, IGFBP7	−110
6	Insulin-like 5, INSL5	−101

conditions and play an important role in cell signaling and immune defense. A robust antioxidant network maintains balance between free radical production and scavenging, ensuring that the overall damage from free radicals is low. However, in the course of aging and in pathological conditions such as inflammation, the balance may shift toward free radical accumulation that can lead to oxidative stress and eventually to cell death [51].

GHK increases gene expression of 14 antioxidant genes and suppresses the expression of 2 prooxidant genes. It increases the expression of the oxidative/inflammatory gene NF-κB2 103% but also increases the expression of two inhibitors of NF-κB, TLE1 by 762% and IL18BP by 295%; thus, it possibly inhibits the activity of the NF-κB protein.

GHK also possesses antioxidant activities in cell culture and *in vivo*.

In dermal wound healing in rats, GHK, attached to biotin to bind it to collagen pads covering wounds, produced a higher production of protein antioxidants in the wound tissue. Superoxide dismutase was increased 80% while catalase was increased 56% [52, 53]. GHK reduced gastric mucosal damage by 75% against lipid peroxidation by oxygen-derived free radicals induced by acute intragastric administration of ethanol [54].

Interleukin 1 beta can induce serious oxidative damage to cultured cells [55, 56]. GHK markedly reduced oxidative damage by interleukin 1-beta to cultured insulin secreting pancreatic cells [57].

In another study, GHK entirely blocked the extent of *in vitro* Cu(2+)-dependent oxidation of low density lipoproteins (LDL). Treatment of LDL with 5 microM Cu(2+) for 18 hours in phosphate buffered saline (PBS) resulted in extensive oxidation as determined by the content of thiobarbituric acid reactive substances. Oxidation was entirely blocked by GHK. In comparison, copper, zinc-superoxide dismutase provided only 20% protection [58].

Acrolein, a well-known carbonyl toxin, is produced by lipid peroxidation of polyunsaturated fatty acids. GHK directly blocks the formation of 4-hydroxynonenal and acrolein toxins created by carbonyl radicals that cause fatty acid decomposition [59, 60]. GHK also blocks lethal ultraviolet radiation damage to cultured skin keratinocytes by binding and inactivating reactive carbonyl species such as 4-hydroxynoneal, acrolein, malondialdehye, and glyoxal [61].

Iron has a direct role in the initiation of lipid peroxidation. An Fe(2+)/Fe(3+) complex can serve as an initiator of lipid oxidation. The major storage site for iron in serum and tissue is ferritin and the superoxide anion can promote the mobilization of iron from ferritin which can catalyze lipid peroxidation. GHK : Cu(2+) produced an 87% inhibition of iron release from ferritin by apparently blocking iron's exit channels from the protein [62].

3.5. Insulin and Insulin-Like Pathways. The insulin/IGF-1-like receptor pathway is a contributor to the biological aging process in many organisms. The gene expression data suggests that GHK suppresses this system as 6 of 9 of the affected insulin/IGF-1 genes are suppressed.

Insulin/IGF-1-like signaling is conserved from worms to humans. *In vitro* experiments show that mutations that reduce insulin/IGF-1 signaling have been shown to decelerate the degenerative aging process and extend lifespan in many organisms, including mice and possibly humans. Reduced IGF-1 signaling is also thought to contribute to the "antiaging" effects of calorie restriction [63].

3.6. COPD. COPD (chronic obstructive lung disease) is a leading cause of death in the world. It is a deadly and painful disease of the lungs that causes difficulty in breathing. In people with COPD, the tissues necessary to support the physical shape and function of the lungs are destroyed. COPD is most often caused by tobacco smoking and long-term exposure to air pollution but is also a component of normal aging. As the lungs get older, the elastic properties decrease, and the tensions that develop can result in areas of emphysema.

The most explored of GHK's actions is the repair of damaged tissues (skin, hair follicles, stomach and intestinal linings, and boney tissue) either by the use of copper-peptide containing creams or by induction of systemic healing. Campbell et al. found that GHK's resetting of gene expression of fibroblasts from COPD patients fits into this category of tissue repair via the TGF beta superfamily. Campbell et al. found that GHK directly increases TGF beta and other family members which activate the repair process [10].

Treatment of human fibroblasts with GHK recapitulated TGF beta-induced gene expression patterns, led to the organization of the actin cytoskeleton and elevated the expression of integrin beta1. Furthermore, addition of GHK or TGF beta restored collagen I contraction and remodeling by fibroblasts derived from COPD lungs compared to fibroblasts from former smokers without COPD.

On another note, persons with severe COPD use air inhalation systems that pump misty, water-filled air in and out of the lungs. Often steroids are added to the solution to suppress the lung inflammation, while this provides short-term help, it also inhibits lung repair. In theory, GHK could be infused into the blood stream of patients to repair the lung tissue, added to a misting solution or used in combination of a carrier like DMSO along with GHK (use a 1 : 1 molar ratio of GHK to DMSO). DMSO and GHK or GHK : Cu(2+) has always worked well together on wound healing. DMSO has been used in the past as a treatment for COPD, so there should be few safety issues.

Also, it may be possible to induce more extensive rebuilding of lung tissue. The mixture of GHK, transferrin, and somatostatin was sufficient to promote branching in the absence of serum in organ culture, all of which could be added to the misting solution [64].

3.7. Cancer. In 2010, Hong et al. identified 54 genes associated with aggressive, metastatic, human colon cancer [8]. The Broad Institute's Connectivity Map was used to find compounds that reverse the differential expressions of these genes. The results indicated that two wound healing and skin remodeling molecules, GHK at 1 micromolar and securinine at 18 micromolar, could significantly reverse the differential expression of these genes and suggested that they may have a therapeutic effect on the metastasis-prone patients.

Normal healthy cells have checkpoint systems to self-destruct if they are synthesizing DNA incorrectly through programmed cell death or the apoptosis system. Matalka et al. demonstrated that GHK, at 1 to 10 nanomolar, reactivated the apoptosis system, as measured by caspases 3 and 7, and inhibited the growth of human SH-SY5Y neuroblastoma cells, human U937 histiocytic lymphoma cells, and human breast cancer cells [9]. In contrast, the GHK accelerated the growth of healthy human NIH-3T3 fibroblasts.

Our analysis of GHK's actions found that it increased gene expression in 6 of the 12 human caspase genes that activate apoptosis. In 31 other genes, GHK altered the pattern of gene expression in a manner that would be expected to inhibit cancer growth. In DNA repair genes there was an increase (47 UP, 5 DOWN) [7]. These results support the idea that GHK may help slow or suppress cancer growth.

Linus Pauling's group once used a copper tripeptide, Gly-Gly-His : Cu(2+) and ascorbic acid as a cancer treatment method. In a recent paper, we used their basic method but with GHK : Cu(2+) and ascorbic acid, which strongly suppressed sarcoma 180 in mice without any evident distress to the animals [7]. GHK altered gene expression in 84 genes (caspases, cytokines, and DNA repair genes) in a manner that would be expected to suppress cell growth. On skin, GHK seems to act most strongly in the late stage of healing, called remodeling, where cellular migration into the wound area is stopped and cellular debris is removed. The anticancer actions of small copper peptides may be a side effect of this system.

The use of GHK : Cu(2+) and ascorbic acid should be investigated in more detail. The mice treated in this manner appeared to remain very healthy and active, in contrast to the toxicities of current cancer chemotherapy.

3.8. GHK as a Clinical Treatment. GHK, abundantly available at low cost in bulk quantities, is a potential treatment for a variety of disease conditions associated with aging. The molecule is very safe and no issues have ever arisen during its use as a skin cosmetic or in human wound healing studies.

GHK has a very high affinity for Cu(2+) (pK of association = 16.4) and can easily obtain copper from the blood's albumin bound Cu(2+) (pK of association = 16.2) [3]. Most of our key experiments used a 1 : 1 mixture of copper-free GHK and GHK : Cu(2+). In wound healing experiments, the addition of copper strongly enhanced healing. However, others often obtain effective results without added copper.

Cells within tissues are under the influence of many other regulatory molecules. Thus, GHK would be expected to influence the cells' gene expression to be more similar to that of a person of age 20–25, an age when the afflictions of aging are very rare. Based on our studies, in which GHK was injected intraperitoneally once daily to induce systemic wound healing throughout the body, we estimate about 100–200 mgs of GHK will produce therapeutic actions in humans. But even this may overestimate the necessary effective dosage of the molecule. Most cultured cells respond maximally to GHK at 1 nanoM. GHK has a half-life of about 0.5 to 1 hour in plasma and two subsequent tissue repair studies in rats found that injecting GHK intraperitoneally 10 times daily lowered the necessary dosage by approximately 100-fold in contrast to our earlier studies [38, 65].

The most likely effective dosage of GHK was given to rats for healing bone fractures. This mixture of small molecules included Gly-His-Lys (0.5 μg/kg), dalargin (1.2 μg/kg) (an opioid-like synthetic drug), and the biological peptide thymogen (0.5 μg/kg) (L-glutamyl-L-tryptophan) to heal bones. The total peptide dosage is about 2.2 μg/kg or, if scaled for the human body, about 140 μg per injection with 10 treatments per day [38, 65].

The use of portable continuous infusion pumps for a treatment might maintain an effective level in the plasma and extracellular fluid with the need for much less GHK. Possibly the peptide could be administered with a transdermal patch [66]. Another approach could be to use peptide-loaded liposomes as an oral delivery system for uptake into the intestinal wall without significant breakdown [67, 68].

4. Conclusion

Most current theories and therapies to treat disease tend to target only one biochemical reaction or pathway. But for human aging, our data suggests that we must think of simultaneously resetting hundreds to thousands of genes to protect at-risk tissues and organs. GHK may be a step towards this gene resetting goal.

Conflict of Interests

The authors declare that there is no conflict of interests regarding the publication of this paper.

Acknowledgments

The authors would like to thank Idelle Musiek, MFA, and Genevieve Pickart, MA, for their invaluable work in the paper preparation.

References

[1] C. Franceschi and J. Campisi, "Chronic inflammation (inflammaging) and its potential contribution to age-associated diseases," *The Journals of Gerontology*, vol. 69, supplement 1, pp. s4–s9, 2014.

[2] A. Brunet and S. L. Berger, "Epigenetics of aging and aging-related disease," *Journals of Gerontology A: Biological Sciences and Medical Sciences*, vol. 69, supplement 1, p. S1720, 2014.

[3] L. Pickart, "The human tri-peptide GHK and tissue remodeling," *Journal of Biomaterials Science, Polymer Edition*, vol. 19, no. 8, pp. 969–988, 2008.

[4] L. Pickart, "The human tripeptide GHK (Glycyl-L-Histidyl-L-Lysine)," in *The Copper Switch, and The Treatment of the Degenerative Conditions of Aging*, R. Klatz and R. Goldman, Eds., chapter 36, pp. 301–312, American Academy of Anti-Aging Medicine, 2009.

[5] H. R. Choi, Y. A. Kang, S. J. Ryoo et al., "Stem cell recovering effect of copper-free GHK in skin," *Journal of Peptide Science*, vol. 18, Article ID 685G690, pp. 685–690, 2012.

[6] S. Jose, M. L. Hughbanks, B. Y. Binder, G. C. Ingavle, and J. K. Leach, "Enhanced trophic factor secretion by mesenchymal stem/stromal cells with Glycine-Histidine-Lysine (GHK)-modified alginate hydrogels," *Acta Biomaterialia*, vol. 10, pp. 1955–1964, 2014.

[7] L. Pickart, J. M. Vasquez-Soltero, F. D. Pickart, and J. Majnarich, "GHK, the human skin remodeling peptide, induces anti-cancer expression of numerous caspase, growth regulatory, and DNA repair genes," *Journal of Analytical Oncology*, vol. 3, no. 2, pp. 79–87, 2014.

[8] Y. Hong, T. Downey, K. W. Eu, P. K. Koh, and P. Y. Cheah, "A 'metastasis-prone' signature for early-stage mismatch-repair proficient sporadic colorectal cancer patients and its implications for possible therapeutics," *Clinical and Experimental Metastasis*, vol. 27, no. 2, pp. 83–90, 2010.

[9] L. E. Matalka, A. Ford, and M. T. Unlap, "The tripeptide, GHK, induces programmed cell death in SH-SY5Y neuroblastoma cells," *Journal of Biotechnology & Biomaterials*, vol. 2, pp. 1–4, 2012.

[10] J. D. Campbell, J. E. McDonough, J. E. Zeskind et al., "A gene expression signature of emphysema-related lung destruction and its reversal by the tripeptide GHK," *Genome Medicine*, vol. 4, article 67, 2012.

[11] K. Yano, J. S. Grove, R. Chen, B. L. Rodriguez, J. D. Curb, and R. P. Tracy, "Plasma fibrinogen as a predictor of total and cause-specific mortality in elderly Japanese-American men," *Arteriosclerosis, Thrombosis, and Vascular Biology*, vol. 21, no. 6, pp. 1065–1070, 2001.

[12] M. Benderly, E. Graff, H. Reicher-Reiss, S. Behar, D. Brunner, and U. Goldbourt, "Fibrinogen is a predictor of mortality in coronary heart disease patients," *Arteriosclerosis, Thrombosis, and Vascular Biology*, vol. 16, no. 3, pp. 351–356, 1996.

[13] E. Kevei and T. Hoppe, "Ubiquitin sets the timer: impacts on aging and longevity," *Nature Structural & Molecular Biology*, vol. 21, pp. 290–292, 2014.

[14] N. Chondrogianni, M. Sakellari, M. Lefaki, N. Papaevgeniou, and E. S. Gonos, "Proteasome activation delays aging in vitro and in vivo," *Free Radical Biology & Medicine C*, vol. 71, pp. 303–320, 2014.

[15] C. Kenyon, "The first long-lived mutants: discovery of the insulin/IGF-1 pathway for ageing," *Philosophical Transactions of the Royal Society B*, vol. 366, no. 1561, pp. 9–16, 2011.

[16] J. Lamb, E. D. Crawford, D. Peck et al., "The connectivity map: using gene-expression signatures to connect small molecules, genes, and disease," *Science*, vol. 313, no. 5795, pp. 1929–1935, 2006.

[17] M. Reich, T. Liefeld, J. Gould, J. Lerner, P. Tamayo, and J. P. Mesirov, "GenePattern 2.0," *Nature Genetics*, vol. 38, no. 5, pp. 500–501, 2006.

[18] C. L. Carty, P. Heagerty, S. R. Heckbert et al., "Interaction between fibrinogen and IL-6 genetic variants and associations with cardiovascular disease risk in the cardiovascular health study," *Annals of Human Genetics*, vol. 74, no. 1, pp. 1–10, 2010.

[19] S. Schagen, R. Voegeli, D. Imfeld, T. Schreier, and C. Zouboulis, "Lipid regulation in SZ95 sebocytes by glycyl-histidyl-lysine," in *Proceedings of the 16th European Academy of Dermatology and Venereology Congress*, May 2007.

[20] A. Gruchlik, M. Jurzak, E. W. A. Chodurek, and Z. Dzierzewicz, "Effect of Gly-Gly-His, Gly-His-Lys and their copper complexes on TNF-α-dependent IL-6 secretion in normal human dermal fibroblasts," *Acta Poloniae Pharmaceutica*, vol. 69, no. 6, pp. 1303–1306, 2012.

[21] N. Mariappan, C. M. Elks, S. Sriramula et al., "NF-κB-induced oxidative stress contributes to mitochondrial and cardiac dysfunction in type II diabetes," *Cardiovascular Research*, vol. 85, no. 3, pp. 473–483, 2010.

[22] W. P. Vermeij, B. I. Florea, S. Isenia, A. Alia, J. Brouwer, and C. Backendorf, "Proteomic identification of in vivo interactors reveals novel function of skin cornification proteins," *Journal of Proteome Research*, vol. 11, no. 6, pp. 3068–3076, 2012.

[23] W. P. Vermeij, A. Alia, and C. Backendorf, "ROS quenching potential of the epidermal cornified cell envelope," *Journal of Investigative Dermatology*, vol. 131, no. 7, pp. 1435–1441, 2011.

[24] C. Liu, H.-J. Liu, Y. Xiang, Y.-R. Tan, X.-L. Zhu, and X.-Q. Qin, "Wound repair and anti-oxidative capacity is regulated by ITGB4 in airway epithelial cells," *Molecular and Cellular Biochemistry*, vol. 341, no. 1-2, pp. 259–269, 2010.

[25] S. Elsøe, J. Ahnström, C. Christoffersen et al., "Apolipoprotein M binds oxidized phospholipids and increases the antioxidant effect of HDL," *Atherosclerosis*, vol. 221, no. 1, pp. 91–97, 2012.

[26] S. L. Kempster, G. Belteki, D. Licence, D. S. Charnock-Jones, and G. C. S. Smith, "Disruption of paraoxonase 3 impairs proliferation and antioxidant defenses in human A549 cells and causes embryonic lethality in mice," *The American Journal of Physiology—Endocrinology and Metabolism*, vol. 302, no. 1, pp. E103–E107, 2012.

[27] D. Novick, S.-H. Kim, G. Fantuzzi, L. L. Reznikov, C. A. Dinarello, and M. Rubinstein, "Interleukin-18 binding protein: a novel modulator of the Th1 cytokine response," *Immunity*, vol. 10, no. 1, pp. 127–136, 1999.

[28] N. Song, J. Wang, H. Jiang, and J. Xie, "Ferroportin1 and hephaestin overexpression attenuate iron-induced oxidative stress in MES23.5 dopaminergic cells," *Journal of Cellular Biochemistry*, vol. 110, no. 5, pp. 1063–1072, 2010.

[29] Y. Gong, G. Wang, Y. Gong, J. Yan, Y. Chen, and F. J. Burczynski, "Hepatoprotective role of liver fatty acid binding protein in

acetaminophen induced toxicity," *BMC Gastroenterology*, vol. 14, article 44, 2014.

[30] G. Wang, Y. Gong, J. Anderson et al., "Antioxidative function of L-FABP in L-FABP stably transfected Chang liver cells," *Hepatology*, vol. 42, no. 4, pp. 871–879, 2005.

[31] M. Rosenblat, R. Karry, and M. Aviram, "Paraoxonase 1 (PON1) is a more potent antioxidant and stimulant of macrophage cholesterol efflux, when present in HDL than in lipoprotein-deficient serum: relevance to diabetes," *Atherosclerosis*, vol. 187, no. 1, pp. 74.e1–74.e10, 2006.

[32] S. Hussain, W. Slikker Jr., and S. F. Ali, "Role of metallothionein and other antioxidants in scavenging superoxide radicals and their possible role in neuroprotection," *Neurochemistry International*, vol. 29, no. 2, pp. 145–152, 1996.

[33] A. Viarengo, B. Burlando, N. Ceratto, and I. Panfoli, "Antioxidant role of metallothioneins: a comparative overview.," *Cellular and Molecular Biology*, vol. 46, no. 2, pp. 407–417, 2000.

[34] G. E. Henry, R. A. Momin, M. G. Nair, and D. L. Dewitt, "Antioxidant and cyclooxygenase activities of fatty acids found in food," *Journal of Agricultural and Food Chemistry*, vol. 50, no. 8, pp. 2231–2234, 2002.

[35] X. L. Chen and C. Kunsch, "Induction of cytoprotective genes through Nrf2/antioxidant response element pathway: a new therapeutic approach for the treatment of inflammatory diseases," *Current Pharmaceutical Design*, vol. 10, no. 8, pp. 879–891, 2004.

[36] N. Mariappan, R. N. Soorappan, M. Haque, S. Sriramula, and J. Francis, "TNF-α-induced mitochondrial oxidative stress and cardiac dysfunction: restoration by superoxide dismutase mimetic Tempol," *The American Journal of Physiology—Heart and Circulatory Physiology*, vol. 293, no. 5, pp. H2726–H2737, 2007.

[37] L. Pickart, "Method of using copper(II) containing compounds to accelerate wound healing," United States Patent 5164367, 1992, http://www.freepatentsonline.com/5164367.html.

[38] V. Y. Cherdakov, M. Y. Smakhtin, G. M. Dubrovin, V. T. Dudka, and I. I. Bobyntsev, "Synergetic antioxidant and reparative action of thymogen, dalargin and peptide Gly-His-Lys in tubular bone fractures," *Experimental Biology and Medicine*, vol. 4, pp. 15–20, 2010.

[39] P. V. Peplow and G. D. Baxter, "Gene expression and release of growth factors during delayed wound healing: A review of studies in diabetic animals and possible combined laser phototherapy and growth factor treatment to enhance healing," *Photomedicine and Laser Surgery*, vol. 30, no. 11, pp. 617–636, 2012.

[40] K. Deonarine, M. C. Panelli, M. E. Stashower et al., "Gene expression profiling of cutaneous wound healing," *Journal of Translational Medicine*, vol. 5, article 11, 2007.

[41] P. J. Murray and S. T. Smale, "Restraint of inflammatory signaling by interdependent strata of negative regulatory pathways," *Nature Immunology*, vol. 13, no. 10, pp. 916–924, 2012.

[42] S. Kachgal, K. A. Mace, and N. J. Boudreau, "The dual roles of homeobox genes in vascularization and wound healing," *Cell Adhesion and Migration*, vol. 6, no. 6, pp. 457–470, 2012.

[43] K. R. Yu and K. S. Kang, "Aging-related genes in mesenchymal stem cells: a mini-review," *Gerontology*, vol. 59, pp. 557–563, 2013.

[44] T. Arodz, D. Bonchev, and R. F. Diegelmann, "A network approach to wound healing," *Advances in Wound Care*, vol. 2, no. 9, pp. 499–509, 2013.

[45] S. Lamouille, J. Xu, and R. Derynck, "Molecular mechanisms of epithelial-mesenchymal transition," *Nature Reviews Molecular Cell Biology*, vol. 15, pp. 178–196, 2014.

[46] N. R. Jana, "Protein homeostasis and aging: role of ubiquitin protein ligases," *Neurochemistry International*, vol. 60, no. 5, pp. 443–447, 2012.

[47] P. J. Hohensinner, J. J. Goronzy, and C. M. Weyand, "Targets of immune regeneration in rheumatoid arthritis," *Mayo Clinic Proceedings*, vol. 89, no. 4, pp. 563–575, 2014.

[48] A. Trusina, "Stress induced telomere shortening: longer life with less mutations?" *BMC Systems Biology*, vol. 8, article 27, 2014.

[49] B. Debrabant, M. Soerensen, F. Flachsbart et al., "Human longevity and variation in DNA damage response and repair: study of the contribution of sub-processes using competitive gene-set analysis," *European Journal of Human Genetics*, vol. 22, no. 9, pp. 1131–1136, 2014.

[50] H. Lodish, A. Berk, P. Matsudaira et al., *Mollecular Biology of the Cell*, W.H. Freeman, New York, NY, USA, 2004.

[51] I. S. Young and J. V. Woodside, "Antioxidants in health and disease," *Journal of Clinical Pathology*, vol. 54, no. 3, pp. 176–186, 2001.

[52] V. Arul, D. Gopinath, K. Gomathi, and R. Jayakumar, "Biotinylated GHK peptide incorporated collagenous matrix: A novel biomaterial for dermal wound healing in rats," *Journal of Biomedical Materials Research B Applied Biomaterials*, vol. 73, no. 2, pp. 383–391, 2005.

[53] V. Arul, R. Kartha, and R. Jayakumar, "A therapeutic approach for diabetic wound healing using biotinylated GHK incorporated collagen matrices," *Life Sciences*, vol. 80, no. 4, pp. 275–284, 2007.

[54] M. Alberghina, G. Lupo, G. La Spina et al., "Cytoprotective effect of copper(II) complexes against ethanol-induced damage to rat gastric mucosa," *Journal of Inorganic Biochemistry*, vol. 45, no. 4, pp. 245–259, 1992.

[55] K. Fukuda, M. Oh, S. Asada et al., "Sodium hyaluronate inhibits interleukin-1-evoked reactive oxygen species of bovine articular chondrocytes," *Osteoarthritis and Cartilage*, vol. 9, no. 4, pp. 390–392, 2001.

[56] B. Meier, H. H. Radeke, S. Selle et al., "Human fibroblasts release reactive oxygen species in response to interleukin-1 or tumour necrosis factor-α," *Biochemical Journal*, vol. 263, no. 2, pp. 539–545, 1989.

[57] C. Vinci, V. Caltabiano, A. M. Santoro et al., "Copper addition prevents the inhibitory effects of interleukin on rat pancreatic islets," *Diabetologia*, vol. 38, no. 1, pp. 39–45, 1995.

[58] C. E. Thomas, "The influence of medium components on Cu^{2+}-dependent oxidation of low-density lipoproteins and its sensitivity to superoxide dismutase," *Biochimica et Biophysica Acta*, vol. 1128, no. 1, pp. 50–57, 1992.

[59] G. Beretta, E. Arlandini, R. Artali, J. M. G. Anton, and R. M. Facino, "Acrolein sequestering ability of the endogenous tripeptide glycyl-histidyl-lysine (GHK): characterization of conjugation products by ESI-MSn and theoretical calculations," *Journal of Pharmaceutical and Biomedical Analysis*, vol. 47, no. 3, pp. 596–602, 2008.

[60] G. Beretta, R. Artali, L. Regazzoni, M. Panigati, and R. M. Facino, "Glycyl-histidyl-lysine (GHK) is a quencher of α,β-4-hydroxy-trans-2-nonenal: a comparison with carnosine. Insights into the mechanism of reaction by electrospray ionization mass spectrometry, 1H NMR, and computational techniques," *Chemical Research in Toxicology*, vol. 20, no. 9, pp. 1309–1314, 2007.

[61] J. Cebrian, A. Messeguer, R. Facino, and J. García Antón, "New anti-RNS and -RCS products for cosmetic treatment," *International Journal of Cosmetic Science*, vol. 27, no. 5, pp. 271–278, 2005.

[62] D. M. Miller, D. DeSilva, L. Pickart, and S. D. Aust, "Effects of glycyl-histidyl-lysyl chelated Cu(II) on ferritin dependent lipid peroxidation," *Advances in Experimental Medicine and Biology*, vol. 264, pp. 79–84, 1990.

[63] C. J. Kenyon, "The genetics of ageing," *Nature*, vol. 464, pp. 504–512, 2010.

[64] S. R. Hilfer, S. L. Schneck, and J. W. Brown, "The effect of culture conditions on cytodifferentiation of fetal mouse lung respiratory passageways," *Experimental Lung Research*, vol. 10, no. 2, pp. 115–136, 1986.

[65] M. Y. Smakhtin, A. I. Konoplya, L. A. Severyanova, A. A. Kurtseva, and V. Y. Cherdakov, "Reparative activity of different functional group peptides in hepatopathyes," *Experimental Biology and Medicine*, vol. 3, pp. 11–17, 2006.

[66] J. J. Hostynek, F. Dreher, and H. I. Maibach, "Human skin penetration of a copper tripeptide in vitro as a function of skin layer," *Inflammation Research*, vol. 60, no. 1, pp. 79–86, 2011.

[67] P. Li, H. M. Nielsen, and A. Müllertz, "Oral delivery of peptides and proteins using lipid-based drug delivery systems," *Expert Opinion on Drug Delivery*, vol. 9, no. 10, pp. 1289–1304, 2012.

[68] J. Swaminathan and C. Ehrhardt, "Liposomal delivery of proteins and peptides," *Expert Opinion on Drug Delivery*, vol. 9, no. 12, pp. 1489–1503, 2012.

Hindawi Publishing Corporation
BioMed Research International
Volume 2014, Article ID 140165, 10 pages
http://dx.doi.org/10.1155/2014/140165

Review Article

Superoxide Dismutase 1 Loss Disturbs Intracellular Redox Signaling, Resulting in Global Age-Related Pathological Changes

Kenji Watanabe,[1,2] Shuichi Shibuya,[1] Yusuke Ozawa,[1] Hidetoshi Nojiri,[3] Naotaka Izuo,[1] Koutaro Yokote,[2] and Takahiko Shimizu[1]

[1] *Department of Advanced Aging Medicine, Chiba University Graduate School of Medicine, Chiba 260-8670, Japan*
[2] *Department of Clinical Cell Biology and Medicine, Chiba University Graduate School of Medicine, Chiba 260-8670, Japan*
[3] *Department of Orthopaedics, Juntendo University Graduate School of Medicine, Bunkyo-ku, Tokyo 113-0033, Japan*

Correspondence should be addressed to Takahiko Shimizu; shimizut@chiba-u.jp

Received 23 April 2014; Revised 29 July 2014; Accepted 6 August 2014; Published 8 September 2014

Academic Editor: Chi-Feng Hung

Aging is characterized by increased oxidative stress, chronic inflammation, and organ dysfunction, which occur in a progressive and irreversible manner. Superoxide dismutase (SOD) serves as a major antioxidant and neutralizes superoxide radicals throughout the body. *In vivo* studies have demonstrated that copper/zinc superoxide dismutase-deficient ($Sod1^{-/-}$) mice show various aging-like pathologies, accompanied by augmentation of oxidative damage in organs. We found that antioxidant treatment significantly attenuated the age-related tissue changes and oxidative damage-associated p53 upregulation in $Sod1^{-/-}$ mice. This review will focus on various age-related pathologies caused by the loss of *Sod1* and will discuss the molecular mechanisms underlying the pathogenesis in $Sod1^{-/-}$ mice.

1. Introduction

Aging is associated with several functional and structural deficits in organs, which are linked to biochemical changes, including oxidative modifications, protein aggregation, and altered gene expression [1]. Reactive oxygen species (ROS) are mainly generated from the electron transport chain in mitochondria and nonspecifically oxidize cellular molecules such as proteins, nucleic acids, and lipids, thus resulting in the accumulation of oxidative damage in organisms [2].

The redox balance is physiologically regulated through the production and degradation of ROS in antioxidant systems to protect cells from oxidative damage. Superoxide dismutase (SOD) enzymes play a major role in the antioxidant system by catalyzing the conversion of superoxide radicals ($O_2^{\bullet -}$) to hydrogen peroxide (H_2O_2) and O_2 [3]. In mammals, there are three SOD isoforms: CuZn-SOD (*Sod1*), which exists in the cytoplasm; Mn-SOD (*Sod2*), which is distributed in the mitochondrial matrix; and extracellular SOD (*Sod3*), which is localized in extracellular fluids, such as lymph, synovial fluid, and plasma.

Mice lacking *Sod2* showed dilated cardiomyopathy, steatosis, and metabolic acidosis, which resulted in neonatal lethality [4]. Therefore, heterozygous ($Sod2^{+/-}$) knockout or tissue-specific knockout mice are used to analyze the physiological role of *Sod2* in various tissues and organs [5, 6]. Carlsson et al. generated *Sod3*-null mutant mice [7]. Although $Sod3^{-/-}$ mice exhibited a shorter survival time than wild-type controls under hyperoxic conditions, the mice grew with no apparent abnormalities until late in life. In contrast, Reaume et al. first described the characterization of global *Sod1*-deficient ($Sod1^{-/-}$) mice. These mice exhibited marked vulnerability to motor neuron loss after axonal injury [8]. Subsequently, $Sod1^{-/-}$ mice showed a significantly shortened mean lifespan by approximately 30% and a high incidence of liver tumors by 20 months of age compared with those of $Sod1^{+/+}$ mice [9]. *In vitro* studies also revealed that $Sod1^{-/-}$ fibroblasts showed a significantly decreased growth rate and higher sensitivity to O_2 stress than $Sod1^{+/+}$ cells [10]. In the following paragraphs, we will introduce the various organ and tissue changes associated with the cellular phenotypes in $Sod1^{-/-}$ mice.

Table 1: The age-related pathologies in *Sod1*$^{-/-}$ mice.

Brain	Acceleration of Alzheimer's disease	[11, 12]
Eye	Macular degeneration	[13, 14]
	Cataract	[15]
	Dry eye	[16, 17]
Ear	Cochlear hair cell loss	[18]
	Hearing loss	[19]
Blood	Hemolytic anemia	[20]
Bone	Osteopenia	[21, 22]
Skin	Skin atrophy	[23, 24]
Muscle	Skeletal muscle atrophy	[25]
Pancreas	Glucose intolerance	[26, 27]
Liver	Hepatocellular carcinoma	[9]
	Fatty deposits	[28]
Ovary	Infertility	[29, 30]
	Luteal degeneration	[31]

2. *Sod1*$^{-/-}$ Mice Exhibit Age-Related Pathological Changes in Various Organs and Tissues

We and other groups have demonstrated that *Sod1*$^{-/-}$ mice show various aging-like tissue changes, such as acceleration of Alzheimer's disease (AD) [11, 12], macular degeneration [13, 14], cataracts [15], dry eye [16, 17], cochlear hair cell loss [18], hearing loss [19], hemolytic anemia [20], osteopenia [21, 22], skin atrophy [23, 24], skeletal muscle atrophy [25], glucose intolerance [26, 27], hepatic carcinoma [9], fatty liver [28], infertility [29, 30], and luteal degeneration [31] (Table 1). Furthermore, the biochemical analyses revealed that *Sod1* loss in organs led to the accumulation of oxidative molecules such as carbonylated proteins, lipid peroxidants, oxidized nucleic acids, and advanced glycation end products (AGEs), which resulted in broadly impaired cellular signaling, gene expression, energy metabolism, cytoskeletal morphology, and cell death in the tissues.

3. Effects on the Individual Organs and Tissues

3.1. Effects on the Brain. Brain function declines in patients with neurodegenerative diseases, as well as during normal aging [32]. Ansari and Scheff reported a strong correlation between oxidative damage levels (total SOD, glutathione, catalase, thiobarbituric acid reactive substances, protein carbonyl, 3-nitrotyrosine, 4-hydroxynonenal, and acrolein) and the variable dementia status of subjects [33]. In addition, we have previously reported a specific reduction of SOD1 protein level, but not SOD2 and SOD3, in neocortex of AD brains [11]. We also reported that a mouse model for AD lacking *Sod1* showed exacerbation of memory loss and behavioral abnormalities associated with accelerated plaque formation and amyloid accumulation [11, 12]. Furthermore, a biochemical analysis also revealed high levels of intracellular Nε-(carboxymethyl) lysine (CML) and 8-hydroxy-2′-deoxyguanosine (8-OHdG) in the mouse brain. In addition, *Sod1* deficiency induced neuronal inflammation, as demonstrated by astrocyte and microglial activation in a mouse model for AD. These findings strongly suggested that SOD1 expression plays a pivotal role in maintaining cellular redox balance and brain function during aging.

3.2. Effects on the Eyes. Several eye diseases, such as age-related macular degeneration, cataracts, dry eye, phacoemulsification, and presbyopia, are closely related to the aging process [32, 34]. *Sod1* deficiency induced the development of drusen-like deposits in the retina, choroidal neovascularization, and retinal pigment epithelium dysfunction, thus resulting in age-related retinal degenerative disorders, including age-related macular degeneration [13, 14]. An immunohistochemical analysis also revealed that CML-positive deposits were abundantly detected in the retinas of aged *Sod1*$^{-/-}$ mice [13]. Moreover, the *Sod1*$^{-/-}$ mouse lens showed twice the level of $O_2^{\bullet-}$ generation compared with that of control mice and had accelerated cataractogenesis following ultraviolet irradiation [15]. Furthermore, Dogru and colleagues reported that *Sod1*$^{-/-}$ mice also exhibited typical dry eye associated with lacrimal gland and meibomian gland changes, and this occurred in an age-dependent manner [16, 17]. The *Sod1*$^{-/-}$ lacrimal and meibomian glands showed increased 4-hydroxy-2-nonenal and 8-OHdG staining, apoptotic cells, and inflammatory infiltrates at 50 weeks of age compared to *Sod1*$^{+/+}$ mice. In addition, electron microscopy observations detected ultrastructural alterations in the mitochondria, including swelling, disorientation, shortening, disorganized cristae, marked fragmentation, shrinkage of the nuclei, and cytoplasmic vacuole formation, as well as the loss of nuclear membranes in *Sod1*$^{-/-}$ mice.

3.3. Changes in the Ears. The cochlear structure in the ear is progressively degenerated during aging, leading to hearing loss [35, 36]. McFadden et al. reported that *Sod1* deficiency morphologically induced a reduction of the inner and outer hair cells during aging [18]. In addition, *Sod1* ablation impacted the noise-induced permanent threshold shifts, leading to hearing loss [18, 19]. On the other hand, systemic overexpression of human *Sod1* protected against age-related and noise-induced hearing loss in C57BL/6 mice [37].

3.4. Changes in the Blood. During aging, the levels of oxidative stress markers, including 8-isoprostane and 2-thiobarbituric acid reactive substances (TBARS), are gradually increased in the plasma and erythrocytes of *Sod1*$^{-/-}$ mice [20]. Furthermore, Iuchi et al. reported that an intracellular ROS indicator, CM-H_2DCFDA (DCF), in erythrocytes was spontaneously elevated in *Sod1*$^{-/-}$ mice. *Sod1*$^{-/-}$ mice also showed hemolytic anemia associated with splenomegaly. In fact, the erythrocyte lifespan from *Sod1*$^{-/-}$ mice was decreased by 60% compared to that of *Sod1*$^{+/+}$ erythrocytes [20]. We independently measured the serum levels of various markers of inflammation in *Sod1*$^{-/-}$

Table 2: The serum biomarker levels in *Sod1*$^{-/-}$ mice.

Markers	Concentrations	*Sod1*$^{+/+}$	*Sod1*$^{-/-}$	*P* value
IL-10	ng/mL	425 ± 54	451 ± 60	0.495
IL-11	pg/mL	39 ± 14.4	33 ± 13.2	0.627
IL-12p70	ng/mL	ND	ND	—
IL-17	pg/mL	ND	ND	—
IL-18	ng/mL	10 ± 1.1	12 ± 1.21	0.105
IL-1alpha	pg/mL	83 ± 63	134 ± 89.4	0.467
IL-1beta	ng/mL	12 ± 1.1	13 ± 1.6	0.268
IL-2	pg/mL	ND	ND	—
IL-3	pg/mL	ND	ND	—
IL-4	pg/mL	20.2 ± 0.0	20.2 ± 0.0	1
IL-5	ng/mL	0.23 ± 0.066	0.19 ± 0.055	0.406
IL-6	pg/mL	4.4 ± 1.7	18 ± 14.3	0.102
IL-7	ng/mL	0.02 ± 0.016	0.05 ± 0.025	0.296
IP-10	pg/mL	99 ± 17.1	150 ± 60.3	0.109
M-CSF	pg/mL	6.9 ± 0.50	6.0 ± 0.25	0.010*
MCP-1	pg/mL	100 ± 34.2	124 ± 60.0	0.457
MCP-3	pg/mL	235 ± 50.9	235 ± 69.3	0.996
MCP-5	pg/mL	18 ± 1.7	24 ± 7.0	0.094
MIP-1alpha	ng/mL	1.6 ± 0.21	1.7 ± 0.09	0.307
MIP-1beta	pg/mL	55 ± 16.5	80 ± 17.5	0.005*
MIP-1gamma	pg/mL	26 ± 3.6	34 ± 3.7	0.013*
MIP-2	pg/mL	18 ± 2.1	20 ± 5.2	0.371
MIP-3beta	ng/mL	1.8 ± 0.37	1.7 ± 0.14	0.349
MDC	pg/mL	547 ± 234	626 ± 42	0.481
RANTES	pg/mL	0.26 ± 0.130	0.45 ± 0.049	0.014*
TNF-alpha	ng/mL	0.066 ± 0.004	0.077 ± 0.010	0.041*
TPO	ng/mL	75 ± 9.4	86.5 ± 5.6	0.049*

ND indicates "not detected". * indicates a significant difference.

mice. A multiplex analysis revealed an altered pattern of inflammation markers, such as macrophage colony stimulating factor (M-CSF), macrophage inflammatory protein-1 beta (MIP-1 beta), macrophage inflammatory protein-1 gamma (MIP-1 gamma), regulated on activation, normal T cell expressed and secreted (RANTES), tumor necrosis factor-alpha (TNF-alpha), and thrombopoietin (TPO) in the *Sod1*$^{-/-}$ mouse sera (Table 2).

3.5. Effects on Bone. Aging stress generally causes bone loss and fragility [38]. We previously clarified that the loss of *Sod1* caused bone loss without leading to developmental skeletal abnormalities in both male and female mice [21]. The three-dimensional computed tomography analyses revealed that there was marked bone loss in both cortical and cancellous bones of *Sod1*$^{-/-}$ mice, which was associated with decreased bone formation and resorption, indicating the presence of low-turnover osteopenia (Figure 1). *Sod1* deficiency also enhanced the intracellular ROS production and the formation of pentosidine, one of the AGEs, in osteoblasts and bone [21]. Furthermore, Wang et al. also reported that young *Sod1*$^{-/-}$ mice showed bone fragility in the femora at the growth stage [39].

Recently, we found that mechanical unloading-induced bone loss associated with intracellular ROS generation in bone-forming cells and bone marrow cells [22]. Interestingly, we also detected specific *Sod1* upregulation at both the RNA and protein levels in bone during mechanical unloading [22]. Notably, *Sod1* deficiency significantly exacerbated the bone loss during mechanical unloading. In addition, *Sod1*$^{-/-}$ mice clearly displayed four-layered structural abnormalities and fragmented tidemarks in the enthesis, indicating tendon enthesis degeneration [40]. These findings suggested that *Sod1* plays a protective role in regulating bone and tendon enthesis homeostasis, as well as the redox balance during unloading and aging in mice.

3.6. Changes in the Skin. Aged skin is characterized by wrinkles, sagging, dryness, and collagen degradation [41, 42]. We have previously reported that *Sod1* deletion caused typical age-related skin thinning [23]. In hematoxylin and eosin stained sections, the epidermis and dermis of the *Sod1*$^{-/-}$ back skin showed remarkable thinning (Figure 2(a)). In addition, the skin weight and hydroxyproline content, which is a unique amino acid present in collagen and elastin, in the *Sod1*$^{-/-}$ mice were compared with those of *Sod1*$^{+/+}$ mice [24].

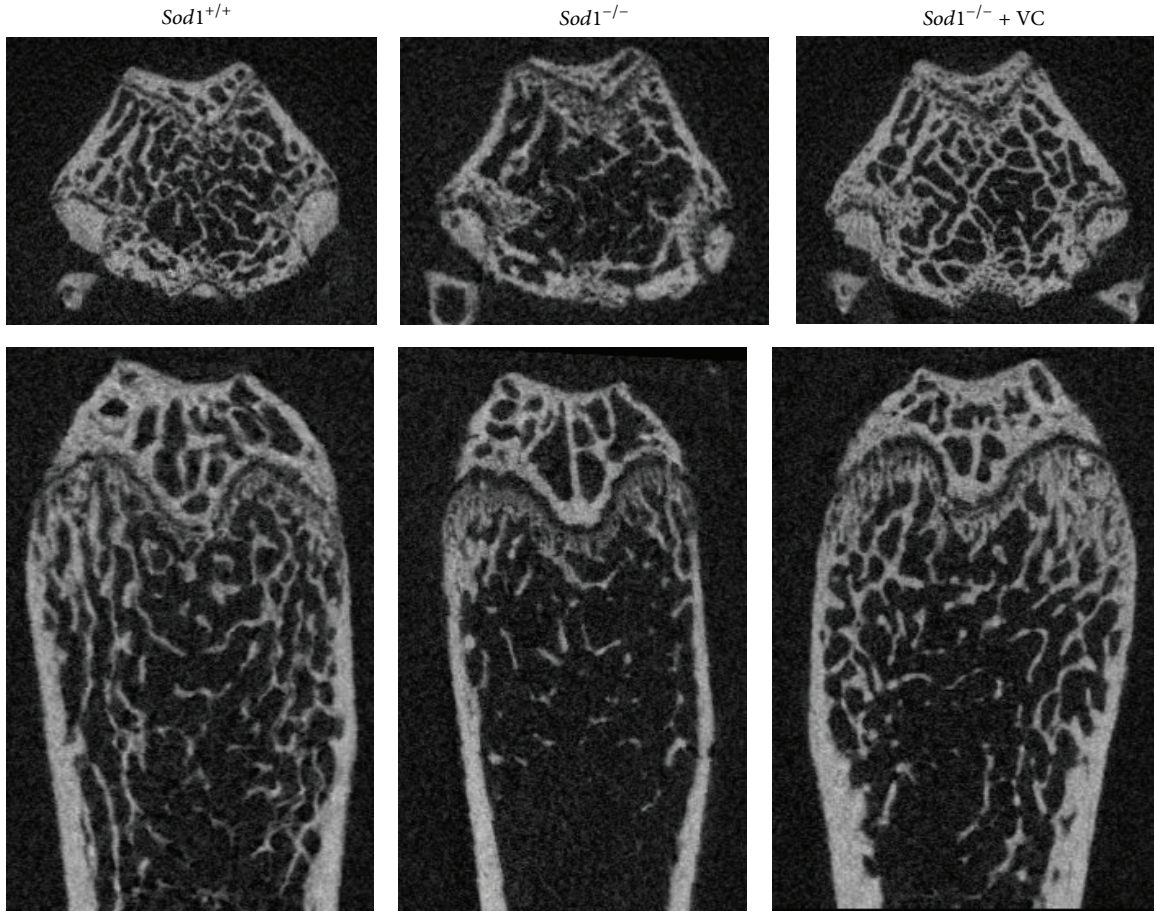

Figure 1: The bone loss in *Sod1*$^{-/-}$ mice. The treatment with 1% vitamin C in drinking water started from 4 weeks of age and continued for 12 weeks. Axial (upper panels) and coronal (lower panels) sections of μCT images of the distal ends of the femora of *Sod1*$^{+/+}$ and *Sod1*$^{-/-}$ females at 16 weeks of age.

An *in vitro* analysis using primary dermal fibroblasts from *Sod1*$^{-/-}$ neonates revealed severe cellular phenotypes, such as apoptosis and growth arrest, under normal conditions (Figure 2(b)). Furthermore, *Sod1*$^{-/-}$ fibroblasts showed excessive intracellular DCF-positive fluorescence (Figure 2(c)). Interestingly, *Sod1*$^{-/-}$ fibroblasts also had a significant enhancement of mitochondrial $O_2^{\bullet-}$ and impairment of the mitochondrial membrane potential [43].

3.7. Effects on Muscle. Aging contributes to the structural and functional changes in skeletal muscle in a wide range of mammals [44]. *Sod1*$^{-/-}$ mice showed significant decreases in the whole hindlimb muscle mass compared with age-matched *Sod1*$^{+/+}$ mice, and this occurred in an age-dependent manner [25]. A biochemical analysis also revealed a significant increase in oxidative damage, such as the formation of F2-isoprostanes, protein carbonyls, and 8-OHdG, in *Sod1*$^{-/-}$ skeletal muscle [25]. *Sod1* loss also induced aberrant mitochondria with abnormal shapes and led to lower ATP production in muscle. Mitochondria isolated from *Sod1*$^{-/-}$ muscle revealed significant increases in $O_2^{\bullet-}$ and H_2O_2 production and no compensatory upregulation of other antioxidant enzymes [45]. Recently, Zhang et al. reported that skeletal muscle-specific *Sod1*$^{-/-}$ mice failed to show muscle loss and ROS production [46]. Interestingly, a neuron-specific *Sod1* transgene in *Sod1*$^{-/-}$ mice prevented muscle loss [47]. The muscle from *Sod1*$^{-/-}$ mice with a brain-specific *Sod1* transgene did not show any differences in the muscle morphology, function, lipid peroxidation, or protein nitration compared with those of *Sod1*$^{+/+}$ muscle, suggesting that *Sod1* insufficiency in neuronal cells could lead to a dysregulation of the muscle mass and function in a nonautonomous manner.

3.8. Effects on the Pancreas. Aging stress also impairs insulin secretion and sensitivity in the pancreas [48]. Wang et al. reported that *Sod1*$^{-/-}$ islets exhibited a decreased β-cell mass, impaired glucose-stimulated insulin secretion, and a decreased ATP content, accompanied by elevated intracellular ROS levels [26]. In addition, *Sod1* ablation also downregulated the duodenal homeobox-1 (*Pdx1*) expression and forkhead box protein A2 (*Foxa2*) pathway in an $O_2^{\bullet-}$-dependent fashion by affecting these targets at the epigenetic, mRNA, and protein levels in the islets [26]. Furthermore, Muscogiuri

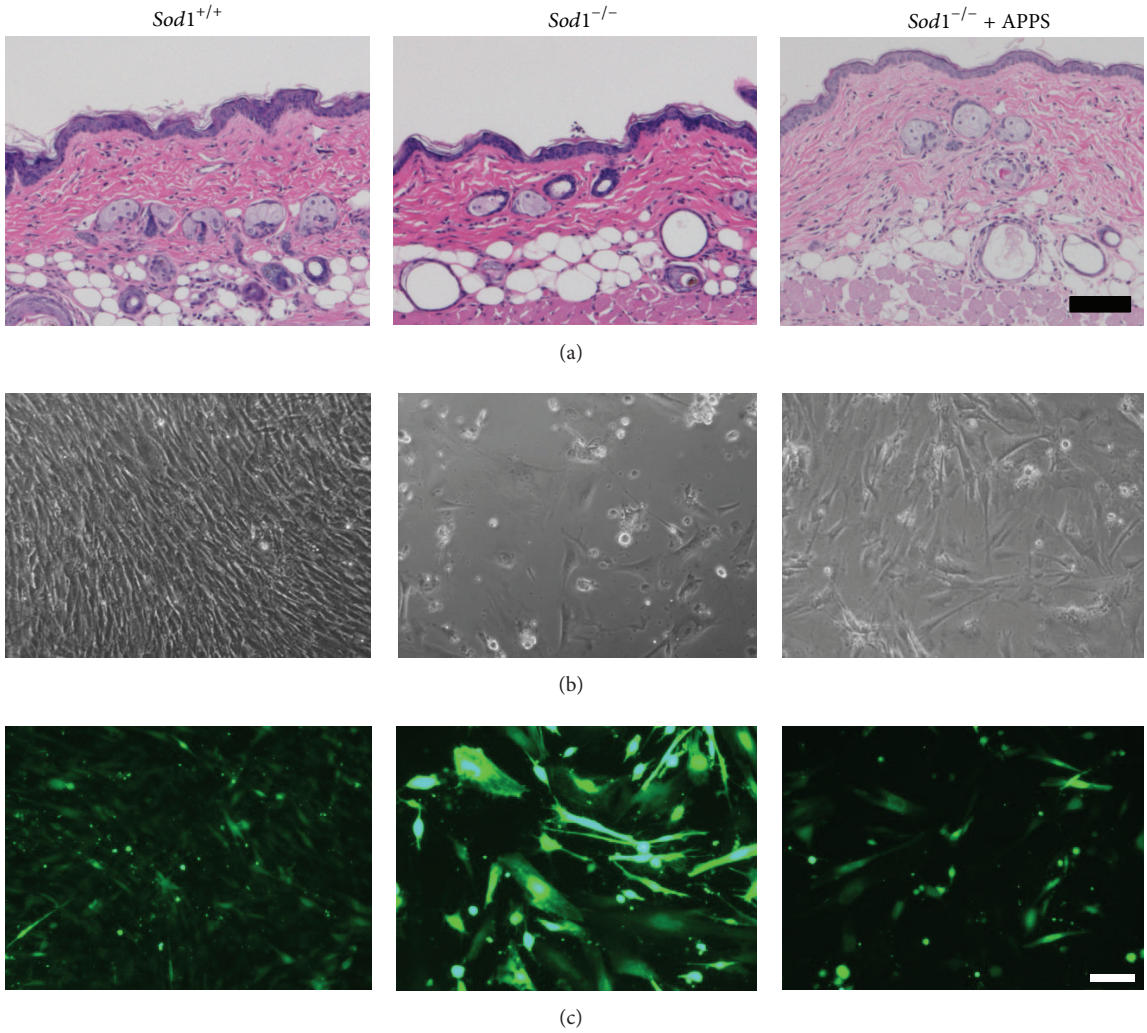

Figure 2: The skin and cellular phenotypes of *Sod1*$^{-/-}$ mice. (a) The hematoxylin and eosin staining of the back skin of *Sod1*$^{-/-}$ and *Sod1*$^{+/+}$ mice. *Sod1*$^{-/-}$ mice (5 months of age) were transdermally treated with 1% L-ascorbyl 2-phosphate 6-palmitate trisodium salt (APPS) for 4 weeks. (b) Dermal fibroblasts were dissected from *Sod1*$^{-/-}$ neonates at 5 days of age. The cells were cultured with or without 10 μM APPS for 48 h under 20% O_2. (c) The intracellular ROS levels in *Sod1*$^{-/-}$ fibroblasts treated with 10 μM APPS were measured by examining the presence of CM-H_2DCFDA. The scale bars represent 100 μm.

et al. also showed that *Sod1* loss significantly impaired the glucose tolerance and led to a reduced β-cell mass, as well as insulin secretion in a hyperglycemic clamp test [27]. Interestingly, *Sod1* ablation failed to alter the peripheral and hepatic insulin sensitivity. These results proved that the absence of *Sod1* impaired β-cell function and glucose tolerance, but not insulin sensitivity, thus resulting in diabetes-like phenotypes.

3.9. Changes in the Liver. Aging of the liver is associated with an increased incidence of tumorigenesis [49]. The liver weight to body weight ratio in *Sod1*$^{-/-}$ mice was significantly higher than that of *Sod1*$^{+/+}$ mice [9]. *Sod1*$^{-/-}$ mice also showed increased oxidative damage such as malondialdehyde (MDA), F2-isoprostane, and 8-OHdG accumulation in their livers [9]. In addition, the *Sod1*$^{-/-}$ livers showed an approximately 30% increase in hepatocarcinogenesis at 20 months of age compared to wild-type mice [9]. We also observed that *Sod1*$^{-/-}$ mice showed significantly accelerated hepatic lipid accumulation and peroxidation and impaired low-density lipoprotein secretion due to apoB degradation that occurred via a posttranslational mechanism [28]. Furthermore, Wang et al. reported that *Sod1* loss enhanced glycolysis and lipogenic signaling but decreased gluconeogenesis in the liver [50]. Recently, Kondo et al. described that the loss of senescence marker protein-30 (SMP30), which is a key enzyme required for L-ascorbic acid biosynthesis [51], accelerated the hepatic steatosis in *Sod1*$^{-/-}$ mice [52]. Both *Sod1* and *Smp30* deficiency led to a remarkable elevation of the triglyceride and cellular $O_2^{\bullet-}$ levels in the liver compared

to those of *Sod1*$^{-/-}$ or *Smp30*$^{-/-}$ mice. These findings indicated that elevated oxidative stress and/or L-ascorbic acid depletion altered the glucose and lipid metabolism in the liver, suggesting that normal SOD1 expression is essential to maintain the hepatic glucose and lipid homeostasis.

In pharmacological studies, acetaminophen (APAP) injection induces glutathione depletion, the formation of reactive nitrogen species, and plasma ALT elevation, resulting in lethal hepatotoxicity in the case of an overdose [53]. Interestingly, *Sod1* deficiency attenuated the APAP-induced hepatotoxicity and lethality owing to its reduction of hepatic APAP-cysteine adducts, protein nitration, and CYP2E1 activity, which acts as an APAP-metabolizing enzyme, in the liver [53, 54]. These data indicated that the increases in intracellular $O_2^{\bullet-}$ caused by *Sod1* deletion inhibited CYP2E1 activity, thus resulting in protection against APAP-induced hepatotoxicity.

3.10. Effects on the Ovaries. Ovarian aging is characterized by a decline in the follicle numbers and sex steroid hormone secretion, which are associated with a gradual decline in fertility [55]. Although *Sod1*$^{-/-}$ female mice had normal estrous cycles and numbers of ovulated ova, their reproductive performance was inferior to that of female *Sod1*$^{+/+}$ and *Sod1*$^{+/-}$ mice [29, 30]. A hormonal analysis revealed that *Sod1*$^{-/-}$ females showed normal plasma levels of follicle-stimulating hormone (FSH), luteinizing hormone (LH), and estradiol at proestrus [31]. On the other hand, the plasma progesterone level was specifically repressed in *Sod1*$^{-/-}$ females compared to that in *Sod1*$^{+/+}$ females during pregnancy. Although *Sod1* loss in the ovaries and oocytes upregulated the intracellular ROS production, *Sod1*$^{-/-}$ oocytes could be normally fertilized and developed to the two-cell stage *in vitro* [31, 56]. However, *Sod1*$^{-/-}$ embryos failed to divide to the four-cell stage under conventional culture conditions (20% O_2) [56]. When *Sod1*$^{-/-}$ embryos were cultured under hypoxic conditions (1% O_2), they developed to the morula stage but could not develop into blastocysts [56], indicating that O_2 stress inhibited the development of *Sod1*$^{-/-}$ embryos at the two-cell stage.

4. Intervention Strategies Using Antioxidants

Vitamin C (VC) is a soluble vitamin and the best characterized antioxidant [57]. In order to evaluate the protective effects of this antioxidant in *Sod1*$^{-/-}$ mice, we treated them with VC to try to rescue the organ phenotypes. Oral administration of VC suppressed the bone loss of *Sod1*$^{-/-}$ mice, indicating that $O_2^{\bullet-}$-induced bone loss could be improved by antioxidant treatment (Figure 1) [21]. In addition, VC treatment also normalized the bone strength and composition of collagen cross-links, without aberrant bone modeling [21]. We further applied a VC derivative, L-ascorbyl 2-phosphate 6-palmitate trisodium salt (APPS), on the *Sod1*$^{-/-}$ mouse skin. APPS is conjugated to a phosphate group and a long hydrophobic chain to promote stability and membrane permeability. The transdermal administration of the APPS reversed the skin atrophy and lipid peroxidation in *Sod1*$^{-/-}$ mice (Figure 2(a)). *In vitro* experiments revealed that APPS treatment completely improved the cell viability and suppressed the intracellular ROS production in *Sod1*$^{-/-}$ fibroblasts (Figures 2(b) and 2(c)). Furthermore, Iuchi et al. reported that oral N-acetyl cysteine (NAC) treatment attenuated the hemolytic anemia and inflammatory response, with ROS suppression, in the erythrocytes for *Sod1*$^{-/-}$ mice [20]. Additionally, we found that NAC treatment also improved the cell viability and decreased the intracellular ROS level in *Sod1*$^{-/-}$ fibroblasts [43].

The oxidative stress induced by *Sod1* deficiency is closely related to the progression of AD. Therefore, we hypothesized that antioxidant treatment would be able to alleviate the progression of AD. In this context, we treated mice with AD-like pathologies with VC. Confirming our hypothesis, chronic VC treatment restored the behavioral abnormalities, apparently by attenuating the oxidative stress in AD model mice [58]. VC also significantly suppressed the soluble Aβ accumulation in the brain, but not the plaque formation in the AD model mice [58]. Recently, we found that VC administration significantly prevented unloading-induced bone loss in wild-type mice [22]. These data strongly indicated that antioxidant intervention has remarkable protective effects against ROS-mediated tissue damage in mice.

5. Molecular Mechanisms Underlying the Organ and Tissue Pathologies in *Sod1*$^{-/-}$ Mice

To analyze the molecular mechanisms underlying the tissue damage induced by *Sod1* deficiency, we have investigated the phenotypes using double-knockout *Sod1* and liver-specific *Sod2* mice. As described above, the *Sod1*$^{-/-}$ mice showed acceleration of hepatic lipid accumulation, accompanied by increased oxidative damage. In contrast, liver-specific *Sod2* knockout mice did not show any obvious morphological abnormalities or spontaneous oxidative damage in the liver [59]. The double-knockout mice had an indistinguishable hepatic phenotype, including lipid peroxidation, lipid accumulation, and TG secretion, from that of *Sod1*$^{-/-}$ mice, indicating that the loss of *Sod2* failed to exacerbate the hepatic changes in *Sod1*$^{-/-}$ mice [28], demonstrating that the different enzymes do not have overlapping functions. Sentman et al. reported that combined *Sod1* and *Sod3* deficiency showed no additive effect on the lifespan and body weight in mice [60]. Likewise, Fujita et al. reported that *Sod1* and *Sod3* double mutant mice showed the same phenotypes, such as $O_2^{\bullet-}$ and NO production and the TBARS level, in the kidneys compared with those of wild-type mice [61]. Moreover, glutathione peroxidase-1 (GPX1) loss also had no impact on the *Sod1*$^{-/-}$ phenotypes in the liver and pancreas [26, 62]. However, *Sod1* loss significantly decreased the GPX1 activity, but not the *Gpx1* level in the liver. The Lei group reported that *Sod1* loss increased the conversion of selenocysteine to dehydroalanine residues in the active site of hepatic GPX1, thus leading to proportional decreases in the activity of the enzyme as a whole [63]. Additionally, many reports have

demonstrated that *Sod1*$^{-/-}$ mice showed no compensatory upregulation of antioxidant enzymes including *Sod2* and *Sod3* [43, 46, 60, 61]. These reports suggested that *Sod2*, *Sod3*, and/or *Gpx1* deficiency failed to further modify the organ pathologies in *Sod1*$^{-/-}$ mice.

Accumulating evidence suggests that both ataxia-telangiectasia mutated (ATM) and p53 play a central role in the DNA damage response induced by oxidative damage in organs and tissues [64]. In this context, Erker et al. investigated the organ phenotypes in mice lacking both *Sod1* and *Atm* to elucidate DNA damage response in the organs. The loss of *Atm* and *Sod1* did not show any interaction with regard to the overall cellular metabolism and survival in mice [65], indicating that *Sod1* regulates organ metabolism and lifespan in an *Atm*-independent manner.

Interestingly, we found that *Sod1*$^{-/-}$ skin displayed obvious p53 activation [43]. Additionally, treatment with a VC derivative remarkably suppressed the *p53* expression and oxidative damage in the skin of *Sod1*$^{-/-}$ mice, suggesting that the antioxidant activity of VC normalized the skin pathologies, at least in part, by suppressing $O_2^{\bullet-}$-mediated p53 activation *in vivo* [43]. Furthermore, the *Sod1* loss induced the phosphorylation of H2AX at Ser139 (γH2AX), a DNA damage marker, and upregulated p21, a target gene of p53, in fibroblasts [43]. Of note, the *Sod1*$^{-/-}$ fibroblasts exhibited a loss of mitochondrial membrane potential and enhanced mitochondria ROS generation. Likewise, Muller et al. reported that *Sod1*$^{-/-}$ skeletal muscle showed significant alterations in mitochondrial function, including increased mitochondrial ROS generation and reduced ATP production [66]. Han et al. also revealed significantly higher levels of p53 and phospho-p53 in nuclei isolated from *Sod1*$^{-/-}$ livers [67]. Moreover, Wang et al. showed that *Sod1* ablation led to increased p53 and phospho-p53 levels in islets [26]. In humans, decreased *Sod1* expression and enhanced p53 expression were observed in AD-affected brain tissues [11, 68], osteoarthritic tissues [69, 70], bones in older individuals [71, 72], and tissues in infertility patients [73, 74]. Taken together, these data suggest that cytoplasmic SOD1 loss induced the DNA damage response, which was associated with p53 upregulation, resulting in age-related pathologies.

6. Conclusion and Perspective

In the present review, we introduced various organ and tissue phenotypes of *Sod1*$^{-/-}$ mice. Using *Sod1*$^{-/-}$ mice, we and other groups have demonstrated that *Sod1* deficiency enhances the intracellular $O_2^{\bullet-}$ production and oxidative damage, resulting in global, age-related pathological changes, including changes in the brain, eyes, ears, blood, bones, skin, muscles, pancreas, liver, and ovaries during aging. Antioxidant treatment prevented or improved the pathological changes in *Sod1*$^{-/-}$ organs and tissues. Interestingly, *Sod1* does not appear to interact with other major antioxidant enzymes, such as *Sod2*, *Sod3*, and *Gpx1,* in terms of the organ and tissues pathologies, as demonstrated using double-knockout mice. These lines of evidence strongly indicated that *Sod1* plays a central role in maintaining the cellular redox balance and organ function *in vivo*. We also suggest that p53 plays a fundamental role in *Sod1*$^{-/-}$-related pathologies. Further analyses will be needed to clarify the contribution of p53 to the molecular signaling and age-related pathological changes induced by *Sod1* deficiency, including those using double mutant mice with *Sod1*$^{-/-}$ and *p53*$^{-/-}$.

Conflict of Interests

The authors declare that there is no conflict of interests regarding the publication of this paper.

Acknowledgments

This study was supported in part by the Program for the Promotion of Basic Research Activities for Innovative Biosciences and Grants-in-Aid for Scientific Research from the Ministry of Education, Culture, Sports, Science and Technology of Japan. The authors would like to thank Dr. Kazuma Murakami, from Kyoto University, and Dr. Daichi Morikawa, Dr. Keiji Kobayashi, Dr. Masato Koike, and Toshihiko Toda, from Chiba University, for their valuable technical assistance.

References

[1] C. López-Otín, M. A. Blasco, L. Partridge, M. Serrano, and G. Kroemer, "The hallmarks of aging," *Cell*, vol. 153, no. 6, pp. 1194–1217, 2013.

[2] T. Finkel and N. J. Holbrook, "Oxidants, oxidative stress and the biology of ageing," *Nature*, vol. 408, no. 6809, pp. 239–247, 2000.

[3] A. Okado-Matsumoto and I. Fridovich, "Subcellular distribution of superoxide dismutases (SOD) in rat liver. Cu,Zn-SOD in mitochondria," *The Journal of Biological Chemistry*, vol. 276, no. 42, pp. 38388–38393, 2001.

[4] Y. Li, T.-T. Huang, E. J. Carlson et al., "Dilated cardiomyopathy and neonatal lethality in mutant mice lacking manganese superoxide dismutase," *Nature Genetics*, vol. 11, no. 4, pp. 376–381, 1995.

[5] T. Shimizu, H. Nojiri, S. Kawakami, S. Uchiyama, and T. Shirasawa, "Model mice for tissue-specific deletion of the manganese superoxide dismutase gene," *Geriatrics and Gerontology International*, vol. 10, supplement 1, pp. S70–S79, 2010.

[6] T. Shimizu, H. Nojiri, and T. Shirasawa, "Tissue-specific deletion of manganese superoxide dismutase in mice," in *Systems Biology of Free Radicals and Antioxidants*, I. Laher, Ed., pp. 475–487, Springer, Berlin, Germany, 2014.

[7] L. M. Carlsson, J. Jonsson, T. Edlund, and S. L. Marklund, "Mice lacking extracellular superoxide dismutase are more sensitive to hyperoxia," *Proceedings of the National Academy of Sciences of the United States of America*, vol. 92, no. 14, pp. 6264–6268, 1995.

[8] A. G. Reaume, J. L. Elliott, E. K. Hoffman et al., "Motor neurons in Cu/Zn superoxide dismutase-deficient mice develop normally but exhibit enhanced cell death after axonal injury," *Nature Genetics*, vol. 13, no. 1, pp. 43–47, 1996.

[9] S. Elchuri, T. D. Oberley, W. Qi et al., "CuZnSOD deficiency leads to persistent and widespread oxidative damage and hepatocarcinogenesis later in life," *Oncogene*, vol. 24, no. 3, pp. 367–380, 2005.

[10] T.-T. Huang, M. Yasunami, E. J. Carlson et al., "Superoxide-mediated cytotoxicity in superoxide dismutase-deficient fetal fibroblasts," *Archives of Biochemistry and Biophysics*, vol. 344, no. 2, pp. 424–432, 1997.

[11] K. Murakami, N. Murata, Y. Noda et al., "SOD1 (copper/zinc superoxide dismutase) deficiency drives amyloid β protein oligomerization and memory loss in mouse model of Alzheimer disease," *The Journal of Biological Chemistry*, vol. 286, no. 52, pp. 44557–44568, 2011.

[12] K. Murakami, N. Murata, Y. Noda, K. Irie, T. Shirasawa, and T. Shimizu, "Stimulation of the amyloidogenic pathway by cytoplasmic superoxide radicals in an Alzheimer's disease mouse model," *Bioscience, Biotechnology and Biochemistry*, vol. 76, no. 6, pp. 1098–1103, 2012.

[13] Y. Imamura, S. Noda, K. Hashizume et al., "Drusen, choroidal neovascularization, and retinal pigment epithelium dysfunction in SOD1-deficient mice: a model of age-related macular degeneration," *Proceedings of the National Academy of Sciences of the United States of America*, vol. 103, no. 30, pp. 11282–11287, 2006.

[14] K. Hashizume, M. Hirasawa, Y. Imamura et al., "Retinal dysfunction and progressive retinal cell death in SOD1-deficient mice," *The American Journal of Pathology*, vol. 172, no. 5, pp. 1325–1331, 2008.

[15] A. Behndig, K. Karlsson, A. G. Reaume, M.-L. Sentman, and S. L. Marklund, "In vitro photochemical cataract in mice lacking copper-zinc superoxide dismutase," *Free Radical Biology and Medicine*, vol. 31, no. 6, pp. 738–744, 2001.

[16] T. Kojima, T. H. Wakamatsu, M. Dogru et al., "Age-related dysfunction of the lacrimal gland and oxidative stress: evidence from the Cu,Zn-superoxide dismutase-1 (*Sod1*) knockout mice," *The American Journal of Pathology*, vol. 180, no. 5, pp. 1879–1896, 2012.

[17] O. M. Ibrahim, M. Dogru, Y. Matsumoto et al., "Oxidative stress induced age dependent meibomian gland dysfunction in cu, zn-superoxide dismutase-1 (*Sod1*) knockout mice," *PLoS ONE*, vol. 9, no. 7, Article ID e99328, 2014.

[18] S. L. McFadden, D. Ding, A. G. Reaume, D. G. Flood, and R. J. Salvi, "Age-related cochlear hair cell loss is enhanced in mice lacking copper/zinc superoxide dismutase," *Neurobiology of Aging*, vol. 20, no. 1, pp. 1–8, 1999.

[19] K. K. Ohlemiller, S. L. McFadden, D.-L. Ding et al., "Targeted deletion of the cytosolic Cu/Zn-superoxide dismutase gene (*Sod1*) increases susceptibility to noise-induced hearing loss," *Audiology and Neuro-Otology*, vol. 4, no. 5, pp. 237–246, 1999.

[20] Y. Iuchi, F. Okada, K. Onuma et al., "Elevated oxidative stress in erythrocytes due to a SOD1 deficiency causes anaemia and triggers autoantibody production," *Biochemical Journal*, vol. 402, no. 2, pp. 219–227, 2007.

[21] H. Nojiri, Y. Saita, D. Morikawa et al., "Cytoplasmic superoxide causes bone fragility owing to low-turnover osteoporosis and impaired collagen cross-linking," *Journal of Bone and Mineral Research*, vol. 26, no. 11, pp. 2682–2694, 2011.

[22] D. Morikawa, H. Nojiri, Y. Saita et al., "Cytoplasmic reactive oxygen species and SOD1 regulate bone mass during mechanical unloading," *Journal of Bone and Mineral Research*, vol. 28, no. 11, pp. 2368–2380, 2013.

[23] K. Murakami, J. Inagaki, M. Saito et al., "Skin atrophy in cytoplasmic SOD-deficient mice and its complete recovery using a vitamin C derivative," *Biochemical and Biophysical Research Communications*, vol. 382, no. 2, pp. 457–461, 2009.

[24] S. Shibuya, K. Kinoshita, and T. Shimizu, "Protective effects of vitamin C derivatives on skin atrophy caused by *Sod1* deficiency," in *Handbook of Diet, Nutrition and the Skin*, V. R. Preedy, Ed., pp. 351–364, Wageningen Academic, Gelderland, The Netherlands, 2012.

[25] F. L. Muller, W. Song, Y. Liu et al., "Absence of CuZn superoxide dismutase leads to elevated oxidative stress and acceleration of age-dependent skeletal muscle atrophy," *Free Radical Biology and Medicine*, vol. 40, no. 11, pp. 1993–2004, 2006.

[26] X. Wang, M. Z. Vatamaniuk, C. A. Roneker et al., "Knockouts of SOD1 and GPX1 exert different impacts on murine islet function and pancreatic integrity," *Antioxidants and Redox Signaling*, vol. 14, no. 3, pp. 391–401, 2011.

[27] G. Muscogiuri, A. B. Salmon, C. Aguayo-Mazzucato et al., "Genetic disruption of SOD1 gene causes glucose intolerance and impairs β-cell function," *Diabetes*, vol. 62, no. 12, pp. 4201–4207, 2013.

[28] S. Uchiyama, T. Shimizu, and T. Shirasawa, "CuZn-SOD deficiency causes ApoB degradation and induces hepatic lipid accumulation by impaired lipoprotein secretion in mice," *Journal of Biological Chemistry*, vol. 281, no. 42, pp. 31713–31719, 2006.

[29] Y.-S. Ho, M. Gargano, J. Cao, R. T. Bronson, I. Heimler, and R. J. Hutz, "Reduced fertility in female mice lacking copper-zinc superoxide dismutase," *Journal of Biological Chemistry*, vol. 273, no. 13, pp. 7765–7769, 1998.

[30] M. M. Matzuk, L. Dionne, Q. Guo, T. R. Kumar, and R. M. Lebovitz, "Ovarian function in superoxide dismutase 1 and 2 knockout mice," *Endocrinology*, vol. 139, no. 9, pp. 4008–4011, 1998.

[31] Y. Noda, K. Ota, T. Shirasawa, and T. Shimizu, "Copper/Zinc superoxide dismutase insufficiency impairs progesterone secretion and fertility in female mice," *Biology of Reproduction*, vol. 86, no. 1, pp. 1–8, 2012.

[32] G. G. Kovacs, H. Adle-Biassette, I. Milenkovic, S. Cipriani, J. van Scheppingen, and E. Aronica, "Linking pathways in the developing and aging brain with neurodegeneration," *Neuroscience*, vol. 269, pp. 152–172, 2014.

[33] M. A. Ansari and S. W. Scheff, "Oxidative stress in the progression of alzheimer disease in the frontal cortex," *Journal of Neuropathology and Experimental Neurology*, vol. 69, no. 2, pp. 155–167, 2010.

[34] J. Ding and D. A. Sullivan, "Aging and dry eye disease," *Experimental Gerontology*, vol. 47, no. 7, pp. 483–490, 2012.

[35] B. J. Walters and J. Zuo, "Postnatal development, maturation and aging in the mouse cochlea and their effects on hair cell regeneration," *Hearing Research*, vol. 297, pp. 68–83, 2013.

[36] A. D. Walling and G. M. Dickson, "Hearing loss in older adults," *American Family Physician*, vol. 85, no. 12, pp. 1150–1156, 2012.

[37] D. E. Coling, K. C. Y. Yu, D. Somand et al., "Effect of SOD1 overexpression on age- and noise-related hearing loss," *Free Radical Biology and Medicine*, vol. 34, no. 7, pp. 873–880, 2003.

[38] R. L. Jilka, "The relevance of mouse models for investigating age-related bone loss in humans," *Journals of Gerontology Series A: Biological Sciences and Medical Sciences*, vol. 68, no. 10, pp. 1209–1217, 2013.

[39] X. Wang, E. A. Gillen, M. C. H. Van Der Meulen, and G. L. Xin, "Knockouts of Se-glutathione peroxidase-1 and Cu,Zn superoxide dismutase exert different impacts on femoral mechanical performance of growing mice," *Molecular Nutrition and Food Research*, vol. 52, no. 11, pp. 1334–1339, 2008.

[40] D. Morikawa, Y. Itoigawa, and H. Nojiri et al., "Contribution of oxidative stress to the degeneration of rotator cuff entheses," *Journal of Shoulder and Elbow Surgery* , vol. 23, no. 5, pp. 628–635, 2014.

[41] J. Khavkin and D. A. F. Ellis, "Aging skin: histology, physiology, and pathology," *Facial Plastic Surgery Clinics of North America*, vol. 19, no. 2, pp. 229–234, 2011.

[42] E. Kohl, J. Steinbauer, M. Landthaler, and R.-M. Szeimies, "Skin ageing," *Journal of the European Academy of Dermatology and Venereology*, vol. 25, no. 8, pp. 873–884, 2011.

[43] K. Watanabe, S. Shibuya, H. Koyama et al., "*Sod1* loss induces intrinsic superoxide accumulation leading to p53-mediated growth arrest and apoptosis," *International Journal of Molecular Sciences*, vol. 14, no. 6, pp. 10998–11010, 2013.

[44] R. A. Fielding, B. Vellas, W. J. Evans et al., "Sarcopenia: an undiagnosed condition in older adults. Current consensus definition: prevalence, etiology, and consequences. International working group on sarcopenia," *Journal of the American Medical Directors Association*, vol. 12, no. 4, pp. 249–256, 2011.

[45] Y. C. Jang, M. S. Lustgarten, Y. Liu et al., "Increased superoxide in vivo accelerates age-associated muscle atrophy through mitochondrial dysfunction and neuromuscular junction degeneration," *FASEB Journal*, vol. 24, no. 5, pp. 1376–1390, 2010.

[46] Y. Zhang, C. Davis, G. K. Sakellariou et al., "CuZnSOD gene deletion targeted to skeletal muscle leads to loss of contractile force but does not cause muscle atrophy in adult mice," *FASEB Journal*, vol. 27, no. 9, pp. 3536–3548, 2013.

[47] G. K. Sakellariou, C. S. Davis, Y. Shi et al., "Neuron-specific expression of CuZnSOD prevents the loss of muscle mass and function that occurs in homozygous CuZnSOD-knockout mice," *The FASEB Journal*, vol. 28, no. 4, pp. 1666–1681, 2014.

[48] D. Elahi, D. C. Muller, J. M. Egan, R. Andres, J. Veldhuis, and G. S. Meneilly, "Glucose tolerance, glucose utilization and insulin secretion in ageing," *Novartis Foundation Symposium*, vol. 242, pp. 222–246, 2002.

[49] A. Anantharaju, A. Feller, and A. Chedid, "Aging liver: a review," *Gerontology*, vol. 48, no. 6, pp. 343–353, 2002.

[50] L. Wang, Z. Jiang, and X. G. Lei, "Knockout of SOD1 alters murine hepatic glycolysis, gluconeogenesis, and lipogenesis," *Free Radical Biology and Medicine*, vol. 53, no. 9, pp. 1689–1696, 2012.

[51] Y. Kondo, Y. Inai, Y. Sato et al., "Senescence marker protein 30 functions as gluconolactonase in L-ascorbic acid biosynthesis, and its knockout mice are prone to scurvy," *Proceedings of the National Academy of Sciences of the United States of America*, vol. 103, no. 15, pp. 5723–5728, 2006.

[52] Y. Kondo, H. Masutomi, Y. Noda et al., "Senescence marker protein-30/superoxide dismutase 1 double knockout mice exhibit increased oxidative stress and hepatic steatosis," *FEBS Open Bio*, vol. 4, pp. 522–532, 2014.

[53] X. G. Lei, J.-H. Zhu, J. P. McClung, M. Aregullin, and C. A. Roneker, "Mice deficient in Cu,Zn-superoxide dismutase are resistant to acetaminophen toxicity," *Biochemical Journal*, vol. 399, no. 3, pp. 455–461, 2006.

[54] J.-H. Zhu, X. Zhang, C. A. Roneker et al., "Role of copper,zinc-superoxide dismutase in catalyzing nitrotyrosine formation in murine liver," *Free Radical Biology and Medicine*, vol. 45, no. 5, pp. 611–618, 2008.

[55] M. Szafarowska and M. Jerzak, "Ovarian aging and infertility," *Ginekologia Polska*, vol. 84, no. 4, pp. 298–304, 2013.

[56] N. Kimura, S. Tsunoda, Y. Iuchi, H. Abe, K. Totsukawa, and J. Fujii, "Intrinsic oxidative stress causes either 2-cell arrest or cell death depending on developmental stage of the embryos from SOD1-deficient mice," *Molecular Human Reproduction*, vol. 16, no. 7, pp. 441–451, 2010.

[57] R. M. Colven and S. R. Pinnell, "Topical vitamin C in aging," *Clinics in Dermatology*, vol. 14, no. 2, pp. 227–234, 1996.

[58] K. Murakami, N. Murata, Y. Ozawa et al., "Vitamin C restores behavioral deficits and amyloid-β oligomerization without affecting plaque formation in a mouse model of alzheimer's disease," *Journal of Alzheimer's Disease*, vol. 26, no. 1, pp. 7–18, 2011.

[59] T. Ikegami, Y.-I. Suzuki, T. Shimizu, K.-I. Isono, H. Koseki, and T. Shirasawa, "Model mice for tissue-specific deletion of the manganese superoxide dismutase (MnSOD) gene," *Biochemical and Biophysical Research Communications*, vol. 296, no. 3, pp. 729–736, 2002.

[60] M.-L. Sentman, M. Granström, H. Jakobson, A. Reaume, S. Basu, and S. L. Marklund, "Phenotypes of mice lacking extracellular superoxide dismutase and copper- and zinc-containing superoxide dismutase," *Journal of Biological Chemistry*, vol. 281, no. 11, pp. 6904–6909, 2006.

[61] H. Fujita, H. Fujishima, K. Takahashi et al., "SOD1, but not SOD3, deficiency accelerates diabetic renal injury in C57BL/6-Ins2Akita diabetic mice," *Metabolism: Clinical and Experimental*, vol. 61, no. 12, pp. 1714–1724, 2012.

[62] J.-H. Zhu and X. G. Lei, "Lipopolysaccharide-induced hepatic oxidative injury is not potentiated by knockout of GPX1 and SOD1 in mice," *Biochemical and Biophysical Research Communications*, vol. 404, no. 1, pp. 559–563, 2011.

[63] S. K. Wang, J. D. Weaver, S. Zhang, and X. G. Lei, "Knockout of SOD1 promotes conversion of selenocysteine to dehydroalanine in murine hepatic GPX1 protein," *Free Radical Biology and Medicine*, vol. 51, no. 1, pp. 197–204, 2011.

[64] S. Ditch and T. T. Paull, "The ATM protein kinase and cellular redox signaling: beyond the DNA damage response," *Trends in Biochemical Sciences*, vol. 37, no. 1, pp. 15–22, 2012.

[65] L. Erker, R. Schubert, S. Elchuri et al., "Effect of the reduction of superoxide dismutase 1 and 2 or treatment with α-tocopherol on tumorigenesis in Atm-deficient mice," *Free Radical Biology and Medicine*, vol. 41, no. 4, pp. 590–600, 2006.

[66] F. L. Muller, W. Song, Y. C. Jang et al., "Denervation-induced skeletal muscle atrophy is associated with increased mitochondrial ROS production," *American Journal of Physiology. Regulatory Integrative and Comparative Physiology*, vol. 293, no. 3, pp. R1159–R1168, 2007.

[67] E. S. Han, F. L. Muller, V. I. Pérez et al., "The in vivo gene expression signature of oxidative stress," *Physiol Genomics*, vol. 34, no. 1, pp. 112–126, 2008.

[68] G. Cenini, R. Sultana, M. Memo, and D. A. Butterfield, "Elevated levels of pro-apoptotic p53 and its oxidative modification by the lipid peroxidation product, HNE, in brain from subjects with amnestic mild cognitive impairment and Alzheimer's disease," *Journal of Cellular and Molecular Medicine*, vol. 12, no. 3, pp. 987–994, 2008.

[69] S. Zhou, J. S. Greenberger, M. W. Epperly et al., "Age-related intrinsic changes in human bone-marrow-derived mesenchymal stem cells and their differentiation to osteoblasts," *Aging Cell*, vol. 7, no. 3, pp. 335–343, 2008.

[70] J. L. Scott, C. Gabrielides, R. K. Davidson et al., "Superoxide dismutase downregulation in osteoarthritis progression and

end-stage disease," *Annals of the Rheumatic Diseases*, vol. 69, no. 8, pp. 1502–1510, 2010.

[71] M. Almeida, "Aging mechanisms in bone," *BoneKEy Reports*, vol. 1, article 102, 2012.

[72] D. Maggio, M. Barabani, M. Pierandrei et al., "Marked decrease in plasma antioxidants in aged osteoporotic women: results of a cross-sectional study," *Journal of Clinical Endocrinology and Metabolism*, vol. 88, no. 4, pp. 1523–1527, 2003.

[73] L. R. Fraga, C. G. Dutra, J. A. Boquett et al., "p53 signaling pathway polymorphisms associated to recurrent pregnancy loss," *Molecular Biology Reports*, vol. 41, no. 3, pp. 1871–1877, 2014.

[74] C. Tatone, M. C. Carbone, S. Falone et al., "Age-dependent changes in the expression of superoxide dismutases and catalase are associated with ultrastructural modifications in human granulosa cells," *Molecular Human Reproduction*, vol. 12, no. 11, pp. 655–660, 2006.

Hindawi Publishing Corporation
BioMed Research International
Volume 2014, Article ID 695797, 9 pages
http://dx.doi.org/10.1155/2014/695797

Research Article

Inhibition of Peroxisome Proliferator-Activated Receptor Gamma Prevents the Melanogenesis in Murine B16/F10 Melanoma Cells

Jiun-Han Chen,[1] Junn-Liang Chang,[2,3] Pei-Ru Chen,[3] Yun-Ju Chuang,[3] Shih-Tsang Tang,[3] Shwu-Fen Pan,[4] Tzer-Bin Lin,[5] Kang-Hua Chen,[6] and Mei-Jung Chen[3]

[1] *Department of Medical Laboratory Science and Biotechnology, College of Medical Technology, Nursing and Wellbeing, Yuanpei University, No. 306 Yuan-Pei Street, Hsinchu 30015, Taiwan*
[2] *Department of Pathology & Laboratory Medicine, Taoyuan Armed Forces General Hospital, Taoyuan 32551, Taiwan*
[3] *Department of Biomedical Engineering, School of Health, Ming Chuan University, No. 5 De-Ming Road, Gui Shan District, Taoyuan County, Taoyuan 333, Taiwan*
[4] *Department of Biotechnology, School of Health, Ming Chuan University, Taoyuan 333, Taiwan*
[5] *Department of Physiology, College of Medicine, Taipei Medical University, No. 250 Wuxing Street, Taipei 110, Taiwan*
[6] *Department of Surgery, Cheng Hsin General Hospital, No. 45 Cheng Hsin Street, Pai Tou, Taipei 112, Taiwan*

Correspondence should be addressed to Mei-Jung Chen; meijungchen@gmail.com

Received 10 July 2014; Accepted 14 August 2014; Published 28 August 2014

Academic Editor: Chi-Feng Hung

The purpose of this study was to investigate if PPARγ plays a role in the melanogenesis. B16/F10 cells were divided into five groups: control, melanin stimulating hormone (α-MSH), α-MSH+retinol, α-MSH+GW9662 (PPARγ antagonist), and GW9662. Cells in the control group were cultured in the Dulbecco's modified Eagle's medium (DMEM) for 48 hrs. To initiate the melanogenesis, cells in all α-MSH groups were cultured in medium containing α-MSH (10 nM) for 48 hrs. Cells were treated simultaneously with retinol (5 μM) in the α-MSH+retinol group. Instead of retinol, GW9662 (10 μM) was cocultured in the α-MSH+GW9662 group. Cells in the final group were cultured in the DMEM with GW9662. All the analyses were carried out 48 hours after treatments. The α-MSH was able to increase cell number, melanin production, and the activity of tyrosinase, the limiting enzyme in melanogenesis. These α-MSH-induced changes were prevented either by retinol or by GW9662. Further analyses of the activities of antioxidant enzymes including glutathione, catalase, and the superoxide dismutase (SOD) showed that α-MSH treatment raised the activity of SOD which was dependent on PPARγ level. According to our results, the α-MSH-induced melanogenesis was PPARγ dependent, which also modulated the expression of SOD.

1. Introduction

Melanocytes distribute in many organs in human beings, such as nervous system, heart, iris, and epidermis [1–3]. They all originate from neural crest cells during embryonic period [4]. One of the functions in melanocytes is synthesis of melanin, indicating melanogenesis. The major rate-limited steps in the melanogenesis are catalyzed by tyrosinase (monophenol, dihydroxy-L-phenylalanine: oxygen oxidoreductase: EC 1.14.18.1) [5]. The gene encoding tyrosinase maps at chromosome 11q14-q21 in humans and chromosome 7 in mice [6]. The tyrosinase controls the initial two distinct reactions of the melanin formation process, namely, the hydroxylation of L-tyrosine to L-3,4-dihydroxyphenylalanine (DOPA) and the subsequent oxidation of DOPA to dopaquinone [7]. Two main types of melanin, eumelanin and pheomelanin, are identified in human beings physically [8]. The amounts, ratios, and types of melanin determine the skin color, and they also play the major photoprotective roles against the harmful effects by ultraviolet (UV) radiation of sunlight, including UVA and UVB [9]. Animal studies demonstrate that these melanin prevent skin from edema [10], erythema,

hyperpigmentation, and inflammation [9] caused by UV exposure.

Several factors secreted from keratinocytes, fibroblasts, and even melanocytes are able to modulate the melanogenesis. For example, proinflammatory factors, IL-1α/β, and hormones, ACTH as well as α-melanocyte stimulating hormone (α-MSH), induce melanogenesis. Instead, endothelin 1, nitric oxide, and nerve growth factor inhibit this process [11]. The most important function of endogenous melanin is absorbing the high energy to prevent penetration of UV radiation, meanwhile scavenging the reactive oxygen species (ROS) burst by UV radiation [12–14]. Subsequently, the bursting accumulation of ROS causes inflammation in epidermis immediately, and also trigger the formation of melanin [8]. Therefore, lots of antioxidants are used to prevent the inflammation by UV exposure [9, 15, 16]. They limit the accumulation and production of ROS in epidermis.

Peroxisome proliferators-activated receptors (PPARs) were discovered in mouse liver by Issemann and Green in 1990 [17]. They are nuclear hormone receptors and are divided into three subtypes, namely, PPARα, PPARβ/δ, and PPARγ. PPARγ expressed in a variety of cell types, including adipocytes, macrophages, vascular smooth muscle cells, and endothelial cells [12–14]. Previous studies focus on the relationships among PPARs, lipid metabolism, and homeostasis [18, 19]. Recent studies showed that PPARγ activation was able to regulate inflammatory responses, cellular proliferation, differentiation, and apoptosis [20]. The highly selective agonist for PPARγ, rosiglitazone (BRL49653), belongs to structure of thiazolidinediones (TZD) and is wildly used as hypoglycemia medicine in clinic [20]. Recent study proved that the production of ROS in macrophages was significantly inhibited by TZD administration, indicating the anti-inflammation by activation of PPARγ [21]. Supporting results were also observed by Jiang et al. [22] that the levels of inflammatory mediators were attenuated by TZD treatment. In our previous study, activation of PPARγ reduced the severity of inflammation and the amount of ROS in pulmonary circulation [23]. Accordingly, it arose the possibility that the expression of PPARγ played an important role in the melanogenesis, which responded to kinds of inflammatory conditions. Therefore, the purpose of this study was to investigate whether PPARγ play a key role in the melanogenesis. According to results in the present study, we proved that the melanogenesis was through the PPARγ-dependent pathway, which was in turn compensation to the expression of antioxidant enzymes.

2. Materials and Methods

2.1. Materials. The B16/F10 cell line was purchased from the Culture Collection and Research Center (Hsinchu, Taiwan); Dulbecco's modified Eagle's medium (DMEM), fetal bovin serum (FBS), phosphate buffer saline (PBS), trypsin-EDTA (TEG), albumin, Bio-Rad protein assays, melanin, L-DOPA, lysis buffer, α-MSH, retinol, and GW9662 were purchased from Sigma company (USA); the catalase assay kit, glutathione assay kit, nuclear extraction kit, PPARγ transcription factor assay kit, and the superoxide dismutase assay kit were purchased from the Cayman Company (USA).

2.2. Cell Culture. The B16/F10 cells, 4×10^5 cells, were seeded at 100 mm diameter of culture dishes containing 7 mL of DMEM with 10% FBS. Cells were then cultured at 37°C in a humid atmosphere containing 5% CO_2. When cells reached 80% confluence, they were changed to the fresh medium and treated with agents as designed for forty-eight hours. There were five groups in this study: control, α-MSH, α-MSH+retinol, α-MSH+GW9662, and GW9662. Cells in the control group were cultured in the 7 mL of DMEM. For stimulating the melanin synthesis, the α-MSH was added to the culture medium as the final concentration as 10 nM. In the third group, cells grew in the DMEM containing 10 nM of α-MSH and 5 μM of retinol. Cells in the α-MSH+GW9662 group accepted the treatments of α-MSH and GW9662 (10 μM). In the last group, cells were treated only with the GW9662 as the final concentration of 10 μM. All the cells grew for 48 hours in the incubator (ULTIMA, REVCO) of the environment at 37°C, a humid atmosphere with 5% CO_2. The cell counts, levels of melanin, the activities of tyrosinase, glutathione, catalase, and superoxide dismutase were further detected in five groups. The PPARγ levels in nucleus were measured in the control, α-MSH, and α-MSH+retinol groups.

Cell morphology was observed under microscopy after treatments. Then the cells were resuspended by TEG for five minutes. After dying with trypan blue, the number of cells in the dish was counted under the microscopy (LeicaDMIL Leica, Leica) in 40x field.

2.3. The Tyrosinase Activity Assays. The tyrosinase activity was determined by the methods of Buscà et al. [24] with minor modification. The B16/F10 cells were deattached by 0.25% trypsin-EDTA (ethylenediaminetetraacetic acid). After washing with PBS and centrifugation at 600 g, 4°C, for 4 minutes, the cell pellets were resuspended in 500 μL of lysis buffer (containing 0.5% Triton X-100 (w/v), 0.1 M PMSF (phenyl methyl sulfonyl fluoride) in PBS) for 30 minutes in ice bath. The lysate was centrifuged (10,000 ×g, 20 minutes, 4°C) in an Eppendorf Biofuge. Finally, the supernatant was collected to analyze the tyrosinase activity and melanin level. The total protein concentration in each sample was determined by Bio-Rad protein assay kit. Ten microliter of each sample was transferred into the 96-well plate. The albumin was used to establish the standard curve. Ten minutes after adding the protein assay solution, the optical absorbance at 620 nm was measured by the spectrometer (V-630 Bio, Biotek). For analyzing the tyrosinase activity, 30 μL of sample was mixed with 170 μL of L-DOPA in the final concentration of 0.85 g/μL, and then the mixture was further incubated at 37°C for 60 minutes. PBS (30 μL) was added to the blank instead of the sample. The optical absorbance at 450 nm was read using the spectrophotometer (Power Wave XS, Biotek). The absorbance difference between the sample and blank (ΔA450) was used to express the amount of product, dopaquinone. The unit of tyrosinase activity was

defined as the relative amount of dopaquinone catalyzed by tyrosinase within one hour in solution containing 1 gram of total proteins. Considering the total protein differences in each sample, therefore, the unit of tyrosinase activity was determined as $\Delta A450/(g \times hr)$. Each sample was detected in triplicate repeat.

2.4. Determination of Melanin Content. Melanin content was determined by the method of Buscà et al. [24] with a few modifications. The cell pellets were dissolved in 0.5 mL of 1 N NaOH at 100°C for 30 min, then determined cell counts, and transferred 30 μL to the well of 96-well plate. The 170 μL of L-DOPA (0.001 g/mL) was mixed to each well to incubate together for 5 min. The melanin content was measured by the optical absorbance at 450 nm and compared with a standard curve generated by melanin with known concentrations in 1 N NaOH (Sigma Chemical Co., St. Louis, MO). The amount of melanin was further normalized by cell counts obtained previously and expressed as g melanin/cell. Each sample was measured in duplicate.

2.5. Measurement of PPARγ Level. The measurement of PPARγ was carried out following extraction of nuclear proteins. The nuclear extraction kit and the PPARγ transcription factor assay kit were used in this measurement. Cells in 10 cm diameter of culture dish were suspended by 1 mL of TEG. Centrifuging to collect the cell pallet, 500 μL of hypotonic buffer (0.5% Triton X-100 (w/v), 0.1 M PMSF (phenyl methyl sulfonyl fluoride) in PBS) was added for 15 minutes in ice bath. Then, the Nonidet P-40 (10%, 50 μL) was added to the mixture. The cell pallet was collected by centrifuging (14,000 ×g, 30 sec, 4°C). It was further mixed with 50 μL of extraction buffer. Samples were prepared as repeated six times of shaker for 30 seconds and ice bath for 10 minutes. The supernatant containing nuclear extraction was collected by centrifuging (14,000 ×g, 10 min, 4°C). The sample, 10 μL, was transferred to the 96-well plate. The transcription factor binding assay buffer 90 μL and the competitor ds DNA 80 μL were further mixed well within the sample. The 100 μL of competitor ds DNA was used as the blank. After incubating for 24 hours then washing out five times, the primary antibody to PPARγ 100 μL was added then incubated in room temperature for one hour. After washing out for five times, the mouse antigoat HRP conjugate, 100 μL, was added to incubate for one hour in room temperature. After washing out again, the developing solution of 100 μL was added to incubate for 30 minutes then the stop solution was followed to each well. The optical absorbance at 450 nm was read using the spectrophotometer (Biotek). The absorbance difference between the sample and blank was normalized to the cell counts. Each sample was detected in duplicate repeat.

2.6. The Glutathione Activity Assay. The total glutathione was measured by the commercial assay kit from Cayman Chemical (USA). After removing the culture medium, cells in 10 cm diameter dish were resuspended by 1 mL of TEG. Fresh medium (0.5 mL) was added and mixed well, then the cells were transferred to a new eppendorf to be centrifuged by 3000 ×g for 10 min at 4°C. Cold buffer (1 mL) was further added to the pallet containing MES and 1 mM EDTA, pH 6~7, to homogenize cells. The suspension was separated from the test sample by centrifuging in 10000 g for 15 min at 4°C. The sample was added the equal volume of *m*-phosphoric acid containing solution to remove extra proteins. After 5 minutes of incubation in room temperature, the suspension was removed by centrifuging at 3000 g for 3 min at 4°C. Each sample was mixed with 50 μL of 4 M of TEAM. The 50 μL of the mixture was then transferred to the well of 96-well plate. The mixture (containing MES buffer, cofactor mixture, enzyme mixture, DTNB, and Q water) was then added for 150 μL to each well. This 96-well plate was then incubated in dark and shook on an orbital shaker. The absorbance was measured at 410 nm when the sample had been incubated for 25 min. The amount of GSH was calculated with the absorbance fitted to the formula established by standards. Each sample and standard was tested in duplicate.

2.7. The Superoxide Dismutase (SOD) Activity Assay. The SOD activity was determined based on the production of O_2^- anions by the xanthine/xanthine oxidase system using a commercial assay kit (Cayman Chemical, USA). After removing the medium by suction, cells were washed with 2 mL of PBS and then 1.5 mL of fresh medium was added with TEG to culture dish. Cells were collected by centrifuging after discarding medium; the cells were rinsed with 2 mL of PBS, pH 7.4; the aforementioned process was repeated again. Cells were collected as pellet by centrifuging and further homogenized with 1 mL of cold HEPES buffer, pH 7.2, containing 1 mM EDTA, 210 mM mannitol, and 70 mM sucrose. The homogenizing tissue was centrifuged at 1,500 g for 5 min at 4°C. The supernatant was removed into a new eppendorf as sample. Each well in the 96-well plate containing 200 μL of the diluted Radical Detector was added 10 μL of sample or standard. The 96-well plate was then incubated for 20 minutes at room temperature when 20 μL of diluted xanthine oxidase had been added. The absorbance was detected at 450 nm using a plate reader finally. The values of standards' absorbance were used to establish the standard curve and formula between absorbance and amounts of product by SOD catalyzing. The values of each sample were fitted to the formula to obtain the amount of product by SOD catalyzing. Finally, the SOD activity was expressed in U/mL. Each sample and standard was tested in triplicate.

2.8. The Catalase Activity Assay. The catalase activity assay was measured by the kit purchased from the Cayman Chemicals. After suction to remove the medium, 2 mL of fresh PBS was added to wash cells and then discarded again. To suspend cells, the 1.5 mL of fresh medium with TEG was then added to culture dish. The cells were then collected by centrifuging. After discarded supernatant, cells were then rinsed with 1.5 mL of PBS, pH 7.4, twice and then collected as pellet by centrifuging. To homogenize cells, the pellet was treated with 1 mL of cold HEPES buffer, pH 7.2. The homogenized cells were then collected as the suspension by centrifuging at 10,000 g for 15 min at 4°C for assay sample. Series concentrations of formaldehyde were prepared well previous as the

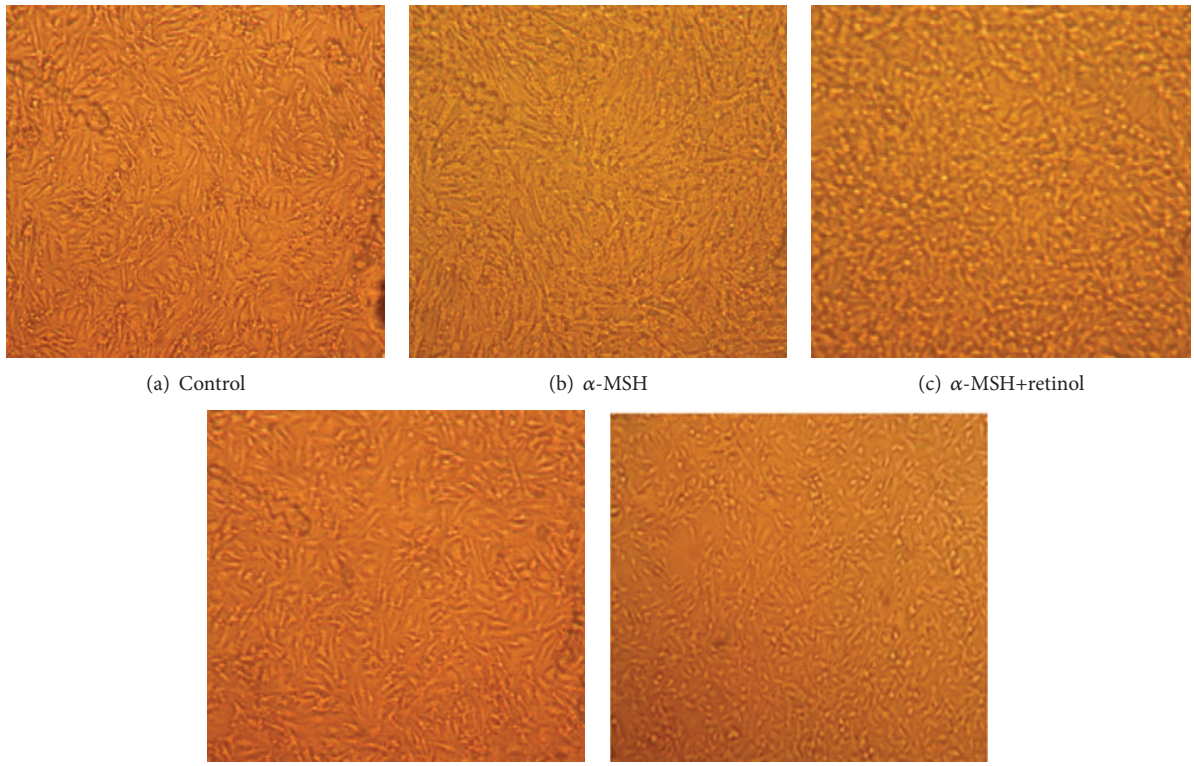

(a) Control (b) α-MSH (c) α-MSH+retinol

(d) α-MSH+GW9662 (e) GW9662

Figure 1: Images of the 5 groups of melanocytes; fixed magnification power of ×40. (a) Control; (b) melanin stimulating hormone (α-MSH); (c) α-MSH+retinol; (d) α-MSH+GW9662; and (e) GW9662.

standards. Each well was added 100 μL of diluted assay buffer, 30 μL of methanol, and 20 μL of standards or samples. The components as positive control were 100 μL of assay buffer, 30 μL of methanol, and 20 μL of CAT. The hydrogen peroxide, 20 μL, was further added to each well to initiate the reaction. The plate was kept in dark to incubate on a shaker for 20 min at room temperature. Potassium hydroxide, 20 μL, was used to terminate the reaction. Catalase Purpald (30 μL) was then added as the chromogen and incubated for 10 min at room temperature. The Catalase Potassium Periodate (10 μL) was then added to each well and incubated together for 5 min at room temperature on a shaker. The absorbance was detected at 540 nm. The linear relationship between the absorbance and concentration was established by standards to calculate the catalase activity of each sample. The catalase activity was expressed in nmol/min/mL. Each sample and standard was tested in duplicate.

2.9. Statistical Analysis. Data were presented as means±SEM. Evaluations of parameters were carried out by one-way analysis of variance. Subsequently, significant differences between any two groups were established using the Newman-Keuls multiple group comparisons. Differences were regarded as significant if $P < 0.05$.

3. Results

The morphology (Figure 1) and cell counts (Figure 2) of B16/F10 cells after treatment in each group are shown. The morphology of cells with variant treatments did not show the obvious transformation (Figure 1). However, adding α-MSH significantly induced the cell growth when compared with the control group (Figure 2). The α-MSH-induced increase in cell counts was attenuated by treatment either with retinol or PPARγ antagonist, GW9662 (Figure 2).

The results of melanin levels in groups are shown in Figure 3. The level in control group was measured as 0.017 ± 0.0002 g/mL. Treatment with α-MSH for two days significantly induced an increase in melanin level, indicating the melanogenesis. This high level caused by α-MSH reached over 2 times of the control level. That α-MSH-induced melanin synthesis was prevented completely by retinol. Adding GW9662 significantly attenuated the increase by α-MSH but still higher than that in the control group.

Further analyzing the activities of tyrosinase, the key enzyme in melanogenesis in five groups is summarized in Figure 4. The results showed similar trends of melanin levels in groups. The treatment of α-MSH for two days elevated significantly the activity of tyrosinase over two times of control group. However, the α-MSH-induced increase in tyrosinase activity was prevented by retinol or by GW9662 (Figure 4).

The GSH contents in all groups are shown in Figure 5. The amount of GSH was obviously decreased by α-MSH treatment. Exogenous antioxidant, retinol, restored the GSH partially but did not reach statistical significance. Adding GW9662 to block the PPARγ did not affect the decrease of

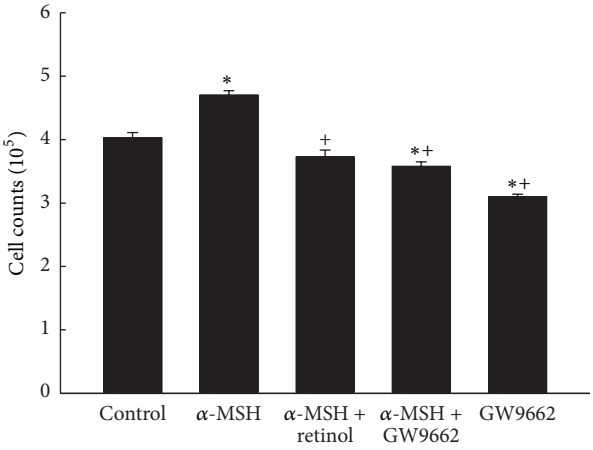

Figure 2: Cell counts in 5 groups. *Significant differences ($P < 0.05$) compared with the control group. #Significant differences ($P < 0.05$) compared with the α-MSH group.

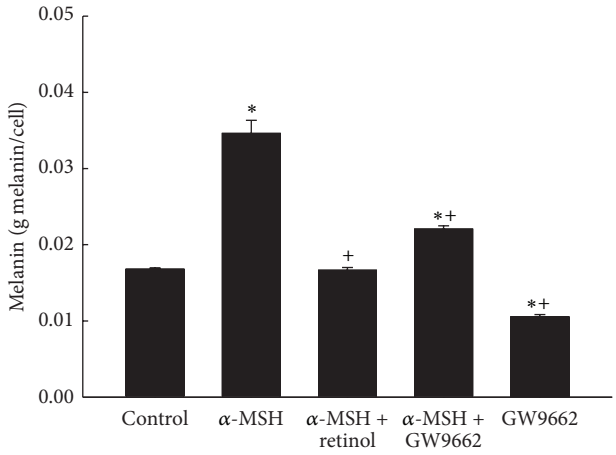

Figure 3: The melanin levels in five groups. Bars represent 1 SE. Significant differences compared with the control group: $^{*}P < 0.05$ and $^{**}P < 0.01$. $^{+}$Significant differences ($P < 0.05$) compared with the α-MSH group.

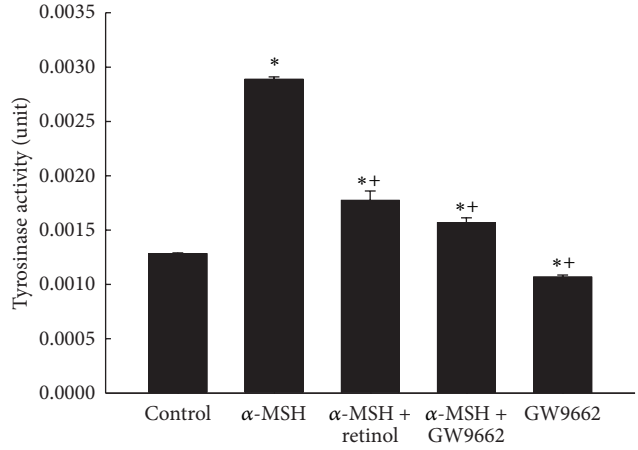

Figure 4: The tyrosinase activities in five groups. Bars represent 1 SE. Significant differences compared with the control group ($^{*}P < 0.05$) or with the α-MSH group ($^{+}P < 0.05$).

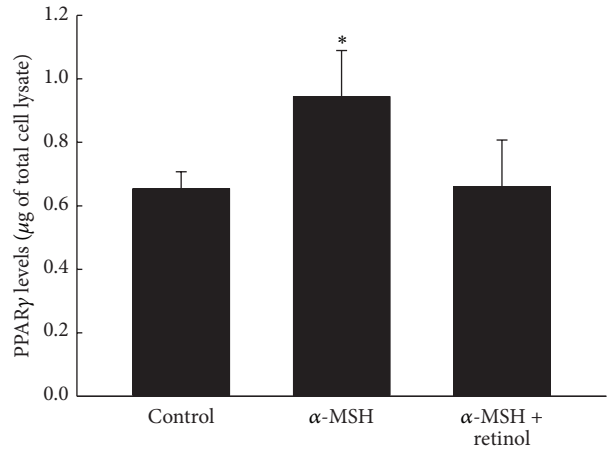

Figure 5: The GSH content in five groups. Bars represent 1 SE. *Significant differences ($P < 0.05$) compared with the control group.

GSH contents by α-MSH. However, there was no influence on the level of GSH by only GW9662 treatment when compared to the control group.

Figure 6 summarized the results of catalase activities in each group. The catalase activity was attenuated over 50% of control group by α-MSH. It restored significantly by coculture with retinol or GW9662 but is still lower than that in control group. Treatment of GW9662 only resulted in obvious decrease in catalase activity when compared with the control group.

Detecting the activities of SOD in each group was summarized in Figure 7. It was induced increase by α-MSH stimulation. The α-MSH-induced increase was prevented by retinol or GW9662. There was no difference between the control group and the group of GW9662 only.

The levels of PPARγ in each group are shown in Figure 8. There was a significant increase in the PPARγ level caused by

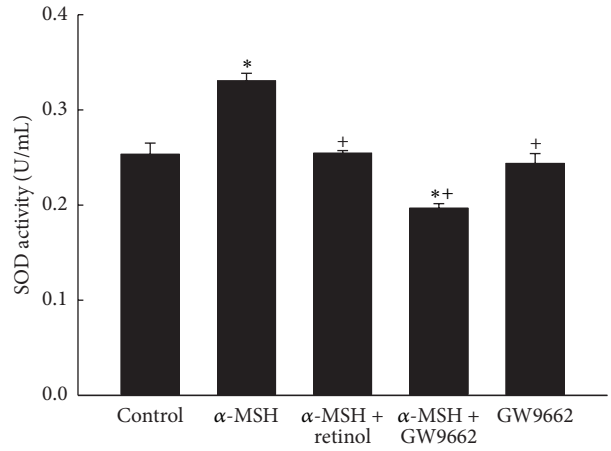

Figure 6: The catalase activities in five groups. Bars represent 1 SE. *Significant differences ($P < 0.05$) compared with the control group.

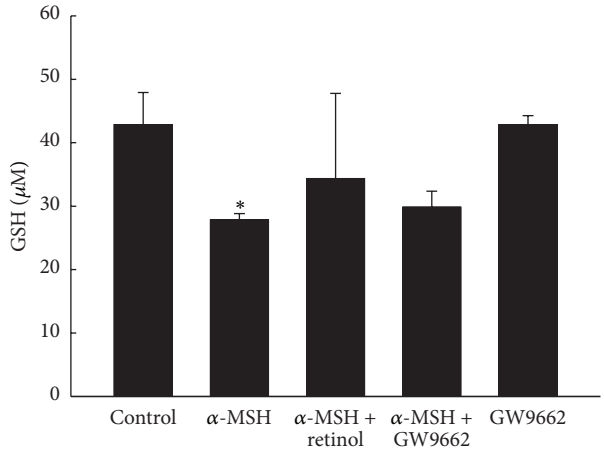

Figure 7: The superoxide dismutase activities in five groups. Bars represent 1 SE. *Significant differences ($P < 0.05$) compared with the control group. +Significant differences ($P < 0.05$) compared with the α-MSH group.

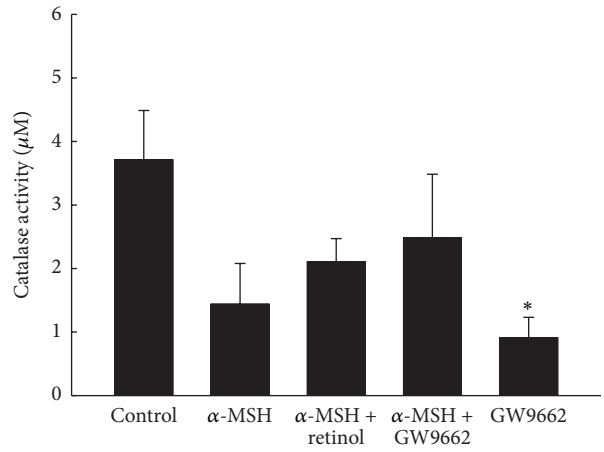

Figure 8: The PPARγ levels in the control, α-MSH, and α-MSH+retinol groups. Bars represent 1 SE. *Significant differences ($P < 0.05$) compared with the control group.

adding α-MSH. Treatment of retinol prevented the increase in PPARγ expression.

4. Discussion

Melanogenesis was demonstrated to protect against the reactive oxygen species (ROS) in many documents. We hypothesized that melanogenesis was via activation of PPARγ, which elevated the tyrosinase activity. In addition, pretreatment of antioxidant retinol was able to prevent these effects. The melanogenesis was well known mediated by tyrosinase, the rate-limiting enzyme in the process of melanin synthesis. Tyrosinase converts the L-tyrosine to dopaquinone for the synthesis of both pheomelanin and eumelanin. Many stimuli to induce melanogenesis processing such as α-MSH [25, 26] and UV radiation exposure [12] were via elevating the oxidative stress. Indexes of melanogenesis, such as melanin contents, tyrosinase activity, and expression, were all augmented by α-MSH [25] and UV radiation exposure [26]. However, pretreatment of retinol significantly reduced above index of melanogenesis in a dose-dependent manner [25]. It was demonstrated that the effects about melanogenesis by α-MSH were via activating melanocortin 1 receptor (MC1R) followed by activation of the CREB/MITF pathway [11]. The protection of melanogenesis against ROS was identified in another kind of cells, primary transformed retinal pigment epithelium cell (RPEC) [27]. When MC1R was blocked either by antagonist or by si RNA, the melanogenesis-related protection was abolished. Furthermore, the melanogenesis-related survival effects on RPECs diminished by Akt inhibitor treatment. Therefore, the functions of melanogenesis were identified as Akt related pathway [27]. Not only melanogenesis but also proliferation was induced by α-MSH [25]. The proliferation index, cell numbers of B16 cell line, was elevated obviously by α-MSH treatment [25]. The cell growth induced by α-MSH (10 nM) was prevented 53% by retinol treatment at 20 μM [25]. In the present study, the increases in cell counts, melanin level, and tyrosinase activity were measured by α-MSH treatment (Figures 2, 3 and 4), supported by the above documents [25, 27]. In addition, both the proliferation and the melanogenesis were reversed by pretreatment of antioxidant retinol (Figures 1, 2, and 3), which was also consistent with the results by Sato et al. [25]. Furthermore, pretreatment PPARγ antagonist, GW9662, prevented the α-MSH-induced increases in melanin level (Figure 3) and tyrosinase activity (Figure 4). We further detected the marked augment in PPARγ level by α-MSH treatment when it was compared with that in control group (Figure 8). Thus, we demonstrated that the melanogenesis in B16F10 cells was dependent on the activation of PPARγ. It is confirmed to our hypothesis that the melanogenesis was via activation of PPARγ and pretreatment of retinol abolished the process.

We hypothesized that the anti-inflammatory effects of melanogenesis depended on the activation of PPARγ to trigger the activity of tyrosinase. The anti-inflammation of melanogenesis was observed in mouse models [9, 28]. UVB exposure (150 mJ/cm^2) led to ICR-Foxn/^{nu} mice dorsal skin erythema, desquamation, and transdermal water loss. Immunostaining results showed an increase in the activation of cyclooxygenase-2 (COX-2) but decreased in catalase activity [9]. Both the COX-2 and the PPARγ were found in melanoma by immunohistological staining [29] and activation of PPARγ by rosiglitazone attenuated COX-2 expression [30]. The ROS not only directly damaged proteins, lipids, and DNA, meanwhile, the increase in intracellular ROS, especially hydroperoxide, also acted as mediators to trigger the MAPK pathway (ERK, p38 and JNK) after UVB exposure [15, 16]. Recently finding reported by Peng et al. [26] demonstrated that the ROS is able to induce increases in tyrosinase and melanin expression by JNK and ERK signaling pathway [26]. Therefore, pretreatment of soy isoflavone, having potent antioxidant activity, significantly protected ICR-Foxn/^{nu} mice from harms by UVB exposure [9]. Another piece of evidence was shown by Luger et al. [28]. When the UV-light exposure was carried out on mice, the

release of α-MSH from keratinocytes was induced to alter the functions of antigen presenting cells and vascular endothelial cells [28]. In addition, administering α-MSH to induce melanogenesis either by intravenous or by topical application to mice inhibited the induction of hypersensitivity reaction, indicating the anti-inflammation [28]. They concluded that the anti-inflammatory effects of melanogenesis were related to the capacity to alter the functions of antigen presenting cells and vascular endothelial cells [28]. Activation of PPARγ leading to anti-inflammation was well known to date. A piece of evidence which also supported our hypothesis was that the inflammation and immune responses caused by UV-light were augmented by inactivation of PPARγ [31]. Acute UVB irradiation, similar to that used by Luger et al. [28], was carried out on epidermal PPARγ knockout mice, Pparg (Pparg-/-(epi)), which was a species of the SKH-1 hairless albino mice [31]. The augments of UVB-induced Caspase 3/7 activity, apoptosis, and inflammation were extremely more obvious than those in wild type littermates [31]. Consistently, increases in apoptosis and inflammation were performed after blocking the PPARγ activity by GW9662 treatment [31]. Above research supported our hypothesis that the anti-inflammatory effects of melanogenesis depended on the activation of PPARγ to trigger the activity of tyrosinase. In our study, both the melanin level and the tyrosinase activity were elevated by α-MSH treatment when compared to those in the control group. However, these increases were attenuated by treatment of GW9662, the antagonist of PPARγ (Figures 3 and 4). Furthermore, we detected the high level of PPARγ in the α-MSH group. Therefore, we demonstrated that the α-MSH caused an increase in PPARγ level, elevating the tyrosinase activity, which followed triggering melanogenesis.

In addition to reducing COX-2 activity and increasing tyrosinase activity, we hypothesized the α-MSH-induced PPARγ increase contributed to the activities of antioxidant(s). Schmilovitz-Weiss reported that PPARγ induced an increase in SOD level [32]. The ultraviolet (UV) light exposure [28] or oxidative stress [27] was known to induce the α-MSH secretion, which had capacity to trigger melanogenesis and proliferation in B16/F10 cells. Cheng et al. [27] recently reported that the α-MSH protected RPEC from hydrogen peroxide- (H_2O_{2-}) induced apoptosis, via melanocortin 1 receptor (MC1R) and the Akt dependent pathway [27]. On the other hand, the relationship between antioxidants and PPARγ was performed in *in vivo* study [32]. The animal model of nonalcoholic fatty liver disease was established by fed rats with fructose-enriched diet for 5 weeks [32]. The gene expression and protein level of both SOD and PPARγ were obviously lower than rats with standard rat chow diet [32]. Daily administration of rosiglitazone (10 mg/kg) during the last 2 weeks of the fructose-enriched diet significantly reversed the changes by fructose-enriched diet, including SOD gene expression and both SOD and PPARγ protein levels [32]. Their results indicated that the activation of PPARγ led to the synthesis of SOD [32]. Interestingly, the responses of SOD, catalase, and GSH to stimulus seemed conflicting in documents. Observations were reported by Shindo et al. [33] that antioxidants, including catalase, GSH, and SOD, in the epidermis and dermis of hairless mice diminished immediately after UV light exposure [9, 33]. However, the activities of antioxidants changed with the patterns of UV irradiation, and the recovery capacities of antioxidants altered during the acute and chronic phases [34]. When the authors irradiated human skin fibroblasts with a single exposure to UV irradiation (1, 6 or 12 J/cm^2) and then examined the activities of antioxidant enzymes over the following days, the catalase activity was attenuated immediately, then restored on the fifth day after UV exposure, indicating adaptive antioxidant response. SOD activity decreased significantly on the third day and then was restored to normal level on the fifth day after UV exposure [34]. Another supporting observation was documented by Poswig et al. in 1999 [35]. The SOD was induced by UVA irradiation and the adaptive antioxidant response was present when repetitive UV exposure [35]. Single exposure of human dermal fibroblasts to UVA irradiation resulted in a dose- and time-dependent increase in specific SOD mRNA levels [35]. When cells are exposed to UVA of 300 kJ per m^2 for 9 to 12 hours, the activity and the amount of SOD reached almost 180% and 200% of control, respectively [35]. Repetitive UVA exposure, especially, on the first three days at a dose rate of 200 kJ per m^2 resulted in a 5-fold induction of SOD mRNA levels, which contributed to eliciting SOD activity [35]. In our study, the treatment of α-MSH for two days continuously significantly caused increases in the PPARγ level (Figure 8) and the activity of SOD (Figure 7). The α-MSH-induced increase in the activity of SOD was prevented by GW9662 administration (Figure 7). However, the conflicting responses to the α-MSH treatment were performed in antioxidants, catalase, and GSH in the present study. The activities of both catalase and GSH decrease after α-MSH treatment though the changes did not reach the statistical significance (Figure 5). We attributed the differences among our study and others to different experiment model including study subjects, stimulus, and especially the analysis timing. In addition to PPARγ, the other member of PPAR family also expressed the capacity of anti-inflammation. UVB exposure (150 mJ/cm^2) to hairless mice 2 (HRM2) every other day for 17 days caused increases in levels of proinflammatory mediators, such as NF-kB, iNOS, and COX-2, whereas activation of PPARα by pretreatment with fenofibrate downregulated these effects of UVB exposure [30]. That indicated the potential anti-inflammation of PPARα.

In conclusion, the results presented here supported the hypothesis that melanogenesis was via activating PPARγ, which also modulated the balance among antioxidants. This is the first study to perform the relationship among antioxidants, melanogenesis, and PPARγ. It is necessary to carry out more studies, such as clinical studies, to understand the details in unknown mechanism. That would offer more helpful information in the treatment and usage in clinic.

Conflict of Interests

The authors declare that there is no conflict of interests regarding the publication of this paper.

Acknowledgments

The authors thank Miss J.-C. Huang and Miss S.-Y. Liao for assistance in this study. This study was supported by a grant from the Ministry of Science and Technology (101-2221-E-130-001).

References

[1] M. Tachibana, "Sound needs sound melanocytes to be heard," *Pigment Cell Research*, vol. 12, no. 6, pp. 344–354, 1999.

[2] F. C. Brito and L. Kos, "Timeline and distribution of melanocyte precursors in the mouse heart," *Pigment Cell and Melanoma Research*, vol. 21, no. 4, pp. 464–470, 2008.

[3] M. Randhawa, T. Huff, J. C. Valencia et al., "Evidence for the ectopic synthesis of melanin in human adipose tissue," *FASEB Journal*, vol. 23, no. 3, pp. 835–843, 2009.

[4] R. O'Rahilly and F. Müller, "The development of the neural crest in the human," *Journal of Anatomy*, vol. 211, pp. 335–351, 2007.

[5] T. Yoshimoto, K. Yamamoto, and D. Tsuru, "Extracellular tyrosinase from Streptomyces Sp. KY-453: purification and some enzymatic properties," *Journal of Biochemistry*, vol. 97, no. 6, pp. 1747–1754, 1985.

[6] D. E. Barton, B. S. Kwon, and U. Francke, "Human tyrosinase gene, mapped to chromosome 11 (q14-q21), defines second region of homology with mouse chromosome 7," *Genomics*, vol. 3, no. 1, pp. 17–24, 1988.

[7] A. Slominski and R. Paus, "Towards defining receptors for L-tyrosine and L-DOPA," *Molecular and Cellular Endocrinology*, vol. 99, no. 2, pp. C7–C11, 1994.

[8] D. G. Graham, S. M. Tiffany, and F. S. Vogel, "The toxicity of melanin precursors," *Journal of Investigative Dermatology*, vol. 70, no. 2, pp. 113–116, 1978.

[9] C. C. Huang, B. Y. Hsu, N. L. Wu et al., "Anti-photoaging effects of soy isoflavone extract (aglycone and acetylglucoside form) from soybean cake," *International Journal of Molecular Sciences*, vol. 12, pp. 4782–4795, 2010.

[10] F. Afaq and H. Mukhtar, "Botanical antioxidants in the prevention of photocarcinogenesis and photoaging," *Experimental Dermatology*, vol. 15, no. 9, pp. 678–684, 2006.

[11] M. Cichorek, M. Wachulska, A. Stasiewicz, and A. Tymińska, "Skin melanocytes: biology and development," *Postepy Dermatologii i Alergologii*, vol. 30, no. 1, pp. 30–41, 2013.

[12] J. Y. Lin and D. E. Fisher, "Melanocyte biology and skin pigmentation," *Nature*, vol. 445, no. 7130, pp. 843–850, 2007.

[13] H. Y. Park, M. Kosmadaki, M. Yaar, and B. A. Gilchrest, "Cellular mechanisms regulating human melanogenesis," *Cellular and Molecular Life Sciences*, vol. 66, no. 9, pp. 1493–1506, 2009.

[14] G.-E. Costin and V. J. Hearing, "Human skin pigmentation: melanocytes modulate skin color in response to stress," *The FASEB Journal*, vol. 21, no. 4, pp. 976–994, 2007.

[15] H.-S. Chiang, W.-B. Wu, J.-Y. Fang et al., "UVB-protective effects of isoflavone extracts from soybean cake in human keratinocytes," *International Journal of Molecular Sciences*, vol. 8, no. 7, pp. 651–661, 2007.

[16] T.-M. Chiu, C.-C. Huang, T.-J. Lin, J.-Y. Fang, N.-L. Wu, and C.-F. Hung, "In vitro and in vivo anti-photoaging effects of an isoflavone extract from soybean cake," *Journal of Ethnopharmacology*, vol. 126, no. 1, pp. 108–113, 2009.

[17] I. Issemann and S. Green, "Activation of a member of the steroid hormone receptor superfamily by peroxisome proliferators," *Nature*, vol. 347, no. 6294, pp. 645–650, 1990.

[18] R. N. DuBois, R. Gupta, J. Brockman, B. S. Reddy, S. L. Krakow, and M. A. Lazar, "The nuclear eicosanoid receptor, PPARγ, is aberrantly expressed in colonic cancers," *Carcinogenesis*, vol. 19, no. 1, pp. 49–53, 1998.

[19] E. Mueller, P. Sarraf, P. Tontonoz et al., "Terminal differentiation of human breast cancer through PPARγ," *Molecular Cell*, vol. 1, no. 3, pp. 465–470, 1998.

[20] P. Escher and W. Wahli, "Peroxisome proliferator-activated receptors: insight into multiple cellular functions," *Mutation Research: Fundamental and Molecular Mechanisms of Mutagenesis*, vol. 448, no. 2, pp. 121–138, 2000.

[21] B. Fischer, A. von Knethen, and B. Brüne, "Dualism of oxidized lipoproteins in provoking and attenuating the oxidative burst in macrophages: role of peroxisome proliferator-activated receptor-γ," *Journal of Immunology*, vol. 168, no. 6, pp. 2828–2834, 2002.

[22] C. Jiang, A. T. Ting, and B. Seed, "PPAR-γ agonists inhibit production of monocyte inflammatory cytokines," *Nature*, vol. 391, no. 6662, pp. 82–86, 1998.

[23] Y.-J. Chen, Y.-W. Lin, J.-H. Chen et al., "Activation of the peroxisome proliferator-activated receptor preventing the monocrotaline-induced pulmonary hypertension," *Adaptive Medicine*, vol. 4, no. 3, pp. 155–164, 2012.

[24] R. Buscà, C. Bertolotto, J. P. Ortonne, and R. Ballotti, "Inhibition of the phosphatidylinositol 3-kinase/p70(S6)-kinase pathway induces B16 melanoma cell differentiation," *Journal of Biological Chemistry*, vol. 271, no. 50, pp. 31824–31830, 1996.

[25] K. Sato, M. Morita, C. Ichikawa, H. Takahashi, and M. Toriyama, "Depigmenting mechanisms of all-trans retinoic acid and retinol on B16 melanoma cells," *Bioscience, Biotechnology and Biochemistry*, vol. 72, no. 10, pp. 2589–2597, 2008.

[26] H. Y. Peng, C. C. Lin, H. Y. Wang, Y. Shih, and S. T. Chou, "The melanogenesis alteration effects of *Achillea millefolium* L. essential oil and linalyl acetate: involvement of oxidative stress and the JNK and ERK signaling pathways in melanoma cells," *PLoS ONE*, vol. 9, no. 4, Article ID e95186, 2014.

[27] L. B. Cheng, L. Cheng, H. E. Bi et al., "Alpha-melanocyte stimulating hormone protects retinal pigment epithelium cells from oxidative stress through activation of melanocortin 1 receptor Akt-mTOR signaling," *Biochemical and Biophysical Research Communications*, vol. 443, no. 2, pp. 447–452, 2014.

[28] T. A. Luger, T. Schwarz, H. Kalden, T. Scholzen, A. Schwarz, and T. Brzoska, "Role of epidermal cell-derived α-melanocyte stimulating hormone in ultraviolet light mediated local immunosuppression," *Annals of the New York Academy of Sciences*, vol. 885, pp. 209–216, 1999.

[29] C. Lee, J. A. Ramirez, J. Guitart, and L. K. Diaz, "Expression of cyclooxygenase-2 and peroxisome proliferator-activated receptor gamma during malignant melanoma progression," *Journal of Cutaneous Pathology*, vol. 35, no. 11, pp. 989–994, 2008.

[30] M. H. Park, J. Y. Park, H. J. Lee et al., "The novel PPAR α/γ dual agonist MHY 966 modulates UVB-induced skin inflammation by inhibiting NF-κB activity,," *PloS ONE*, vol. 8, no. 10, Article ID e76820, 2013.

[31] R. P. Sahu, S. C. Dasilva, B. Rashid et al., "Mice lacking epidermal PPARγ exhibit a marked augmentation in photocarcinogenesis associated with increased UVB-induced apoptosis, inflammation and barrier dysfunction," *International Journal of Cancer*, vol. 131, no. 7, pp. E1055–E1066, 2012.

[32] H. Schmilovitz-Weiss, E. Hochhauser, M. Cohen et al., "Rosiglitazone and bezafibrate modulate gene expression in a rat model of non-alcoholic fatty liver disease—a historical prospective," *Lipids in Health and Disease*, vol. 12, article 41, 2013.

[33] Y. Shindo, E. Witt, and L. Packer, "Antioxidant defense mechanisms in murine epidermis and dermis and their responses to ultraviolet light," *Journal of Investigative Dermatology*, vol. 100, no. 3, pp. 260–265, 1993.

[34] Y. Shindo and T. Hashimoto, "Time course of changes in antioxidant enzymes in human skin fibroblasts after UVA irradiation," *Journal of Dermatological Science*, vol. 14, no. 3, pp. 225–232, 1997.

[35] A. Poswig, J. Wenk, P. Brenneisen et al., "Adaptive antioxidant response of manganese-superoxide dismutase following repetitive UVA irradiation," *The Journal of Investigative Dermatology*, vol. 112, no. 1, pp. 13–18, 1999.

Hindawi Publishing Corporation
BioMed Research International
Volume 2014, Article ID 692061, 9 pages
http://dx.doi.org/10.1155/2014/692061

Research Article

Amelioration of LPS-Induced Inflammation Response in Microglia by AMPK Activation

Chin-Chen Chen,[1] Jiun-Tsai Lin,[2] Yi-Fang Cheng,[2] Cheng-Yi Kuo,[2] Chun-Fang Huang,[2] Shao-Hsuan Kao,[3] Yao-Jen Liang,[1,4] Ching-Yi Cheng,[5] and Han-Min Chen[1,2,4]

[1] *Institute of Applied Science and Engineering, Catholic Fu-Jen University, New Taipei City 24205, Taiwan*
[2] *Energenesis Biomedical Co., Ltd., New Taipei City 24205, Taiwan*
[3] *Institute of Biochemistry and Biotechnology, Chung Shan Medical University, Taichung City 40201, Taiwan*
[4] *Department of Life Science, Catholic Fu-Jen University, New Taipei City 24205, Taiwan*
[5] *Research Center for Industry of Human Ecology, Graduate Institute of Health Industry Technology, Department of Cosmetic Science, Chang Gung University of Science and Technology, Taoyuan 33303, Taiwan*

Correspondence should be addressed to Han-Min Chen; steven@energenesis-biomedical.com

Received 31 March 2014; Revised 22 May 2014; Accepted 30 May 2014; Published 17 June 2014

Academic Editor: Nicole Clarke

Adenosine 5′-monophosphate-activated protein kinase (AMPK) is a key regulator of cellular energy homeostasis via modulating metabolism of glucose, lipid, and protein. In addition to energy modulation, AMPK has been demonstrated to associate with several important cellular events including inflammation. The results showed that ENERGI-F704 identified from bamboo shoot extract was nontoxic in concentrations up to 80 μM and dose-dependently induced phosphorylation of AMPK (Thr-172) in microglia BV2 cells. Our findings also showed that the treatment of BV2 with ENERGI-F704 ameliorated the LPS-induced elevation of IL-6 and TNF-α production. In addition, ENERGI-F704 reduced increased production of nitric oxide (NO) and prostaglandin E2 (PGE2) via downregulating the expression of inducible nitric oxide synthase (iNOS) and cyclooxygenase 2 (COX-2), respectively. Moreover, ENERGI-F704 decreased activated nuclear translocation and protein level of NF-κB. Inhibition of AMPK with compound C restored decreased NF-κB translocation by ENERGI-F704. In conclusion, ENERGI-F704 exerts inhibitory activity on LPS-induced inflammation through manipulating AMPK signaling and exhibits a potential therapeutic agent for neuroinflammatory disease.

1. Introduction

Homeostasis of proinflammatory and anti-inflammatory response in brain is shifted towards a proinflammatory state with age, so neuroinflammation has been implicated as an important etiological factor in several aging-related neurodegenerative diseases, such as Alzheimer's disease and Parkinson's disease [1–3]. Due to the involvement of inflammation in pathogenesis, many studies were devoted to the therapy of neurodegenerative diseases using anti-inflammatory strategies [4]. Microglia are myeloid-lineage cells residing in the central nervous system. As a neuron protector, microglia are sensitive to microenvironment and readily become activated in response to immunological stimuli, toxin, or injury [5]. Upon activation, however, microglia secrete a variety of proinflammatory cytokines or other cytotoxic factors, which are believed to exacerbate neurodegeneration. It has been reported that lipopolysaccharides (LPS) and/or interferon-γ enhanced the production of NO in microglia via inducible nitric oxide synthase (iNOS) and caused neuron death within 48 hours [6]. In addition, the increased proinflammatory cytokines such as TNF-α, IL-1β, and IL-6 in either cell culture or animal models induce neuron degeneration [7–12].

NF-κB, a transcriptional factor, regulates several proinflammatory cytokines and inflammation-related protein expression such as TNF-α, IL-1β, IL-6, COX-2, and iNOS [13]. Upon stimulation, activated IκB kinase (IKK) phosphorylates IκB, which results in the dissociation of NF-κB-IκB complex and thereby translocation of active NF-κB into nucleus. Activation of NF-κB has been found in several

neurodegenerative diseases including Alzheimer's disease, Parkinson's disease, and Huntington's disease [14–16] and has also been considered as an important target for therapy of neurodegenerative diseases.

AMP-activated kinase (AMPK) is a key regulator of energy homeostasis and metabolic stress [17]. Conditions of glucose deprivation, ischemia, or oxidative stress activate AMPK through upstream kinases such as liver kinase B1 (LKB1) and Ca^{2+}/calmodulin dependent kinase kinase β (CaMKKβ) by phosphorylation on conserved Thr-172 residue of α subunit [18, 19]. Upon activation, AMPK directly phosphorylated downstream targets such as acetyl-CoA carboxylase to inhibit anabolic pathways such as fatty acid/cholesterol synthesis, protein synthesis, and gluconeogenesis [20] and increase cellular ATP level. In particular, recent studies reveal that AMPK might also be involved in modulating inflammatory response [21–24]. It has been demonstrated that an AMPK activator, 5-aminoimidazole-4-carboxamide ribose (AICAR), suppressed LPS-induced proinflammatory secretion and attenuated nuclear factor-κB (NF-κB) activation in glial cells [25].

In the present study, we investigated the anti-inflammatory effects of ENERGI-F704, a purine compound identified from bamboo (*Phyllostachys edulis*) shoot extract [26], in microglia BV2 cells stimulated by LPS. We examined the effects of ENERGI-F704 on AMPK activation. We also assessed its anti-inflammation functions by monitoring the secretion of proinflammatory cytokines, the production of NO and PGE2, and the expression of corresponding enzymes in various conditions. It was found that ENERGI-F704 might attenuate LPS-induced inflammation and the nuclear translocation of NF-κB via AMPK activation in BV2 cells.

2. Materials and Methods

2.1. Reagents. All reagents were purchased from Sigma-Aldrich (St. Louis, MO, USA) except where otherwise specified. Dulbecco's modified Eagle's medium (DMEM) and fetal bovine serum (FBS) were purchased from Invitrogen (Carlsbad, CA, USA). ENERGI-F704 was a proprietary compound generously provided by Energenesis Biomedical Co., Ltd. (New Taipei, Taiwan).

2.2. Cell Culture. The murine microglial cell line (BV2) was given by Professor Kao (Chung Shan Medical University, Taichung, Taiwan) and routinely maintained in Dulbecco's modified Eagle's medium (DMEM) supplemented with 10% fetal bovine serum (FBS), 4 mM L-glutamine, 2 mM sodium pyruvate, and 100 μg/mL penicillin-streptomycin (Invitrogen GibcoBRL, Carlsbad, CA, USA). Cells were incubated at 37°C under 5% CO_2 and 95% relative humidity. The cells used in this experiment were between passages 3 and 8.

2.3. In Vitro Cytotoxicity Assay. The cytotoxicity of ENERGI-F704 in BV2 cells was analyzed by XTT assay. In Brief, BV2 cells were seeded into 96-well microplates in a density of 1×10^4 cells/well. After incubation overnight, cells were treated with various concentration of ENERGI-F704 (0, 5, 10, 20, 40, or 80 μM) for 24 h. After the end of treatment, 125 μL of XTT (2,3-bis-(2-methoxy-4-nitro-5-sulfophenyl)-2H-tetrazolium-5-carboxanilide) reagent was added to the final concentration of 1 mg/mL. Then, the plates were incubated at 37°C for further 4 h in the dark. The absorbance was measured at 490 nm with a reference wavelength set at 690 nm using VersaMax ELISA microplate reader (Molecular device, Sunnyvale, CA, USA). Data was presented as relative absorbance values to untreated cell.

2.4. Western Blot Assays. Cells were collected, washed twice with ice-cold PBS (PH 7.4), and lysed in cell lysis buffer containing 10 mM Tris-HCl pH 7.5, 150 mM NaCl, 1 mM EDTA, 0.5% Triton-X 100, 1x protease inhibitor cocktail (Roche, Basel, Switzerland), and 1x PhosSTOP phosphatase inhibitor cocktail (Roche) at 4°C for 30 min. Cell lysate was centrifuged at 15,000 g, 4°C for 1 min, and the supernatant was stored at −70°C until further analysis. 30 mg of protein samples was subjected to 10% SDS-PAGE and subsequently transferred onto Immobilon polyvinylidene difluoride (PVDF) membranes (Millipore, Bedford, MA, USA). After blocking with 5% BSA in PBS, the membranes were incubated with primary antibodies, including anti-phospho-AMPK (Thr172) antibody (1 : 2000, number 2535, Cell Signaling Technology, Danvers, MA, USA), anti-AMPKα1 antibody (1 : 2000, number 2603, Cell Signaling Technology), anti-iNOS antibody (1 : 2000, number 2977, Cell Signaling Technology), anti-COX-2 antibody (1 : 2000, number 12282, Cell Signaling Technology), anti-p65 antibody (1 : 2000, number 8242, Cell Signaling Technology), or anti-actin antibody (1 : 5000, NB600-501, Novus Biologicals, Littleton, CO, USA) at 4°C overnight. Resulting membranes were washed and incubated with corresponding secondary antibodies coupled with horseradish peroxidase in 1 : 20000 dilution at room temperature for 1 h. Chemiluminescence of the immunoreactive bands was developed by LumiFlash Prime Chemiluminescent Substrate, HRP (Visual Protein, Taipei, TW), and detected by Kodak XAR-5 film (Rochester, NY, USA). The images were scanned and quantified using ImageJ software (http://imagej.nih.gov/ij/).

2.5. Enzyme-Linked Immunosorbent Assay (ELISA). Production of proinflammatory cytokine and PGE2 was analyzed using ELISA assay. The supernatant of cell culture was harvested and assessed. The cytokines IL6 and TNF-α were evaluated using Mouse DuoSet ELISA kits (R&D Systems, Minneapolis, MN, USA) and the extracellular PGE2 was assessed using Prostaglandin E2 parameter assay kit (R&D Systems). All the manipulations were performed following the manufacturer's protocol.

2.6. Nitric Oxide Determination. Production of nitric oxide was measured using the Griess assay. In brief, 100 μL of supernatant sample was mixed with equal volume of Griess reagent containing 1% sulfanilamide, 0.1% N-(1-naphthyl)-ethylenediamine dihydrochloride, and 5% H_3PO_4. After 5 min incubation, the absorbance was measured at 550 nm with a reference wavelength set at 630 nm using VersaMax ELISA microplate reader. A standard curve made from a series of standard nitrite concentrations (0, 6.25, 12.5,

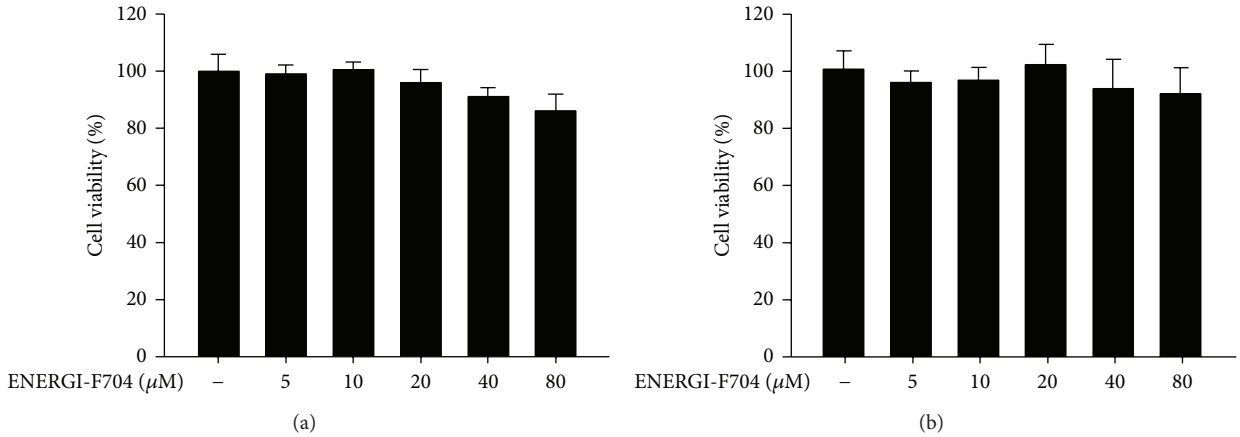

Figure 1: Cytotoxicity of ENERGI-F704. BV2 cells induced either without (a) or with (b) LPS were treated with indicated concentrations of ENERGI-F704 for 24 h. The cell viability of each condition was analyzed using XTT assay. The relative cytotoxicity is calculated as relative absorbance values to untreated cell. Data are statistically analyzed by one-way ANOVA and presented as the mean ± SEM of three independent experiments.

50, 66.7, 100, and 200 μM) was used for sample calibration.

2.7. NAD Assay. NAD level was determined by NADH cycling enzymatic reaction using NAD/NADH quantification colorimetric kit (Biovision, Milpitas, CA, USA) according to the manufacturer's instructions. In brief, 2×10^5 cells were harvested and extracted with 400 μL NAD/NADH Extraction Buffer by two freeze/thaw cycles (20 min on dry-ice, then 10 min at RT), followed by vortex and centrifugation at 14000 rpm for 5 min. The supernatants were examined for the total level of NAD plus NADH by mixing with NAD Cycling Mix for conversion of NAD to NADH and measured for the free NADH by heat decomposing of NAD at 60°C for 30 min. The colorimetric assay of NADH was developed by adding NADH developer and it was incubated at RT for 1 h. The absorbance was measured at 450 nm using VersaMax ELISA microplate reader (Molecular device, Sunnyvale, CA, USA). Data was presented as relative absorbance values to untreated cell. A standard curve made from a series of standard NADH amounts (0, 20, 40, 60, 80, and 100 pmol) was used for sample calibration. The NAD level was calculated as NAD = total of NAD + NADH − NADH. The data were normalized with total cell lysate protein (NAD/mg protein) and presented as relative concentration to untreated cell.

2.8. Immunocytochemistry. Cells were cultured on glass coverslips in the DMEM based medium. The cultures were treated with LPS incorporating with ENERGI-F704 or compound C in indicated concentrations for 1 h at 37°C. The cells were fixed with 4% paraformaldehyde and subsequently incubated with anti-p65 antibody (1 : 200, number 8242, cell Signaling Technology) at 4°C overnight followed by the incubation with Alex Fluor 488-labeled secondary antibody (1 : 1000, Abcam, Cambridge, UK) for 1 h at room temperature. The nuclei of cells were counterstained with DAPI. Coverslips were mounted with ibidi mounting medium (ibidi GmbH, Martinsried, Germany) and the immunofluorescence was imaged by OLYMUS 1X71 inverted microscope. The resulting images were quantified using ImageJ software.

2.9. Statistical Analysis. All results were presented as means ± SEM of three independent experiments. Statistical analysis was performed by one-way ANOVA or two-way ANOVA using SPSS software (Armonk, NY, USA).

3. Results

3.1. ENERGI-F704 Activates AMPK in BV2 Cells. We examined the cytotoxicity of ENERGI-F704 in microglial BV2 cells using XTT assay. As shown in Figure 1, ENERGI-F704 at concentrations up to 80 μM exerted no toxic effect on the BV2 cells treated with or without LPS. We next determined the AMPK activating property of ENERGI-F704 in BV2 cells using Western blot analysis. According to Figure 2, a significant increase in the phosphorylation of AMPK was observed in the presence of ENERGI-F704 in a dose-dependent manner.

3.2. ENERGI-F704 Reduces Proinflammatory Cytokines Production in LPS-Induced BV2 Cells. AMPK has been reported for its role in suppressing inflammatory responses. Therefore, we next evaluated whether ENERGI-F704 suppresses the production of proinflammatory cytokines such as TNF-α and IL-6 in LPS-treated BV2 cells. LPS-treated BV2 cells were treated with either ENERGI-F704 or the pharmacological AMPK activator, 5-aminoimidazole-4-carboxamide 1-β-D-ribofuranoside (AICAR), for 24 h. The changes in levels of TNF-α and IL-6 were determined using ELISA assay. The exposure of BV-2 cells to LPS resulted in a significant secretion of IL-6 and TNF-α after 24 h incubation (Figures 3(a) and 3(b)). The elevations in TNF-α and IL-6 production

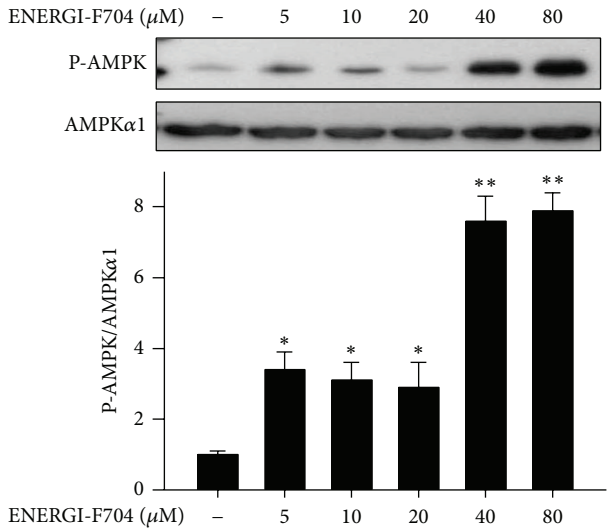

Figure 2: ENERGI-F704 activates AMPK in microglial BV2 cells. BV2 cells were treated with serial concentrations of ENERGI-F704 for 3 h. Cell lysates were used to determine the phosphorylation of AMPK using Western blot analysis. Data are presented as the mean ± SEM of three independent experiments (one-way ANOVA; **, $P < 0.01$; specific comparison to vehicle treated control). Representative images of three independent experiments are shown.

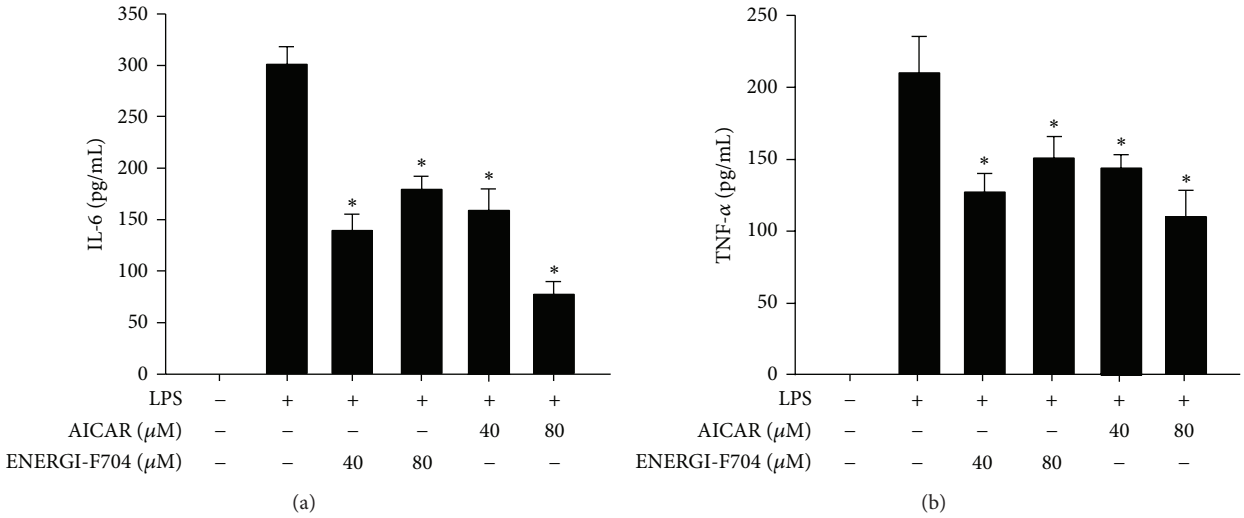

Figure 3: ENERGI-F704 reduced LPS-induced IL-6 and TNF-α secretion in BV2 cells. BV2 cells were incubated with 200 ng/mL LPS in the presence of ENERGI-F704 or AICAR for 24 h. The levels of IL-6 (a) and TNF-α (b) in culture medium of each condition were accessed using ELISA analysis. Data are presented as the mean ± SEM of three independent experiments (one-way ANOVA; *, $P < 0.05$; specific comparison to LPS-treated control).

were reduced significantly in the presence of ENERGI-F704. A similar inhibitory phenomenon was observed in the cells treated with AICAR.

3.3. ENERGI-F704 Suppresses NO Production and iNOS Expression in LPS-Induced BV2 Cells. Nitric oxide (NO) acts as signaling molecule in inflammation. The excessive production of NO in response to LPS stimulation might lead to activation of apoptotic signaling in brain tissue [27]. To evaluate the effects of ENERGI-F704 on NO production induced by LPS, BV2 cells stimulated with LPS were treated with ENERGI-F704 or AICAR for 24 h, and concentration of NO was analyzed. As shown in Figure 4(a), treatment with ENERGI-F704 at concentrations of 40 and 80 μM significantly inhibited NO production of LPS-treated BV-2 cells, whereas AICAR inhibited NO production as well. To explore the mechanism underlying inhibitory effect of ENERGI-F704 on LPS-induced NO production, expression of iNOS in each experimental group was assessed using Western blotting. The elevated expressions of iNOS in LPS-induced BV2 cells were significantly reduced by treatment with ENERGI-F704 or AICAR (Figure 4(b)), whereas use of AMPK inhibitor,

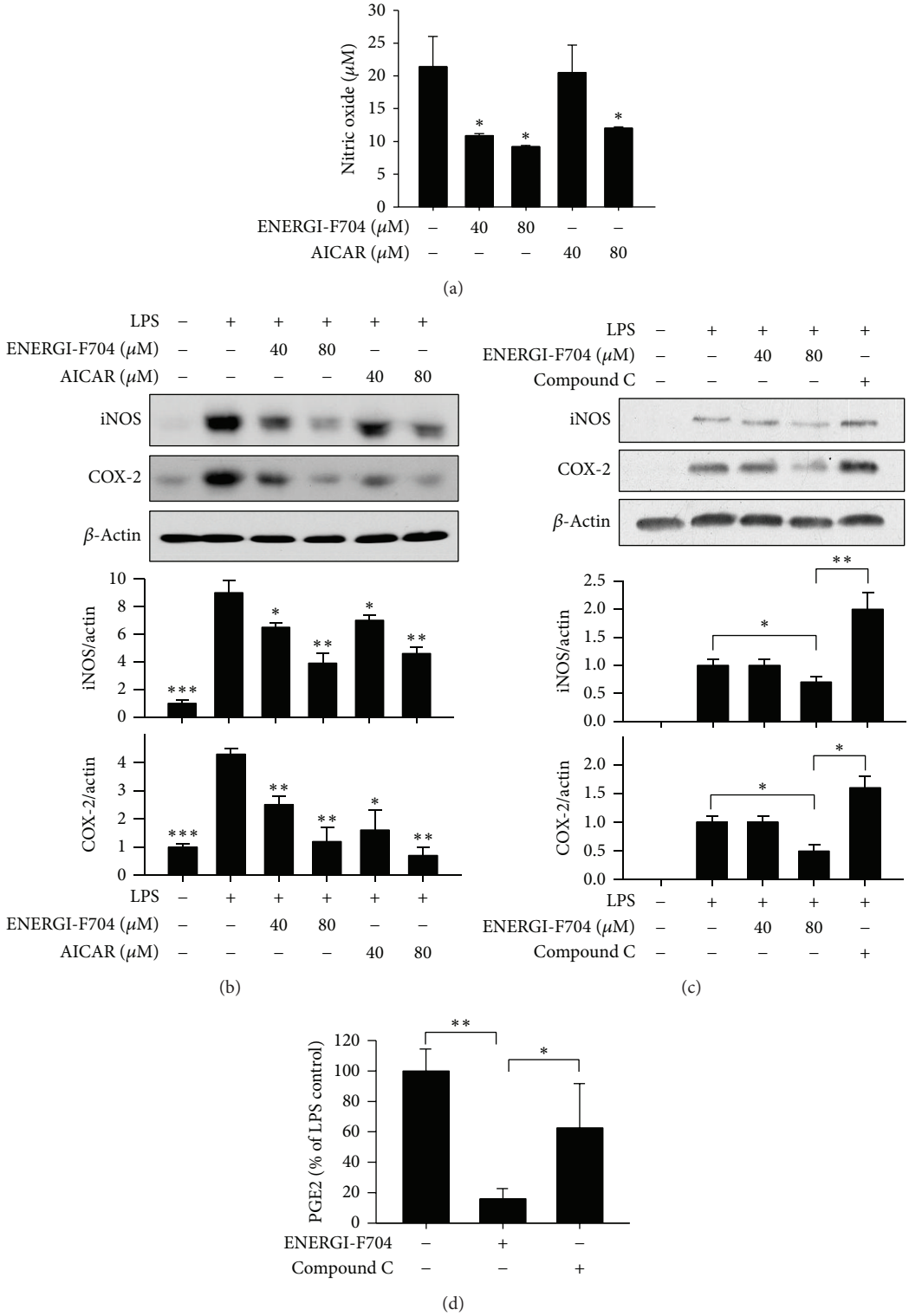

Figure 4: ENERGI-F704 decreases LPS-induced NO, iNOS, COX-2, and PGE2 production in BV2 cells. BV2 cells were stimulated with 200 ng/mL LPS and subsequently treated with either ENERGI-F704 or AICAR for 24 h. (a) Levels of NO in the culture of BV2 cell were determined. (b) After treatments, cell lysates were used to determine the level of iNOS and COX-2 using Western blotting. (c) LPS-treated BV2 cells were treated with ENERGI-F704 in cotreatment with or without compound C for 24 h. Cell lysates were used to determine the level of iNOS and COX-2 using Western blotting. (d) LPS-induced BV2 cells were treated with ENERGI-F704 in cotreatment with or without compound C for 48 h, and the level of PGE2 in the culture medium was determined. Data are presented as the mean ± SEM of three independent experiments (two-way ANOVA; *, **, and ***, $P < 0.05$, $P < 0.01$, and $P < 0.01$; specific comparison to LPS-treated control). Representative images of three independent experiments are shown.

compound C, led to negatively compensated expression of iNOS (Figure 4(c)).

3.4. ENERGI-F704 Inhibited LPS-Induced Cyclooxygenase 2 Expression and PGE2 Production. We further evaluated the effect of ENERGI-F704 on COX-2 expression in BV2 cells challenged with LPS using Western blot assay. As shown in Figure 4(b), the expression of COX-2 was upregulated upon LPS stimulation. The upregulated expression of COX-2 was ameliorated by ENERGI-F704 or AICAR (Figure 4(b)), whereas the treatment with compound C remarkably reversed the suppression (Figure 4(c)). As expected, when measuring the product of COX-2, as shown in Figure 4(d), the concentration of extracellular PGE2 in LPS-induced BV2 cells was diminished by ENERGI-F704, which can be offset in the presence of compound C.

3.5. ENERGI-F704 Attenuates LPS-Induced Nuclear Translocation and Production of NF-κB. NF-κB is known for its critical role in inflammation through regulating transcription of proinflammatory cytokines such as IL-1β, IL-6, TNF-α, and iNOS. To examine the effects of ENERGI-F704 on NF-κB activation, LPS-stimulated BV2 cells were treated with ENERGI-F704 for 1 h and examined for nuclear translocation of NF-κB. As shown in Figure 5, NF-κB stained green retained in cytosol and translocated into nuclei in response to LPS stimulation. The treatment of LPS-induced BV2 cells with ENERGI-F704 attenuated the translocation of NF-κB to nuclei. The inhibitory effect of ENERGI-F704 on NF-κB translocation was reversed in the presence of compound C. Furthermore, our data revealed that the expression level of P65 was reduced significantly in a dose-dependent manner (Figure 5(c)).

Activation of AMPK leads to the deacetylation activity of SIRT1 mediated by the increase of NAD^+ and acetylation of P65 is required for the stability of NF-κB [28–30]. We next determined the effect of ENERGI-F704 on the NAD^+ level. As shown in Figure 6, the treatment with ENERGI-F704 dose-dependently increased the level of NAD^+. Interestingly, increased level of NAD^+ in response to ENERGI-F704 treatment was largely reversed in the presence of compound C.

4. Discussion

Accumulating evidence shows that AMPK is a repressor of inflammation. However, there are limited studies addressed on the effect of AMPK activators on LPS-induced microglia. In the present study, ENERGI-F704, a proprietary compound identified from bamboo shoots extract, exerts AMPK activation activity in human microglial cell model BV2. ENERGI-F704 suppressed LPS-induced IL-6 and TNF-α secretion. Moreover, ENERGI-F704 decreased LPS-induced iNOS and COX-2 expression as well as the production of NO and PGE2 in BV2 cells. In the testing condition, our data suggest ENERGI-F704 with anti-inflammatory activity without apparent cytotoxicity. In fact, our previous study has reported that ENERGI-F704 can trigger the phosphorylation of AMPK in human umbilical vein endothelial cells [26]. All the results indicate that ENERGI-F704 acts as an AMPK activator to ameliorate that the NF-κB-involved inflammation response is reliable and not cell type restricted.

Some AMPK activators such as AICAR and metformin have also been demonstrated for their potential to modulate inflammation via NF-κB [25, 31, 32]. Our results had showed ENERGI-F704 as a feasible mean to attenuate LPS-induced inflammatory responses in BV2 and other cell lines. As the anti-inflammatory effects of ENERGI-F704 were diminished in the presence of AMPK inhibitor, compound C, it again suggests that the amelioration of LPS-induced inflammation in microglia BV2 cells by ENERGI-F704 is mediated by AMPK activation. In addition, the activation of AMPK can activate SIRT1 activity via increasing intracellular NAD^+ levels [28]. It has been demonstrated that SIRT1 could deacetylate p65 subunit of NF-κB complex at lysine 310 and consequently enhance the set-mediated methylation of lysines 314 and 315 [29, 30]. Moreover, the methylation of lysines 314 and 315 resulted in degradation of p65 through triggering ubiquitin-proteasome system. In the present study, we did observe an increase in the level of NAD and a reduction in the level of p65 subunit under the treatment of ENERGI-F704 (Figure 4(d)). Therefore, it is possible that destabilization of p65 protein might be another way of ENERGI-F704 to modulate NF-κB activity. Indeed, the LPS-induced expression of p65 downstream targets, iNOS and COX-2, can be suppressed in the presence of ENERGI-F704 (Figures 4(b) and 4(c)).

Numerous studies showed that manipulation of NF-κB signaling provides beneficial effects in treating neuron injury. It has been examined that suppression of NF-κB activity by using IKK inhibitors, AS602868 and BAY 11-7082, exerts long-lasting protection of primary neurons and oligodendrocytes under N-methyl-D-aspartate induced excitotoxicity [33, 34]. In a mouse model of focal cerebral ischemia, transgenic expression of NF-κB suppressor or pharmacological inhibitor of IKK reduced the infarct size [35]. Besides neuron injury, activation of NF-κB has been found in several aging-related neurodegenerative diseases including Alzheimer's disease and Parkinson's disease, which was considered as a pivotal target for therapy of neurodegenerative diseases [14, 15]. In addition, recent studies further revealed that the neuron immune crosstalk of NF-κB, IKK, and microglia in hypothalamus is important in systemic ageing progression, so immune inhibition can be a potential strategy for lifespan extension [36]. Considering AMPK activation effectively manipulating the NF-κB signaling, AMPK activators, including ENERGI-F704, are potential therapeutic agents for neurodegenerative diseases. Further studies are awaited to elucidate the underlying mechanism of ENERGI-F704 on AMPK.

5. Conclusions

In conclusion, ENERGI-F704 suppressed inflammatory responses and induced AMPK activation in LPS-treated BV-2 cells. Anti-inflammatory effect of ENERGI-F704 was attributed to modulating the nuclear translocation and stability of NF-κB. The anti-inflammatory effects of ENERGI-F704 were diminished in the presence of AMPK inhibitor. It

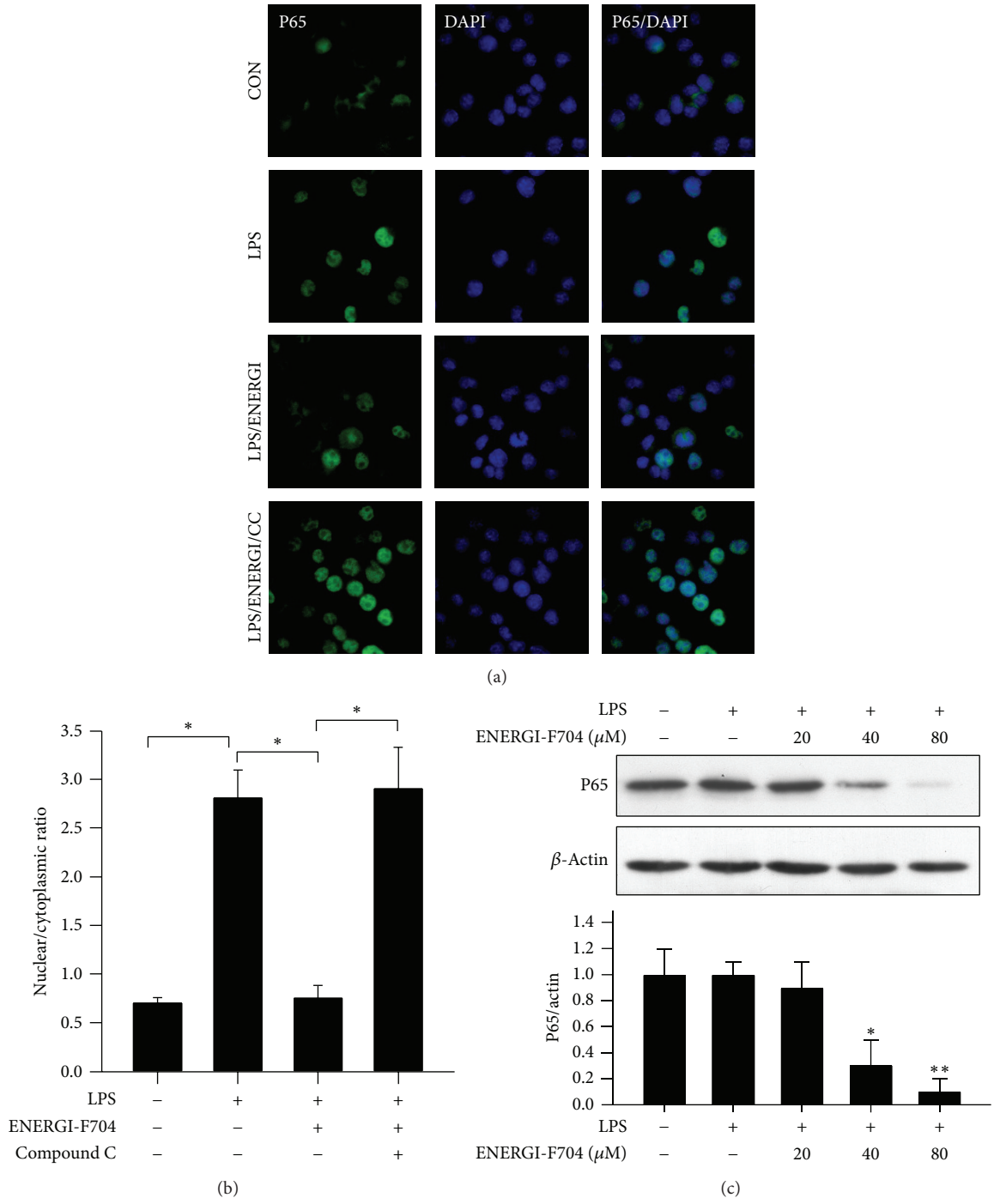

Figure 5: ENERGI-F704 attenuates LPS-induced nuclear translocation and production of NF-κB in BV2 cells. BV2 cells were stimulated with 200 ng/mL LPS and subsequently treated with ENERGI-F704 incorporating with or without compound C for 1 h. (a) After treatments, cells were fixed for immunocytochemical staining. NF-κB and nuclei were visualized using Alexa Fluor 488 (green) and DAPI (blue), respectively. (b) Ratio of nuclear: cytoplasmic immunofluorescence of NF-κB was assessed by microscopy image and quantified using ImageJ software. Ratio < 1 indicates brighter cytoplasmic staining for NF-κB, whereas ratios > 1 indicate brighter nuclear staining for NF-κB. (c) BV2 cells were incubated with 200 ng/mL LPS in the presence of ENERGI-F704 for 24 h. After treatments, cell lysates were used to determine the levels of NF-κB using Western blotting. Data are presented as the mean ± SEM of three independent experiments (one-way ANOVA; * and **, $P < 0.05$ and $P < 0.01$; specific comparison to LPS-treated control). Representative images of three independent experiments are shown.

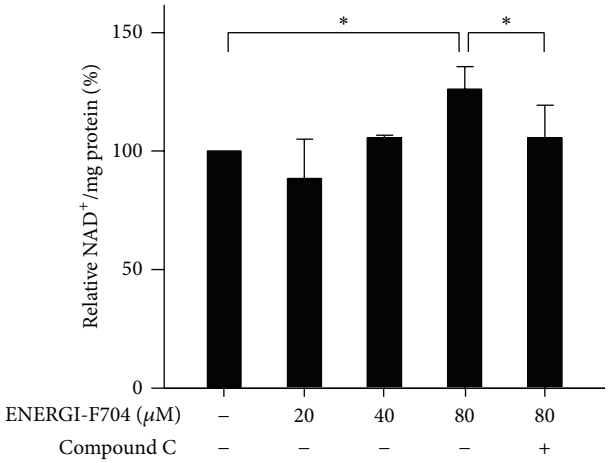

Figure 6: ENERGI-F704 increases the level of NAD in BV2 cells. BV2 cells were incubated with 200 ng/mL LPS in the presence of ENERGI-F704 or compound C for 24 h. Cell lysates collected from each condition were used to determine the level of NAD using NAD/NADPH colorimetric analysis. Data are presented as the mean ± SEM of three independent experiments (one-way ANOVA; *, $P < 0.05$).

is suggested that ENERGI-F704 has a potential to act as anti-inflammatory agent for treating neuroinflammatory diseases through AMPK activation. Further studies are necessary to elucidate the actual mechanism underlying anti-inflammatory activity of ENERGI-F704.

Conflict of Interests

The authors declare that there is no conflict of interests regarding the publication of this paper.

Authors' Contribution

Chin-Chen Chen and Jiun-Tsai Lin contributed equally to this work.

References

[1] C. Holmes, C. Cunningham, E. Zotova et al., "Systemic inflammation and disease progression in Alzheimer disease," *Neurology*, vol. 73, no. 10, pp. 768–774, 2009.

[2] H.-M. Gao, B. Liu, W. Zhang, and J.-S. Hong, "Synergistic dopaminergic neurotoxicity of MPTP and inflammogen lipopolysaccharide: relevance to the etiology of Parkinson's disease," *FASEB Journal*, vol. 17, no. 13, pp. 1957–1959, 2003.

[3] X.-G. Luo, J.-Q. Ding, and S.-D. Chen, "Microglia in the aging brain: relevance to neurodegeneration," *Molecular Neurodegeneration*, vol. 5, no. 1, article 12, 2010.

[4] B. Liu and J.-S. Hong, "Role of microglia in inflammation-mediated neurodegenerative diseases: mechanisms and strategies for therapeutic intervention," *Journal of Pharmacology and Experimental Therapeutics*, vol. 304, no. 1, pp. 1–7, 2003.

[5] G. W. Kreutzberg, "Microglia: a sensor for pathological events in the CNS," *Trends in Neurosciences*, vol. 19, no. 8, pp. 312–318, 1996.

[6] A. Bal-Price and G. C. Brown, "Inflammatory neurodegeneration mediated by nitric oxide from activated glia-inhibiting neuronal respiration, causing glutamate release and excitotoxicity," *Journal of Neuroscience*, vol. 21, no. 17, pp. 6480–6491, 2001.

[7] L. Yuan and A. H. Neufeld, "Tumor necrosis factor-alpha: a potentially neurodestructive cytokine produced by glia in the human glaucomatous optic nerve head," *Glia*, vol. 32, pp. 42–50, 2000.

[8] U. Schlomann, S. Rathke-Hartlieb, S. Yamamoto, H. Jockusch, and J. W. Bartsch, "Tumor necrosis factor α induces a metalloprotease-disintegrin, ADAM8 (CD 156): implications for neuron-glia interactions during neurodegeneration," *Journal of Neuroscience*, vol. 20, no. 21, pp. 7964–7971, 2000.

[9] K. Hemmer, L. Fransen, H. Vanderstichele, E. Vanmechelen, and P. Heuschling, "An in vitro model for the study of microglia-induced neurodegeneration: involvement of nitric oxide and tumor necrosis factor-α," *Neurochemistry International*, vol. 38, no. 7, pp. 557–565, 2001.

[10] I. Figiel and K. Dzwonek, "TNFα and TNF receptor 1 expression in the mixed neuronal-glial cultures of hippocampal dentate gyrus exposed to glutamate or trimethyltin," *Brain Research*, vol. 1131, no. 1, pp. 17–28, 2007.

[11] C. C. Ferrari, M. C. Pott Godoy, R. Tarelli, M. Chertoff, A. M. Depino, and F. J. Pitossi, "Progressive neurodegeneration and motor disabilities induced by chronic expression of IL-1β in the substantia nigra," *Neurobiology of Disease*, vol. 24, no. 1, pp. 183–193, 2006.

[12] R. A. Quintanilla, D. I. Orellana, C. González-Billault, and R. B. Maccioni, "Interleukin-6 induces Alzheimer-type phosphorylation of tau protein by deregulating the cdk5/p35 pathway," *Experimental Cell Research*, vol. 295, no. 1, pp. 245–257, 2004.

[13] P. J. Barnes and M. Karin, "Nuclear factor-κB—a pivotal transcription factor in chronic inflammatory diseases," *New England Journal of Medicine*, vol. 336, no. 15, pp. 1066–1071, 1997.

[14] G. P. García-Ospina, M. Jiménez-Del Río, F. Lopera, and C. Vélez-Pardo, "Neuronal DNA damage correlates with a positive detection of c-Jun, nuclear factor κB, p53 and Par-4 transcription factors in Alzheimer's disease," *Revista de Neurologia*, vol. 36, no. 11, pp. 1004–1010, 2003.

[15] S. Hunot, B. Brugg, D. Ricard et al., "Nuclear translocation of NF-κb is increased in dopaminergic neurons of patients with Parkinson disease," *Proceedings of the National Academy of Sciences of the United States of America*, vol. 94, no. 14, pp. 7531–7536, 1997.

[16] M. Napolitano, D. Zei, D. Centonze et al., "NF-kB/NOS cross-talk induced by mitochondrial complex II inhibition: implications for Huntington's disease," *Neuroscience Letters*, vol. 434, no. 3, pp. 241–246, 2008.

[17] D. G. Hardie, "Minireview: the AMP-activated protein kinase cascade: the key sensor of cellular energy status," *Endocrinology*, vol. 144, no. 12, pp. 5179–5183, 2003.

[18] M. J. Abbott, A. M. Edelman, and L. P. Turcotte, "CaMKK is an upstream signal of AMP-activated protein kinase in regulation of substrate metabolism in contracting skeletal muscle," *The American Journal of Physiology: Regulatory Integrative and Comparative Physiology*, vol. 297, no. 6, pp. R1724–R1732, 2009.

[19] A. Woods, S. R. Johnstone, K. Dickerson et al., "LKB1 is the upstream kinase in the AMP-activated protein kinase cascade," *Current Biology*, vol. 13, no. 22, pp. 2004–2008, 2003.

[20] D. G. Hardie, S. A. Hawley, and J. W. Scott, "AMP-activated protein kinase—development of the energy sensor concept," *Journal of Physiology*, vol. 574, no. 1, pp. 7–15, 2006.

[21] S. Galic, M. D. Fullerton, J. D. Schertzer et al., "Hematopoietic AMPK β1 reduces mouse adipose tissue macrophage inflammation and insulin resistance in obesity," *Journal of Clinical Investigation*, vol. 121, no. 12, pp. 4903–4915, 2011.

[22] S. J. Park, K. S. Lee, S. R. Kim et al., "AMPK activation reduces vascular permeability and airway inflammation by regulating HIF/VEGFA pathway in a murine model of toluene diisocyanate-induced asthma," *Inflammation Research*, vol. 61, no. 10, pp. 1069–1083, 2012.

[23] X. Zhao, J. W. Zmijewski, E. Lorne et al., "Activation of AMPK attenuates neutrophil proinflammatory activity and decreases the severity of acute lung injury," *The American Journal of Physiology: Lung Cellular and Molecular Physiology*, vol. 295, no. 3, pp. L497–L504, 2008.

[24] R. Prasad, S. Giri, N. Nath, I. Singh, and A. K. Singh, "5-Amino-imidazole-4-carboxamide-1-beta-4-ribofuranoside attenuates experimental autoimmune encephalomyelitis via modulation of endothelial-monocyte interaction," *Journal of Neuroscience Research*, vol. 84, no. 3, pp. 614–625, 2006.

[25] S. Giri, N. Nath, B. Smith, B. Viollet, A. K. Singh, and I. Singh, "5-aminoimidazole-4-carboxamide-1-β-4-ribofuranoside inhibits proinflammatory response in glial cells: a possible role of AMP-activated protein kinase," *Journal of Neuroscience*, vol. 24, no. 2, pp. 479–487, 2004.

[26] H.-M. Chen, J.-T. Lin, C.-Y. Kuo, and C.-F. Huang, "The effects of novel AMPK activator on human vascular endothelial cells," *Journal of Medical and Bioengineering*, vol. 3, no. 2, pp. 144–148, 2014.

[27] G. A. Czapski, M. Cakala, M. Chalimoniuk, B. Gajkowska, and J. B. Strosznajder, "Role of nitric oxide in the brain during lipopolysaccharide-evoked systemic inflammation," *Journal of Neuroscience Research*, vol. 85, no. 8, pp. 1694–1703, 2007.

[28] C. Cantó, Z. Gerhart-Hines, J. N. Feige et al., "AMPK regulates energy expenditure by modulating NAD + metabolism and SIRT1 activity," *Nature*, vol. 458, no. 7241, pp. 1056–1060, 2009.

[29] X.-D. Yang, E. Tajkhorshid, and L.-F. Chen, "Functional interplay between acetylation and methylation of the RelA subunit of NF-κB," *Molecular and Cellular Biology*, vol. 30, no. 9, pp. 2170–2180, 2010.

[30] F. Yeung, J. E. Hoberg, C. S. Ramsey et al., "Modulation of NF-κB-dependent transcription and cell survival by the SIRT1 deacetylase," *EMBO Journal*, vol. 23, no. 12, pp. 2369–2380, 2004.

[31] Y. Hattori, K. Suzuki, S. Hattori, and K. Kasai, "Metformin inhibits cytokine-induced nuclear factor κB activation via AMP-activated protein kinase activation in vascular endothelial cells," *Hypertension*, vol. 47, no. 6, pp. 1183–1188, 2006.

[32] S.-H. Tsai, S.-Y. Lin-Shiau, and J.-K. Lin, "Suppression of nitric oxide synthase and the down-regulation of the activation of NFκB in macrophages by resveratrol," *British Journal of Pharmacology*, vol. 126, no. 3, pp. 673–680, 1999.

[33] I. Sarnico, F. Boroni, M. Benarese et al., "Targeting IKK2 by pharmacological inhibitor AS602868 prevents excitotoxic injury to neurons and oligodendrocytes," *Journal of Neural Transmission*, vol. 115, no. 5, pp. 693–701, 2008.

[34] M. Pizzi, I. Sarnico, F. Boroni, A. Benetti, M. Benarese, and P. F. Spano, "Inhibition of IκBα phosphorylation prevents glutamate-induced NF-κB activation and neuronal cell death," *Acta Neurochirurgica*, no. 93, pp. 59–63, 2005.

[35] M. Schwaninger, I. Inta, and O. Herrmann, "NF-κB signalling in cerebral ischaemia," *Biochemical Society Transactions*, vol. 34, no. 6, pp. 1291–1294, 2006.

[36] G. Zhang, J. Li, S. Purkayastha et al., "Hypothalamic programming of systemic ageing involving IKK-β, NF-κB and GnRH," *Nature*, vol. 497, no. 7448, pp. 211–216, 2013.